DEPARTMENT OF PATHOLOGY
SCHOOL OF MEDICINE
CARDIFF UNIVERSITY

Investigating the mechanistic basis of telomeric fusions

A thesis submitted to the School of Medicine, Cardiff University in partial fulfilment for the degree of Doctor of Philosophy

BY
NICOLE H. HEPPEL

2011

UMI Number: U567010

All rights reserved

INFORMATION TO ALL USERS
The quality of this reproduction is dependent upon the quality of the copy submitted.

In the unlikely event that the author did not send a complete manuscript
and there are missing pages, these will be noted. Also, if material had to be removed,
a note will indicate the deletion.

UMI U567010
Published by ProQuest LLC 2013. Copyright in the Dissertation held by the Author.
Microform Edition © ProQuest LLC.
All rights reserved. This work is protected against
unauthorized copying under Title 17, United States Code.

ProQuest LLC
789 East Eisenhower Parkway
P.O. Box 1346
Ann Arbor, MI 48106-1346

Declaration

This work has not previously been accepted in substance for any degree and is not concurrently submitted in candidature for any degree.

Signed ..... (candidate) Date 31. March 2011

STATEMENT 1

This thesis is being submitted in partial fulfillment of the requirements for the degree of .....PhD.....(insert MCh, MD, MPhil, PhD etc, as appropriate)

Signed ..... (candidate) Date 31. March 2011

STATEMENT 2

This thesis is the result of my own independent work/investigation, except where otherwise stated.
Other sources are acknowledged by explicit references.

Signed ..... (candidate) Date 31. March 2011

STATEMENT 3

I hereby give consent for my thesis, if accepted, to be available for photocopying and for inter-library loan, and for the title and summary to be made available to outside organisations.

Signed ..... (candidate) Date 19. Sept. 2011...

STATEMENT 4: PREVIOUSLY APPROVED BAR ON ACCESS

I hereby give consent for my thesis, if accepted, to be available for photocopying and for inter-library loans **after expiry of a bar on access previously approved by the Graduate Development Committee.**

Signed ..... (candidate) Date .....

Acknowledgements

I would like to thank my supervisor Dr Duncan Baird, for his continuous support and guidance through out the project. First and foremost I would like to thank him for giving me the opportunity to undertake this PhD in the first place.

Furthermore, I would like to thank all the other members of the STELA group: Jan Rowson, Dr. Maira Tankinmanova, Dr. Bethan Britt-Compton, Dr Laureline Roger, Dr Thet Thet Lin, Dr Rhiannon Robinson and Biotelo Letsolo for all their advice and encouragement in the last four years. I also would like to thank all the technical staff in the Pathology department for their help. A special thank you goes to Rebecca Capper, Jane Bond and Amy Brook, which have been a tremendous help in tissue culture.

I especially would like to thank my family and friends who have been a continual support and encouragement during the course of this PhD. A huge thank you goes to my dad and my brother who have been supporting me both financially and mentally over the course of the last 7 years. They have been home in everyway possible even if they were hundreds of kilometres away. Most importantly I have to thank my friend Laureline, without her strength and support this PhD thesis would not have been possible.

Finally, I would like to thanks Tennessee Williams and Marlon Brando for perfectly summarising my feelings about single telomere length analysis (STELA).

***Stanley Kowalski**: Hey, STELLA.*

Tennessee Williams *A Streetcar named Desire*

Summary

Telomeres are essential nucleoprotein structures located at the ends of chromosomes that provide both end protection and avoid recognition through the DNA damage response. In humans, telomeres consists of arrays of TTAGGG repeats which associate with, and are protected by, shelterin, a complex of telomere binding proteins. Dysfunctional telomeres arise by either gradual telomere erosion as a result of the end replication problem to critical lengths, or by the removal of telomere binding proteins. It is widely accepted that short dysfunctional telomeres are recognised as DNA double strand breaks. The aberrant repair of telomeric double strand breaks and the subsequent formation of dicentric chromosomes, can initiate cycles of anaphase bridging, breakage and fusion that can drive genomic instability. In eukaryotes, double strand breaks are repaired by either error-free homologous recombination or error-prone non-homologous end joining.

In this thesis, single molecule approaches were used to observe the telomere dynamics of DNA repair deficient fibroblast cultures and to characterise possible fusion events in cells undergoing crisis following the forced expression of HPV16 E6E7 oncoproteins.

All the DNA repair deficient human fibroblast strains observed in this thesis exhibited a similar limited replicative capacity. In contrast to previous reports, the data presented here supports the assumption that DNA repair deficiency does not result in accelerated telomere erosion and therefore the reduced replicative lifespan of these fibroblast cultures appears to be telomere independent.

The main aspect of this thesis was to examine the role that components of the DNA repair mechanisms might play in the fusion of short dysfunctional telomeres. The results presented here indicate that the fusion of short dysfunctional telomeres is largely independent of DNA Ligase I and DNA Ligase IV. These observations lead to the assumption that DNA Ligase III might be the predominant ligase involved in the fusion of short dysfunctional telomeres.

Furthermore, NBS1 deficiency results in a paucity of sporadic telomere deletion events which is consistent with the hypothesis that NBS1 is involved in the resolution of Holliday junctions within T-loops creating telomeric deletion events. In contrast, DNA Ligase IV deficiency and PARP1 inhibition caused distinct short telomere length distributions. Both these phenotypes might be related to problems with telomere replication.

Table of Contents

Abbreviations

3-AB	3-aminobenzamid
53BP1	p53 Binding Protein 1
ABC	ATP Binding Cassette
AdD	Adenylation Domain
ADP	Adenosine Diphosphate
ALT	Alternative Lengthening of Telomeres
AMP	Adenosine Monophosphate
A-NHEJ	Alternative NHEJ
ARH3	ADP-ribosylhydrolase 3
AT	Ataxia Telangiectasia
ATLD	ataxia telangiectasia-like disorder
ATM	Ataxia Telangiectasia Mutated
ATP	Adenosine Triphosphate
ATR	ATM and Rad3 Related
BER	Base Excision Repair
BFB	Breakage-Fusion-Bridge
BLM	Bloom Syndrome Helicase
Bp	Base pair
BRCA1	Breast Cancer 1
BRCT	Breast Cancer C-terminal domain
BrdU	Bromodeoxyuridine
BS	Bloom Syndrome
BSA	Bovine Serum Albumin
CD	Cell division
Cdc	Cell division cycle
CDC25	Cell Division Cycle 25
cDNA	Complementary DNA
CHK1	Checkpoint kinase 1
CHK2	Checkpoint kinase 2
C-NHEJ	Classic NHEJ
C-terminus	Carboxyl-terminus
D melanogaster	*Drosophilia melanogaster*
DAB	Diaminobenzidine
DBD	DNA Binding Domain
DC	Dyskeratosis Congenita
DDR	DNA Damage Repair
DIQ	1,5-Isoquinolinediol
DKC1	Dyskerin
D-loop	Displacement loop
DMEM	Dulbecco's Modified Eagle's Medium
DMS	Dimethylsulfate

DMSO	Dimethyl sulfoxide
DNA	Deoxyribonucleic Acid
DNA-PK_{cs}	DNA-dependent protein kinase catalytic subunit
DSB	DNA double Strand break
EMEM	Eagle's minimum essential medium
FEN1	Flap Endonuclease 1
FHD	Fork Head associated Domain
G0	Quiescence
G1	Gap phase 1
G2	Gap phase 2
G418	Geneticin
GTP	Guanosine triphosphate
HeLa	Henrietta Lacks
HeT-A	Drosophila telomeric non-LTR retrotransponson
HPV	Human Papillomavirus
HR	Homologous Recombination
IR	Ionizing Radiation
Kb	Kilo base
kDA	Kilo Dalton
LTR	Long Terminal-Repeat
M musculus	*Mus Musculus*
MBD	Mre11 Binding Domain
MDC1	Mediator of DNA damage Checkpoint 1
Mdm2	Murine double minute 2
MMEJ	Microhomology Mediated End Joining
MRE11	Meiotic recombination II protein
MRN	Complex containing MRE11/RAD50/NBS1
MRX	Homolog in yeast of MRN
NAD	Nicotinamide Adenine Dinucleotide
NBS1	Nijmegen Breakage Syndrome protein
NEO	Neomycin
NHEJ	Non-Homologous End Joining
NIMA	Never In Mitosis A
Nt	Nucleotide
NTase	Nucleotidyltransferase
N-terminus	Ammino-terminus
NTP	Nucleoside triphosphate
NuMA	Nuclear Mitotic Apparatus protein
OB	Oligonucleotide Binding fold
pADPr	Poly ADP-ribose
PAR	Poly ADP-ribose
PARG	Poly (ADP-ribose) glycohydrolase
PARP	Poly ADP-ribose polymerase
PBS	Phosphate Buffered Saline
PCNA	Proliferating Cell Nuclear Antigen
PCR	Polymerase Chain Reaction
PD	Population doubling

PIN2	Protein interacting with NIMA
PINX1	Pin2/TRF1 interacting protein
PIP1	Pot1 interacting protein
PNK	Mammalian polynucleotide kinase
POT1	Protein-protection Of Telomeres 1
pRB	Retinoblastoma susceptibility gene product
PTOP	Pot1 interacting protein
RAD50	Radiation sensitive protein
RAD51D	RAD51/RecA-related gene
RAP1	Repressor Activator Protein 1
RNA	Ribonucleic Acid
RNase	Ribonulease
ROS	Radical Oxygen Species
RS	Replicative senescence
RT	Room temperature
S cerevisiae	*Saccharomyces cerevisiae*
S phase	DNA synthesis phase
S pombe	*Saccharomyces pombe*
SAβ-gal	Senescence-associated mammalian β-galactosidase
SCE	Sister Chromatide Exchange
SD	Standard Deviation
SE	Standard error
SIPS	Stress induced premature senescence
STELA	Single Telomere Length Analysis
T brucei	*Trypanosoma brucei*
T cruzi	*Trypanosoma crizi*
TAE	Tris-acetat-EDTA
TAHR	Drosophila telomeric non-LTR retrotransponson
TART	Drosophilia telomeric non-LTR retrotransposons
Taz1	Telomere associated in *Schizosaccharomyces pombe*
TBE	Tris Borate EDTA
T-circles	Telomeric circle
TERC	Telomerase RNA
TERT	Telomerase reverse transcriptase
TIN2	TRF interacting protein 2
TINT1	TIN2 interacting protein
T-loop	Telomere loop
TNKS	Tankyrase 1
TNKS2	Tankyrase 2
TPP1	Thiamine pyrophosphate enzyme
TRD	Telomere rapid deletion
TRF	Terminal Restriction Fragment
TRF1	Telomere Repeat binding Factors 1
TRF2	Telomere Repeat binding Factors 2
TRFH	TRF homodimerisation domain
TVR	Telomere Variant Repeat
UV	Ultraviolet

WRN	Werners syndrome gene
WS	Werner Syndrome
XPF	Human nucleotide excision repair protein
XRCC	X-ray repair cross-complementing
Xrs2	NBS1 homolog in yeast
γH2AX	Histone H2AX phosphorylated on serine 139

Chapter 1: Introduction

1.1 History of Telomeres

At the end of the 1930's, two independent researches made a seminal observation (McClintock, 1939, Mueller, 1938). The disruption of the chromosome following X-ray treatment resulted in various types of internal rearrangements including translocations, inversions and deletions. However, most interestingly, the chromosome ends were excluded from these chromosomal alterations. The geneticist Herman Müller speculated that an unidentified structure protected the end of the chromosomes in *Drosophila melanogaster* which prevented chromosomal modifications and maintained the integrity of the chromosome. He named these structures "telomeres" derived from the Greek words *telos* (end) and *meros* (part) (Fig 1.1a). At the same time, in 1939, Barbara McClintock's observations in maize (Zea Mays) provided evidence that the loss of these end structures following X-irradiation induces frequent sister chromatid fusion events. These fusion events created dicentric chromosomes which formed a "bridge" between the two "daughter" cells during the meiotic anaphase. The cell separation at the end of anaphase stretches and breaks the dicentric chromosome inducing an unequal break site in the two daughter chromosomes. Mitosis of the "daughter" cell can induced continuous cycles of replication, chromatid fusion and unequal breakage which are termed "breakage-fusion-bridge" (BFB) events. Consequently several BFB cycles can lead to chromosomal abnormalities, gene amplifications and gene loss. Further experiments showed that BFB cycles were only maintained in non-embryonic tissue. In embryonic cells the continuous BFB events were interrupted and the incipient chromosomal breakage were permanently healed (McClintock, 1941).

1.2 Structure of Telomeres

Even though telomeres were identified in the 1930's, it took another 40 years until the first telomeric DNA sequence could be identified in the protozoa *Tetrahymena thermophilia* (Blackburn and Gall, 1978). Telomeric DNA is highly conserved amongst eukaryotes despite displaying variability in telomeric sequence and length. The TTAGGG repeats sequence is thought to be the oldest telomeric sequence as it is observed in the telomeres of protozoa, fungi, plants and mammalians. Even as the telomere repeats vary between species, most telomeres are composed of a G-rich strand (G-strand) at the chromosomal 3'end and a C -rich strand (C-strand) at the 5'end (Meyne et al., 1989). Rather than ending in a blunt end, the G-strand protrudes over the C-strand in a single stranded extensions forming a G-rich 3'-overhang (Fig 1.1b). G-strand overhangs are present at both chromosome ends (Cervantes and Lundblad, 2002, Makarov et al., 1997, McElligott and Wellinger, 1997). It has been suggested that the G-rich overhang at the 3' end of the chromosome is a result of the end replication problem. In contrast to this, the overhang of the 5' end is generated by either degradation of the C-rich strand or elongation of the G-rich strand by telomerase (Dionne and Wellinger, 1996, Makarov et al., 1997, McElligott and Wellinger, 1997). The overhangs are maintained throughout the replicative capacity of the cell (Chai et al., 2005).

The 3 -overhang is thought to fold back into the telomere repeat region forming a secondary telomeric DNA structures termed the t-loop. By invading the double stranded DNA a single stranded displacement loop (D-loop) is created (Fig 1.1c). The t-loop protects telomere ends from degradation, DNA repair activity and regulates telomerase activity (Griffith et al., 1999, Palm and de Lange, 2008). The formation of the t-loop is supported by members of the shelterin complex (de Lange, 2004). T-loops have been observed in protozoan, plants and humans and to some extend in yeasts (Cesare et al., 2003, Griffith et al., 1999, Munoz-Jordan et al., 2001, Tomaska et al., 2004). However very little is known about the dynamics of T-loop assembly and whether each chromosome end is capped by a t-loop. Furthermore it is not clear whether the t-loop is

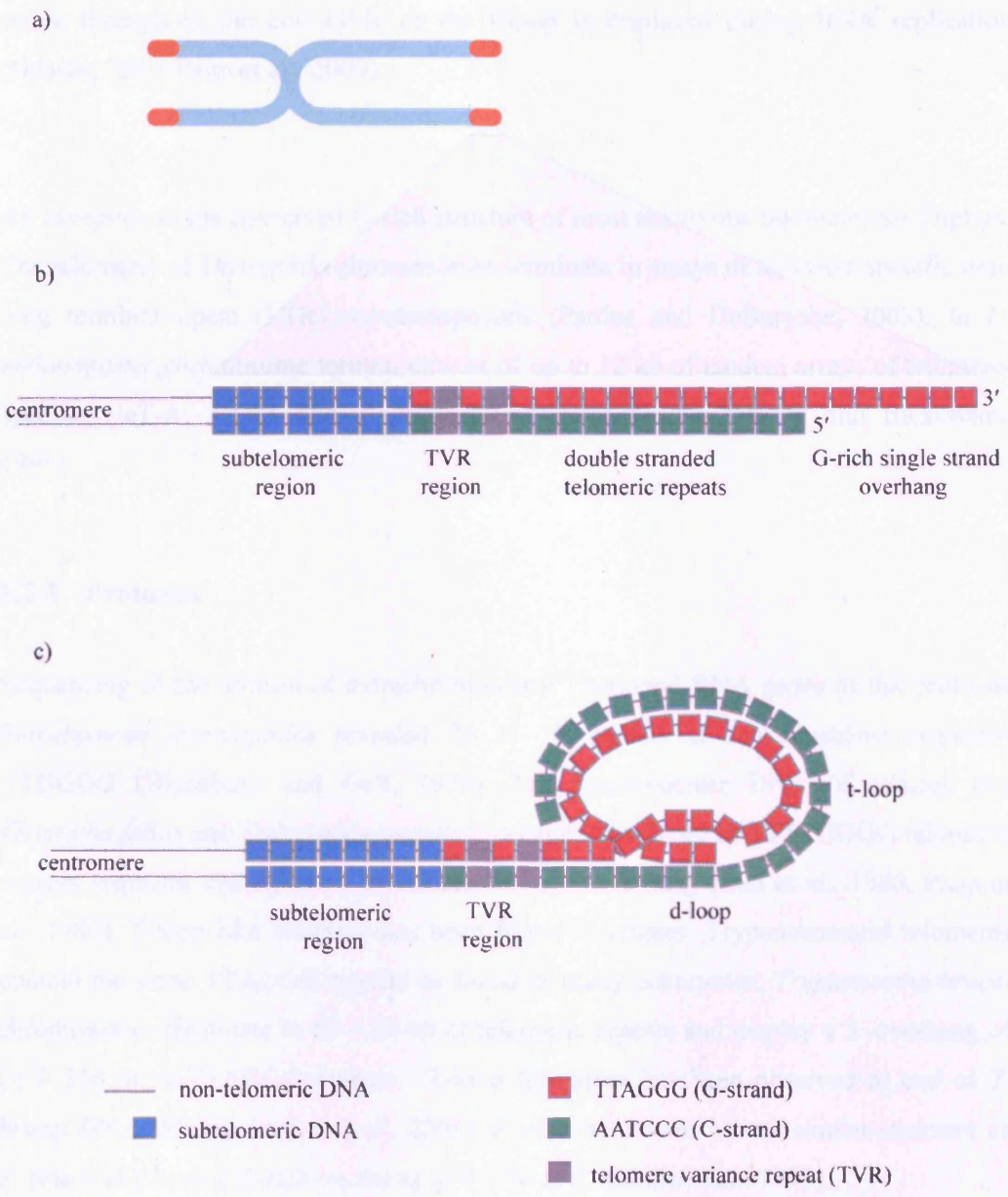

Figure 1.1 The structure of telomeres

stable throughout the cell cycle or the t-loop is displaced during DNA replication (Denchi, 2009, Palm et al., 2009).

An exception to the conserved G-rich structure of most eukaryotic telomeres are Diptera. The telomeres of *Drosophila* chromosomes terminate in arrays of telomere-specific non-long terminal-repeat (LTR) retrotransposons (Pardue and DeBaryshe, 2003). In *D. melanogaster* chromosome termini consist of up to 12 kb of tandem arrays of telomere-specific HeT-A, TART and TAHR LTR retrotransposons (Mason and Biessmann, 1995).

1.2.1 Protozoa

Sequencing of the termini of extrachromosomal ribosomal RNA genes of the protozoa *Tetrahymena thermophilia* revealed 20 to 70 repeats of the repetitive sequence TTGGGG (Blackburn and Gall, 1978). The macronuclear DNA of ciliates like *Oxytricha fallax* and *Stylanychia pustulata* is capped by 20 bp of TTTTGGGG telomeric repeats sequence ending in an additional 16 bp 3′-overhang (Oka et al., 1980, Pluta et al., 1982). T-loop like structure has been found in ciliates. Trypanosomatid telomeres contain the same TTAGGG repeats as found in many eukaryotes. *Trypanosoma brucei* chromosomes terminate in 10 – 20 kb of telomeric repeats and display a 3 -overhang of 21 – 250 nt of TTAGGG repeats. T-loop formation has been observed at end of *T. brucei* DNA (Munoz-Jordan et al., 2001). *T. cruzi* telomeres have a similar structure as *T. brucei* and have a G-rich overhang of 9 – 50 nt (Chiurillo et al., 1999).

1.2.2 Fungi

The telomeric sequence found at the chromosome termini of budding yeast *Saccharomyces cerevisiae* consists of 120 to a 150 bp of $G_{2\text{-}3}(TG)_{1\text{-}6}$ repeats. An additional more distal domain contains varying number of $TG_{1\text{-}7}$ repeats (Shampay et al.,

1984, Wang and Zakian, 1990). In *S. cerevisiae*, the two telomeric arrays form an alternative higher order structure which differs from t-loop observed in other eukaryotes (de Bruin et al., 2001). The telomeres of fission yeast *Schizosaccharomyces pombe* contain approximately 300 bp of the degenerated telomeric repeat sequence, $TTAC(A)(C)G_{2\text{-}8}$ (Hiraoka et al., 1998). T-loop formation has been observed in *S. pombe* and appears to be dependent on Taz1, a component of the fission yeast shelterin complex (Tomaska et al., 2004). Both budding and fission yeast have a G-rich single stranded overhang at their chromosome termini. In contrast to mammalian cells where the length of the G-rich overhang appears to be constant (Makarov et al., 1997), the amount of G-rich overhang of *S. cerevisiae* and *S. pombe* increases during S-phase (Wellinger et al., 1993).

1.2.3 Plants

In almost all plants, the chromosomal termini are composed of canonical TTTAGGG repeats (Fajkus et al., 2005, Riha and Shippen, 2003). However the telomere length varies between different plants species. For example, the *Arabidopsis* telomere spans an area of 2 to 5 kb (Riha and Shippen, 2003) whereas the telomere repeat regions in tobacco plants reaches 150 kb (Fajkus et al., 1995). Exceptions from the normally TTTAGGG repeat observed in plants are the algae *Chlamydomonas* and member of the Asparagles species. In the *Chlamydomonas*, telomeres contain the repeat sequence TTTTAGGG (Petracek et al., 1990). In Asparagales, a single nucleotide change causes a switch to the repeat motif TTAGGG which is normally observed in humans (Fajkus et al., 2005). In contrast to other plants, members of the *Alliaceae* family (onions) lack any kind of G-rich telomere repeats and display a completely unknown telomere structure (Pich et al., 1996). Like the telomere length, the length of G-rich 3'-overhang is highly variable in plants ranging from 20 to 30 nt in *Arabidopsis* (Riha and Shippen, 2003) to 75 kb in *Pisum sativum* (common garden pea)(Cesare et al., 2003). Most interestingly, not all chromosomal termini in plants end in a G-rich 3'-overhang indicating a so far unknown telomere structures in plants (Riha et al., 2000, Watson and Riha, 2010).

1.2.4 Mammalian

The chromosome ends of mammalians are capped by telomeres containing the conserved TTAGGG repeat sequence (Meyne et al., 1989). However the telomere length varies between different species and subspecies. For instance the wild forms of *Mus musculus* and *Mus spretus* have telomeres in the range of 5-20 kb whereas the telomere length is significantly longer in inbred strains of *M. musculus*. The mouse strain DBA/2 displays a telomere length ranging from 20 to 150 kb, whereas the strain C57BL/6 has telomeres of 20-65 kb in length (Kipling and Cooke, 1990).

Human telomeres are composed of pure TTAGGG repeat arrays ranging from 5 to 20 kb. In addition to this highly conserved telomere repeat sequence, human telomeres contain 1 to 2 kb of telomere variance repeats (TVR) such as TTGGGG, TGAGGG and TCAGGG at the proximal end of the telomere (Baird et al., 1995, Brown et al., 1990, de Lange et al., 1990).

1.3 Telomere Associated Proteins

Human telomere repeats arrays interact with a specialised multi-protein complex termed shelterin complex. The components of this complex are abundant at the chromosome termini throughout the cell cycle. The six core proteins of the shelterin complex are the telomere repeat binding factors 1 and 2 (TRF1 and TRF2), the TRF-interacting protein 2 (TIN2), protection of telomeres 1 (POT1), the POT1-TIN2 organizing protein (TPP1, also known as TINT1, PTOP or PIP1) and repressor/activator protein 1 (RAP1) (de Lange, 2005, Palm and de Lange, 2008)(Fig 1.2). Only TRF1, TRF2 and POT1 bind directly to telomeric DNA, with TRF1 and TRF2-binding to telomeric double stranded DNA and POT1 binding to the G-rich single stranded 3 -overhang. The other components of the shelterin complex associate with the chromosomal termini via the interaction with the 3 telomere binding proteins.

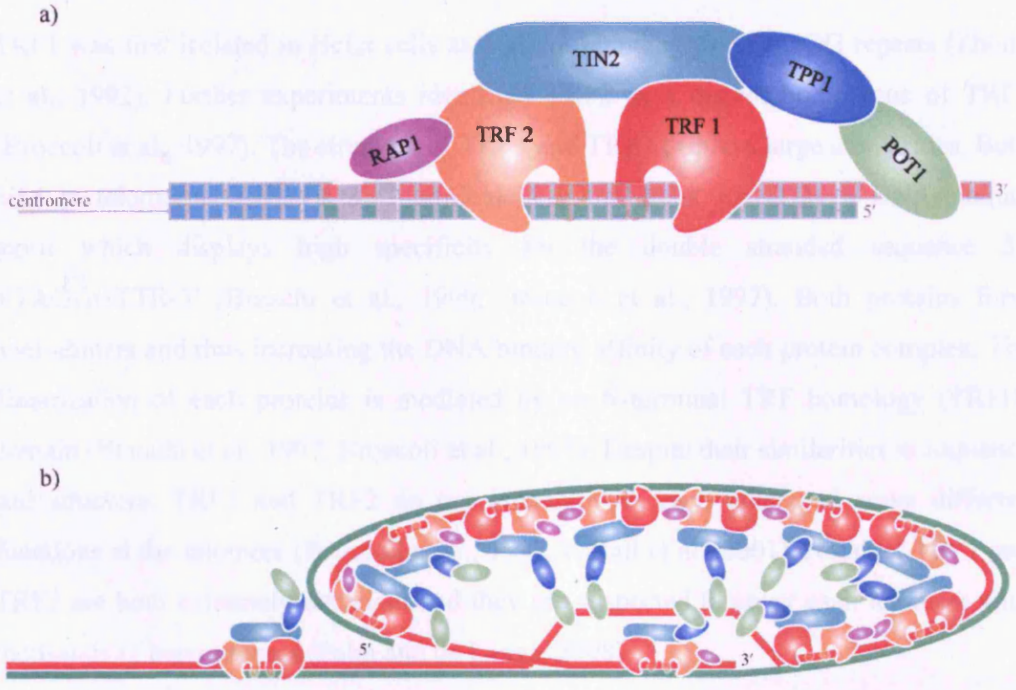

Figure 1.2 The shelterin complex. a) The six core components of the shelterin complex. b) the shelterin complex interacting with a telomere in t-loop configuration . Since TRF 1 and TRF 2 bind indepentently to telomeric repeats and TIN2, the resutling subcomplexes are presented in this scheme (modified from Denchi 2009, Martinez 2010)

1.3.1 The Shelterin complex

1.3.1.1 Telomere Repeat Binding Factors 1 and 2 (TRF1 and TRF2)

TRF1 was first isolated in HeLa cells as a protein binding to TTAGGG repeats (Zhong et al., 1992). Further experiments identified TRF2 as a distant homologue of TRF1 (Broccoli et al., 1997). The structure of TRF1 and TRF2 displays large similarities. Both bind to telomeric DNA via a C-terminal helix-turn-helix SANT/Myb DNA-binding motif which displays high specificity for the double stranded sequence 5 - YTAGGGTTR-3′ (Bianchi et al., 1999, Broccoli et al., 1997). Both proteins form homodimers and thus increasing the DNA binding affinity of each protein complex. The dimerization of each proteins is mediated by an N-terminal TRF homology (TRFH) domain (Bianchi et al., 1997, Broccoli et al., 1997). Despite their similarities in sequence and structure, TRF1 and TRF2 do not interact with each other and serve different functions at the telomere (Broccoli et al., 1997, Fairall et al., 2001). Notable, TRF1 and TRF2 are both extremely abundant and they are suspected to cover each telomere with thousands of heterodimers (Palm and de Lange, 2008).

TRF1 has DNA remodelling activity which might stimulate the T-loop formation (Bianchi et al., 1997, Griffith et al., 1998). TRF1 has been shown to contribute to telomere length regulation (Smogorzewska et al., 2000, van Steensel and de Lange, 1997). However it role in telomere protection has not been established. TRF1 promotes the replication of telomere repeats and prevents the stalling of replication forks (Sfeir et al., 2009). TRF1 deletion in mouse is lethal (Iwano et al., 2004, Karlseder et al., 2003). TRF1 is a negative regulator of telomere length in telomerase-positive cells, whereas TRF2 is important for telomere capping (Kim et al., 2004). The poly(ADP-ribosyl)ation of TRF1 inhibits the binding of TRF1 to telomeres and therefore leaves the chromosome termini accessible for telomerase (Cook et al., 2002, Smith and de Lange, 2000, Smith et al., 1998). TRF1 interacts with TIN2, TNKS1, the Ku70/80 heterodimer, Bloom's

syndrome helicase (BLM), ATM kinase, PinX1 (Hsu et al., 2000, Kim et al., 2004, Lillard-Wetherell et al., 2004, Smith et al., 1998).

TRF2 can form t-loop like structures in the presence of model telomere substrates. (Stansel et al., 2001). The Ku70 subunit of the Ku 70/80 heteromere has been shown to interact with TRF2. Ku70/80 also associates with the hTERT component of telomerase, indicating an involvement in telomere length maintenance (Chai et al., 2005, Hsu et al., 2000, O'Connor et al., 2004, Ye et al., 2004a). TRF1 also recruits ERCC1/XPF to the telomere, removing the 3′ overhang from uncapped telomeres allowing non-homologous end joining (NHEJ), The ERCC1/XPF is also implemented to prevent telomere recombination with chromosome internal sites (Zhu et al., 2003). Other proteins which interact with TRF2 are the MRN complex and Werner syndrome helicase (WRN) (Opresko et al., 2002, Zhu et al., 2000, Zhu et al., 2003).

1.3.1.2 TIN2

TIN2 (TRF1- and TRF2-interacting nuclear factor 2) provides a stabilizing scaffold for the shelterin complex as it binds to TRF1, TRF2 and TPP1 (Houghtaling et al., 2004, Kim et al., 2004, Ye et al., 2004a, Ye et al., 2004b). The TIN2 protein contains 3 distinct binding sites for each binding partner (Chen et al., 2008, Ye et al., 2004a). The binding site for TRF1 is located on the C-terminus of TIN2, whereas the N-terminus is associated with binding to TRF2. Both binding sites on TIN2 interact with the TRFH domain in the corresponding protein. TIN2 recruits TPP1-POT to telomeres using a third binding site located in its N-terminus and thereby linking double stranded and single stranded telomeric repeats (Chen et al., 2008, Houghtaling et al., 2004, Kim et al., 2004, Ye et al., 2004a). Furthermore, TIN2 is an important stabilisation factor for TRF1 and TRF2. TIN2 prevents the poly(ADP-ribosyl)ation of TRF1 through tankyrase1 which results in the modification of TRF1 and consequently in the release of TRF1 from DNA. (Smith et al., 1998, Ye et al., 2004b). In addition, the link, TIN2 forms between TRF1 and TRF2, further stabilises TRF2's binding to telomeric DNA (Kim et al., 2004, Ye et al., 2004a). In human cells, the expression of TIN2 with a truncated N-terminus leads to

aberrant telomere elongation, whereas the over-expression of TIN2 inhibits telomere elongation. This suggests that TIN2 along with TRF1 and TRF2 limits the access of telomerase to the chromosome end and therefore acts as a negative telomere length regulator (Kim et al., 1999).

1.3.1.3 TPP1

POT1-TIN2 organizing protein (TPP1, also known as TINT1, PTOP or PIP1) was first identified by two hybrid screens with TIN2. It acts as a linker protein between POT1 and TIN2 (Houghtaling et al., 2004, Liu et al., 2004b, Ye et al., 2004b). The C-terminus of TPP1 binds to TIN2 whereas the central domain of the protein interacts with POT1 (Liu et al., 2004b, Ye et al., 2004b). Furthermore, a serine rich region is located between the two protein binding domains but its function is unknown at the moment (Palm, de Lange 2008). Recent findings indicate that the N-terminus of TPP1 contains a telomerase-interacting domain which implements a role for TPP1 in the telomerase recruitment and regulation of telomerase activity at chromosome ends (Xin et al., 2007, Ye et al., 2004a). TPP1 is essential for the recruitment of POT1 to telomere. However, several reports have claimed that POT1 can localise at chromosome ends in the absence of functional TPP1 (Colgin et al., 2003, He et al., 2006). In addition, TPP1 is crucial for proper localisation of POT1 in the nucleus (Chen et al., 2007). The expression of a non-functional TPP1 results in removal of all POT1 from the chromosome end and sub-consequently leads to a telomere de-protection and telomere length phenotype which is similar to the one observed after POT1 loss (Denchi and de Lange, 2007, Liu et al., 2004a, Xin et al., 2007).

1.3.1.4 POT1

POT1 (Protection of Telomeres 1) was first identified through its homology to the cilicate telomere protein TEBPα (Baumann and Cech, 2001). Human POT1 contains two oligonucleotide/oligosaccharide-binding (OB) folds that are highly specific' for 5 -

(T)TAGGGTTAG-3′ sequence. Surprisingly, it appears that POT1 only binds to telomeric DNA in the presence of TPP1 (Baumann and Cech, 2001, Loayza and De Lange, 2003, Loayza et al., 2004). However, several reports have indicated that POT1 can localise to chromosome ends in the absence of functional TPP1 (Colgin et al., 2003, He et al., 2006). In addition, POT1 appears to require TPP1 for nuclear localisation (Chen et al., 2007). Knock down of human POT1 caused telomere elongation and only a few telomeres fused (34 -37). Moreover, POT1 is thought to stabilise the t-loop formation as it binds to the displacement G-strand in the D-loop (Loayza et al., 2004, Palm and de Lange, 2008).

1.3.1.5 Rap1

Human Rap1 (Repressor/Activator Protein 1) is recruited to the chromosomal termini by TRF2 (Li et al., 2000) and depends on TRF2 to remain stable (Celli and de Lange, 2005). Rap1 contains 3 different domains; a Myb domain to interact with an unknown protein partner (Hanaoka et al., 2001), an N-terminal BRACT (BRAC1 C-terminal) motif and a C-terminal domain which enables the binding to TRF2 (Palm and de Lange, 2008). In contrast to yeast Rap1, human Rap1 does not directly bind to telomeric DNA (Li and de Lange, 2003). The exact function of human Rap1 has not been established yet. Nevertheless based on its structure, human Rap1 might be involved in protein-protein interactions (Denchi, 2009). However more recent suggest the RAP1 might be involved in the inhibition of NHEJ (Bae and Baumann, 2007, Sarthy et al., 2009).

1.3.2 Transient Associated Telomeres Proteins

In contrast to the six shelterin proteins which reside at telomeres throughout the cell cycle, several proteins have been reported which transiently associate with chromosome ends. Most of these proteins are involved in DNA damage response or DNA damage repair. Several components of homologous recombination (HR) have been observed at mammalian telomeres. These proteins include the MRN complex (Zhu et al., 2000),

Rad51D (Tarsounas et al., 2004), Blooms syndrome helicase (BLM) (Lillard-Wetherell et al., 2004, Opresko et al., 2005, Opresko et al., 2002) and WRN RecQ helicase (Crabbe et al., 2004, Opresko et al., 2002). In addition to HR proteins, non-homologous end joining (NHEJ) core components associate with telomere (DNA-PKcs (d'Adda di Fagagna et al., 2001, Hsu et al., 1999), Ku 70/80 (Hsu et al., 1999, O'Connor et al., 2004). Other proteins include PinX1 (Kim et al., 2004), PARP1 (O'Connor et al., 2004), tankyrase 1 and tankyrase 2 (Cook et al., 2002, Smith et al., 1998). Almost all of these proteins are recruited to the telomere by TRF1 and TRF2 (Chen et al., 2008, Palm and de Lange, 2008).

1.3.2.1 PinX1

PinX1 is a TRF binding protein that directly inhibits telomerase activity. The protein, along with its interacting partner MCRS2 (a cell cycle dependant protein that accumulates in S-phase), negatively regulates telomeric length, binding directly to TERT and TRF1(Zhou and Lu, 2001). PinX1 binds to the region of TERT that associates with TERC RNA subunit with the telomerase complex, thereby preventing it association with the RNA telomerase template (Banik and Counter, 2004).

1.3.2.2 Tankyrase1 and Tankyrase2

Tankyrase 1 (TNKS) and Tankyrase 2 (TNKS2) are both poly(ADP-ribose) polymerases (PARPs) (Cook et al., 2002, Smith et al., 1998). TNKS is a 140 kDA protein which was first identified in a yeast two hybrid screen (Smith et al., 1998). TNKS shares 80% of overall amino acid content with TNKS2 (Lyons et al., 2001). In humans, TNKS and TNKS2 localise to telomeres and are involved in telomere length maintenance. They both interact with and poly(ADP-ribosyl)ated TRF1. The poly(ADP-ribosyl)ation of TRF1 inhibits the binding of TRF1 to telomeres and therefore leaves the chromosome termini accessible for telomerase (Cook et al., 2002, Smith and de Lange, 2000, Smith et al., 1998). Moreover, TNKS interacts with mitotic apparatus protein NuMA regulating

for mitotic spindle function (Chang et al., 2005). TNKS knockdown cells display defects in assembly of bipolar spindles as well as other spindle and microtubule defects (Hsiao and Smith, 2008). In addition TNKS is essential for the resolution of sister telomeres during mitosis. TNKS deficiency leads to fusion between the two de-protected sister chromatids. The sister telomeres are fused by NHEJ (Hsiao and Smith, 2009). TNKS2 functions are not so clear; it appears it shares similar functions with TNKS however further studies are needed to define them (Cook et al., 2002).

1.4 Telomere Repeat Containing RNA (TERRA)

Telomeres establish a heterochromatic state at chromosome ends. Heterochromatin states are characterised by the presence of trimethylated lysines at position 9 in histone H3 and 20 in histone H4, histone hypoacetylation, the accumulation of several isoforms of heterochromation protein 1 and hypermethylation of cytosines in CpG-dinucleotides present in subtelomeric regions (Blasco, 2007, Ottaviani et al., 2008). Telomeric chromatin states contribute to chromosome positioning and movement within the nucleus and also to the regulation of telomerase. Abnormal telomeric chromatin states have been linked to severe stochastic telomere loss and thus suggesting a crucial role of this structure during telomere replication (Yehezkel et al., 2008, Michishita et al., 2008). Recent studies have identified telomeric repeat containing RNA (TERRA) in several eukaryotes including yeasts, plants and mammals. TERRA localizes to telomeres throughout the entire cell cycle and forms an integral component of telomeric heterochromatin. TERRA-associated functions are still mostly a mystery. However, several discoveries have been made in TERRA biogenesis (Azzalin et al., 2007, Schoeftner and Blasco, 2008, Luke et al., 2008, Luke and Lingner, 2009).

Mammalian TERRA is a heterogeneous non-coding RNA that consists of telomeric UUAGGG repeats, and ranges in length from approximately 100 bases up to more than 9 kb (Azzalin et al., 2007, Schoeftner and Blasco, 2008, Luke and Lingner, 2009). TERRA is transcribed in a centromere to telomere direction and contains both telomeric and subtelomeric RNA. This may suggest that the transcription site of TERRA lies

within the subtelomeric sequence. The DNA-dependent RNA polymerase II (RNAPII) is thought to be the main polymerase to transcribe TERRA and uses the C-rich telomeric strand of the telomere as template. Evidence for this assumption is provided by the fact that RNAPII physically associate with mammalian telomeres and with TRF1, a sheltering component. Furthermore, a proportion of mammalian and yeast TERRA is 3′ polyadenylated, a circumstance which is shared with the majority of RNAPII products. However, more recent studies indicated that other RNA polymerases like RNAPI and RNAPIII may also have a potential function in TERRA transcription (Azzalin et al., 2007, Schoeftner and Blasco, 2008, Luke and Lingner, 2009, Dejardin and Kingston, 2009).

The non-sense-mediated RNA decay (NMD) machinery, which plays an important role in the degradation of mRNAs containing pre-mature termination codons, has been implicated in TERRA localisation at human telomeres (Azzaline 2007, Chawla Azzalin 2008). It has been demonstrated that three of the key players in the NMD pathway (UPF1, SMG1 and hEST1A/SMG6) associate directly with telomeres and depletion of these proteins results in a significant increase in the amount of TERRA foci at telomeres. Furthermore, both TERRA half-life and total TERRA levels were unaffected by the depletion of these three proteins (Azzalin et al., 2007, Luke and Lingner, 2009).

1.5 Telomeric Function

1.5.1 Capping the Chromosome termini

Observations in *Drosophila melanogaster* and in maize (McClintock, 1939, Mueller, 1938) showed that disrupted chromosomes following X-ray treatments lead to various types of chromosomal rearrangements. However the chromosome ends were excluded from these alterations. This lead to the hypothesis that chromosomes are capped and this "capping" somehow distinguishes the chromosome end from a DNA double strand break. Electron microscopy analysis of chromosome ends revealed a large duplex loops

referred to as t-loop which might provide this capping function (Griffith et al., 1999). T-loop formation depends on TRF1 and TRF2 which have been proposed to remodel telomeric DNA into large loops (Bianchi et al., 1997, Griffith et al., 1999, Stansel et al., 2001).

In addition to the t-loop, quadruplex (four-stranded) structures might provide a cap for the chromosome ends. The quadruplex structures can be formed by sequences of telomeric DNA which contain repetitions of the GGTTAG motif. The four individual guanines from each strand form planar G.G.G.G tetrad arrangements, consequently aligning all four DNA strands parallel, with the three linking trinucleotide loops positioned on the exterior of the quadruplex core (Chang et al., 2003, Granotier et al., 2005, Parkinson et al., 2002, Wang and Patel, 1993). Furthermore, quadruplex conformation of telomeric DNA might be able to impair telomerase activity. This function depends on small molecules which bind and stabilize quadruplex structures *in vivo* (Gomez et al., 2003, Riou et al., 2003).

1.5.2 Protection from DNA Damage Response (DDR)

One of the key functions of telomeres is protect the chromosome termini from inappropriate DNA damage repair and distinguish them from DNA double strand breaks. Two members of the shelterin complex, TRF2 and POT1, play a major role in the interaction of telomeres with the DNA damage response (DDR). For example, the expression of a dominant-negative mutant of TRF2 results in the recognition of telomeres as DNA double strand breaks which in turn leads to the activation of the ATM/p53 damage response pathway (Karlseder et al., 1999, van Steensel et al., 1998). TRF2 is also thought to be capable to directly inhibit the autophosphorylation and self-activation of ATM and thereby abrogating the ATM signalling pathway (Bradshaw et al., 2005, Karlseder et al., 2004). Furthermore, the core shelterin components TRF2 and POT1, both repress DNA damage signalling pathways. The two proteins act independently from each other. TRF2 prevents the activation of ATM kinase, whereas POT1 represses ATR (Denchi and de Lange, 2007). However proteins which are

involved in the detection of DNA damage, DNA damage repair and DDR signalling also localise to functional telomeres. Recent studies have shown that functional telomeres require the DDR machinery for telomere replication (Denchi, 2009, Dimitrova and de Lange, 2009, Verdun et al., 2005, Zhu et al., 2000).

1.5.3 Telomeres in mitosis and meiosis

During meiosis, homologous chromosomes align with each other, recombine and synapse. In order to align with each other, chromosomes attach to the nuclear envelop (NE) and cluster to form a structure which resembles a bouquet of flowers. The "bouquet" formation process has been observed in nearly all eukaryotes except *Caenorhabditis elegans* and *Drosophila* (Dernburg et al., 1995, McKee, 2004, Scherthan, 2001). Observations in maize, human and mice indicated that telomeres attach randomly to the NE during leptotene and move around the NE until they approach each other (Bass et al., 1997, Scherthan et al., 1996). The process appears to be a highly active mechanism which is tightly regulated and is switched off in early pachytene. It has been assumed that the bouquet formation assists the efficiency of meiotic prophase (Harper et al., 2004). In human cells, it appears that that tethering of the chromosome termini to the nuclear envelop is dependent on the two TRF proteins (Luderus et al., 1996).

Meiosis is separated in different stages. In the first stage called lepotene, the de-condensed clouds of chromatin are organised into long thin fibres. At the end of leptotene or the beginning of zygotene, telomeres attach to the NE and cluster together forming the bouquet. During the zygotene stage, homologous chromosomes begin to associate tightly along their length or synapse when the central element of the synatonemal complex is installed. The bouquet formation is perpetuated throughout the zygotene phase and into early pachytene. By mid-pachytene, synatonemal complex formation is complete and meiotic recombination between homologes is resolved. The telomeres are no longer clustered. After the bouquet is dispersed, the cells continue through diplotene, when the synatonemal complex disassembles and chiasmata, which

hold the homologous together until anaphase I, become visible. In diakinesis, the chromosome under go a final stage of chromosome condensation just before NE breakdown and the initiation of metaphase (Harper et al., 2004).

1.6 Telomere dynamics in somatic cells

A majority of eukaryotic somatic cells do not express telomerase and divide only a finite number of times (Hayflick limit) before entering a non-dividing nevertheless biologically active growth arrest known as replicative senescence (RS) (Allsopp et al., 1995, Hayflick, 1965). The Hayflick limit is dependent on telomere length and therefore cells with longer telomeres have a larger replicative capacity compared to cells with shorter telomeres (Allsopp et al., 1992). The telomeric loss of 50 – 200 bp with each cell division cycle is progressive and is thought to be a consequence of the end replication problem (Baird et al., 2003, Harley et al., 1990, Henderson et al., 1996). This gradual attrition of telomeric DNA acts as an intrinsic mechanism to count cell division and is therefore thought to be a benchmark for cellular aging. The introduction of active telomerase can reverse the end replication problem, avoid the onset of replicative senescence and extend the replicative capacity of cells indefinitely (Bodnar et al., 1998). In somatic cells, the eroding telomeres gradually loose their telomeric function, until a small subset of short telomeres triggers a DNA damage response and replicative senescence is induced (Hemann et al., 2001a, Hemann et al., 2001b, Martens et al., 2000). Replicative senescence is thought to be a potent tumour suppressor mechanism in young cells providing a barrier to unlimited cell proliferation. However new evidence shows that accumulation of senescent cells in aging tissue can induce cancer progression (Campisi and d'Adda di Fagagna, 2007).

1.6.1 The End Replication Problem

Following the discovery of the DNA replication mechanism and the fact that the discontinuous or lagging strand requires a RNA-DNA primer to initiate 5 to 3′ replication, a problem with the semi-conservative replication of linear DNA at the chromosomal termini became apparent (Olovnikov, 1971). Whereas the leading strand is continuously replicated in a 5′ to 3′ direction after the firing of the replication origin, the delayed synthesis of the lagging strand occurs in short defined Okazaki fragments (50-150 nt). A DNA polymerase α/primase complex synthesises a RNA-DNA primer (40 nt, including 10 nt of RNA) generating a free 3 -OH group which provides the basis for 5 to 3′ elongation through DNA polymerase δ. The synthesis of a new Okazaki fragment is discontinued after pol δ complex reaches the previous Okazaki fragment. In order to produce a continuous DNA strand, two nucleases, RNase HI and FEN1, completely remove the initial RNA primer and after filling the small gap between the two fragments, the two matured Okazaki fragments are joined by DNA ligase I (Waga and Stillman, 1998). However, at the end of the chromosome, the removal of the RNA primer from the lagging strand creates an unfilled gap ranging in size from a single RNA primer to a complete Okazaki fragment (10 - 150 nt). In consequence the truncated lagging strand would drive a gradual shortening of the chromosome end with each successive replication cycle. The deliberation was termed the end replication problem (Fig 1.3).

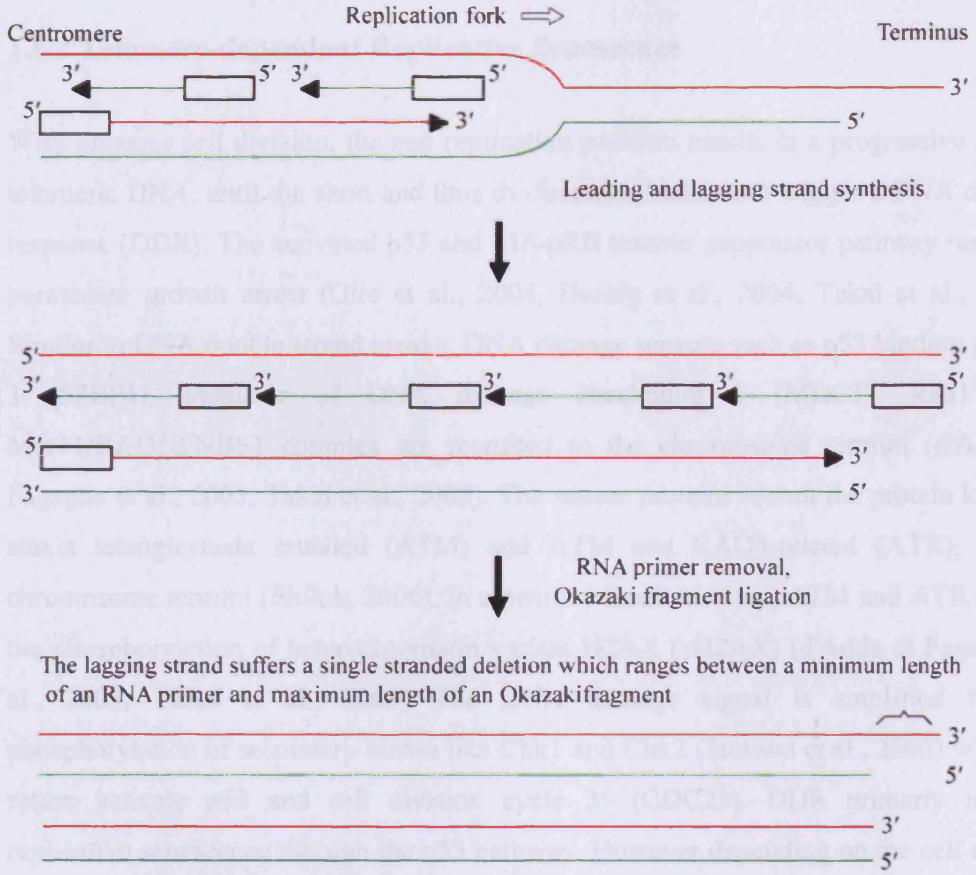

Figure 1.3 End replication problem (modified from Baird 2007)

1.6.2 Telomere-dependant Replicative Senescence

With ongoing cell division, the end replication problem results in a progressive loss of telomeric DNA, until the short and thus dysfunctional telomeres trigger a DNA damage response (DDR). The activated p53 and p16-pRB tumour suppressor pathway results in permanent growth arrest (Gire et al., 2004, Herbig et al., 2004, Takai et al., 2003). Similar to DNA double strand breaks, DNA damage sensors such as p53 binding protein 1 (53BP1), mediator of DNA damage checkpoint 1 (MDC1), Rad17 and Mre11/RAD50/NBS1 complex are recruited to the chromosome termini (d'Adda di Fagagna et al., 2003, Takai et al., 2003). The sensor proteins recruit the protein kinases, ataxia telangiectasia mutated (ATM) and ATM and RAD3-related (ATR), to the chromosome termini (Shiloh, 2006). In a positive feedback loop, ATM and ATR trigger the phosphorylation of heterochromatin variant H2AX (γH2AX) (d'Adda di Fagagna et al., 2003, Takai et al., 2003) The DNA damage signal is amplified by the phosphorylation of secondary kinase like Chk1 and Chk2 (Jackson et al., 2002) which in return activate p53 and cell division cycle 25 (CDC25). DDR primarly induces replicative senescence through the p53 pathway. However depending on the cell type or species, DDR can also permanently arrest cells through the p16-pRB pathway (Campisi and d'Adda di Fagagna, 2007).

1.6.3 Telomere-independent Replicative Senescence

Telomere erosion is not the sole cause of replicative senescence. Also oxidative stress, DNA damaging agents and oncogene over expression can induce premature replicative senescence and thereby limit the replicative lifespan of human fibroblasts significantly (Dumont et al., 2000, Robles and Adami, 1998, Serrano et al., 1997). Replicative senescence caused by the end replication problem can be circumvented by the ectopic expression of TERT, the catalytic protein component of human telomerase (Bodnar et al., 1998). However telomerase can not prevent replicative senescence caused by other senescence inducers (Campisi and d'Adda di Fagagna, 2007, Chen et al., 2001).

Accumulation of DNA damage causes many cell types to undergo senescence (Di Leonardo et al., 1994, Parrinello et al., 2003). Like telomere dependent senescence, DNA damage induced sensences relies on p53 and are usually accompanied by expression of p21 (Di Leonardo et al., 1994, Herbig et al., 2004). This gave rise to the hypothesis that DNA damage inducing chemotherapy might cause senescence in tumour cells. However, tumour cells with functional p53 are more likely to senesce than the ones with mutated p53, at least in cell culture or cancer-prone mouse models (Roberson et al., 2005, Schmitt et al., 2002).

The forced over-expression of active oncogenes in normal cell leads to premature senescence. The transformation of human primary cells with ras, a cytoplasmic transducer of mitogenic signals results in an early onset of cellular senescence (Serrano et al., 1997). Similar results were achieved following the over-expression of other members of the ras signalling pathway (Lin et al., 1998, Michaloglou et al., 2005, Zhu et al., 1998) and the proliferative nuclear proteins like E2F-1 (Dimri et al., 2000). Since oncogenes like member of the ras signalling pathway stimulate cell growth and therefore can drive uncontrolled cell proliferation, it is assumed that oncogene induced senescence evolved as a tumour suppressor mechanism, preventing tumourgenesis (Braig and Schmitt, 2006). Similar to telomere-dependent senescence, oncogene-induced senescence elicits a DNA damage response (DDR). However, DDR plays a significant role in initiation and maintaining oncogene-induced senescence, since down-regulation of DDR components results in cell proliferation and oncogenic transformation (Di Micco et al., 2006).

1.7 Telomeric Elongation

1.7.1 Telomerase

Telomerase is a ribonucleoprotein reverse transcriptase (RT) that synthesises telomeric repeats in germline cells and cancer cells. Like telomeric repeats, telomerase was first identified in *Tetrahymena thermophilia* (Greider and Blackburn, 1985). Since then telomerase activity has been detected in protozoa (Shippen-Lentz and Blackburn, 1989, Zahler and Prescott, 1988), in fungi (Cohn and Blackburn, 1995, Lingner et al., 1997) and mammals (Morin, 1989, Prowse et al., 1993).

Active human telomerase consist out of 3 core elements, the telomerase RNA component (TERC), the reverse transcriptase telomerase (TERT) and the TERC-binding protein dyskerin (DKC1) (Fig 1.4). In addition to the core elements, several species-specific accessory proteins are associated with active telomerase forming a holoenzyme. These species-specific accessory proteins control the biogenesis, cellular localisation and function of telomerase (Wyatt et al.). Amongst these proteins in humans are the two NTPase proteins NHP2 and NOP10; the two closely related ATPases potin and reptin; and TCAB1 (telomerase Cajal body protein 1) (Cohen et al., 2007, Fu and Collins, 2007, Venteicher et al., 2009, Venteicher et al., 2008).

Dyskerin is a putative pseudouridine synthase, which also recognizes the H/ACA sequence motif. This motif can be found in TERC (Mitchell et al., 1999). Dyskerin functions to support telomerase biogenesis and TERC stability (Mitchell et al., 1999). Recent reports indicate that dyskerin, NHP2 and NOP10 are necessary for the accumulation and stabilisation of TERC (Fu and Collins, 2007). Pontin interacts directly with both TERT and dyskerin. The amount of TERT bound to pontin and reptin peaks in S phase, providing evidence for cell-cycle-dependent regulation of TERT. Depletion of pontin and reptin markedly impairs TERT accumulation, indicating an essential role in telomerase assembly. These findings suggest an alternative approaches for inhibiting

telomerase in cancer (Venteicher et al., 2008). The depletion of TCAB1 by using RNA interference prevents TERC from associating with Cajal bodies, disrupts telomerase-telomere association, and abrogates telomere synthesis by telomerase. Thus, TCAB1 controls telomerase trafficking and is required for telomere synthesis in human cancer cells (Venteicher et al., 2009).

Telomerase is stringently repressed in the majority of somatic cells with the exception of a low activity level in S-phase, which may participate in the maintenance of the telomeric overhang in normal human cells (Dionne and Wellinger, 1998). In contrast to normal human cells, 90% of all human cancer display telomerase re-activation (Broccoli et al., 1997, Broccoli et al., 1995, Kim et al., 1995). TERC is constitutively expressed in all types of tissue, whereas the expression of hTERT is a highly regulated (Kolquist et al., 1998, Masutomi and Hahn, 2003). However, the level of telomerase activity and telomere length is not related to the expression levels of hTERC and hTERT (Swiggers et al., 2004). Telomerase elongates telomeres by catalysing multiple rounds of copying its own RNA template. In the first step, the telomere RNA template anneals to the free 3' end of the DNA substrate. In the second step, new nucleotides are added to the DNA substrate until the '5end of the template sequence is reached. In the final step, telomerase relocates and realigns to the newly synthesised '3end where the next round of telomere synthesis is initiated (Greider and Blackburn, 1996, Wyatt et al.).

a)

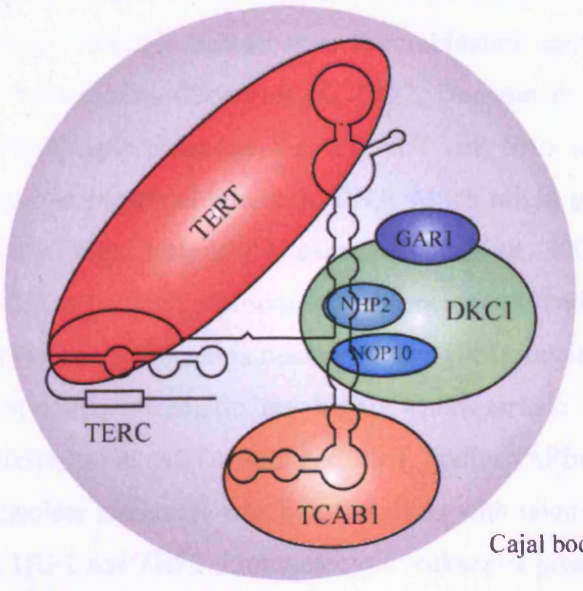

b)

Figure 1.4 Telomerase. a) telomerase holoenzyme in a Cajal body outside of S phase (modified from Venteicher 2009). b)

1.7.2 Alternative Lengthening of Telomeres (ALT)

Alternative lengthening of telomeres (ALT) has been described in 15% of all human cancers, where telomerase activity is un-detectable. Telomere length maintenance in these cancers occurs through homologous recombination and the mis-regulation of normal telomere homeostasis (Bryan et al., 1997, Dunham et al., 2000, Muntoni and Reddel, 2005). Phenotypic characteristics of ALT cell lines and tumours include an abundance of extrachromosomal telomeric DNA which might presents itself as double-stranded telomeric circles (t-circles) (Cesare and Griffith, 2004, Wang et al., 2004). Telomeric DNA (either extrachromosomal or chromosomal) and associated proteins can be found in promyelocytic leukaemia nuclear bodies (PML nuclear bodies). PML bodies which contain telomeric chromatin are highly characteristic for ALT cells and are therefore also referred to as ALT-associated PML bodies (APBs) (Yeager et al., 1999). APBs are large nuclear structures which co-localises with telomeric DNA and telomere binding proteins TRF1 and TRF2. Promyelocytic leukaemia proteins are essential for the accumulation of p53 in response to DNA damage. These proteins display a neutralizing effect on the negative p53 regulator Mdm2 (Louria-Hayon et al., 2003). APBs also contain replicative factor A, RAD51, RAD52 and the MRN complex, all proteins involved in DNA synthesis and recombination (Wu et al., 2000, Yeager et al., 1999, Zhu et al., 2000). APBs might drive the homologous recombination resulting in ALT, although there is still a debate of APBs exact function.

1.8 Telomeres and Disease

Telomere dysfunction can lead to genomic instability. Direct evidence has been observed in telomerase deficient p53 mutant mice. Telomere erosion in ageing telomerase-deficient p53 mutant mice results in repetitive cycles of fusion-bridge breakage and consequently leads to the formation of complex non-reciprocal translocations. This process facilitates the progression of epithelial cancers (Artandi et al., 2000). Furthermore, severe chromosomal instability, as a result of non-functional

telomeres, promotes secondary genetic changes which in turn promote carcinogenesis (Artandi and DePinho, 2000b). Some genomic instability syndromes are caused by mutated genes which directly interfere with telomere dynamics. The resulting telomere instability has a major effect upon the integrity of the chromosome. However, in most cases, it is not entirely clear how the mutated gene interferes with telomere biology.

1.8.1 Cancer

A cancer cell is described as a cell which grows out of control, ignoring signals to stop dividing and is unable to recognize its own natural boundaries. Cancer progression is thought to be a somatic evolution, in which certain mutagens give rise to a cell which has selective proliferative advantages (Cahill et al., 1999). Current opinion states that most cancers derive from rare stem cells that are able to proliferate indefinitely. These stem cells promote carcinogenesis through improper homeostatic mechanisms that govern tissue repair and stem cell self-renewal (Beachy et al., 2004, Reya et al., 2001). Telomerase negative cells lose their telomeric function due to the gradual attrition of their telomeres which results in non-reciprocal translocations and chromosomal fusion events. These cells may evade replicative senescence by circumventing the p53 and pRB checkpoints and therefore driving the formation of cancer (Artandi and DePinho, 2000a, Chin et al., 1999, Hara et al., 1991).

Most cancer cells and tumours maintain their telomere length through re-activation of telomerase (Holt and Shay, 1999, Kim et al., 1994, Shay and Bacchetti, 1997). The expression of the hTERC and hTERT telomerase subunits is up regulated in almost all human malignant tumours. Therefore, telomerase activity is a significant indicator of outcome and progression of cancer (Hiyama and Hiyama, 2002, Hiyama et al., 2004, Keith, 2003). Subsequently telomerase is a prime target for developing anti-cancer therapies (Keith et al., 2004).

In contrast to the cancers types which avoid senescence via activation of telomerase, 15% of all human cancers maintain their telomere length by one or more mechanisms

named alternative lengthening of telomeres (ALT) (Bryan et al., 1997, Dunham et al., 2000, Muntoni and Reddel, 2005). ALT is predominant in tumours of mesenchymal origin indicating a tendency of mesenchymal stem cells to activate ALT (Lafferty-Whyte et al., 2009). Other tumours types display ALT include glioblastoma multiform (most common form of malignant brain tumour in adults), osteosarcoma and some type of soft tissue sarcoma (Cesare and Reddel, 2010).

Telomerase activity alone does not always immortalise cells (Kiyono et al., 1998). For many cancers, telomerase re-activation is a late stage event. The exact contribution of telomerase to cancer development and progression, apart from telomere maintenance, is not clearly defined (Blasco and Hahn, 2003).

1.8.2 Telomere Dysfunction in Disease

1.8.2.1 Dyskeratosis Congenita

Dyskeratosis Congenita (DC) is an inherited disease which is characterised by abnormal skin pigmentation, bone marrow failure, nail dystrophy and leucoplakia (Marrone and Mason, 2003, Mason, 2003). Two distinct types of dyskeratosis congenita have been observed; X-linked recessive DC and autosome dominant DC. The X-linked form is linked to mutations in the DKC1 gene at Xq28. The encoded protein, dyskerin, is associated with a sub group of both small nucleolar RNAs and the RNA component of the telomerase complex (TERC) (Mitchell et al., 1999). The autosomal dominant form of the disease is caused by mutations in TERC itself (Vulliamy et al., 2001), in the catalytic subunit of telomerase TERT (Vulliamy et al., 2005) and in the member of the shelterin complex TIN2 (Savage et al., 2008). Both dyskeratosis congenital forms feature short dysfunctional telomeres.

1.8.1.2 Bloom's Syndrome

Bloom's syndrome (BS) is an autosomal recessive disorder and is characterized by stunted growth, sun sensitive telangiectasia skin, severe impaired immune response and a predisposition to cancer (Bloom, 1954). Cellular key features of BS patients are very high levels of sister chromatide exchange (SCE) after treatment with DNA damaging agents (German et al., 1977) and symmetrical quadriradials, chromosomal re-arrangements between homologous chromosomes at homologous sites (German et al., 1965). The affected protein in BS is a RecQ ATP-dependent DNA helicase (Ellis et al., 1995, Karow et al., 1997). The BLM helicase is involved in homologous recombination, Holliday branch migration and is essential for genome stability (Karow et al., 2000, Wu et al., 2001). POT1 stimulates WRN and BLM to unwind long telomeric duplexes and D-loop structures. This suggests that the two helicases are involved in resolving of telomeres and possibly protecting the free 3′ overhang during the DNA unwinding (Opresko et al., 2005). BLM co-localises with TRF2 in ALT. cells suggesting a possible role for BLM in ALT telomere maintenance (Lillard-Wetherell et al., 2004).

1.8.2.3 Ataxia Telangiectasia

Ataxia Telangiectasia (AT) is a rare recessive disease caused by mutations in the ataxia telangiectasia mutated (ATM) gene on chromosome 11q22 (Savitsky et al., 1995). The clinical symptoms include progressive neurodegenerative dysfunction, immunodeficiency, radiation sensitivity, ocular telangiectasia, hypogonadism, genome instability and a predisposition to cancer (Kastan and Lim, 2000, Lavin and Shiloh, 1997, Meyn, 1999, Savitsky et al., 1995). Furthermore, patients with AT have a short stature and display signs of premature aging such as grey hair, wrinkled skin, skin atrophy and sclerosis (Lavin and Shiloh, 1997, Savitsky et al., 1995). The ATM kinase is involved in mitogenic signal transduction, cell cycle control and DNA damage response (Hoekstra, 1997, Kastan and Lim, 2000). AT patients appear to have accelerated telomere attrition as well as an elevated number of chromosomal fusion events (Metcalfe

et al., 1996). Fibroblasts derived from patients with AT undergo early senescence and are sensitive to oxidative stress (Tchirkov and Lansdorp, 2003).

1.8.1.4 Werner Syndrome

Werner Syndrome (WS) is an autosomal recessive disease caused by mutations in the WRN gene located on chromosome 8p (Yu et al., 1996). Clinical features of WS include cataract skin atrophy, soft tissue calcifications, type II diabetes, atherosclerosis and osteoporosis, all indicators of old age (Martin, 1982). In addition, WS is associated with genomic instability and an early onset of cancer (Davis and Kipling, 2009). In line with the premature aging, 90% of all WS cells prematurely senescence (Tollefsbol and Cohen, 1984). Initially this was thought to be a consequence of accelerated telomere attrition (Faragher et al., 1993, Schulz et al., 1996), However STELA analysis of clonal WS cultures disproved this hypothesis, showing that WS fibroblast erode at similar rates then normal fibroblasts (Baird et al., 2004). The reason why WS fibroblasts display an attenuated replicative capacity is not understood so far, but may involve replicative stress (Davis et al., 2005). WS cells tend to develop chromosomal rearrangements including translocations, inversions, and deletion (Salk, 1982). Furthermore, the cells display an increased frequency of chromosomal deletions (Fukuchi et al., 1989).

1.8.1.5 Idiopathic Pulmonary Fibrosis

Idiopathic pulmonary fibrosis (IPF) is a normally fatal lung disorder with a so far unknown pathogenetic mechanism. Its main symptom is progressive scarring (fibrosis) of the supporting framework of both lungs, which results in an irreversible destruction of the lung's architecture (Selman and Pardo, 2002). The disease appears to be age related, with most cases diagnosed in patients older than 50. IPF is caused by heterozygous mutations in TERT or TERC which result in short telomeres (Alder et al., 2008, Armanios et al., 2007).

1.9 DNA Repair Mechanism

DNA double strand breaks (DBSs) and single-strand breaks (SSBs) are an every day occurrence in primary human fibroblasts caused by ionising radiation, ultraviolet light, reactive oxygen species, errors during DNA replication, enzymes during meiosis and V(D)J recombination. The repair of these DSBs and SSBs is essential to maintain genomic fidelity and stability. In order to combat DBSs and SSBs, cells have developed multiple distinct DNA repair mechanisms which detect damaged DNA, signal its presence and promote the repair of the damage (Jackson and Bartek, 2009, Weterings and Chen, 2008). One of these mechanisms is base excision repair (BER). BER is a multi-step process that corrects non-bulky damage to bases resulting from oxidation, methylation, deamination, or spontaneous loss of the DNA base itself. In BER, DNA glycosylase recognises the damaged base and mediates base removal before proliferating cell nuclear antigen (PCNA), polymerase β and DNA ligase I or DNA Ligase III complete the repair process (Jackson and Bartek, 2009, David et al., 2007, Hoeijmakers, 2001). Nucleotide excision repair (NER) is perhaps the most flexible of the DNA repair pathways. NER recognises and repairs lesions which are caused by helical distortion of the DNA duplex and pyrimidine dimers (cyclobutane pyrimidine dimers and 6-4 photoproducts) which are caused by the UV component of sunlight. Other NER substrates include bulky chemical adducts, DNA intrastrand crosslinks, and some forms of oxidative damage. Two distinct NER pathways exist: transcription-coupled NER which focuses on lesion blocking transcriptions and global genome NER which surveys the entire genome for distorting damage (Jackson and Bartek, 2009, David et al., 2007, Hoeijmakers, 2001, Loeb and Monnat, 2008). DNA mismatch repair (MMR) pathway plays an essential role in the correction of replication mistakes such as base-base mismatches resulting from errors of DNA polymerases which escaped the proof reading function and insertion/deletion loops caused by template slippage. Mutations in several human MMR genes can cause a predisposition to hereditary nonpolyposis colorectal carcinoma (HNPCC), as well as a variety of sporadic tumours that display microsatellite instability (Jackson and Bartek, 2009, David et al., 2007, Hoeijmakers, 2001, Loeb and Monnat, 2008, Jiricny, 2006).

In eukaryotes, DSBs are repaired by either homologous recombination (HR) or non-homologous end joining (NHEJ). Both pathways require the MRN complex to bind to unprocessed DNA breaks, tethering the ends and aligning them for DSB repair (Williams et al., 2008). The error-free HR is limited to late S and G2 phase and utilises homologous repeat sequences like the sister chromatids to repair DNA damage. NHEJ-mediated DNA repair is relatively error-prone and is composed of two distinct pathways termed classic NHEJ (C-NHEJ) and alternative NHEJ (A-NHEJ). C-NHEJ can be observed throughout the cell cycle and is dependent on Ku70/80 and DNA Ligase IV/XRCC4. In contrast, A-NHEJ is associated with G2 phase and requires PARP1 and DNA ligase III/XRCC1 or DNA ligase I (San Filippo et al., 2008, Weterings and Chen, 2008)(Fig 1.5).

1.9.1 Homologous Recombination

Homologous recombination (HR) is a very accurate DNA repair mechanism and is restricted to the S and G2 phase of the cell cycle (Hartlerode and Scully, 2009). HR is initiated after a DSB has appeared. After the DSB formation, the DNA ends are processed by nucleolytic resection to give single-strand tails with free 3′-OH ends. These ends become the substrate for the HR protein machinery in order to form the recombinase filament on the single stranded DNA end. After a successful homology search, strand invasion occurs to form a nascent D-loop intermediate. DNA polymerase synthesizes new DNA and thereby extents from the 3′ end of the invading strand. The second DSB is captured to form a D-loop intermediate, which contains two crossed strands or Holliday junctions. The reaction is completed by gap-filling DNA synthesis and ligation. Finally Holliday junctions are resolved to give a crossover and non-crossover product (Fig. 1.5 A) (Weterings and Chen, 2008, Rass et al., 2010).

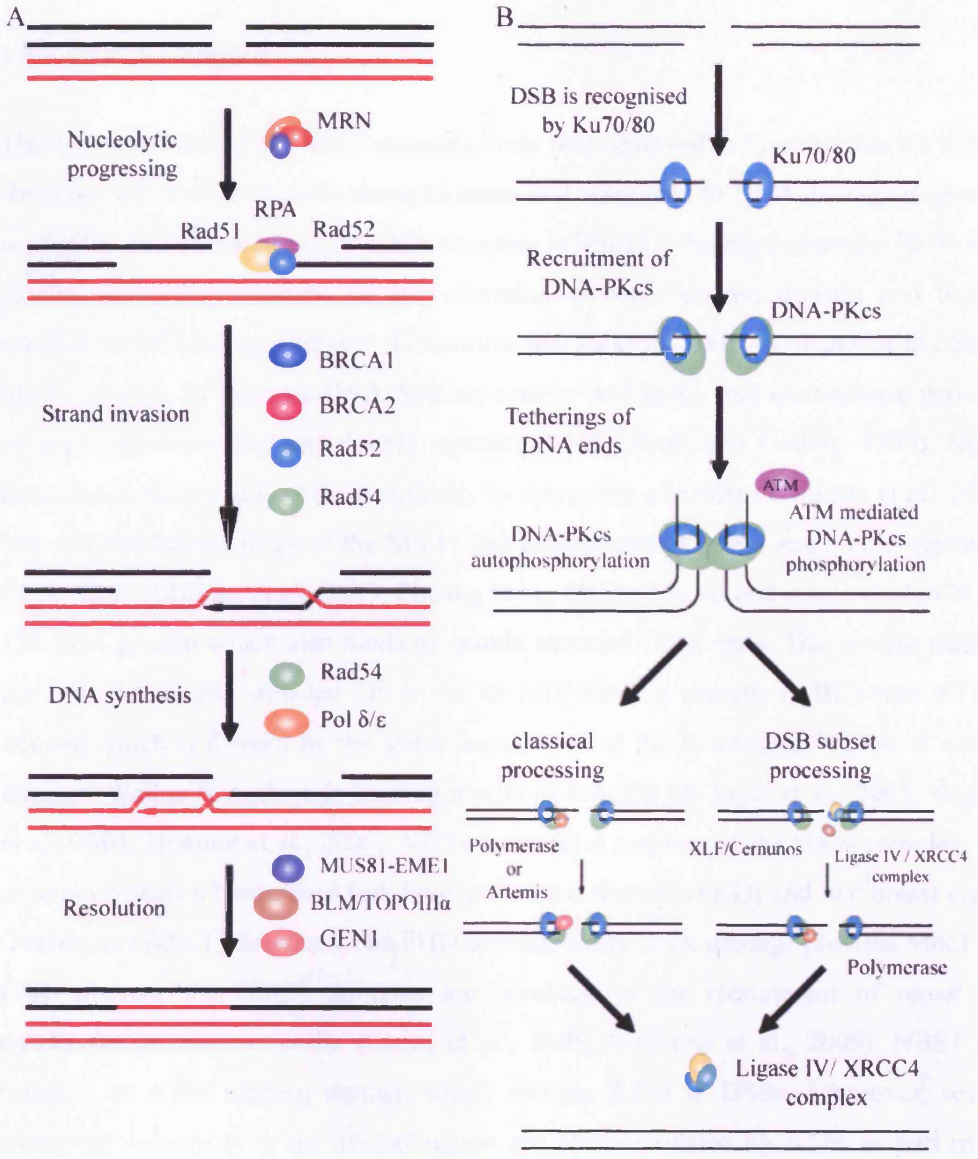

Figure 1.5 Overview of homologous recombination (HR) and non-homologous end-joining (NHEJ) A) HR B) NHEJ (Adapted from Weterings & Chen 2008, Rass et al 2010)

1.9.1.1 MRN Complex

The three members of the MRN complex were first observed in *S. cerevisiae* via screens for genes involved in meiotic recombination and resistance to DNA damage (Ogawa et al., 1995). The first member of MRN complex is Mre11, a highly conserved 70-90 kDA protein which is composed of an N-terminal phosphoesterase domain and two C-terminal DNA-binding domains (D'Amours and Jackson, 2002, Williams et al., 2007). Mre11 possess an intrinsic DNA binding activity and endo- and exonuclease activities against single-stranded and double stranded DNA (Paull and Gellert, 1999). Mre11 forms homodimers and binds specifically to open ends of DSBs (Williams et al., 2008). The endonuclease activity of the Mre11 has been observed in HR and NHEJ-dependent DNA repair (Milman et al., 2009, Zhuang et al., 2009). The second member, Rad50, is a 150 kDA protein which also binds to double stranded DNA ends. The protein partially unwinds the double stranded DNA via its ATP-binding cassette (ABC)-type ATPase domain which is formed by the stable association of the N-terminal Walker A and C-terminal Walker B nucleotide binding motifs of RAD50 (de Jager et al., 2001, Hopfner et al., 2001, Hopfner et al., 2000). NBS1 is the third member of the MRN complex. The protein contains a N-terminal fork head associated domain (FHD) and two breast cancer C-terminal (BRCT) domains. The FHD domain binds DNA damage proteins Mdc1 and Ctp1 whereas the BRCT domains are involved in the recruitment of repair and checkpoint proteins to DSBs (Lloyd et al., 2009, Williams et al., 2009). NBS1 also contains an ATM binding domain which recruits ATM to DSBs. Moreover, several conserved sequences in the central region are phosphorylated by ATM as part of the DNA damage response (Falck et al., 2005, You and Bailis, 2010). Mre11, RAD50 and NBS1/Xrs2 were shown to interact physically with each other (Trujillo et al., 1998). Each subunit of the Mre11 dimer binds one Rad50 molecule creating the $Mre11_2Rad50_2$ core of the MRN complex (de Jager et al., 2001, Hopfner et al., 2001). The $Mre11_2Rad50_2$ core complex is recruited to the end of double stranded DNA and its coiled-coil arms tether the DNA termini together. This function depends on the protein concentration. It is believed that the Mre11 dimer facilitates short-range interaction while Rad50 enables long-range tethering of DNA ends (Hopfner et al., 2002, Williams

et al., 2008). NBS1 interacts with Mre11 and is responsible for the translocation of the $Mre11_2Rad50_2$ complex from the cytoplasm into the nucleus (Desai-Mehta et al., 2001, Williams et al., 2009).

The MRN complex has multiple roles in DNA damage repair, checkpoint activation, telomere maintenance, meiosis and DNA replication. Firstly, MRN acts as an early sensor on DSBs in the DNA damage response activating the signal transduction cascades that lead to cell cycle checkpoints (Petrini and Stracker, 2003). Furthermore the MRN complex in association with other proteins like CtIP shifts the DNA damage sensing to DNA repair (You and Bailis, 2010). In addition, the MRN complex plays a pivotal role in telomere maintenance. Both Mre11 and NBS1 sequester at telomeres in meiotic human fibroblasts. The MRN complex associates with TRF2 though out the cell cycle, where as NBS1 only accumulates at telomeres in S-phase (Lombard and Guarente, 2000, Verdun et al., 2005, Zhu et al., 2000). Further investigation showed that knockdown of Mre11 or NBS1 reduces the length of the 3′ G-overhangs of telomeres, demonstrating that MRN can promote telomere function by recruiting telomerase to fully capped telomeres (Verdun et al., 2005, Zhu et al., 2000). On the other hand, several report showed that the MRN complex can prevent the fusion of newly replicated telomeres by activating the ATM signalling in order to induce a DNA damage response (Attwooll et al., 2009, Dimitrova and de Lange, 2009, Deng et al., 2009). Moreover, studies of dysfunctional telomeres following the abolishment of TRF2 have revealed that depending on the stage of the cell cycle, MRN can either promote or suppress NHEJ-mediated fusion of short dysfunctional telomeres (Deng et al., 2009, Dimitrova and de Lange, 2009).

1.9.2 Classic Non-homologous End Joining (C-NHEJ)

The core elements in mammalian classic NHEJ are the heterodimer Ku70/80, the catalytic subunit of DNA-dependent protein kinase (DNA-Pk_{cs}), and the DNA Ligase IV – XRCC4 complex. The mechanism for C-NHEJ is presented in Fig 1.5 B. C-NHEJ is initiated by the binding of the Ku70/80 heterodimer to two broken ends of the DSB. The two Ku heterodimers are presumed to provide a scaffold for the members of C-NHEJ

and thereby allowing the modification of both DNA ends in preparation for joining. The two Ku proteins in turn recruit DNA-PK_{cs}, thus linking the two DNA ends and thereby forming the active DNA-PK complex. Active DNA-PK interacts with different nucleases and polymerases and starts DNA processing by phosphorylating several proteins like Ku and itself. In a final step, the DNA ligase IV/XRCC4 complex is recruited, further stabilising the broken DNA ends and finally mediating the rejoining of the modified break side. The recently discovered XLF/Cernunnos protein is thought to enhance the ligation process (Lieber, 2010, Lieber, 2008, Weterings and Chen, 2008).

1.9.2.1 Ku 70/80 Heterodimer

The Ku 70/80 heterodimer was first identified in patients suffering from polymyositis-scleroderma overlap syndrome, The Ku complex is one of the most abundant nuclear proteins and is formed by Ku70 and Ku 80 subunits (Ma et al., 2005, Mimori et al., 1981). The Ku heterodimer has roles in DNA replication, transcription regulation and telomere maintenance (Cohen et al., 2004, Sawada et al., 2003). Ku70/80 is one of the core components of the C-NHEJ repair pathway. The protein complex displays a strong binding affinity to double stranded DNA. It binds to blunt ends, to 5′ and 3′ single stranded overhangs or to hairpin structures (Arosio et al., 2002, Dynan and Yoo, 1998).

Ku70 and Ku80 proteins share a similar structure. Both contain a N-terminal α/β domain, a central β-barrel domain and a helical C-terminus arm. The central β-barrel domains of the two proteins form a double ring which encircles the DNA molecule. The N-terminal and C-terminal domains of Ku70 and Ku80 for binding of other DNA repair proteins (Walker et al., 2001).

In classic NHEJ, Ku70/80 is implicated to be involved in strand alignment and synapsis, suppression of exonuclease resection, end ligation and the recruitment of further DNA processing factors. The Ku complex initiates C-NHEJ by the binding to two broken ends of the DSB (Lieber et al., 2003, Ma et al., 2005). Furthermore, the Ku70/80 heteromer contributes to protecting DSBs from nucleolytic processing. Several reports have shown

that the absence of functional Ku70/80 leads to excessive end processing resulting in the deletion of large segments of DNA (Boulton and Jackson, 1996, Feldmann et al., 2000, Li and Comai, 2002). Besides, it has been reported, the Ku complex might also encourage break ligation by on the one hand sterically aligning the two DNA ends (Kysela et al., 2003, Ramsden and Gellert, 1998) and on the other hand recruiting the DNA Ligase IV/XRCC4 complex (Chen et al., 2000, Nick McElhinny et al., 2000). In addition the Ku complex stimulates the association of polymerase μ and δ with DNA fragments. Both polymerases are implicated in gap filling during the alignment of DNA ends (Ma et al., 2004).

1.9.2.2 DNA-PK_{cs}

The DNA-dependent protein kinase catalytic subunit (DNA-PK_{cs}) is a member of the phosphoinositide-3-kinase-related family, which includes ATM and ATR DNA damage signalling proteins. The large protein kinase, consisting of 4128 amino acids (aa), has a molecular weight of 469 kDA (33, 85-87). DNA-PK_{cs} associates with the Ku70/80 heterodimer and forms a catalytic active DNA-PK holoenzyme (Falck et al., 2005). The kinase activity of DNA-PK_{cs} is activated upon interaction with a free DNA. The protein can bind to DNA fragments in absence of the Ku complex. However its kinase activity appears to be much lower (Hammarsten and Chu, 1998). DNA-PK_{cs} mediates the synapsis and ligation of the two DNA fragments (Block et al., 2004, DeFazio et al., 2002, Kysela et al., 2005). The auto-phosphorylation of DNA-PK_{cs} results in the remodelling of DNA-Pk (Block et al., 2004). Moreover, DNA-PK phosphorylates the histons H2AX and H1.This might indicate that DNA-PK modifies chromatin structure to facilitate the access of other DNA repair complexes to DSBs (Kysela et al., 2005).

1.9.2.3 Artemis

The endonuclease Artemis was first recognised as an essential factor in V(D)J recombination, stimulating the opening of hairpin structures (Moshous et al., 2001,

Rooney et al., 2002). However following the observation that Artemis deficiency leads to ionizing radiation (IR) sensitivity, it became apparent that Artemis might play a role in DSB repair (Ma et al., 2002). Purified Artemis protein displays single-strand-specific 5′ to 3′ exonuclease activity. Following the recruitment of Artemis to the DSB by DNA-PK_{cs}, Artemis acquires endonuclease activity on 5and 3′ overhangs, as well as hairpin structures (Ma et al., 2002). Furthermore, Artemis is phosphorylated by both the ATM kinase and to a minor extent by DNA-PK_{cs} kinase (Dahm, 2007). However it is not clear, if this phosphorylation of Artemis is essential for the activation of the endonuclease activity as observations are contradictory (Weterings and Chen, 2008).

1.9.2.4 DNA Ligase IV/XRCC4 complex

DNA Ligase IV and XRCC4 form a complex which is essential for C-NHEJ. The complex mediates the final ligation of the processed DNA ends (Lieber, 2010, Lieber, 2008, Weterings and Chen, 2008). DNA Ligase IV and XRCC4 deficiency is lethal in mice (Barnes 1998, Gao 1998). Crystallographic analysis of the DNA Ligase IV/XRCC4 complex revealed that one DNA Ligase IV protein binds to two XRCC4 proteins (Sibanda et al., 2001). XRCC4 is crucial for DNA Ligase IV activity as it stabilises the localisation of DNA Ligase IV at DSBs (Bryans et al., 1999, Chen et al., 2000, Costantini et al., 2007). Interaction between Ku70/80 and the DNA Ligase IV/XRCC4 complex is important for efficient NHEJ (Nick McElhinny et al., 2000). DNA-PK_{cs} also interacts with XRCC4, providing further stability to the ligation process (Chen et al., 2000, Costantini et al., 2007).

1.9.2.5 XLF/Cernunnos

XRCC4-like factor (XLF) or Cernunnos is the most recently identified component of C-NHEJ (Ahnesorg et al., 2006, Buck et al., 2006).The 33 kDa protein displays sequence and structural homology to XRCC4 (Andres et al., 2007). It is assumed that XLF/Cernunnos is recruited by the Ligase IV/XRCC4 complex to the DSB where it either enhances or modulates the efficiency of the ligation reaction (Ahnesorg et al.,

2006). Furthermore, the presence of XLF/Cernunnos facilitates the joining of mis-matched and non-cohesive DNA ends, thereby limiting the nucleotide loss through C-NHEJ (Ahnesorg et al., 2006, Tsai et al., 2007, Weterings and Chen, 2008).

1.9.3 Alternative Non-homologous End Joining (A-NHEJ)

Recent studies described an alternative non-homologous end-joining (NHEJ) pathway which is independent of DNA-PKcs and Ku70/80. Instead the pathway relies on poly(ADP-ribose) polymerase 1 (PARP-1) and XRCC1/DNA Ligase III complex (Audebert et al., 2004, Audebert et al., 2006, Wang et al., 2005). This slower back-up process (A-NHEJ) can be observed in wild-type cells and cells with defects in DNA-PK dependent NHEJ (C-NHEJ). The pathway utilizes microhomologies and is prone to missjoining (Roth and Wilson, 1986, Verkaik et al., 2002). In addition, the joining process is biased to a high G:C content at the joining point (Audebert et al., 2008).

1.9.3.1 PARP

Poly(ADP-ribose) polymerase 1 (PARP1) generates large chains of poly(ADP-ribose) (pADPr or PAR), a polymer composed of two ribose moieties and two phosphates. Poly(ADP-ribosyl)ation through PARP1 transfers ADP-ribose subunits from nicotinamide adenine dinucleotide (NAD^+) to target proteins forming long pADPr polymers (Kameshita et al., 1984, Rouleau et al., 2010).

The nuclear protein PARP1 is comprised of three functional domains. The N-terminal end contains a DNA-binding domain consisting of three zinc fingers of which two are essential for single stranded and double stranded DNA binding (Gradwohl et al., 1990, Hassa and Hottiger, 2008). The third one plays an important role in linking damage induced alterations in the DNA binding domain to changes in the PARP catalytic activity (Langelier et al., 2008, Tao et al., 2008). The central domain allows the auto-poly(ADP-ribosyl)ation of PARP1 (Altmeyer et al., 2009, Tao et al., 2009). It contains a

BRCA1 carboxy-terminal (BRCT) domain which can be found in many members of the DNA damage response pathway (Rouleau et al., 2010). The catalytic domain of PARP1 is located at the C-terminus, executing the poly(ADP-ribosyl)ation of target proteins (Kameshita et al., 1984).

Following the induction of DNA damage, PARP1 is rapidly recruited and starts immediately to transfer ADP-ribose subunits from NAD^+ to the receptor, thereby creating large pADPr chains (Haince et al., 2008, Hassa and Hottiger, 2008), However, most of the pADPr ribbons are attached to PARP1 itself. The pADPr polymers initiate the recruitment of other proteins to the DSB (Ahel et al., 2009, Kraus, 2009, Timinszky et al., 2009). Some of these proteins like XRCC1 bind directly to pADPr (Masson et al., 1998). Furthermore, the auto-poly(ADP-ribosyl)ation of PARP1 creates an auto-regulatory feedback loop as the synthesis of pADPr diminished the binding affinity of PARP for DNA. pADPr polymers provide a mechanism to remove PARP1 from the DSB allowing access of other DNA repair proteins and consequently inhibiting further poly(ADP-ribosyl)ation (Kraus, 2009, Satoh and Lindahl, 1992, Timinszky et al., 2009).

In addition to recognising DNA damage, PARP1 is involved in the rapid recruitment of MRN and ATM (Haince et al., 2007, Haince et al., 2008), indicating PARP1 is involved in HR, in NHEJ (Audebert et al., 2004, Veuger et al., 2004, Wang et al., 2004), in BER(Masson et al., 1998), and in the restarting of the replication fork (Bryant et al., 2009).

1.9.3.2 XRCC1

X-ray cross-complementing group 1 (XRCC1) is a 70 kDA protein which contains 3 domains: a C-terminal BRCT II domain, a central BRCT I domain and an N-terminal DNA binding domain. XRCC1 has no known enzymatic activity (Mani et al., 2004, Marintchev et al., 1999). The protein associates easily with nicked and gapped DNA, implying a role as a strand-break sensor (Mortusewicz and Leonhardt, 2007). These reports suggest that XRCC1 functions as a scaffold protein which is able to coordinate

and facilitate the steps of various DNA repair pathways (Mani et al., 2004, Mortusewicz and Leonhardt, 2007). XRCC1 binds to PNK and enhances its capacity for damage discrimination (Mani et al., 2007). Furthermore, the stabilization of DNA ligase IIIα is dependent on its interaction with the BRCT II domain of XRCC1 (Taylor et al., 1998). XRCC1 interacts with automodified PARP-1 (Masson et al., 1998) as does DNA ligase IIIα. This might provide another mechanism to recruit the XRCC1-ligase IIIα complex to sites of DNA damage (Thompson et al., 1982).

1.9.3.3 DNA Ligase III

Human DNA Ligase III functions in several different DNA repair pathways, including single-strand repair, base excision repair and nucleotide excision repair. More recent studies report that DNA Ligase III is also involve in an alternative NHEJ pathway (Moser et al., 2007, Wang et al., 2005, Wang et al., 2006). DNA Ligase III is the only DNA Ligase present in human mitochondria and provides all DNA repair and replication activities in this organelle (Bogenhagen et al., 2001, Lakshmipathy and Campbell, 2001). Moreover, DNA Ligase III contains a PARP-like zinc finger (ZnF) that increases the extent of DNA nick joining and intermolecular DNA ligation. This type of zinc finger is only present in DNA Ligase III and therefore distinguishes Ligase III from the other two mammalian DNA Ligases (Cotner-Gohara et al., 2008, Kulczyk et al., 2004, Mackey et al., 1999). DNA Ligase III deficiency in mice leads to early embryonic lethality (Puebla-Osorio et al., 2006).

1.9.3.5 DNA Ligase I

Members of the DNA Ligase I family can be found in all eukaryotes. In *Saccharomyes cerevisiae*, cell division cycle mutant cdc9 is defective in DNA Ligase I (Nasmyth, 1978). The temperature sensitive strain is both impaired for DNA replication and DNA damage repair (Johnson et al., 1979, Nasmyth, 1978). Human Ligase I and *S. cerevisiae* cdc9 only share 40% of homology; however both have similar functional domains. Both

contain a N-terminal DNA binding domain (DBD) and a conserved carboxyl-terminal catalytic core composed of a oligonucleotide binding (OB) fold and an adenylation domain (AdD). All three domains interact together to allow the flexible enzyme structure to completely engulf the DNA substrate (Barnes et al., 1990, Pascal et al., 2004). The N-terminal DBD contains a proliferating cell nuclear antigen (PCNA) binding site allowing the recruitment of DNA Ligase I to nicked DNA to initiate the final ligation step, thus sealing breaks in the phosphodiester bonds formation (Levin et al., 1997, Levin et al., 2000). Like all eukaryotic DNA ligases, DNA Ligase I is a nucleotidyltransferase (NTase) reviewed in (Martin and MacNeill, 2002). The ATP-dependent ligase interacts with members of the replication complex (Li et al., 1994) and catalyzes the joining of Okazaki fragments during lagging strands synthesis (Waga et al., 1994). In addition, DNA Ligase I ligates DNA nicks during base pair excision repair (BER) (Prasad et al., 1996).

1.10 This Work

Previous studies in our group have shown that short telomeres have the potential to undergo fusion with other short telomeres and thus increase the risk of genomic instability, a hallmark of cancer (Capper et al., 2007). Sequence analysis of fusions between short telomeres have identified a distinct mutational profile comprising large deletions into the telomere-adjacent DNA, short patches of microhomologies at the fusion point and low amount of TTAGGG repeats (Capper et al., 2007, Letsolo et al., 2009). This profile is consistent with MMEJ first described in *S. cerevisiae* (Ma et al., 2003) and an alternative NHEJ pathway in humans (Feldmann et al., 2000) which are both Ku independent. In contrast to fusion of critical short telomeres, the TRF2 knock down in embryonic mouse fibroblasts creates chromosomal fusion events which display several kilo bases of telomeric repeats at the fusion point and are dependent on DNA Ligase IV, Ku 70/80 and DNA PKcs, all components of C-NHEJ (Smogorzewska et al., 2002, van Steensel et al., 1998).

Since both mutational profiles indicate an aberrant DNA damage repair pathway driving chromosomal fusion events, the main focus of this study will be examine the possible pathways involved in the fusion of short dysfunctional telomeres. This will be done by generating short dysfunctional telomeres in patient derived cells which are deficient in DNA repair mechanisms. Furthermore, the direct sequencing of possible fusion events should clarify the role of different DNA repair proteins in the mechanistic basis of telomere fusion. The forced expression of human papillomavirus HPV16 E6E7 oncoproteins results in the abrogation of functional RB and p53 and thus allows cells to bypass senescence and continue to grow until crisis (Bond et al., 1999, Shay et al., 1993). By taking advantage of this fact and the unaltered telomere dynamics of the transformed cells, our group has previously shown that telomeres eroding beyond a certain threshold length undergo fusion (Capper et al., 2007).

Moreover, as STELA is a chromosome specific method to analyse telomeres, telomere dynamics of DNA repair deficient patient derived fibroblast cultures will be observed. In order to compare and consequently exclude the influence of oxidative stress from telomere dynamics, the fibroblast cultures are going to be cultured under physiological and normal oxygen culture conditions.

Chapter 2: Material and Methods

2.1 Tissue Culture

2.1.1 Cells

Ligase IV syndrome cells (GM17523 and GM16088), Ligase I deficient cells (GM16096), Nijmegen Breakage Syndrome (GM07166) were received from Coriell - Institute for Medical Research, Camden, New Jersey, USA. Fibroblast strains GM17523, GM16088, GM16096 and GM07166 were maintained in monolayer culture at 20% and 3% oxygen, re-fed once a week and re-seeded at a confluence of ~90%. For further details see table 2.1.

Human embryonic kidney cells HEK293 and the clonal derivative of MRC-5 E6E7 human diploid fibroblasts were described previously (Capper et al., 2007, Letsolo et al., 2009). Both cell lines were cultured in monolayer at 20% oxygen. The medium of MRC-5 E6E7 clone 1 and HEK293 cells was changed every 3-4 days and cells were passaged at a confluence of ~75%. For further details see table 2.1.

2.1.2 Medium and Inhibitors

All cells, except MRC-5 E6E7 and HEK293, were cultured in Eagle's minimum essential medium (EMEM, Invitrogen) supplemented with Earle's salts containing Sodium Bicarbonate (7.5% solution, Gibco), 2x nonessential amino acids (Sigma), 2x essential amino acids (Sigma), 2x vitamins (Sigma), 10% (v/v) fetal calf serum (Autogenbioclear), 1x 10^5 U/l penicillin, 100 mg/l streptomycin and 2mM glutamine (all Sigma). MRC-5 E6E7 clone 1 fibroblasts were cultured in EMEM (Invitrogen) supplemented with Earle's salts containing Sodium Bicarbonate (7.5% solution, Gibco), 2x nonessential amino acids (Sigma), 10% (v/v) fetal calf serum (Autogenbioclear),

Table 2.1 Cell lines

Name / ID	GM17523	GM16088	GM16096	GM07166	MRC-5 E6E7	HEK293
Description	LIG4 Syndrome	LIG4 Syndrome	Ligase I, DNA, ATP-dependent LIG1	Nijmegen breakage syndrome		
Cell Type	fibroblast	fibroblast	fibroblast	fibroblast	fibroblast	epithelial
Tissue Type	Skin	Skin	Skin	/	Lung	Kidney
Species	Homo sapiens	Homo sapiens	Homo sapiens	Homo sapiens	Homo sapiens	Homo sapiens
Transformant	Untransformed	Untransformed	Untransformed	Untransformed	HPV 16 E6E7 Transformed	Transformed With adenovirus 5 DNA
Age	10 years	15 years	18 years	20 years	14 weeks	fetus
Sex	female	male	female	female	male	
Race	Caucasian	Caucasian	Caucasian	Caucasian	Caucasian	
Telomerase	no	no	no	no	no	yes
Clinically affected	yes	yes	yes	yes	no	no
Mutated Gene	LIG4	LIG4	LIG1	NBS1		
Chromosomal location of mutated gene	13q22-q34	13q22-q34	19q13.2-q13.3	8q21		
Identified Mutations	GLY469GLU ARG814TER	ARG278HIS	GLU566LYS; ARG771TRP	5-BP DEL, NT657-661;	none	der(1)t(1;15) (q42;q13), der(19)t(3;19) (q12;q13), der(12)t(8;12) (q22;p13),
Reference	(O'Driscoll 2001)	(O'Driscoll, 2001)	(Webster, 1992)	(Varon, 1998)	(Capper 2007, Letsolo 2009)	(Capper 2007, Letsolo 2009)

25mM HEPES Buffer, 1x 10^5 U/l penicillin, 100 mg/l streptomycin and 2 mM L-glutamine (all Sigma). The fibroblasts were continuously treated with PARP inhibitor 1,5 – Dihydroxyisoquinoline (DIQ, Sigma). The inhibitor was dissolved in dimethyl-sulfoxide (DMSO, Sigma) and was added to the cell culture medium at 10 µM and 100 µM. The inhibitor was replenished with each medium exchange.

HEK293 cells were cultured in Dulbecco's Modified Eagle's Medium (DMEM, Invitrogen) supplemented with 10% (v/v) fetal calf serum (Autogenbioclear), 1x 10^5 U/l penicillin, 100 mg/l streptomycin and 2 mM L-glutamine (all Sigma).

2.1.3 Typsinising and passaging cells

After aspirating used medium, cells were washed with pre-warmed 1x trypsin (0.05% trypsin and 0.2% EDTA (Gibco)) to remove all remaining serum. An appropriate volume of fresh 1x trypsin was added to the flask and the cells were incubated for up to 40 minutes at 37°C until the cells were rounded. Fresh medium was added to deactivate tryspin. The cell suspension was transferred to a 15 ml tube. For re-plating, sufficient numbers of cells (N_1) and fresh medium was added to a new flask or well. For further details see table 2.2.

2.1.4 Counting cells and PD calculations

To monitor population doubling (PD) of the cell lines, cells were counted at every passage. After trypsinizing, 10 µL of cell suspension were counted in a haemocytometer (Improved Neubauer, Hawksley). Total cell number N_2 was determined as follows:

$$N_2 = \text{number of counted cells} \times 10^4 \times \text{volume of cell suspension (in mL)}$$

The population doublings (PDs) for each culture were recorded during every experiment. PDs were calculated with following formula:

$$PD = [\log N_2 \text{ (total cell number)} - \log N_1 \text{ (seeded cell number)}]/\log 2 \text{ cm}^2$$

Table 2.2 Trypsinising and plating cells

	Surface areas (cm^2)	Media Volume (ml)	Trypsin (ml)	Medium to deactivate trypsin (ml)	N1 (Untransformed cells lines)	N1 (MRC-5 HPV 16 E6E7 transformed)	N1 (HEK293, transformed with andenovirus)
T175	176.71	25	3	12	$4-6 \times 10^5$	/	/
T75/100 mm dish	78.54	10	2	8	$0.5-2 \times 10^5$	$4-6 \times 10^5$	$4-6 \times 10^5$
T25/60mm dish	28.27	5	1	4	$2-8 \times 10^4$	$0.5-1 \times 10^5$	$0.5-1 \times 10^5$
6 well	9.62	2	0.5	2	$< 2 \times 10^4$	/	/
24 well	1.76	1	0.1	0.5	$< 1 \times 10^3$	/	/

2.1.5 Cell freezing

Cells were frequently frozen to serve as a back-up for further experiments or in case of a contamination of the culture. For freezing, the cells were trysinized as usual and were pelleted by centrifugation at 1000 rpm for 5 min in a Centaur-2 centrifuge. The cells were re-suspended in 0.5 mL of culture medium and an equal amount of freezing mix (20% dimethyl-sulfoxide (DMSO, Sigma) in culture medium). The suspension then was transferred to a freezing ampoule which was placed in a freezing box containing iso-propanol. The freezing mix and iso-propanol allows a gentle gradual freezing procedure preventing ice crystal formation in the cells. Cells were frozen at -80°C and were kept at this temperature for short term storage. For long term storage, cells were transferred into liquid nitrogen at -196°C.

2.1.6 Thawing cells

Cells were removed from -80° or liquid nitrogen and thawed rapidly in a water bath (Grant) at 37°C. To remove all traces of DMSO, 9 mL of fresh culture medium were added drop wise. The slow dilution minimised the damage through osmotic shock and

increased the survival rate of the cells. The cell suspension was centrifuged at 1000 rpm for 5 min in a Centaur-2 centrifuge at room temperature (RT). After aspirating the supernatant, the pellet was re-suspended in an appropriate volume of fresh culture medium and re-plated. See Table 2.2 for seeding densities.

2.1.7 Measurement of DNA Synthesis of Senescent Cells by BrdU labelling

The onset of replicative senescence was defined as at least 4 weeks of no cell growth and bromodeoxyuridine (BrdU) labelling indices of < 3% (Bond et al., 1999). BrdU incorporation enables the detection of dividing cells in a cell population. For the assay, cells were seeded onto coverslips at a concentration of 2.0 – 5.0 x 10^4 cells per 35 mm dish. Cells were re-fed with fresh medium 2 days prior to the BrdU labelling. The cells were incubated with BrdU (50µmol/l, Boehringer) for 1 hour at 37 °C. To remove excess BrdU, cells were washed three times in 1x PBS and afterwards fixed for 30 minutes in pre-cooled 70% ethanol (Fisher Scientific) at 4°C. The coverslips were then extensively washed in 1x PBS and left to re-hydrate for 10 minutes in 1x PBS. In order to depurinate the DNA, the coverslips were incubated in 4 M HCl (Fisher Scientific) for 10 minutes at RT. Afterwards the coverslips were rinsed once in 1x PBS and then incubated with 0.1 M Borax, ph 8.5 (Sigma) for 5 minutes at RT. After washing the coverslips three times in 1 x PBS, coverslips were transferred into a humidified chamber and were incubated with an anti-BrdU monoclonal antibody (Dako M0744, Dako Cytomation), diluted to 1:100 in 0.6% bovine serum albumin (BSA, Roche) in 1x PBS, for 50 minutes at 37°C. Again, the cells were washed 3 times in 1x PBS and then incubated with rabbit anti-mouse antibody (Dako P0260 Dako Cytomation), diluted 1:100 in 0.6% BSA in 1x PBS, for a further 50 minutes at 37°C. The coverslips were washed in 1x PBS and developed with diaminobenzidine (DAB) solution for less than 5 minutes. The DAB solution was prepared immediately before use by adding 1 ml of DAB stock solution to 9 ml of 1x PBS and then adding 3.4 ml of hydrogen peroxide to the solution. DAB was washed off with three 1x PBS washes, followed by a wash with tap water. To finish the BrdU labelling, coverslips were stained with Meyers

hematoxylin for 30 to 60 seconds, followed by 3 washes with tap water. The hematoxylin staining was monitored under the microscope. As a final step, coverslips were dehydrated by quickly washing them in H_2O, followed by two quick washes in 100% ethanol and two quick washes in Xylene. Coverslips were mounted on glass slide and left to dry overnight. BrdU labelling index (%) was determined by counting dividing cells (stained brown) and comparing them with the total amount of fixed cells.

BrdU labelling index (%) = (number of stained cells / total number of cells)*100

2.1.8 Retroviral Infection

The recombinant retrovirus expressing HPV16E6E7 from a pLXNS construct, packaged in amphotropic PA317 cells was described previously (Halbert et al., 1991). As an empty vector control, a pBABEneo vector, packed in ψCRIP producer cells was used (Wyllie et al., 1993). Retroviral gene transfer was carried out as described previously (Bond et al., 1999, Capper et al., 2007).

Ligase IV syndrome cells (GM17523 and GM16088), Ligase I deficient cells (GM16096), Nijmegen Breakage Syndrome (GM07166) were infected individually with both the pLXNS-E6E7 and pBABE-NEO control retrovirus supernatants. All cells were plated at a concentration of 2.0 -2.5 x 10^5 cells per 60 mm dish on the day prior to infection. Cells were incubated with fresh medium containing 8 μg/ml polyprene (Aldrich) for at least one hour before the infection. 2 - 4 mL of virus-containing harvest medium were taken from storage at -80°C and thawed in a 37°C water bath (Grant). Supernatants were filtered with a 0.45 μm filter (Pall corporation) using a 5 mL syringe (Tyco Heatlhcare Kendall) and a kwill (Avon) and were transfered into a bijou (Sterilin). Polyprene was added to the retroviral suspension so that the final polyprene concentration was 8 μg/mL. After removing the medium from the cells, 2- 4 mL of medium containing the retroviral vector were added to each 60 mm dish and were left to

incubate for 4 – 6 hours at 37°C. After the incubation, the harvest medium was filled up with fresh culture medium to 5 mL. 48 hours after infection, the cells were re-plated in 100 mm dishes with normal culture medium at 1/2, 1/10, 1/50, 1/100 1/250 fold dilutions (Fig. 2.1). By using a non-selective medium, cells were giving time to reattach to the dish surface increasing the infection rate. The next day, cells were re-fed with selective medium containing 0.4 mg/ml geneticin (G-418, Invitrogen). The selection process took approximately 14 days, in which the cells were fed once a week with selective medium. The 1/2 and 1/10 fold dilution were used for bulk populations whereas 1/50, 1/100 1/250 fold dilution yielded individual clones. Clones were isolated using cloning rings. They were trypsinised and passed into 24 well plates after reaching a local densitiy of 90%. Both bulk populations and single clones were trypsinised and re-seeded like non-infected cells but were re-fed only with selective medium containing G418 every week.

2.1.9 Preparations of cell samples for further experiments

Cells were alternatively either frozen or sampled for single telomere length analysis (STELA) and fusion assays to obtain a complete overview of the telomere dynamics before senescence and/or crisis. The cells were pelleted by centrifugation at 1000 rpm for 5 minutes at RT. The supernatant was aspirated and the cell pellet was washed with 1x PBS to remove residue culture medium. After centrifuging at the same conditions and removing the supernatant again, the cell pellet was frozen and stored at -20°C for up to 12 months.

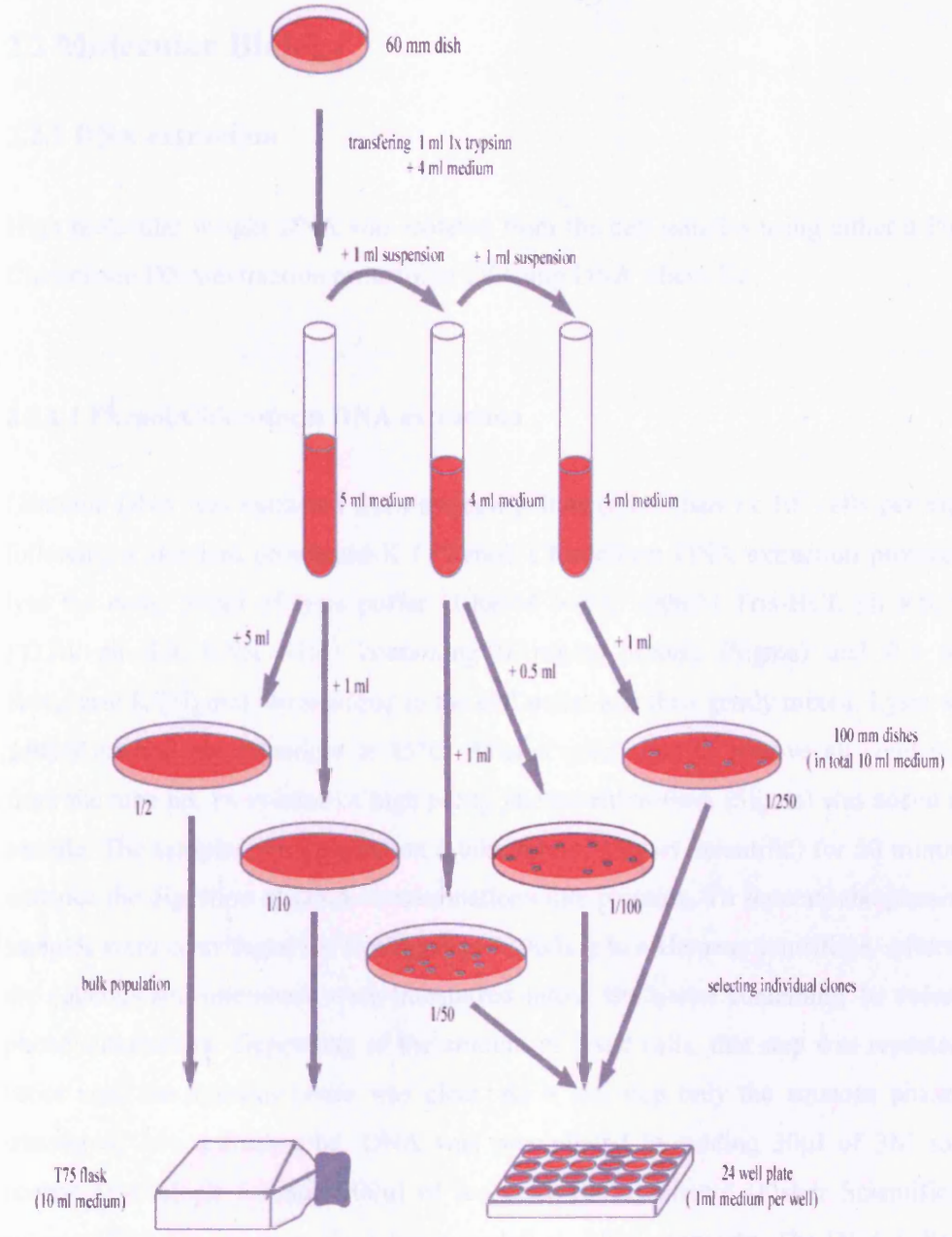

Figure 2.1 Retroviral Infection

2.2 Molecular Biology

2.2.1 DNA extraction

High molecular weight DNA was isolated from the cell samples using either a Phenol/ Chloroform DNA extraction protocol or QIAamp DNA Micro Kit.

2.2.1.1 Phenol/Chloroform DNA extraction

Genomic DNA was extracted from the cell pellets (more than 1x 10^5 cells per sample) following a standard proteinase K / Phenol/ Chloroform DNA extraction protocol. To lyse the cells, 300µl of lysis puffer (100mM NaCl, 100mM Tris-HCL ph 8.0, 5mM EDTA ph 8.0, 0.5% SDS) containing 0.1mg/ml RNase (Sigma) and 0.2 mg/ml Proteinase K (Sigma), were added to the cell pellet and then gently mixed. Lysis was in general carried out overnight at 45°C. After a quick spin to remove all condensation from the tube lid, 1x volume of high purity phenol/chloroform (Sigma) was added to the sample. The samples were placed on a tube rotator (Stuart Scientific) for 30 minutes to enhance the digestion of DNA contaminations like proteins. To separate the phases, the samples were centrifuged for 5 minutes at 13000x g in a Heraeus centrifuge. Afterwards the aqueous and interphase were transferred into a fresh tube containing 1x volume of phenol/chloroform. Depending of the amount of lysed cells, this step was repeated 2-4 times until the aqueous phase was clear. As a last step only the aqueous phase was transferred into a fresh tube, DNA was precipitated by adding 30µl of 3M sodium acetate (NaAc) ph 5.2 and 900µl of ice cold 100% Ethanol (Fisher Scientific). To support DNA precipitation, the tubes were left at -20°C overnight. The DNA pellet was recovered by centrifuging 18000xg at 4°C for 30 minutes in a Camlab centrifuge. The pellet was washed in 70% ethanol and after removing the ethanol, was dried at room temperature for up to 2 hours. The dried pellet was re-suspended in corresponding amount of 1x EcoRI buffer or 10mM Tris-HCl ph 8.0 (50µl for large, 25µl for medium and 15µl for small pellets). DNA samples were stored at 4°C allowing the DNA to

solubilize again. Large pellets were further solubilized by restriction enzyme digestion with 12 units of *Eco*RI (New England Biolabs) for 6 hours at 37°C, followed by heat inactivation at 65°C for 10 minutes.

2.2.1.2 DNA extraction using QIAamp DNA Micro Kit

For cell samples which contained less then 1x 10^5 cells, genomic DNA was extracted using QIAamp DNA Micro Kit. The kit enables the purification of genomic DNA from small samples sizes by binding the DNA to a silica-based membrane. DNA was extracted from the cell pellets by adding 100µl of the provided ATL buffer (tissue lysis buffer) and 10µl of the provided Proteinase K solution. After adding 100µl of the provided AL buffer (containing guanidinium chloride to denature proteins), the samples were pulse-vortexed for 15s. The lysis of the samples was carried out at 45°C for 10 min. After a quick spin to remove all condensation from the tube lid, 50µl 100% ethanol was added to the sample. Afterward the sample was pulse-vortexed for 15s and incubated at RT for 3 min. The entire lysate was transferred to the QIAamp MinElute Column. The samples were centrifuged for 1 min at 6000x g in a Heraeus centrifuge to bind the DNA to the silica-based membrane. Residual contaminations were removed by washing twice with the provided buffers AW1 (containing guanidinium chloride to denature proteins) and AW2 (70% ethanol to remove salt). The DNA was eluted from the column with 30µl 10mM Tris-HCl pH 8.0.

2.2.2 Single Telomere Length Analysis (STELA) and Fusion Assay

The solubilised genomic DNA was quantified in triplicate using Hoechst 33358 fluorometry (BioRad). Hoechst 33358 is a fluorescent dye which binds to DNA in high salt concentrations and allows quantitative DNA measurements by comparing the fluorescence emission of the unknown DNA sample against the emission of a known DNA sample. The dye was diluted in TEN buffer (10 mM Tris/HCL pH 8.0, 1mM EDTA, 100mM NaCl) to a final concentration of 1µl/mL. 1µl of each DNA sample was added to 1ml of freshly prepared TEN buffer containing Hoechst 33358 and the fluorescence emission is measured with the fluorometer (BioRad). Later on genomic DNA was quantified in triplicate using NanoDrop (Thermo Scientific). NanoDrop is a micro-volume UV to visible light Spectrophotometer. After pipetting 1µl of the DNA sample on the pedestal, the machine automatically adjusts the path length for measurement and gives a concentration reading.

Each DNA sample was diluted in 10 mM Tris-HCL pH 8 (Sigma) to 10 ng/µl. In case the sample contained less than 10 ng/µl of DNA, undiluted DNA was used for the STELA working dilution or the fusion assay. The single telomere length analysis (STELA) and the single molecule fusion PCR were performed according to the existing protocols (Baird et al., 2003, Britt-Compton and Baird, 2006, Capper et al., 2007, Letsolo et al., 2009).

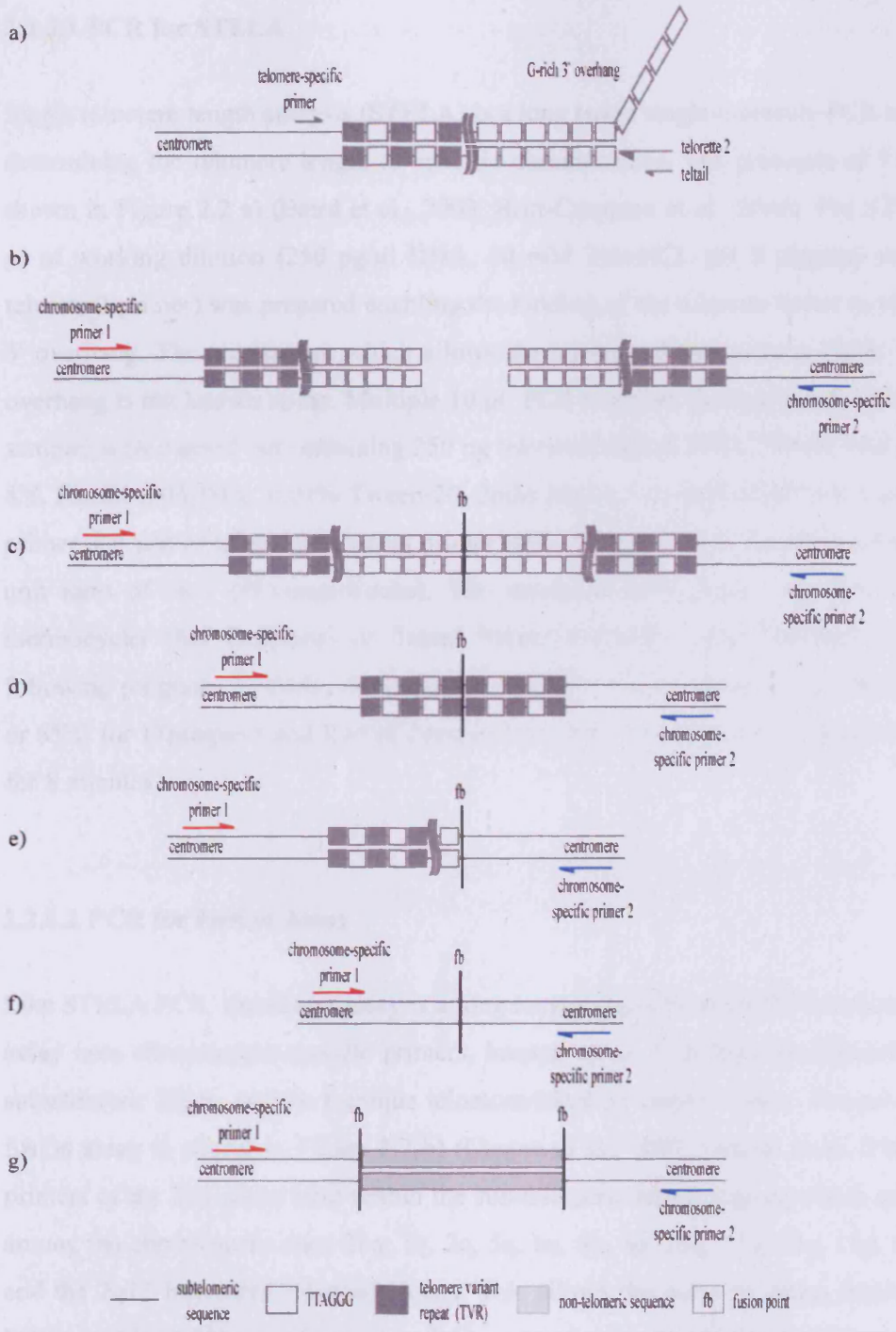

Figure 2.2 Single Telomere Length Analysis and Fusion Assay. a) Principle of STELA, b) principle of the fusion assay c- g) examples for telomere - telomere fusion events: c) "Head to Head" fusion containing large amounts of TTAGGG d-g) deletion events during the fusion process d) deletion into the TVR region of both telomere, e + f) deletion into the subtelomeric DNA sequence of either one or both chromosomes g) example of an insertion of non-telomeric DNA into the fusion

2.2.2.1 PCR for STELA

Single telomere length anlaysis (STELA) is a long range single-molecule PCR technique determining the telomere length of specific chromosomes. The principle of STELA is shown in Figure 2.2 a) (Baird et al., 2003, Britt-Compton et al., 2006). For STELA, 40 µl of working dilution (250 pg/µl DNA, 10 mM Tris-HCL pH 8 (Sigma) and 1 µM telorette2 primer) was prepared enabling the binding of the telorette linker to the G-rich 3′ overhang. The mechanism which allows the binding of the telorette linker to the 3′ overhang is not known so far. Multiple 10 µl PCR reactions (normally 4-6 reactions per sample) were carried out containing 250 pg telorette2-linked DNA, 75mM Tris-HCL pH 8.8, 20mM $(NH_2)SO_4$, 0.01% Tween-20, 2mM $MgCl_2$, 1.2 mM dNTP's, 0.5 µM teltail primer, 0.5 µM of telomere-adjacent primer (table 2.3) and 0.5 U *Taq/Pwo* mixture at a unit ratio of 10:1 (Promega/Roche). The reactions were cycled in a MJ PTC-225 thermocycler (MJ Research) or Tetrad Peltier Thermal Cycler (BioRad) using the following program: 22 cycles of denaturation at 94°C for 20 seconds, annealing at 59°C or 65°C for 17pseqrev1 and XpYpE2 respectively for 30 seconds and elongation at 68°C for 8 minutes.

2.2.2.2 PCR for Fusion Assay

Like STELA PCR, the fusion assay is a long range single-molecule PCR technique. The assay uses chromosome-specific primers, located up to 3 kb from the telomere in the subtelomeric DNA, to detect unique telomere-telomere fusion events. The principle of fusion assay is shown in Figure 2.2 b) (Capper et al., 2007, Letsolo et al., 2009). The primers of the 21q group bind within the sub-telomeric repeat regions which are shared among the chromosome ends 21q, 1q, 2q, 5q, 6q, 6p, 8p, 10q, 13q, 17q, 19p, 19q, 22q and the 2q13 interstitial telomeric locus. This allows the assay to detect fusion events between at least 35% of telomeres in the human genome. In addition to fusions between Xp, Yp, 17p and the above mentioned chromosome ends, the assay can detect sister chromatid-type fusion events as long as there has been a deletion of at least one of the telomeric repeat arrays. However, fusion events which contain perfect inverted repeat

sequences present a problem as a perfect sequence match can not be separated during sequencing. Furthermore, observations in our group have shown that the 21q group primers can generate additional non-specific products which can not be re-amplified. This artifical product is dependent on the DNA sample and the amount of DNA used in the fusion assay. Therefore the fusions detected with the 21q primer were not used to determine the fusion frequency of the analysed samples (Letsolo et al., 2009, Capper et al., 2007).

Multiple 10 µl PCR reactions (normally 9 or 18 reactions per sample) were carried out containing 10 ng DNA, 75mM Tris-HCL pH 8.8, 20mM $(NH_2)SO_4$, 0.01% Tween-20, 2mM $MgCl_2$, 1.2 mM NTP's, 0.5 µM XpYpM primer, 0.5 µM 17p6 primer, 0.5 µM 21q1 primer and 0.5 U *Taq/Pwo* mixture at a unit ratio of 10:1 (Promega/Roche). The reactions were cycled in a MJ PTC-225 thermocycler (MJ Research) or Tetrad Peltier Thermal Cycler (BioRad) using following program: 25 cycles of denaturation at 94°C for 20 seconds, annealing at 59°C or 65°C for 17p and XpYp respectively for 30 seconds and elongation at 68°C for 8 minutes.

2.2.2.3 Gel Electrophoresis for STELA and Fusion Assay

The amplified DNA fragments created by STELA or fusion PCR were resolved by horizontal submarine gel electrophoresis. After adding 2 µl of a 6x Ficol based gel loading dye (5% bromophenol blue, 5% xylene and 15% ficol) to the PCR reactions, 5 µl of each reaction was loaded on a 0.5% Tris-acetat-EDTA (TAE) agarose gel (Roche) containing 0.1% ethidium bromide (EtBr, Fisher Scientific). To track the molecular weight of the PCR products, a DNA ladder containing 0.5 µl of 1 kb DNA ladder (Stratagene) and 0.5 µl of 2.5 kb DNA ladder (Stratagene) was loaded onto the gel. Gels were run overnight at 110 Volt for at least 15 hours. The gel tanks and power packs used were from Bio-Rad.

2.2.2.4 Southern Blot

Gels were trimmed to size by visualising the DNA ladder on a UV tansilliuminator (FOTODYNE Incorporated) and removing excess gel. After DNA depurination for 2x 6 minutes in 0.25M HCL, the DNA fragments were denaturated in 1.5M NaCl, 0.5M NaOH for 15 minutes. The separated fragments were then transferred to a positively charged membrane (Hybond XL, GE Healthcare) by alkaline southern blotting. The denaturation buffer was used as transfer buffer. Southern blot construction is shown in Figure 2.3. The transfer was stopped after 4 – 6 hours, afterwards the membrane was quickly washed in H_2O and allow to dry at room temperature.

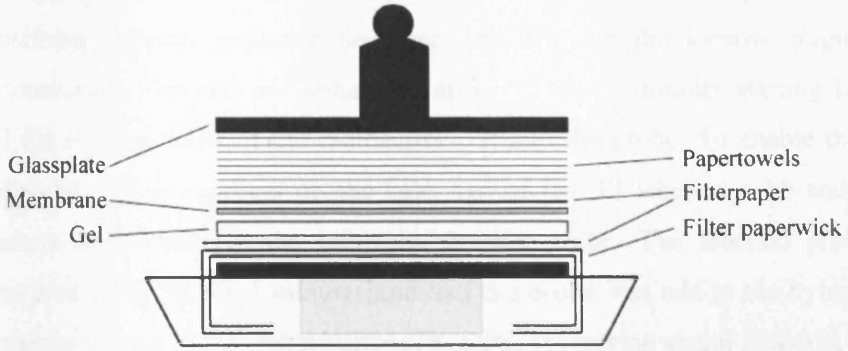

Figure 2.3 Southern Blot (modified from Cornel Mülhardt, *The Experimentator*, Spektrum Akademischer Verlag; 6 edition (2008). Print)

2.2.2.5 Southern Hybridisation Probes for STELA and Fusion Assay

Telomere adjacent probes and the probe binding telomere repeats for the detection of STELA products by southern hybridisation were generated by PCR (2.2.4.1) using the following oligonucleotides (table 2.3): For 17p STELA: 17p2 and 17p7; for XpYp STELA: XpYpE2 and XpYpB2.

Hybridisation probes for the detection of fusion assay products by southern hybridisation were generated by PCR (2.2.4.1) using the following oligonucleotides (table 2.3): For 17p: 17p7 and 17pseq3; for XpYp: XpYpE and XpYpB; for 21q group members: 21q1 and 21qseqrev1.

2.2.2.6 Southern Hybridisation

The hybridisation probes for STELA and fusion assay were labelled by using the rediprime random hexamer labelling kit (GE Healthcare). 25 ng of the probe template was denatured at 96 °C for 5 minutes and snap chilled on ice for 5 minutes. The denaturated DNA and [α-^{33}P] dCTP was added to the ready-made labelling mix containing random sequence hexamers, dNTPs and the klenow fragment of DNA polymerase I. The mix was incubated at 37 °C for 15 minutes starting DNA synthesis and the incorporation of the radioactive ^{33}P into the probe. To enable the detection of molecular weight markers on the blot, 1µl of [α-^{33}P] labelled 1 kb and 2.5 kb DNA markers was added to the telomere specific probe. The labelled probe was again denatured at 96 °C for 5 minutes and half the probe was add to the hybridisation tubes containing 15 ml of Church's buffer (7% SDS, 1% bovine serum albumin, 1 mM EDTA, 0.5 M sodium phosphate, pH 7.0) and the southern blot. Hybridisation was carried out overnight at 60 °C in a hybridisation oven (ThermoHybaid).

2.2.2.7 Hybridisation Washes and Fragment Analysis

After hybridisation overnight, the blots were washed with 0.1 x SSC/0.1% SDS at 60 °C for 1-2 h. The wash solution was exchanged several times to maximize the removal of all non-specific bound hybridisation probe. The blots were dried and the hybridized fragments were detected by phosphoimaging with a Molecular Dynamics Storm 860 PhoshorImager (GE Healthcare). Prior to re-hybridisation with additional probes, blots were stripped with boiling 0.1% SDS for at least 6 hours. The molecular weights of the DNA fragments were enumerated and sized by using the software package Phoretic 1D

quantifier (Nonlinear Dynamics). Each data set was transferred into a separate Microsoft Excel Spread sheet (Microsoft, Seattle, USA). All mean values, standard deviations (SD), standard errors (SE) and median values were calculated with Microsoft Excel. Modal telomere distributions of each sample were determined as peaks in the histogram depicting the calculated individual and cumulative frequencies of the different telomere lengths. The frequency of occurrences of a value in the data set was generated by the histogram analysis tool of Microsoft Exel (Microsoft, Seattle, USA).

2.2.3 Oligonucleotides

Primers were synthesised by MWG. All used primers were designed previously in the group and were based on telomere adjacent sequences (Baird et al., 2003, Britt-Compton and Baird, 2006, Capper et al., 2007, Letsolo et al., 2009). All used primers are detailed in Table 2.3.

Table 2.3 Oligonucleotides

	STELA primers	Tm (°C)	Reference
Telorette2 (Tel2)	5'-TGCTCCGTGCATCTGGCATCTAACCCT-3'		(Baird 2003)
Teltail	5'-TGCTCCGTGCATCTGGCATC-3'	various	(Baird 2003)
XpYpE2	5'-TTGTCTCAGGGTCCTAGTG-3' (406 bp)	65	(Baird 2003)
17pseqrev1	5'-GAATCCACGGATTGCTTTGTGTAC-3' (311bp)	59	(Britt-Compton 2006)

	Fussion assay primer	Tm (°C)	Reference
XpYpM	5'-ACCAGGTTTTCCAGTGTGTT-3'	59	(Capper 2007)
17p6	5'-GGCTGAACTATAGCCTCTG-3'	59	(Britt-Compton 2006)
21q1	5'-CTTGGTGTCGAGAGAGGTAG-3'	59	(Letsolo 2009)

	Probe generation	Tm (°C)	Reference
XpYpB2	5'-TCTGAAAGTGGACC(A/T)ATCAG-3'		(Baird 2003)
17p2	5'-GAGTCAATGATTCCATTCCTAGC-3'		(Britt-Compton 2006)
17p7	5'-CCTGGCATGGTATTGACATG-3'		(Capper 2007)
17pseq3	5'-AGAATCCTGTCCTCAACAAGT-3'		(Britt-Compton 2006)
21qseq1rev	5'-AGCTAGCTATCTACTCTAACAGAGC-3'		(Letsolo 2009)
21qseq1	5'-TGGTCTTATACACTGTGTTC-3'		(Letsolo 2009)

	Reamplification primers	Tm (°C)	Reference
XpYpO	5'-CCTGTAACGCTGTTAGGTAC-3'		(Capper 2007)
21q1B	5'-TTGGTGTCGAGAGAGGTAGC-3'		Baird unpublished

	Sequencing primers	Tm (°C)	Reference
17p-33G	5'-GCACCCGGGCTCATACCTG-3'	50	(Capper 2007)
21q2ct	5'-AGTAGCATCTCYAGTGCTGGAG-3'	50	(Letsolo 2009)
21q3	5'-CTGCAGTTGTCCTAGTCGC-3'	50	(Letsolo 2009)
10q1	5'-AGGTTCCACTCGTCTCTGCG-3'	50	(Letsolo 2009)
10q2	5'-TGCAATGTCCCTAGCTGCCAG-3'	50	(Letsolo 2009)
8p1	5'-TGCACAGGACTCTTAGGCTG-3'	50	(Letsolo 2009)
Subtel2	5'-GAATCCTGCGCACCGAGATTCTC-3'	50	(Letsolo 2009)
21qseq2	5'-TGCCCCAATCATCATTCACTCTGC-3'	50	(Letsolo 2009)
6p1	5'-CTGCACAGGACTCCTAGGATG-3'	50	(Letsolo 2009)

2.2.4 Polymerase Chain Reaction (PCR) and Gel Electrophoresis

2.2.4.1 PCR for generating probes

To generate probes for Southern Hybridisation, the template DNA was diluted in 10mM Tris-HCl (ph 8.8) to 50 ng/µl. The PCR reaction volume of 10µl contained 100 ng/µl DNA , 75mM Tris-HCL pH 8.8, 20mM $(NH_2)SO_4$, 0.01% Tween-20, 2mM $MgCl_2$, 1.2 mM NTP's, 1 µM primer 1, 1 µM primer 2 and 1 U of 10:1 ratio of *Taq* (Promega) and *Pwo* polymerase (Roche). The reactions were cycled in a MJ PTC-225 thermocycler (MJ Research) or Tetrad 2 Peltier Thermal Cycler (Bio Rad) using following program: 32 cycles of denaturation at 96°C for 20 seconds, annealing temperature Tm (table 2.3) for 30 seconds and elongation at 68°C for 8 minutes.

2.2.4.2 Reamplification PCR

Fusion products were reamplified as described previously (Capper et al., 2007, Letsolo et al., 2009). First-round PCR reactions containing fusion events were diluted 1:20 in H_2O. A second PCR reaction (end vol. 30µl) with nested primers (XpYpO, 17p7, 21qseq1 or 21q1B, Table 2.3) was carried out containing 3µl diluted PCR reaction, 75mM Tris-HCL pH 8.8, 20mM $(NH_2)SO_4$, 0.01% Tween-20, 2mM $MgCl_2$, 1.2 mM of dNTPs, 0.5 µM primer 1, 0.5 µM primer 2 and 0.5 U of 10:1 ratio of *Taq* (Promega) and *Pwo* polymerase (Roche). The reactions were cycled in a MJ PTC-225 thermocycler (MJ Research) or Tetrad 2 Peltier Thermal Cycler (Bio Rad) using following program: 32 cycles of denaturation at 94°C for 20 seconds, annealing at 59°C for 30 seconds and elongation at 68°C for 8 minutes.

2.2.4.3 Agarose Gel Electrophoresis

DNA fragments were resolved using horizontal submarine gel electrophoresis. After adding 6 µl of a 6x Ficol based gel loading dye to the PCR reactions, the complete reaction was loaded on a 1x TAE or 1x TBE (45mM Tris-borate, 1 mM EDTA) agarose gel (Fisher Scientific) containing 0.1% ethidium bromide (EtBr, (Fisher Scientific). To estimate the molecular weight of the PCR products, a DNA ladder containing 0.5 µl of 1 kb DNA ladder (Stratagene) and 0.5 µl of 2.5 kb DNA ladder (Stratagene) was loaded onto the gel. Gels were run either overnight at 45 Volt or at 120 Volts for 1-2 hours. The used gel tanks and power packs were Bio-Rad.

2.2.4.4 DNA Gel Extraction

The resolved DNA fragments were visualised with a UV tansiluminator (FOTODYNE Incorporated) and appropriate fragments were cut from the gel using a clean scalpel. The DNA was extracted from the agarose block using QIAamp Gel extraction Kit. The kit

enables the separation of DNA and agarose by binding the DNA to a silica-based membrane. After several washing steps, the DNA was eluted from the column with 30µl 10mM Tris-Cl, ph 8.5.

2.2.5 Sequencing Analysis of Fusion events

Sequencing was carried out using Big Dye 3.1 or Big Dye 3.0 GTP. The 10µl reaction contained 4.4 µl of reamplified fusion product, 1.6 µl 1µM primer and 4.0 µl of Big Dye mix (PE applied Biosystems). The sequencing reaction was then cycled in a MJ PTC-225 thermocycler (MJ Research) or Tetrad 2 Peltier Thermal Cycler (Bio Rad) using following program: 25 cycles of denaturation at 96°C for 30 seconds, annealing at 50°C for 15 seconds and elongation at 60°C for 4 minutes. Unincorporated dye terminators were removed from the sequencing reaction using gel-filtration technology (DyeEx Spin 2.0 Kit, Qiagen). The purified reactions were resolved and sequences were generated using an Applied Biosystems Genetic Analyzers (3130xl), Data Collection software version 3.0 and Sequencing Analysis software version 5.2.

2.3 Statistical Analysis

All tissue culture and sequence analysis data was entered into Microsoft Excel Spread sheets (Microsoft, Seattle, USA). All mean values, standard derivations (SD), standard errors (SE) and median values were calculated with Microsoft Excel. All presented diagrams were generated in Microsoft Excel.

2.3.1 Determination of erosion rates

To establish the erosion rate in the exponential growth phase of the cells, the telomere length determined by STELA was plotted against the corresponding PD. The slope of the regression line of the data points gave the erosion rate in base pairs (bp) per PD. R^2 values were used to assess correlations between telomere length and PDs. In order to

decide whether the telomere erosion rates at the two oxygen concentrations are significantly different, or whether the differences might just be due to chance standard errors (also standard error of the mean, SE) was chosen as error bars. SE is defined as $SE = SD/\sqrt{n}$. (Cumming et al., 2007)

2.3.2 Frequency of fusion events

In order to calculate the frequency of fusion events, the number of bands generated by each fusion reaction was counted and divided by the estimated number of input molecules into the reaction. The number of input molecules was estimated from the amount of DNA analysed in each reaction divided by the size of a diploid human genome of 6 pg.

Frequency = number of fusion events/[amount of DNA used in analysis (pg) / 6 pg]

2.3.3 T-test

A paired t-test was used to determine of one sample measured at two conditions differed from each other. It was assumed that the data sets were approximately normally distributed and the variances of the two sets were homogenous. No differences between the two data set and the implication that both could be from the same source was postulated to be the null hypothesis H_0. The t-test was calculated in Microsoft Excel using a 2-tailed, 2 sample equal variance t-test. The calculated p-value is the probability of the null hypothesis H_0 being true. At a p-value below 0.05 the null hypothesis H_0 was rejected.

2.3.4 Chi-Square test

A Chi-Square test (χ^2) was used to determine if the observed frequencies conformed to the expected frequencies of the category. In this thesis the expected frequencies were derived from previous observations in the group. For the null hypothesis H_0 , it was assumed that the observed and the expected frequencies did not differ from each other. The $\aleph^2$ –test was calculated in GraphPAD Prism V.4.01 (GraphPAD Inc., San Diego, USA). At a p-value below 0.05 the null hypothesis H_0 was rejected.

2.3.5 Repeat Measure ANOVA

A repeat measure ANOVA (analysis of variance) was used to determine if there was a significant difference between one sample subjected to three or more different treatments. No difference between the different treatments was stated as the null hypothesis H_0. The repeat measure ANOVA was calculated in GraphPAD Prism V.4.01 (GraphPAD Inc., San Diego, USA). At a p-value below 0.05 the null hypothesis H_0 was rejected.

Chapter 3: DNA Ligase I Deficiency

3.1 Abstract

The human fibroblasts strain GM16096 is derived from a patient with DNA ligase I syndrome. The cells are characterised by a reduction of Ligase I activity levels to less than 5 % and the delayed joining of Okazaki fragments. The aim of this work was to investigate if DNA Ligase I modulates telomere dynamics and the role that DNA Ligase I may play in the mechanism that underlies the fusion of short dysfunctional telomeres.

The telomere dynamics were investigated using STELA. The telomere dynamics in DNA Ligase I deficient human fibroblasts were not significantly different from those observed in normal human fibroblasts. This suggests that the limited replicative capacity is not a result of accelerated telomere attrition and that impaired Okazaki fragment joining does not modulate telomere dynamics.

In order to investigate whether DNA Ligase I deficiency plays a role in the mechanisms behind chromosomal fusion events, cells were forced to divide beyond senescence to "crisis" by the expression of HPV16 E6E7 abrogating the function of p53 and RB. The resulting fusion events found in E6E7 expressing DNA Ligase I deficient cells were investigated on a molecular level and a distinct mutational profile for telomere-telomere fusion events was observed. Telomere fusion involving the 17p telomere and members of the 21q group of related telomeres were detected. This was consistent with the observed loss of the 17p telomere. In contrast, the XpYp telomere remained intact and was not subjected to fusion. No clear differences in the fusion profile (sub-telomeric deletion and microhomology at the fusion point) compared to the profile of normal human fibroblast strains could be observed. However, due to the limited data set, no statistically significant conclusion about the requirement of DNA Ligase I in the fusion of short dysfunctional telomeres could be drawn.

3.2 Introduction

3.2.1 DNA Ligase I

DNA Ligase I is one of three DNA ligases in human cells which perform a vital role in DNA replication and repair (Martin and MacNeill, 2002). Like all eukaryotic DNA Ligases, DNA Ligase I is a nucleotidyltransferase (NTase). The ATP-dependent ligase interacts with members of the replication complex (Li et al., 1994) and catalyzes the joining of Okazaki fragments during lagging strands synthesis (Waga and Stillman, 1994). In addition, DNA Ligase I ligates DNA nicks during base pair excision repair (BER) (Prasad et al., 1996).

3.2.2 DNA Ligase I Deficiency

Only one human being has been diagnosed with DNA Ligase I deficiency. A female patient (46BR) showed symptoms of growth retardation, sun sensitivity, severe immune deficiency and chromosomal instability, symptoms similar to those of Bloom's syndrome and ataxia telangiectasia (AT). The patient developed lymphoma and died shortly after from pneumonia at the age of nineteen (Webster et al., 1992). A fibroblast cell line (46BR cell line or GM16096) was established from a skin sample of the patient. Early biochemical studies showed that double strand breaks (DBS) induced by the treatment with ultraviolet (UV) radiation or DMS persist longer in the 46BR cell line than in normal cells (Teo et al., 1983). Furthermore, the cells display retarded joining of Okazaki fragment and are lethally affected by 3-aminobenzamid (3'-AB), an inhibitor of poly(ADP-ribose) polymerase (PARP) (Creissen and Shall, 1982, Henderson et al., 1985). All these studies supported the hypothesis that 46BR cells have a basic defect in DNA Ligase activity. Following the identification of the human gene encoding DNA Ligase I (LIG1) located on chromosome 19 (q13.2 – 13.3) (Barnes et al., 1990), two different missense mutations in both alleles of DNA Ligase I were identified in the patient derived cell line, 46BR (Barnes et al., 1992). The first mutation, an arginine-771 to tryptophan transition within the OB fold domain was inherited from the mother of the patient and can also be found in the patient's siblings. The second mutation, two amino

acids away from the key active-site lysine on the other allele, replacing glutamic acid-566 with lysine was either inherited from the father or occurred spontaneously. Both mutations retain the Ligase I enzyme with less than 5% activity (Barnes et al., 1992, Lehmann et al., 1988, Prigent et al., 1994).

The fibroblast cell line is highly sensitive to DNA damaging agents and shows a slightly increased level of sister chromatid exchange (SCE) after treatment with UV irradiation and methylating agents. Most interestingly, DNA Ligase I deficient fibroblasts have a defect in Okazaki fragment joining and single strand nick sealing during DNA damage repair (Prasad et al., 1996, Prigent et al., 1994). Several studies have shown that the ligation kinetics of 46BR are affected. In contrast to an unaffected ligation reaction, the reaction is retarded due to an accumulation of the two normally transient intermediate products, Ligase I-AMP and nicked DNA-AMP (Henderson et al., 1985, Lonn et al., 1989, Prigent et al., 1994).

Cytotoxic DNA lesions caused by oxidative damage are normally repaired by base excision repair (BER) (Laval et al., 1998). Two sub-pathways have been identified which are distinguished by the nucleotide replacement size and proliferating cell nuclear antigen (PCNA) dependency (Fortini et al., 1999, Frosina et al., 1996). The short patch BER pathway is dependent on polymerase-β and results in the removal and replacement of a single nucleotide. The strand re-ligation is carried out by either DNA Ligase I or III. In contrast to short patch BER, long-patch BER is dependent on PCNA and involves the removal of an oligonucleotide (2-11 nts) from the DNA lesion. The nicked DNA is sealed by DNA Ligase I. Not surprisingly, DNA Ligase I deficiency results in the favouring of the short patch BER in 46BR cells (Levin et al., 2000). Western Blot analysis of GM16096 fibroblasts showed that DNA Ligase I levels are significantly lower (Liang et al., 2008) whereas DNA Ligase III levels are enhanced compared to normal cells (Moser et al., 2007) and therefore are thought to compensate for DNA Ligase I deficiency. In conjunction with the PARP inhibitor lethality (Lonn et al., 1989), these observations suggest that the survival of GM16096 fibroblasts depends on PARP1 and DNA Ligase III. The DNA damage response (DDR) in 46BR.1G1 cells, the human

simian virus 40-transformed form of 46BR (GM16096) is altered. However there is only a moderate delay in cell cycle progression as the cells do not activate the S-phase specific ATR/Chk1 checkpoint (execution of mitosis). In contrast, the ATM-mediated DNA damage checkpoint appears to be chronically activated (Soza et al., 2009).

Surprisingly, there is no defect in V(D)J recombination to explain the immune deficiency instead it appears to result from a defect in B and T cells proliferation after stimulation (Hsieh et al., 1993, Petrini et al., 1994).

The absence of functional DNA Ligase I in mice is developmentally lethal due to insufficient foetal liver erythropoiesis. However, in early stages of embryogenesis another ligase compensates for the lack of DNA Ligase I in other foetal tissues (Bentley et al., 1996). DNA Ligase I null mice primary fibroblasts also fail to convert the ligation reaction intermediates resulting in a delayed DNA joining process. In contrast to human patient derived primary fibroblasts; mouse cells display no lethal sensitivity to DNA damaging agents and to the PARP inhibitor 3'- AB. They also show normal level of SCE (Bentley et al., 2002). A mouse model (46BR mice) mimicking the mutation observed in the patient with DNA Ligase I deficiency was created by introducing Arg-771 to Trp replacement mutation into mice. The 46BR mice are challenged in their foetal erythropoiesis but evolve into mature animals though at the slower pace than wild type mice. Primary fibroblasts from 46BR mice have a significantly increased level of genomic instability due to the same abnormal DNA ligation mechanism as seen in human 46BR primary fibroblasts. Old 46BR mice display an increased risk of cancer and develop rare epithelial tumours (Harrison et al., 2002).

3.2.3 Oxidative Stress and Telomeres

The proliferative capacity of normal fibroblast populations is dependent on seeding densities and oxygen concentration (Balin et al., 1984). Lowering the oxygen concentration or supplementing the growth media with antioxidants reduces the level of oxidative stress on the cells and therefore facilitates an increase in replicative lifespan of

the cells (Chen et al., 1995). The same effect has been observed in cultures from human colorectal mucosa, mouse leukaemia cells and primary melanoma cells (Gupta and Eberle, 1984, Pritchett et al., 1985, Joyce and Vincent, 1983). Several more recent studies have demonstrated that IMR90 human fibroblast enter premature senescence following the treatment with hydrogen peroxide (H_2O_2). This reactive oxygen species induces oxidative stress which has been attributed to induce varying levels of DNA damage resulting in the damaged cell exiting the cell cycle within the first 24 hours after treatment (Chen et al., 1998, Chen et al., 1995, Chen et al., 2001). H_2O_2 treatment initiates a DNA damage response via p53, p21 and p16 activation resulting in the cell cycle arrest in S-phase (Cheng et al., 2004). Further data suggest a link between oxidative damage and telomere biology. Observation in WI38 cell showed that high oxygen levels (40%) lead to premature senescence. Interestingly, the telomere lengths at senescence were similar to those observed at 20% oxygen. This lead to the hypothesis that the elevated telomere erosion rate in WI38 cells cultured at high oxygen levels were due to oxidative stress (von Zglinicki, 2002). Similar results were achieved when culturing IMR90 at 20% oxygen compared to cells cultured at 5% oxygen (von Zglinicki, 2002). Furthermore, IMR90 fibroblasts cultured at 20% oxygen failed to immortalise with the forced expression of telomerase (Wright and Shay, 2001). However the cells easily immortalise when cultured in 3% oxygen (Britt-Compton et al., 2009, Forsyth et al., 2003). In contrast to IMR90 cells, MRC5 and HCA3 fibroblast strains show no differences in cell proliferation and telomere erosion at varying oxygen tension (Lorenz 2001, Britt-Compton 2009). The controversy concerning oxidative stress as a direct cause of telomere loss is further helped with observation in G6PD deficient primary foreskin fibroblasts HFF1 and HFF3 which both prematurely senesce after H_2O_2 treatment, but none of these cells display elevated telomere erosion rates (Cheng et al., 2004).

3.2.4 Aims

The aim of this work was to investigate if DNA Ligase I modulates telomere dynamics and the role that DNA Ligase I may play in the mechanism that underlies the fusion of short dysfunction telomere.

3.3 Results

3.3.1 Optimising the replicative lifespan of DNA Ligase I deficient cells

Previous studies have shown that oxidative stress can reduce the replicative lifespan of primary human fibroblasts (Forsyth et al., 2003). It is conjectured that radical oxygen species induce varying levels of DNA damage leading to premature cell cycle arrest. Large quantities of non-proliferating cells can imply a raised telomere erosion rate (Chen et al., 1995). Furthermore, other studies indicate that the telomere erosion rate is directly influenced by DNA damage in the telomeric region resulting from oxygen tension (von Zglinicki, 2002). DNA damage caused by oxygen radials is normally repaired by BER (Laval et al., 1998). DNA Ligase I deficient fibroblasts are impaired in BER and favour the short patch BER pathway (Levin et al., 2000). Consequently oxidative stress may impede the replicative capacity of the Ligase I deficient fibroblast and thus influence the telomere dynamics observed in the cells. Therefore parental Ligase I deficient cells at PD 7.99 were either cultured under normal culture conditions (20% O_2) or under physiological oxygen levels of 3% to reduce oxidative stress. The fibroblasts were passaged serially in culture and the accumulated PDs were documented as a function of time (Fig. 3.1). After 20 passages the replicative capacity of GM16096 was exhausted at both oxygen concentrations and the cell numbers drop significantly.

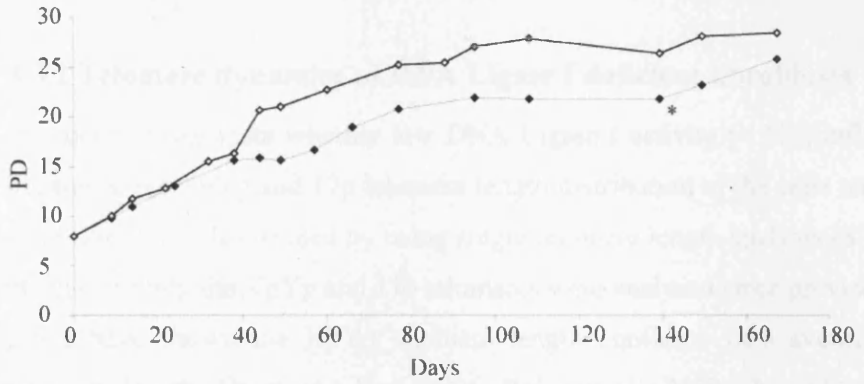

Figure 3.1 Growth curves of DNA Ligase I deficient cells cultured in 3% and 20% Oxygen. Plotting growth curves as function of population doublings (PD) versus time in days. Filled markers represent cells cultured at 20% oxygen and open markers represent those cultured in 3% oxygen.

Growth curves for both cultures conditions are similar except for a clonal outgrowth of the 20% O_2 culture close to senescence (indicated with *). Compared to the cultures at 20% O_2, culturing DNA Ligase I deficient fibroblasts at 3% O_2 increased the proliferating lifespan of the cells by 6.7 PDs. The mean growth rate during the exponential growth phase of the two cultures at 3% and 20% O_2 was determined to be 0.244 PD/day ± 0.199 and 0.152 PD/day ± 0.099 respectively. The slight increase in growth rate resulting from the lower oxygen concentration accounted for the extended lifespan of the cells at 3% oxygen.

Although the GM16096 was derived from a relative young individual (age 18), the fibroblasts had a limited replicative capacity of 26 and 28 PD at 20 and 3% O_2 respectively. This is in contrast to normal human fibroblast which undergo 40 to 70 PDs before they enter a stable proliferative arrest termed replicative senescence (Hayflick, 1965). Replicative senescence is defined by a characteristic morphology of high endogenous senescence-associated mammalian β-galactosidase activity index (>90%), a very low (<3%) BrdU labelling index and very low death rates (Bond et al., 1999). After 4 weeks of no apparent growth in both cultures, cell proliferation was tested by BrdU labelling. The cells at 20% O_2 presented a BrdU index of 23% in PD 21.74. For the cells at 3% O_2, a BrdU index of 1.8% in PD 26.36 was determined indicating that the cells had reached senescence.

3.3.2 Telomere dynamics of DNA Ligase I deficient fibroblasts

In order to investigate whether low DNA Ligase I activity (< 5%) influences telomere dynamics, the XpYp and 17p telomere length distribution of the cells under both culture conditions were determined by using single telomere length analysis (STELA) (Baird et al., 2003). Only the XpYp and 17p telomeres were analysed since previous studies in our group have shown the XpYp telomere length conforms with average chromosomal telomere length (Baird and Farr, 2006, Baird et al., 2003). In addition, the telomere erosion rates resulting from the end-replication problem are similar at most chromosome ends (Britt-Compton et al., 2006). Several samples were taken during the course of the experiment and were analysed.

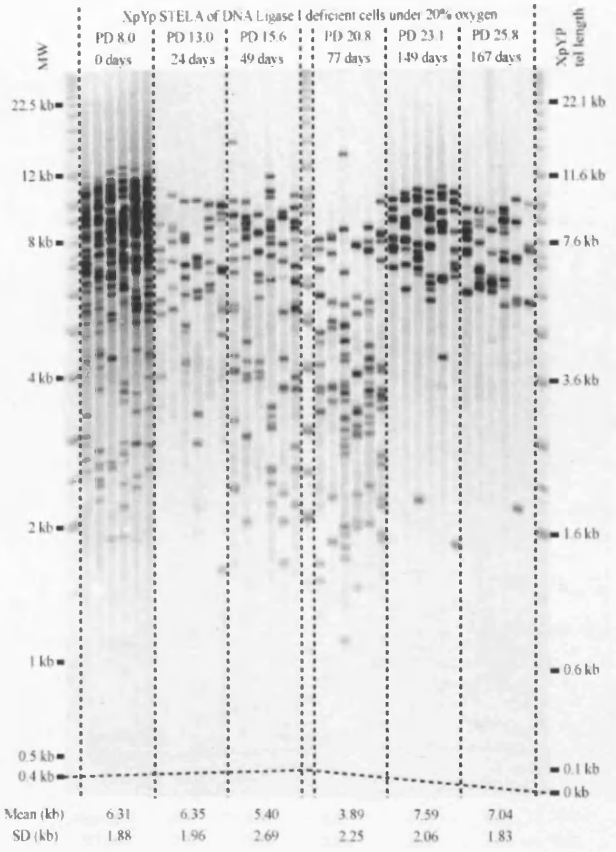

Figure 3.2 a). XpYp STELA gel displaying the telomere length profile in DNA Ligase I deficient cells under 20% oxygen. Starting from the point fibroblast were taken into culture, population doublings (PD) are presented abowe the gel.Also displayed above the gel are the number of days the fibroblasts were kept in culture . Molecular weight (MW) is indicated on the left and the corrected telomere length is indicated on the right. Mean telomere length and corresponding standard deviation (SD) are detailed below the gel.

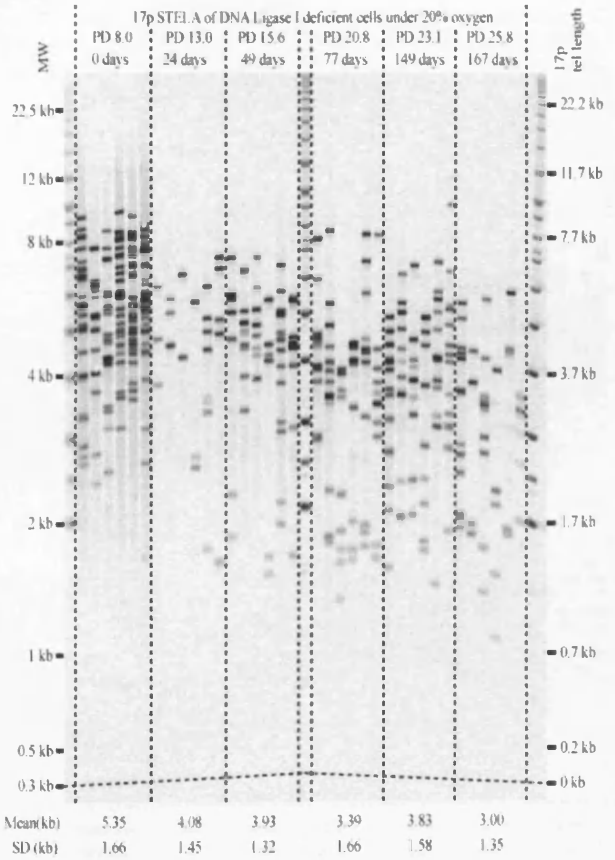

Figure 3.2 b) STELA gel displaying the 17p telomere length profile of DNA Ligase I deficient fibroblast under 20% oxygen. Starting from the point cells were taken into culture, population doublings (PD) are presented above the gel. The number of days the fibroblast were kept in culture is displayed above the gel. Molecular weight (MW) is indicated on the left and corrected telomere length is indicated on the right. Mean telomere length and corresponding standard deviation (SD) are detailed below the gel.

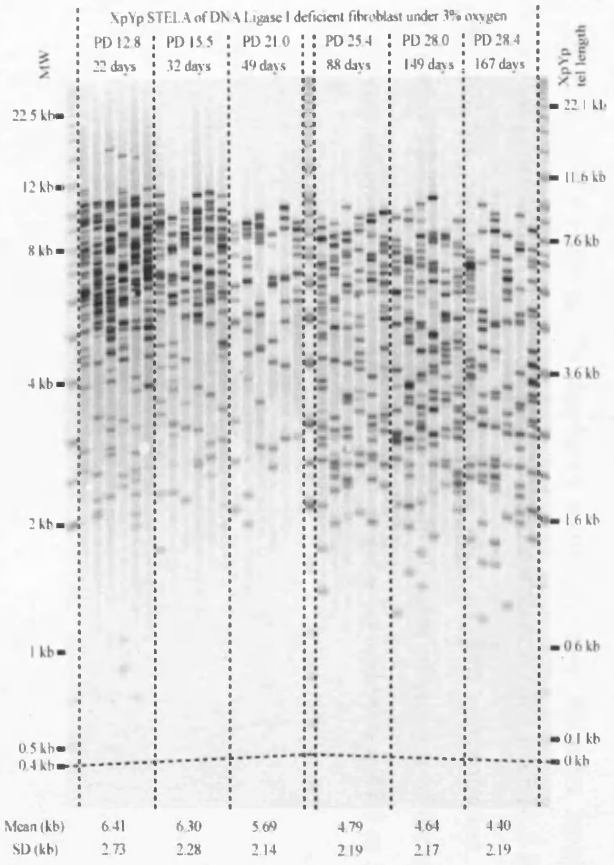

Figure 3.3 a) STELA gel displaying the XpYp telomere length profile of DNA Ligase I deficient cells under pysiological oxygen concentrations. Starting from the point cells were taken into culture, population doublings (PD) are presented above the gel. Also displayed above the gel are the number of days the fibroblasts were kept in culture. Molecular weight (MW) is indicated on the left. Corrected telomere length is indicated on the right. Mean telomere length and corresponding standard deviation (SD) are detailed below the gel.

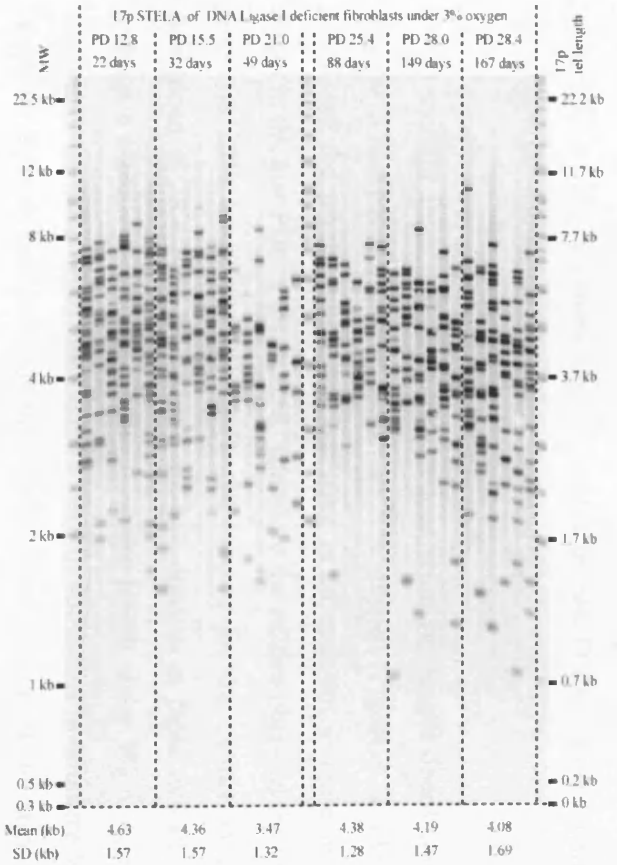

Figure 3.3 b) 17p STELA displaying the telomere length profile of DNA Ligase I deficient fibroblasts under physiological oxygen concentrations. Starting from the point cells were taken into culture, PDs are presented above the gel. In the second line above the gel displays the the days cells were kept in culture. Molecular weight (MW) is indicated on the left. Corrected telomere length is indicated on the right. Mean telomere length and corresponding standard deviation (SD) are detailed below the gel.

with STELA. The telomere length profiles for the DNA Ligase I deficient fibroblast strain GM16096 are shown in figures 3.2 and 3.3.

It was evident from the more homogenous telomere length distribution that a clonal outgrowth had occurred in the culture at 20% oxygen (Figure 3.2a, PD 23.1 and 25.8), overtaking the whole culture and resulting in an apparent increase in XpYp telomere length in the last PDs of the culture. Therefore the culture obtained the minimal telomere length in 20% oxygen at PD 21.71. Senescence for the culture in 3% oxygen was determined at 28.4 PDs. Comparing the two cultures at these two PD points, STELA revealed a significantly longer XpYp telomere length under 3% oxygen at the point of senescence (p-value <0.01, two tailed t test). In contrast, 17p telomere length appears to be similar for both culture conditions at senescence (p-value 0.569, two tailed t test).

From the growth curve (Fig. 3.1) the culture at 20% O_2 exited the exponential growth phase after 77 days. The lower oxygen level of 3% O_2 increased the exponential growth phase of the cells for 17 days. In the 20% O_2 culture, mean telomere length decreased by 2.61 kb at the XpYp telomere and by 1.54 kb at the 17p telomere at senescence over 13.9 PDs. The culture at 3% displayed a loss in mean telomere length of 2.01 kb at XpYp telomere and of 0.55 kb at 17p telomere at senescence over 16.7 PDs. The erosion rates for the XpYp and 17p telomere at each oxygen concentration were calculated separately and are shown in Fig. 3.4. The mean rates of erosion of the two chromosome ends were determined to be 180.1 ± 27.5 at 20% O_2 and 99.6 ± 47.5 at 3% O_2 (bp/PD ± SE).

a)

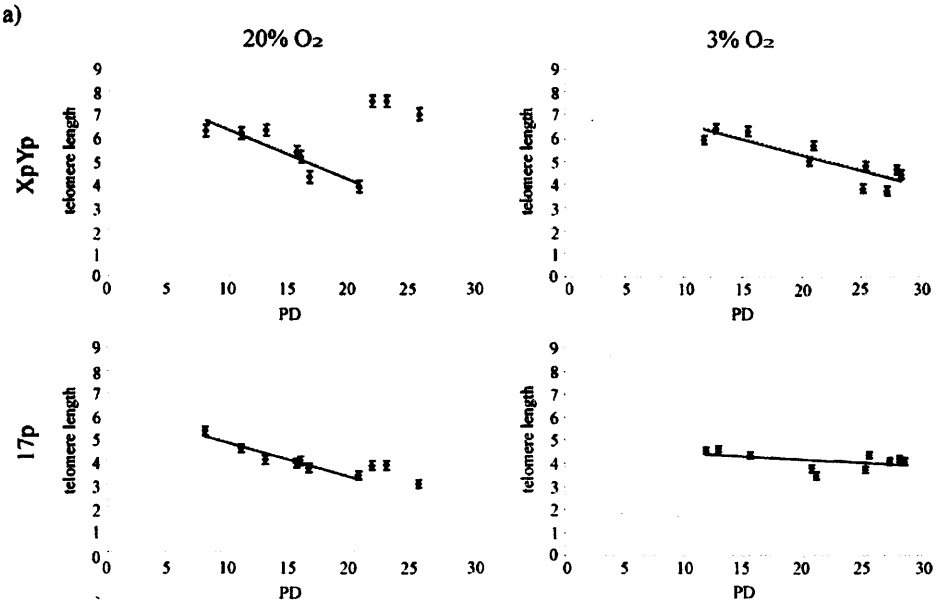

b)

telomere	Erosion rate bp/PD	20% O_2 R2	Number of Data points	Erosion rate bp/PD	3% O_2 R2	Number of Data points
XpYp	213	0.81	7	135	0.76	10
17p	146	0.92	7	29	0.23	10
overall mean	180.1		overall mean	99.6		
overall SE	27.5		overall SE	47.5		

Figure 3.4 Summarising the telomere erosion rate data from DNA Ligase I deficient fibroblasts in 3% and 20% oxygen. a) Telomere erosion rate is calculated as the slope of the regression line after plotting the mean telomere length against the corresponding PD. Individual Telomeres are detailed on the right, oxygen concentration is displayed above; error bars are ± standard error; y-axis presents mean telomere length; x-axis represents PD. b) Erosion rates, accompanying R2 and the number of data points for each chromosome are displayed.Overall mean and corresponding standard errors are also detailed.

3.3.3 Telomere dynamics of DNA Ligase I deficient fibroblasts expressing HPV16 E6E7 oncoproteins

Given the overlapping function of DNA Ligase I in base excision repair and Okazaki fragment joining, the key objective for investigating DNA Ligase I deficient cells was to examine the role that DNA Ligase I could play in telomere fusion events. In order to do so, telomere length of Ligase I deficient cells was pushed into the range in which telomeres become unprotected and undergo fusion (Capper et al., 2007). This was achieved by the forced expression of the human papillomavirus HPV16 E6E7. These oncoproteins abrogate the function of p53 and Rb allowing the cells to bypass senescence and continue to divide to crisis. The expression of E6E7 did not extend the replicative life span of the DNA Ligase I deficient cells to the same extend as normal human fibroblasts, where typically 26 – 28 PDs can be achieved (Capper et al., 2007). Instead the Ligase I deficient cells reached crisis 5-10 PDs after senescence making it difficult to obtain sufficient amounts of cells for STELA and fusion assay samples. The problem was avoided by altering the existing protocol and transfecting the cells with HPV16 E6E7 in PD 12 instead of 3-4 PDs before reaching senescence. Since abrogation of p53 and Rb does not influence growth rate and phenotype of the cells (Capper et al., 2007), only four clones expressing E6E7 (clones 7, 8, 9 and 17) and two clones expressing empty vector (Neo clones 1 and 5) achieved sufficient cell numbers (average for E6E7 clones: 5×10^4 cells, for Neo clones: 2.5×10^4 cells) for STELA and fusion assay samples.

STELA was used to track the telomere dynamics as the cells divide through to crisis. As the E6E7 clones approached crisis, the cell cultures ceased to expand resulting in a decline in the calculated PDs. This decline is completely artificial and a result of the methodology (see chapter 2.1.4). In order to indicate that the cells were still proliferating the number of days, the cells were kept in culture after infection, are displayed below the calculated PDs in figure 3.5. As expected, following the expression of HPV16 E6E7, the XpYp telomere of the E6E7 clones continued to erode beyond the length of the senescent control cells (NEO clones 1 and 5) (Fig. 3.5 a). The 17p telomere of the E6E7 clones eroded beyond a threshold length where it was no longer detectable with STELA

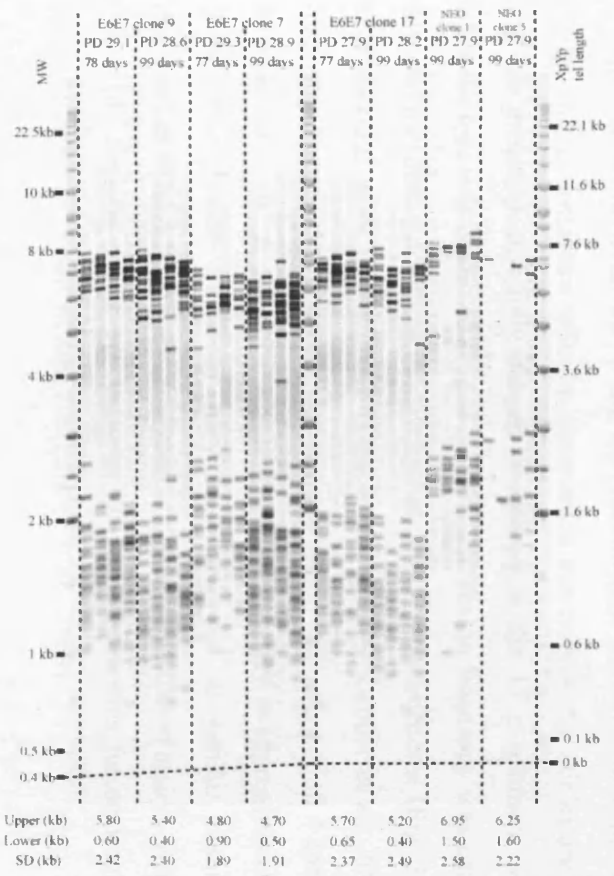

Figure 3.5 a) XpYp Stela displaying the telomere length profile of DNA Ligase I deficient fibroblasts expressing either HPV E6E7 oncoproteins or the empty Neo control vector under 3% oxygen. The calculated PDs starting from the point cells were taken into culture are presented in the first line above the gel. In the second line above the gel displays the the days cells were kept in culture after infection. Molecular weight (MW) is indicated on the left and corrected telomere lenght is indicated on the right. Modal telomere lengths and corresponding standard deviation (SD) are detailed below the gel.

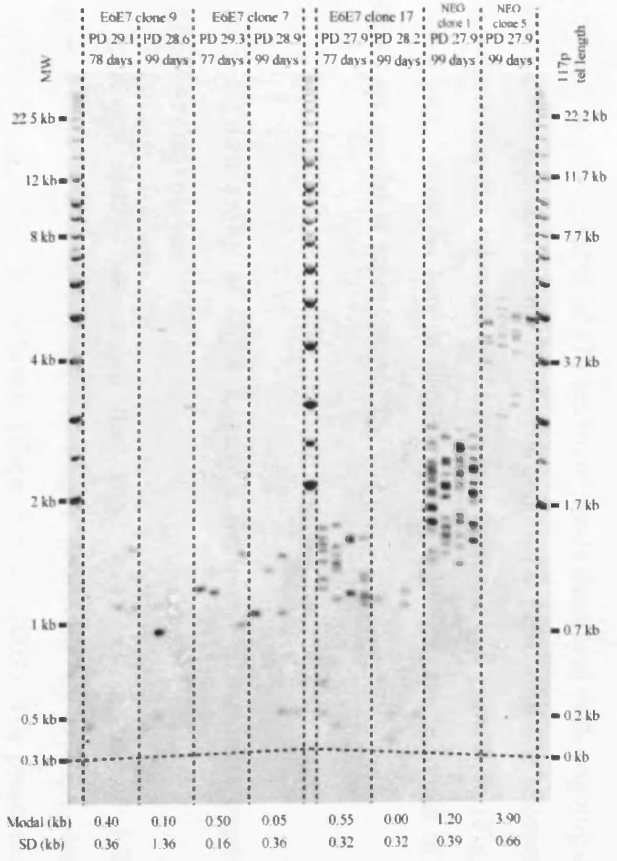

Figure 3.5 b) 17p Stela displaying the telomere length profile of DNA Ligase I deficient fibroblasts expressing either HPV E6E7 oncoproteins or the empty Neo control vector under 3% oxygen. The calculated PDs starting from the point cells were taken into culture are presented in the first line above the gel. In the second line abov the gel displays the days cells were kept in culture after infection with HPV16 E6E7. Molecular weight (MW) is indicated on the left and corrected telomere lenght is indicated on the right. Modal telomere lengths and corresponding standard deviation (SD) are detailed below the gel.

(Fig 3.5 b). The number of 17p telomere bands decreased with ongoing cells division, so that on average less then 4 % of cells retained a detectable 17p telomere at crisis. This indicated that this telomere had been lost from the cell population (Figure 3.5 b). Both Neo clones show no loss of detectable 17p telomere; the amounts of XpYp and 17p bands are similar at senescence (Fig. 3.5).

3.3.4 Fusion assay of DNA Ligase I deficient fibroblasts expressing HPV16 E6E7 oncoproteins

A previous study has shown that short telomeres in normal MRC5 fibroblasts approaching crisis, which are no longer detectable by STELA, have become de-protected and can undergo fusion (Capper et al., 2007). The presence and quantity of telomere-telomere fusion events in DNA Ligase I deficient fibroblasts was determined using long-range single–molecules PCR amplifications with 3 primers for 17p, XpYp and 21q group telomeres (21q, 1q, 2q, 5q, 6q, 6p, 8p, 10q, 13q, 17q, 19p, 19q, 22q and the 2q13 interstitial telomeric locus) (Letsolo et al., 2009) (Fig. 3.6). It was not possible to detect fusion between XpYp and the chromosome ends of 17p or members of the 21q group. This is consistent with the observation that both XpYp alleles are relatively long and are probably still fully capped compared to the 17 p telomere where complete telomere loss was observed (Fig. 3.5, 3.6). The fusion frequency was calculated for the 17p chromosome since most fusions include the 17p chromosome (Fig. 3.6, 3.7). In line with previous work in our group (Letsolo et al., 2009, Capper et al., 2007), the fusion frequency increased near crisis. The average fusion frequency of all 4 analysed clones at crisis is $1.7 \times 10^{-3} \pm 1.1 \times 10^{-3}$. Notably, this frequency is approximately 4 to 5 times higher than fusion frequency previously observed in similar manipulated E6E7 transformed MRC5 fibroblasts analysed using the same fusion assay. With an estimated 3.9×10^{-4} fusions events per analysed DNA molecule this fusion frequency was the highest frequency observed thus far (Letsolo et al., 2009).

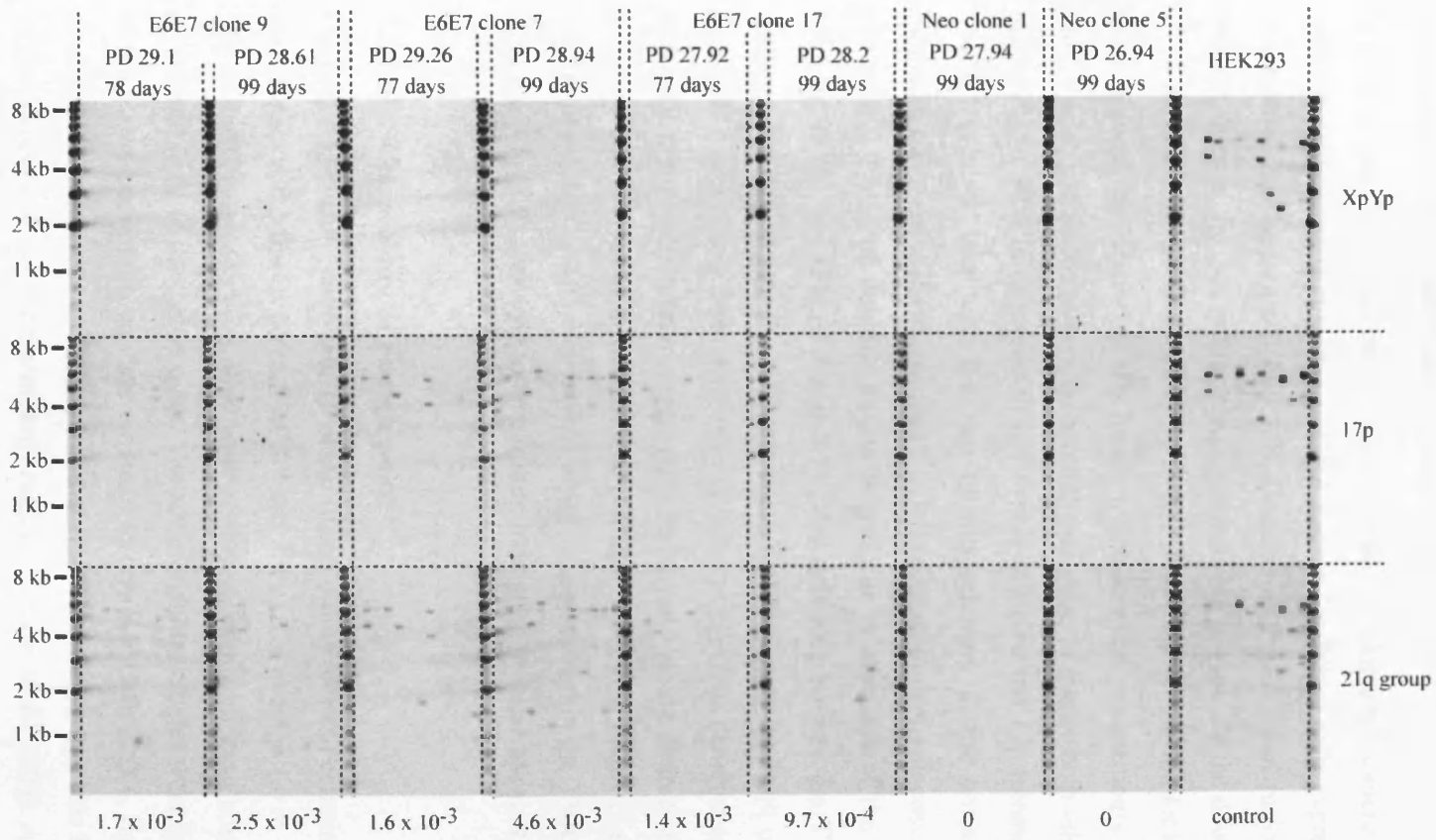

Figure 3.6 Fusion assays in DNA Ligase I deficient cells expressing either HPV16 E6E7 or empty NEO control vector for the XpYp, 17p and 21q group chromosomes. HEK293 was used as reaction control. Each reaction contains 5 ng of DNA and are detected by the chromosome specific probe detailed on the right. The calculated PDs and the days cells were kept in culture after infection are displayed above the gel. The fusion frequency was calculated for the 17p chromosome and is stated below each sample. Molecular weight markers are indicated on the left.

3.3.5 Internal Structure of Fusions in Ligase I deficient fibroblasts expressing HPV16 E6E7 oncoproteins

In order to gain insight in the mechanistic basis of telomere-telomere fusion events, 25 telomere-telomere fusion events in DNA Ligase I deficient cells expressing E6E7 were re-amplified and sequenced (Fig. 3.7). Because of the nature of fusion events between two members of the 21q group, it was not possible to separate the double sequence data of 10 fusions (data not shown). Only in one case (Fig. 3.7 d), the location of the fusion point allowed the separation of a fusion event between two members of the 21q group. The 15 analysed fusion events involved the deletion of one or both telomeres (Fig. 3.7). Interestingly, 87% of analysed fusion events involved the 17p telomere (Fig. 3.6, 3.9) which was consistent with the loss of this telomere in the crisis cells (Fig. 3.5). However, only one of these included a deletion into telomere-adjacent DNA sequence of 17p (Fig. 3.7 c). The deletion events only occur in members of the 21q group (mean 1916 bp ± 764 bp) (Fig. 3.7 and 3.8). The deletions include the TVR region of the telomere and extend into the telomere-adjacent DNA up to the limit of the fusion assay for the 21q group at 3.2 kb. This is in contrast to previous observations in MRC5 cells where all investigated chromosome ends displayed varying degrees of telomere repeat sequence and several kb of the telomere-adjacent DNA deletions (Letsolo et al., 2009, Capper et al., 2007). The distribution of fusion points within the TVR region of the 17p telomere (Fig. 3.9) appeared to be random; indicating no clear hot spot for fusion points.

3.3.6 Microhomology at Fusion point

Out of the 15 fusions analysed, 10 of the fusion points (66.6%) contained nucleotide (nt) homologies at the fusion point (Fig. 3.7 and 3.8 a). On average 1.0 nt ± 0.22 nt (mean ± SE) of 100% sequence homology were observed, with additional homologies in the 20 bp left and right of the fusion point. The additional homologies were found on both sides of the fusion point, with no clear tendency to one side (left: 22.3%, right 18.6%, overall mean 20.5%). Previous analysis of normal fibroblasts revealed a bias in the G:C content of the sequence of the microhomology regions (Letsolo et al., 2009). A G:C bias was not

observed in the fusion molecules derived from the Ligase I deficient cells. However this may be accounted simply by the small sample size.

3.3.7 TTAGGG repeat content at fusion point

Only 37.5 % of the analysed fusion events contained telomeric TTAGGG repeats at the fusion point (Fig 3.8 b) with a mean of 1.1 ± 0.38 nt (mean ± SE) and a maximum 5 repeats. All the observed repeats could be allocated in the TVR region of the 17p telomere (Fig 3.9). All fusion events had only TTAGGG repeats on one side of the fusion. This is consistent with the hypothesis, that telomere have to erode into TVR region to loose the protection through the shelterin complex and undergo fusion (Capper et al., 2007).

3.3.8 Complex fusion events

Most of the analysed fusion events involve only the 17p telomere and a member of the 21q group. However two of the fusion events are more complex including large patches of non-telomere sequences in the fusion. One of these fusion events is depicted in Fig. 3.7 e. The fusion event between a member of the 21q group and the 11p chromosome contains an insert derived from a sequence located near 3p24. It is noteworthy that the 3p24 sequence is within the vicinity of the FRA3A fragile site and the fusion point with the 11p chromosome is close to the FRA11C site (Debacker and Kooy, 2007, Debacker et al., 2007). Both sites are common fragile sites which are present in nearly all individuals and are thought to be part of the chromosomal structure (Debacker et al., 2007, Durkin et al., 2008). Previous data has indicated that telomere fusion with non-telomeric loci may preferentially occur adjacent to fragile sites (Letsolo et al., 2009). The second fusion event containing non-telomeric DNA was only partly sequenced due to the limited amount of DNA. Nevertheless it was possible to identify an insert derived from 15p13 nested between the involved 10q telomere and 17p telomere. From the limited size of the analysed data set, it was apparent that no statistical significant conclusion can be drawn.

3.3.9 Increased Frequency of Single Nucleotide Mutations in DNA Ligase I Deficient cells

While analysing the sequence of the observed fusion events in DNA Ligase I deficient human fibroblast expressing HPV E6E7, an increased frequency of single nucleotide mutations has been observed in the sub-telomeric sequence of the 17p telomere and members of the 21q group (data not shown). The sequence variances made it difficult to differentiate between the individual chromosomes in the 21q group. Due to the limited amount of DNA used for the sequence analysis of the fusion events, it was not possible to gain a re-presentable overview of the frequency and position of these single nucleotide mutations (data not shown).

Figure 3.7 DNA sequences data of fusion events in DNA Ligase I deficient fibroblasts expressing E6E7. a) 13q:17p fusion b) 13q:17p fusion c) 19q:17p, the only fusion with a subtelomeric deletion of 17p. d)13q:21q group, an example for a fusion between two members of the 21q group e) 21q group:3p:11p, fusion with an insertion. Telomere-adjacent DNA is shown in multicolor, TTAGGG repeats (T)in black, variant reparts (V) in red and inserts in brown. Fusion points, deletions size in bp, microhomoloy (bold and underlined) and number of T and V repeats are indicated below.

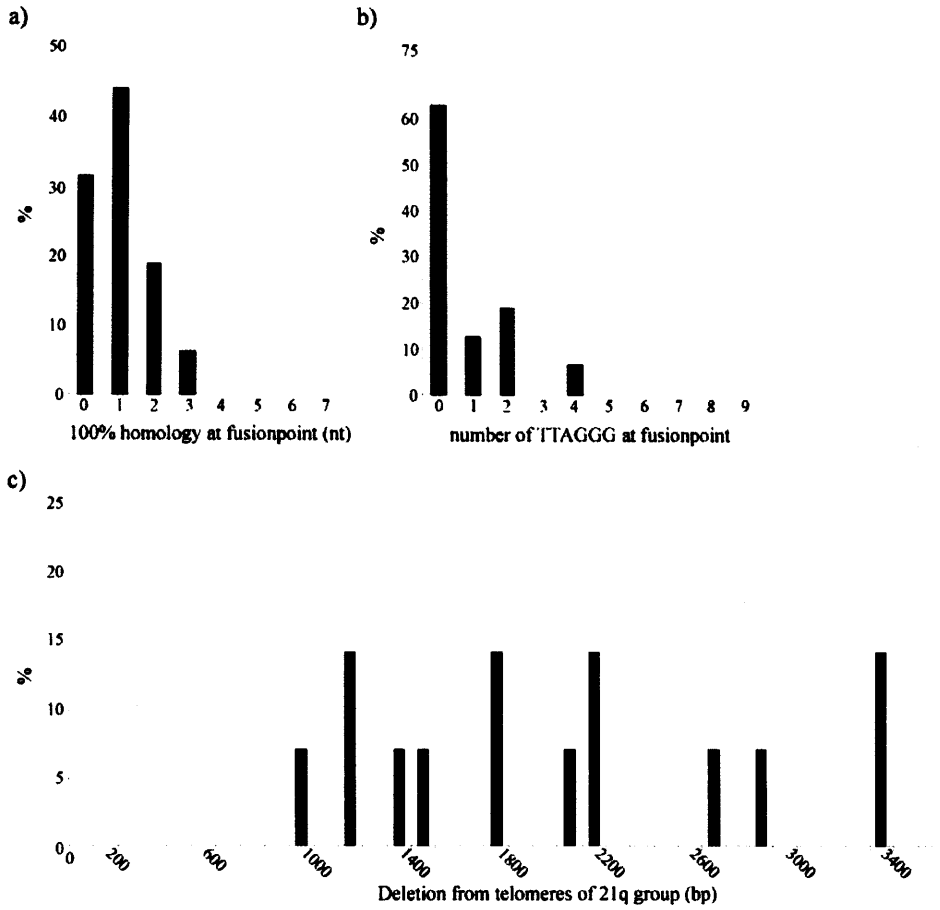

Figure 3.8 Histograms summarizing the telomere fusion data in DNA Ligase I deficient fibroblasts expressing E6E7. a) size of 100% sequence homology at the fusion point. b) the number of TTAGGG repeats ajacent to the fusion point c) the deletion size from the start of the telomeres of the 21q group.

Figure 3.9 Fusion point in the 17p telomere. Fusion points highlighted in yellow.

3.4 Discussion

3.4.1 Replicative Lifespan, Oxidative Stress and Telomere Erosion in Ligase I deficient cells

The replicative lifespan of GM16096 is limited with a maximum of 26-27 PDs obtained prior to replicative senescence. Cells were obtained from the Corriel Cell Repository, no further information of the proliferative history of the cells was available prior to this study. Other studies (Cabuy et al., 2005, Soza et al., 2009) indicate that the proliferative capacity of DNA ligase I deficient cells GM16096 is significantly reduced compared to normal fibroblast where 40 to 70 PDs at the points of replicative senescence are expected (Hayflick, 1965). The replicative capacity of Ligase I deficient fibroblasts is in line with that observed in other DNA repair deficient fibroblasts cultures such as Werner (Tollefsbol and Cohen, 1984, Martin et al., 1970), DNA Ligase IV syndrome (chapter 4 in this thesis) and NBS1 deficient fibroblast (chapter 5 in this thesis).

Soza et al 2009 demonstrated that DNA Ligase I deficiency leads to an increased number of single-stranded and double-stranded DNA breaks in 46BR.1G1 cells, the human simian virus 40-transformed form of 46BR (GM16096). It was also apparent that Ligase I deficiency results in moderate delays to cell cycle progression as Okazaki fragments remain in the intermediate form (DNA Ligase I-AMP and nicked DNA-AMP) for a prolonged time (Prigent et al., 1994, Levin et al., 2000). The resulting DNA damage in the newly synthesised DNA strand does not activate the S-phase specific ATR/Chk1 checkpoint which takes care of problems encountered by replication fork (Lukas and Bartek, 2004). The presence of a persistent DNA damage response is likely to result in an increase of quantity of cells exiting the cell cycle, thus creating a discrepancy between the actual cell divisions of the cultures and the calculated population doublings (PDs). In this situation the majority of growth in the culture will be driven by the proliferation of a smaller number of cells. This will have the effect of both attenuating the replicative lifespan of the culture and will exacerbate the apparent rate of erosion as a function of PD. This may account for the attenuated replicative capacity of the Ligase I cell culture, and how lower oxygen tensions, that are considered to reduce the extent of oxidative stress (Forsyth et al., 2003) and DNA damage, result in

an increase in the replicative capacity. Consistent with this hypothesis, Cabuy et al 2005 also reported elevated levels of telomere erosion in GM16096, ranging from 120 bp/PD to 200 bp/PD depending on the method used to determine telomere length (Southern blot and Flow-FISH). Furthermore this may provide an explanation for the increased rate of telomere erosion that was apparent in these cells at 20% O_2 that was reduced in lower oxygen tensions.

An alternative explanation for the increased rates of telomere erosion, observed at 20% oxygen, might be that the absence of Ligase I changes the biochemistry of the end-replication problem, for example by increasing the size for Okazaki fragment and thus increasing the amount of DNA lost from the terminus with each cell division. However, there is no evidence that Ligase I deficient cell exhibit an increase in Okazaki fragment size. Furthermore if changes in Okazaki fragments size accounted for this difference, culturing the cells in different oxygen tension would not be predicted to decrease the rates of erosion, as was observed in this study. A further explanation may also be that Ligase I deficient cells exhibit an impaired repair ability to repair double-stranded DNA breaks, double-strand breaks within the telomere would have the effect of increasing the rates of erosion. However this also appears unlikely as no evidence of any increases in telomere length heterogeneity could be observed in these cells, indeed the telomere length distributions of these was in distinguishable for that observed in normal fibroblast cell cultures (Baird et al., 2003, Britt-Compton et al., 2006, Capper et al., 2007).

3.4.2 Telomere Fusion in DNA Ligase I Deficient human fibroblasts

The expression of HPV E6E7 yielded 4 clonal cell populations, whilst there was no apparent proliferative lifespan extension as determined by estimating the population doublings by cell counting, the fact that the telomeres were considerably shorter when these cells entered 'crisis' compared the control clones, suggest that there was indeed a lifespan extension. These cell populations exhibited homogenous telomere length distributions that were consistent with clonal growth, there were no apparent differences in these distributions compared to clonal populations of normal human fibroblasts (Baird et al., 2003, Capper et al., 2007). Bimodal distributions were observed at the XpYp

telomere that were consistent with allelic telomere length variation. At the point of crisis the bimodal distributions at XpYp were intact, however 96% of cell had completely lost the 17p telomere. Telomere fusion was readily detected in these cells, consistent with the telomere length data, telomere fusion could not be detect involving the intact XpYp telomere, and the majority (84%) of fusion involved the 17p telomere that showed complete loss. Interestingly the maximum telomere fusion frequency (4.6×10^{-3}) was 10 fold higher than that detected in normal MRC5 cells expressing HPVE6E7 (3.9×10^{-4}) (Capper et al., 2007, Letsolo et al., 2009) which had lost the 17p and XpYp telomeres and were analysed using the same fusion technology. An explanation for this is not immediately apparent. However it is of interest to note that Ligase I deficient cells exhibit an up-regulation of Ligase III (Moser et al., 2007) and favour short patch base excision repair which is Ligase III dependent and involves the removal of a single nucleotide (Levin 2000). Long patch base excision repair, in contrast, requires Ligase I and involves the removal of larger patches of DNA surrounding the lesion (2-12 nt). Ligase III is considered to play a key role in Ku independent error prone end joining process alternative NHEJ (Zhu et al., 2000, Wang et al., 2005, Audebert et al., 2006, Audebert et al., 2004). It may also be pertinent to note that in this study a reduction, of borderline statistical significance, in the amount of microhomology at the fusion point was observed.

A further aspect of the telomere fusion data in Ligase I deficient cells was that in a sample of 15 fusion events involving the 17p only one displayed a sub-telomeric deletion event. Again the explanation for this is unclear. However, the increase in the fusion frequency (×5) suggests the possibility that the fusion process is more efficient and thus short dysfunctional telomere may be subjected to fusion prior to substantive end-processing creating large deletion events. This observation may also provide an alternative explanation of the apparent increased frequency of fusion, the lack of sub-telomeric deletions at 17p may render the fusion assay more efficient as the paucity of sub-telomeric deletion preserves the 17p telomere-adjacent primer sites.

3.5 Conclusion

DNA Ligase I deficient fibroblasts display an attenuated replicative lifespan. However, only the cells cultured at 20% oxygen present an elevated telomere erosion rate compared to normal fibroblast. Thus it could be speculated that premature senescence in these cells is not the result of increased telomere attrition as telomere erosion rates at 3% oxygen are in the range observed in normal fibroblasts. Instead it might be possible that DNA Ligase I deficient fibroblasts are sensitive to oxidative stress. Telomere fusion can be readily detected in Ligase I deficient cell undergoing crisis. The elevated rates of fusion may be related to the bias in the use of short patch base excision repair.

Chapter 4: DNA Ligase IV syndrome

4.1 Abstract

DNA Ligase IV is a core component of classic non-homologous end joining (C-NHEJ). Two patient derived Ligase IV syndrome fibroblast cultures were analysed in this study. Both fibroblast strains contain hypomorphic mutations in LigIV gene resulting in residual DNA ligase IV activity and impaired C-NHEJ.

The telomere dynamics in Ligase IV deficient fibroblast were investigated using STELA. An accumulation of critically short telomeres could be detected in the parental fibroblast cultures. It appears that premature senescence of DNA Ligase IV syndrome cells is not a result of elevated telomere attrition as telomere erosion rates are in the range observed in normal human fibroblasts. However the distribution of short telomeres could trigger a DNA damage response inducing premature senescence.

Another aspect of this study was to examine the role of Ligase IV in telomere fusion. However the expression of HPV16 E6E7 in DNA Ligase IV syndrome strains failed to drive average telomere length of DNA Ligase IV deficient fibroblasts into the length range at which telomeres become unprotected and undergo fusion. Nevertheless the investigation of the parental cultures displayed a low but significantly elevated fusion frequency. This is in contrast to telomere fusion following the experimental abrogation of TRF2 which are dependent on DNA Ligase IV. These data are consistent with the view that classical NHEJ is not the predominant mechanism underlying the fusion of telomeres.

4.2 Introduction

4.2.1 DNA Ligase IV

As with DNA ligase I, DNA ligase IV is an ATP-dependent nucleotidyltransferase (NTase) (Martin and MacNeill, 2002). DNA Ligase IV functions in non-homologous end joining (NHEJ) and V(D)J recombination. The Ligase forms a complex with XRCC4 and is unstable in the absence of XRCC4 (Critchlow et al., 1997). Interestingly, DNA Ligase IV has the ability to join DNA ends which are non-complementary because of mismatches and small gaps (Gu et al., 2007).

4.2.2 DNA Ligase IV Syndrome

14 individuals with DNA Ligase IV Syndrome have been reported, each with a hypomorphic mutation in the DNA Ligase IV gene (O'Driscoll et al., 2004, Rucci et al., 2010). The first case with DNA Ligase IV deficiency was discovered in a 14 year old acute lymphoblastic leukaemia patient (180BR) who displayed an extreme sensitivity to radiation therapy and died following radiation morbidity (Plowman et al., 1990). Previously to the diagnosis with leukaemia, the patient was clinically normal and did not share the more severe symptoms of the other individuals with DNA Ligase IV syndrome. The symptoms include "bird-like" features, microcephaly, pancytopenia, skin abnormalities, growth retardation, neurological abnormalities, occurrences of malignancy and varying degrees of immune deficiencies (O'Driscoll et al., 2001, O'Driscoll et al., 2004). All these symptoms are reminiscent of Nijmegen Breakage Syndrome (NBS) and Ataxia Telangiectasia (AT)(Girard et al., 2000).

Two patient derived fibroblast strains were analysed in this study. GM16088 were derived from a forearm skin biopsy of the radiation sensitive leukaemia patient 180BR (Arlett and Priestley, 1984); GM17523 were derived from a 9 year old individual (99PO149) displaying the clinically more severe characteristics of DNA Ligase IV syndrome (O'Driscoll et al., 2001).

Both fibroblast cultures are viable due to residual Ligase IV activity (Girard et al., 2004, O'Driscoll et al., 2001, Riballo et al., 2001). In mice Lig4 null mutations result in embryonic lethality (Barnes et al., 1998, Gao et al., 1998). In order to create a Ligase IV syndrome model in mice, two mice strains with hypomorphic mutations in the Lig4 gene have been established. The ligase IV activity in both strains is reduced 10 fold and similar symptoms to humans with Ligase IV syndrome are observed (Nijnik et al., 2009, Rucci et al., 2010).

4.2.3 GM16088 or 180BR

Radiation sensitivity is a characteristic of AT (Davis and Kipling, 2009). However, in contrast to AT, normal levels of DNA synthesis inhibition were observed in cells from the180BR patient following radiation (Plowman et al., 1990). Further studies revealed that even low levels of radiation and consequently low quantities of induced DSBs are lethal for cells derived from patient 180BR. This suggested a pre-existing defect in DNA double strand repair and an increased sensitivity to chromosomal breakage (Badie et al., 1995a, Badie et al., 1995b). However members of the DNA-PK complex (Ku70, Ku80 and DNA-PKcs) are expressed at normal levels in these cells. Furthermore, the DNA end binding activity of Ku and DNA-PK activity are indistinguishable from normal cells (Badie et al., 1997). Interestingly, in contrast to AT and NBS, 180BR cells are not compromised in their ability to arrest at cell cycle checkpoints (Badie et al., 1997). The sequencing of the DNA Ligase IV cDNA revealed a homozygous G to A missense mutation at position 833. The substitution of arginine with a histidine (R278H) results in the remodelling of a highly conserved motif close to the active lysine site of the ligase (Riballo et al., 1999). The structural change reduces the ability of DNA Ligase IV to form a stable enzyme-adenylation complex retaining the adenlylation activity in 180BR below 5% of wild type activity (Riballo et al., 1999). In addition to the low adenylation activity, the R278H mutation impairs the double strand and nick ligation ability of Ligase IV in 180BR leaving the Ligase with less then 10% of wild type ligation ability (Girard et al., 2004, Riballo et al., 2001). The mutation also impacts on the V(D)J recombination by inducing imprecise signal end joining (Riballo et al., 2001). V(D)J

joining in 180BR fibroblasts is carried out at a lower frequency than wild type comprising large deletions (2-40 nt) and fewer microhomologies at the joining point (Riballo et al., 2001). Taking this together, the R278H mutation leaves the DNA Ligase IV conformationally unstable and with a ligase activity of less than 10%. In contrast to patient 99PO149, the residual activity of DNA Ligase IV in 180BR is enough to ensure normal development explaining why the patient did not display the more severe symptoms of DNA Ligase IV syndrome (Girard et al., 2004).

4.2.4 GM17523 or 99PO149

Patient 99PO146 displayed characteristic symptoms of NBS but did not have a mutation in NBS1 and produced normal levels of nibrin protein (Cerosaletti et al., 1998, Hiel et al., 2001). Further analysis revealed the patient to be a compound heterozygote for two mutations in the DNA Ligase IV gene (O'Driscoll et al., 2001). The first mutation, a C to T substitution at position 2440 (R814X) results in a truncation of the DNA Ligase IV protein between the two C-terminal BRCT domains present in Lig4. The mutation interferes with the XRCC4 binding ability of Ligase IV leaving the protein complex unstable (Girard et al., 2004, O'Driscoll et al., 2001). The R814X mutation leaves DNA Ligase IV with a barely detectable adenylation activity and a residual double strand ligation activity of 10 – 15% compared to wild type activity (Girard et al., 2004). The second mutation, 1406G>A, converts the amino acid glycine at position 469 in the ligase domain to glutamic acid (G469E), impairing ligase IV function without interfering with the XRCC4 interaction (O'Driscoll et al., 2001). The G469E mutation yields protein with no detectable adenylation and double strand ligation activity. Additionally, only residual nick ligation activity could be detected (Girard et al., 2004). Summing up, both mutations leave GM17523 with less then 1% of DNA Ligase IV activity accounting for the more severe phenotype of patient 99PO146 (Girard et al., 2004).

4.2.5 Aims

The aim of this work was to determine if DNA Ligase IV deficiency influences telomere dynamics and most interestingly, if DNA Ligase IV is involved in the mechanistic pathway fusing short dysfunctional telomeres.

4.3 Results

4.3.1 Optimising the replicative lifespan of DNA Ligase IV syndrome cells

Radical oxygen species like superoxides, hydrogen peroxide and hydroxyl radicals (Halliwell, 1996) can induce different levels of DNA damage in primary human fibroblast cultures resulting in premature cell cycle arrest and a significant reduction of the replicative lifespan of the cells (Forsyth et al., 2003). Large quantities of non-proliferating cells in a culture can create an artificial increase in the telomere erosion rate (Chen et al., 1995). Furthermore, other studies suggest that oxygen tension directly influences the telomere erosion rate by inducing DNA damage in the telomeric regions (von Zglinicki, 2002). Both DNA Ligase IV deficient cell lines are impaired in their ability to repair DNA damage (Badie et al., 1995b). Therefore oxidative stress may aggravate the cells phenotype and consequently attenuate the cultures replicative lifespan and influence the telomere dynamics observed in these cells.

In order to determine the influence of oxidative tension on the DNA Ligase IV syndrome cells strains GM16088 and 17523, both fibroblast lines were either cultured under physiological oxygen levels of 3% O_2 or normal culture conditions of 20% oxygen. The cells were passaged serially and the accumulated PDs were plotted as a function of time (Fig. 4.1). In line with a previous study (Badie et al., 1997), the replicative lifespan of both DNA ligase IV syndrome cultures was limited and the cells ceased to grow after 20 – 25 passages.

For the cells derived from the DNA ligase IV syndrome patient 180BR (GM16088), the growth curves for both culture conditions are similar (Fig. 4.1a) No increase in replicative lifespan could be achieved by culturing the cells at physiological oxygen concentrations (3% O_2). The cells at 20% and 3% oxygen reached their replicative limit PD 25 and PD 27, respectively. The growth rates of both cultures, calculated for the exponential growth phase of the cells, were determined to be 0.195 PD/day ± 0.115 PD/day at 20% O_2 and 0.206 PD/day ± 0.127 PD/day at 3% O_2.

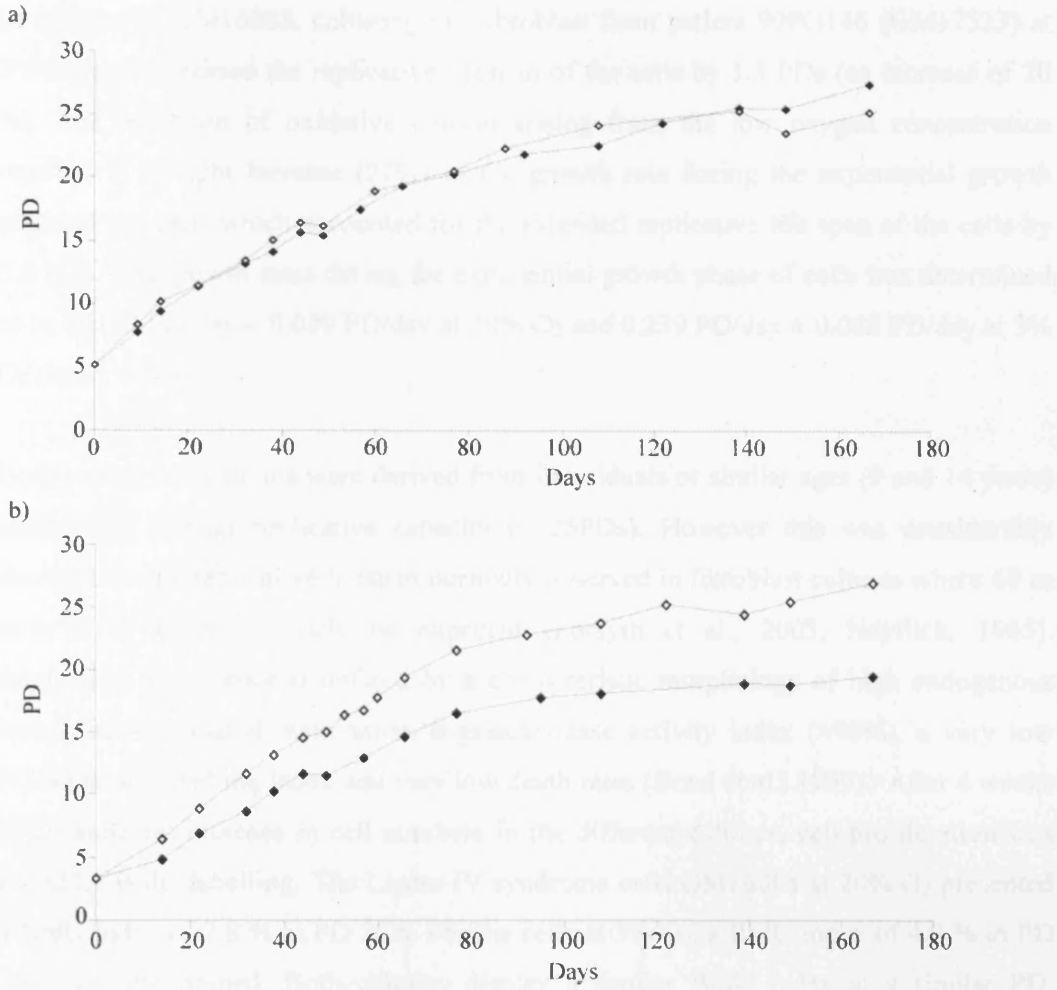

Figure 4.1 Growth curves of DNA Ligase IV syndrome firoblast strains GM16088 and GM 17523 cultured in 3 and 20% oxygen. Growth curves were plotted as a function of population doublings (PD) versus time in days. a) cells derived from patient 180BR (GM16088) b) fibroblast derived from patient 99PO146 (GM17523). Filled markers represent fibroblast cultured at 20% oxygen and open markers represent those cultured in 3% oxygen.

In contrast to GM16088, culturing the fibroblast from patient 99PO146 (GM17523) at 3% oxygen increased the replicative lifespan of the cells by 5.5 PDs (an increase of 20 %). The reduction of oxidative tension arising from the low oxygen concentration resulted in a slight increase (27%) in the growth rate during the exponential growth phase of the cells which accounted for the extended replicative life span of the cells by 5.5 PDs. The growth rates during the exponential growth phase of cells was determined to be 0.173 PD/day ± 0.089 PD/day at 20% O_2 and 0.239 PD/day ± 0.088 PD/day at 3% O_2 (mean ± SD).

Both primary cell strains were derived from individuals of similar ages (9 and 14 years) exhibited a similar replicative capacity (~ 25PDs). However this was considerably shorter than the replicative lifespan normally observed in fibroblast cultures where 60 or more PDs would typically be expected (Forsyth et al., 2003, Hayflick, 1965). Replicative senescence is defined by a characteristic morphology of high endogenous senescence-associated mammalian β-galactosidase activity index (>90%), a very low (<3%) BrdU labelling index and very low death rates (Bond et al., 1999). After 4 weeks of no apparent increase in cell numbers in the different cultures, cell proliferation was tested by BrdU labelling. The Ligase IV syndrome cells GM16088 at 20% O_2 presented a BrdU index of 7.8 % in PD 25.6. For the cells at 3% O_2, a BrdU index of 4.9 % in PD 25.3 was determined. Both cultures display a similar BrdU index at a similar PD, supporting the assumption that lower oxygen levels do not extend the replicative capacity of these cells.

The second fibroblast strain GM17523, a BrdU index of 3.4 % at PD 19.0 in 20% O_2 and a BrdU index of 38 % at PD 24.5 at 3% O_2 were established. All 4 cultures were allowed to proliferate for an additional 3 weeks. However after this time, the average cell number in both fibroblast cultures at both oxygen concentrations had diminished to less then 7×10^4 cells. In order to gain sufficient amount of DNA for STELA and Fusion assay, no BrdU labelling was carried out for the last sample of the cultures. It was assumed that all cultures except GM 17523 at 3% O_2 had reached senescence.

4.3.2 Telomere dynamics of the DNA Ligase IV syndrome cells

In order to investigate whether residual DNA Ligase IV activity influences telomere dynamics, the XpYp and 17p telomere length distribution of GM16088 and GM17523 under both culture conditions were determined by using single telomere length analysis (STELA)(Baird et al., 2003). In line with previous studies in the group (Baird and Farr, 2006, Baird et al., 2003, Britt-Compton et al., 2006), only the XpYp and 17p telomere were analysed, as average telomere length conforms to the mean XpYp telomere length and telomere erosion resulting from the end replication problem is similar at most chromosome ends. Multiple samples were taken during the proliferative lifespan of the cultures and subjected to STELA.

The STELA profiles for DNA ligase IV deficient fibroblast derived from patient 180BR (GM16088) cultured at 20 and 3% oxygen are displayed in figure 4.2 to 4.4. It was apparent that the telomere distributions were complex with bimodal distributions observed at the XpYp telomere in both culture conditions (Fig. 4.2 a and 4.4 a). These distributions changed as the cells reached the end of their replicative capacity and the loss of the lower distribution could be observed. Although less obvious, bimodal distributions were also observed at the 17p telomere in both oxygen concentration (Fig. 4.2 b and 4.4 b). Again it was apparent that the lower distribution was lost as the cells in 3% oxygen reached the end of their replicative lifespan. The same loss could not be observed in the cells at 20% oxygen. Comparing the STELA analysis of GM16088 at both oxygen concentration with the growth curves (Fig. 4.1 a), it was evident that both cultures of GM16088 exited the exponential growth phase after approximately 77 days in culture. The loss of the lower distributions in XpYp and 17p STELA at 20 and 3% oxygen in the last PDs of the cultures resulted in an artificial increase in telomere length (for 20% O_2: PD 25.5 and 27.5 in Fig. 4.2 and 4.5; for 3% O_2: PD 23.7 and PD 25.3 in Fig. 4.4 and 4.5). Therefore the minimal telomere length in senescent non-proliferating GM16088 cells at both oxygen concentrations was determined at PD 20.5 prior to the loss of the lower distribution. Examining both cultures of GM16088 at this PD point showed that the bimodal XpYp telomere length

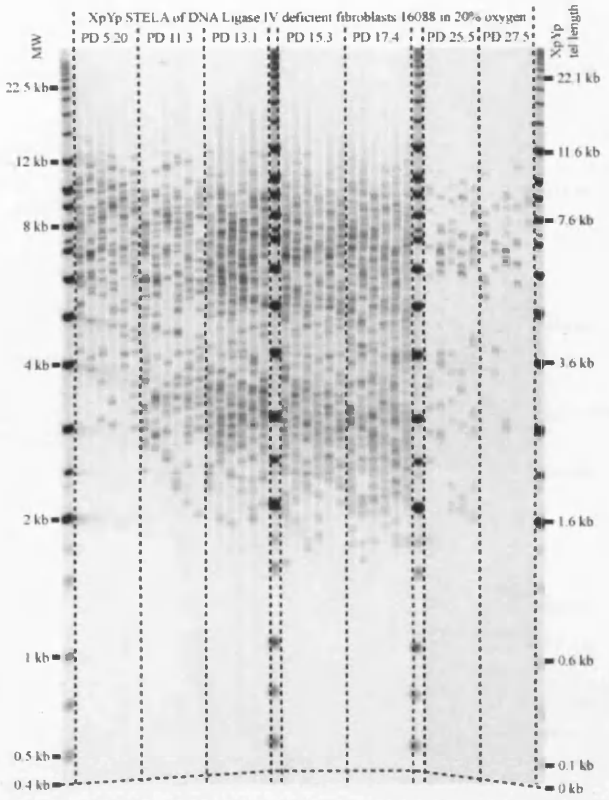

Upper (kb)	7.80	7.20	6.60	5.50	5.40	5.40	5.40
Lower (kb)	N.A.	2.40	2.20	2.15	1.90	2.35	N.A.
SD (kb)	2.41	2.46	2.38	2.37	2.41	2.28	1.76

Figure 4.2 a. XpYp STELA gel displaying the telomere length profile of DNA Ligase IV deficient fibroblast 16088 in 20% oxygen. Starting from the point cells were taken into culture, population doublings (PD) are presented above the gel. Molecular Weight (MW) is indicated on the left and the corrected telomere length is indicated on the right. Modal upper and lower telomere length and corresponding standard deviation (SD) are detailed below the gel. N.A. Not applicable because no telomere molecules were present. PCR products were detected using the telomere repeat probe.

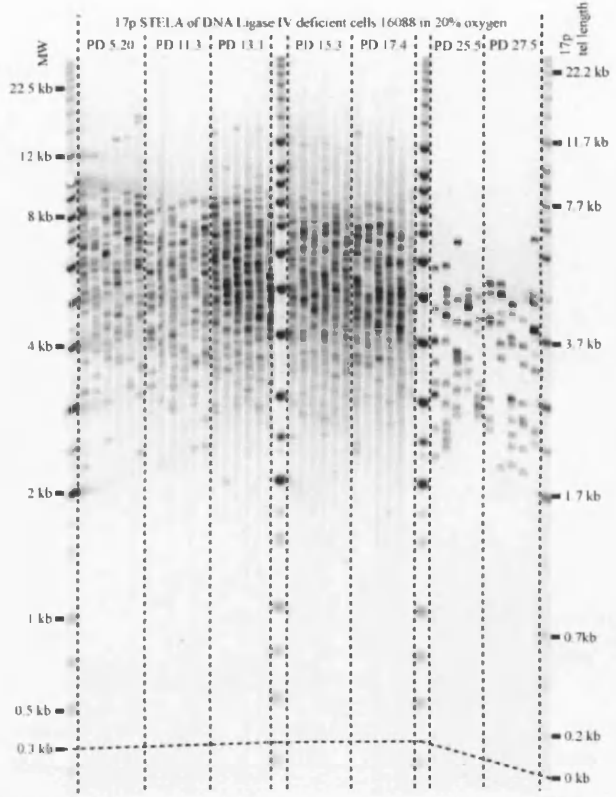

Median (kb)	5.90	4.90	5.05	4.86	4.73	3.33	3.64
SD (kb)	2.46	1.56	1.87	1.72	1.77	0.95	1.06

Figure 4.2 b STELA gel displaying the 17p telomere length profile of DNA Ligase IV deficient fibroblast 16088 in 20% oxygen. Starting from the point cells were taken into culture, population doublings (PD) are presented above the gel. Molecular Weight (MW) is indicated on the left and corrected telomere length is indicated on the right. Mean telomere length and corresponding standard deviation (SD) are detailed below the gel. PCR products were detected using telomere repeat probe.

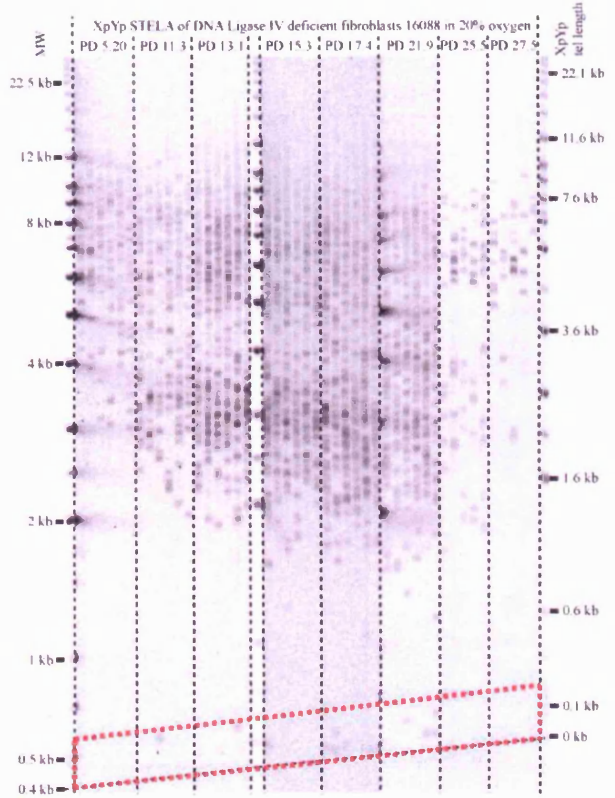

Upper (kb)	7.80	7.20	6.60	5.50	5.40	5.25	5.40	5.40
Lower (kb)	N.A.	2.40	2.20	2.15	1.90	1.85	2.35	N.A.
SD (kb)	2.41	2.46	2.38	2.37	2.41	2.19	2.28	1.76

Figure 4.3 a XpYp STELA gel displaying the telomere length profile of DNA Ligase IV deficient fibroblast 16088 in 20% oxygen. The gel was probed with the telomere adjacent probe. Starting from the point cells were taken into culture, population doublings (PD) are presented above the gel. Molecular Weight (MW) is indicated on the left and the corrected telomere length is indicated on the right. Mean telomere length and corresponding standard deviation (SD) are detailed below the gel.

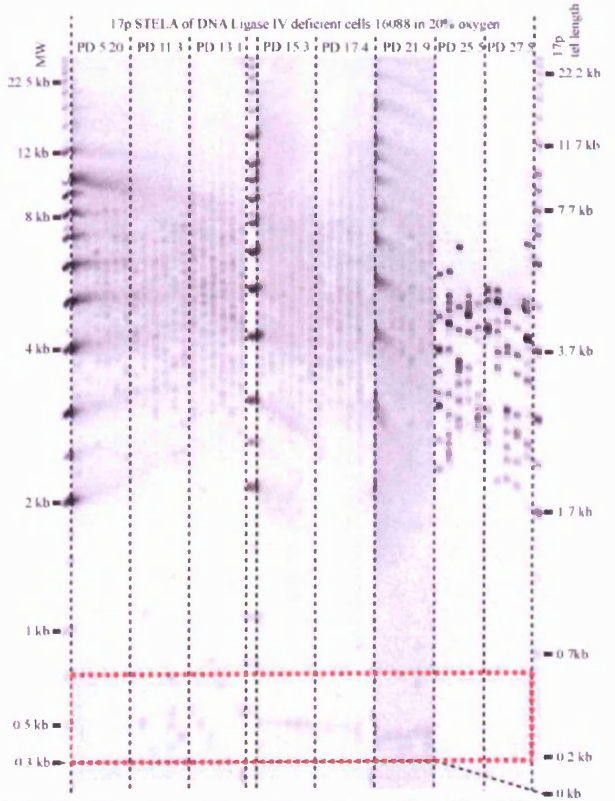

Median (kb)	5.90	4.90	5.05	4.86	4.73	4.37	3.33	3.64
SD (kb)	2.46	1.58	1.87	1.72	1.77	1.44	0.95	1.06

Figure 4.3 b STELA gel displaying the 17p telomere length profile of DNA Ligase IV deficient fibroblast 16088 in 20% oxygen. The gel was probed with the telomere adjacent probe. Starting from the point cells were taken into culture, population doublings (PD) are presented above the gel. Molecular Weight (MW) is indicated on the left and corrected telomere length is indicated on the right. Mean telomere length and corresponding standard deviation (SD) are detailed below the gel.

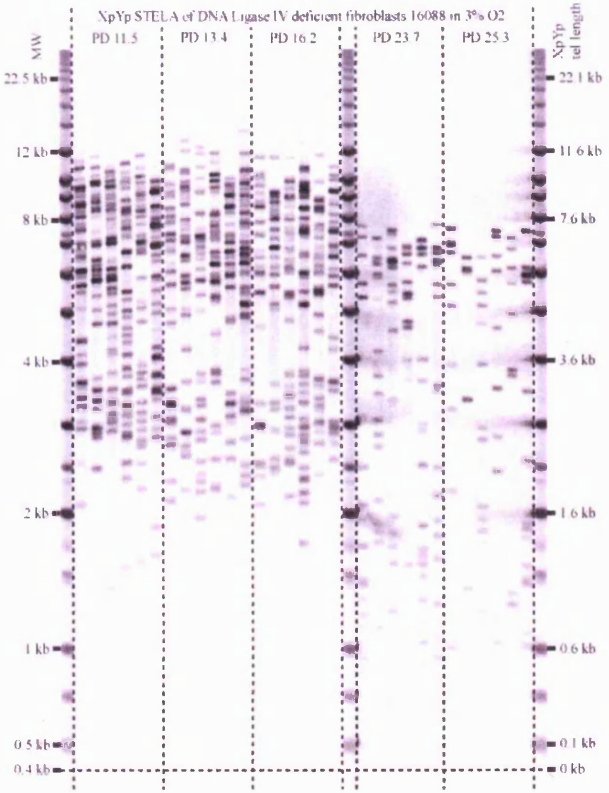

Upper (kb)	5.50	5.20	5.20	5.65	5.35
Lower (kb)	2.40	2.10	2.00	0.60	0.60
SD (kb)	2.51	2.57	2.37	2.29	2.30

Figure 4.4.a XpYp STELA gel dislaying the telomere length profile in DNA Ligase IV deficient cells 16088 in 3% oxygen. Starting from the point fibroblasts were taken into culture, population doublings (PD) are presented above the gel. Molecular Weight (MW) is indicated on the left and the corrected telomere length is indicated on the right. Upper and lower modal telomere length and corresponding standard deviation (SD) in kb are detailed below the gel.

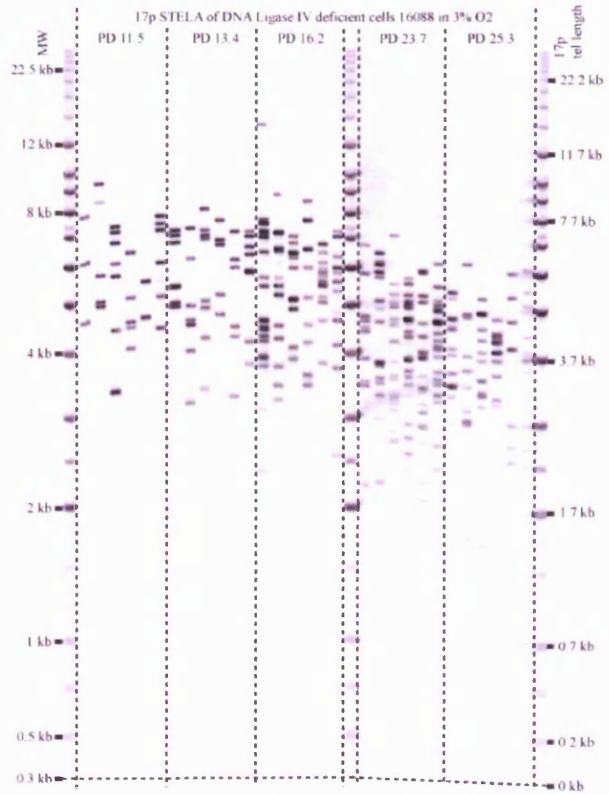

Mean (kb)	6.40	6.30	5.52	3.87	3.72
SD (kb)	1.77	1.58	1.77	1.34	1.07

Figure 4.4.b STELA gel displaying the 17p telomere length profile of DNA Ligase IV deficient cells 16088 in 3% oxygen. Starting from the point fibroblasts were taken into culture, population doublings (PD) are presented above the gel. Molecular Weight (MW) is indicated on the left and corrected telomere length is indicated on the right. Mean telomere length and the corresponding standard deviation (SD) are detailed below the gel.

a)

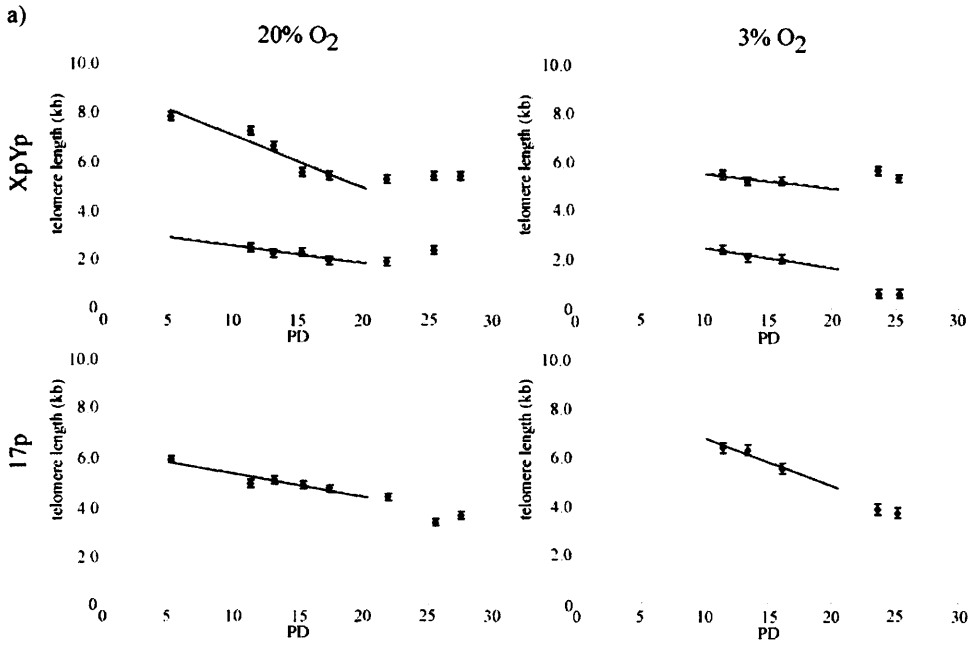

b)

telomere	Erosion rate bp/PD	20% O_2 R2	Number of Data points	Erosion rate bp/PD	3% O_2 R2	Number of Data points
XpYp	211.8	0.891	5	60.2	0.665	3
	70.3	0.788	4	82.6	0.866	3
17p	93.2	0.865	5	194.5	0.897	3
Overall mean	125.4		Overall mean	112.4		
Overall SD	43.9		Overall SD	41.5		

Figure 4.5 Summarising the telomere erosion rate data of DNA Ligase IV deficient cells 16088 in 20 and 3% oxygen. a) Telomere erosion rate is calculated as the slope of the regression line after plotting the median telomere length against the corresponding PD. Individual telomere are detailed on the right, oxygen concentration is displayed above, error bars are ± standard error, y-axis presents median telomere length, x-axis presents PD. b) Erosion rates, accompanying R2 and the number of data points for each chromosome are displayed. Overall median and corresponding standard deviation are also detailed.

distribution obtained similar minimal values at senescence in both culture conditions (it was not possible to calculate a p-value for the bimodal distributions).

The upper and lower XpYp modal distribution reached a telomere length at senescence of 5.2 kb and 1.9 kb respectively (Figure 4.2 a and 4.4 a). Moreover the 17p median telomere length of both cultures obtained similar values of 5.0 kb at senescence (Fig. 4.2 b and 4.4 b) (p-value: 0.441, two tailed t-test). This was consistent with the similar replicative histories of the cells in the two oxygen concentrations.

The fastest growth rates were observed in the first 15 PDs of the culture, with a gradual slowing of the growth rate as the cells entered the end of their replicative capacity. During the first 15 PDs at 20% O_2, the bimodal XpYp telomere length distribution decreased by 2.6 kb at the upper modal length whereas the lower distributions decreased by 0.5 kb. For the 17p telomere, the culture at 20% O_2 displayed a loss of 0.9 kb in the median 17p length whereas at 3% O_2 a decrease of 1.5 kb at the mean 17p length could be observed. The telomere erosion rate data for DNA ligase IV deficient fibroblasts GM16088 for 20% and 3% oxygen is summarised in Fig. 4.5. XpYp and 17p telomere erosion rates were calculated separately. The erosion rate of both GM16088 cultures the combined average erosion rate of both telomere ends was determined to be 125.4 ± 43.9 in 20% O_2 compared to 112.4 ± 41.5 in 3% O_2 (bp/PD $\pm$ SE).

STELA requires the sequential hybridisation of the blots with two hybridisation probes; a telomere-adjacent probe and then the telomere-repeat containing probe. This allows the detection of shorter molecules that do not contain many TTAGGG repeats with the telomere-adjacent probe. Interestingly, the telomere adjacent probe for XpYp and 17 (Fig 4.3) revealed the presence of an additional distribution of very short telomeres in cells cultured at 20% oxygen (red box). These short telomeres are in a length range at which fusion has been detected (< 252 bp) (Capper et al., 2007, Letsolo et al., 2009). The frequency of these short XpYp telomeres (on average < 1% of the analysed molecules, Fig 4.3 a) did not appear to be different than those observed in normal fibroblasts (Baird et al., 2003, Britt-Compton et al., 2006). However in these previous

studies, the calculated frequencies refer to the presence of stochastically significantly shorter telomeres in unimodal distribution. Due to the bimodal distribution of the XpYp telomere in Ligase IV deficient cells GM16088, it was not possible to determine whether these short telomeres are either significantly shorter than the normal distribution of telomeres or just a distribution of accumulating short telomeres. The frequency for the 17p telomere (Fig. 4.3 b) was only calculated for PD 11.3 and 13.1, since it was not feasible to exclude that the recurring band in PD 15.3 to PD 21.9 was not a contamination of the STELA reaction or a hybridisation artefact. On average 3.8 % of the 17p telomere in GM 16088 are shorter than 450 bp (it was not possible to determine if this is significant due to the bimodal distribution of the 17p telomere).

The telomere length profiles for the second DNA Ligase IV syndrome culture GM17523 at 20% and 3% oxygen are shown in figure 4.6 and 4.7. Again, these displayed complex telomere length profiles. At 20% O_2 bimodal distributions were evident at both the XpYp and the 17p telomere. However a clear tri-modal distribution occurred as the cells progressed to the end of their replicative capacity. The appearance of the additional distribution appeared to coincide with a substantial decrease in the upper distribution between PDs 16.5 and 17.8. As the BrdU index is less than 3.4 % for the cells at 20% O_2, it was not possible to determine the minimal telomere length at senescence due to the unusual telomere distribution. At 3% O_2, the cells displayed a telomere length distribution that was markedly shorter at the 17p telomere (Fig. 4.7 b). This is distinct from any other telomere length distribution recorded by STELA (Baird and Farr, 2006, Baird et al., 2003, Britt-Compton et al., 2006). The distribution remained constant through out the first 23 PDs of the culture and represents on average 14.4 % (ranging from 10.3 % to 20.3 %) of the total number of telomeres. The distribution disappeared in later samples.

In order to define the rates of telomere erosion in GM17523 fibroblast at both oxygen concentrations, the growth curves were compared with the STELA analysis of the cells. Like GM16088, both cultures exit exponential growth approximate 77 days in

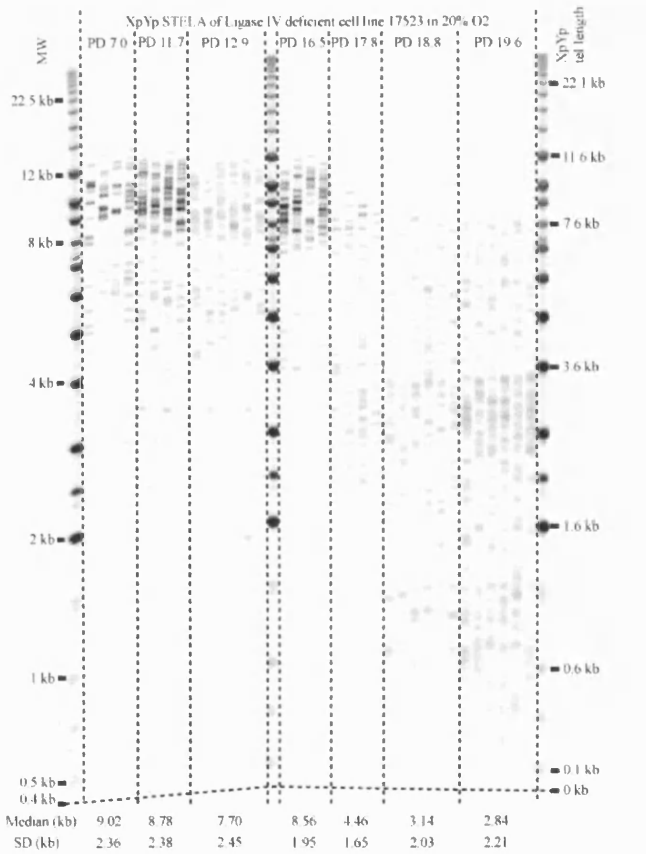

Figure 4.6 a STELA gel displaying the XpYp telomere length profile of DNA Ligase IV syndrome fibroblasts 17523 in 20% oxygen. Starting from the point cells were taken into culture, population doublings (PD) are presented above the gel. Molecular Weight (MW) is indicated on the left and the corrected telomere length is indicated on the right. Median telomere length and corresponding standard deviation (SD) in kb are detailed below the gel.

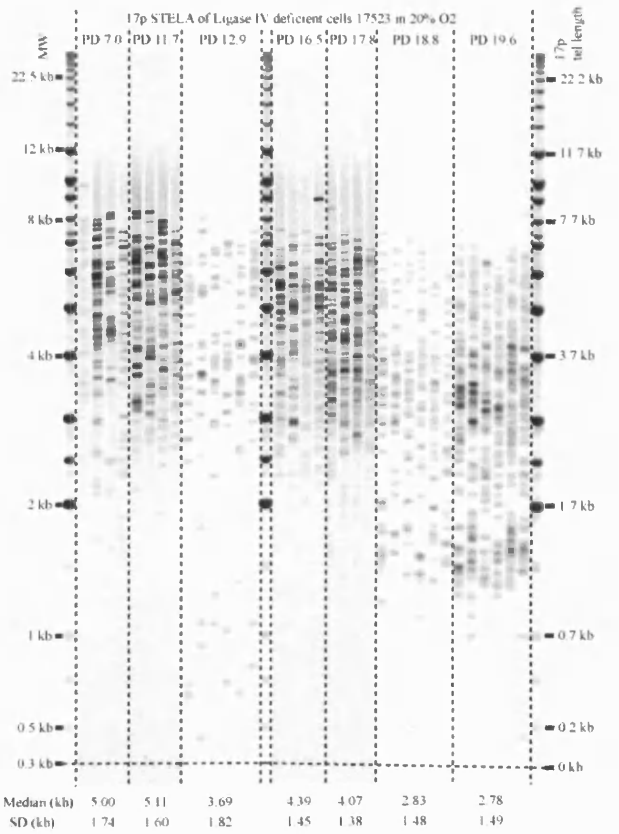

Figure 4.6 b 17p STELA gel displaying the telomere length profile in DNA Ligase IV syndrome cells 17523 in 20% oxygen. Starting from the point fibroblasts were taken into culture, population doublings (PD) are presented above the gel. Molecular Weight (MW) is indicated on the left and the corrected telomere length is indicated on the right. Median telomere length and corresponding standard deviation (SD) in kb are detailed below the gel.

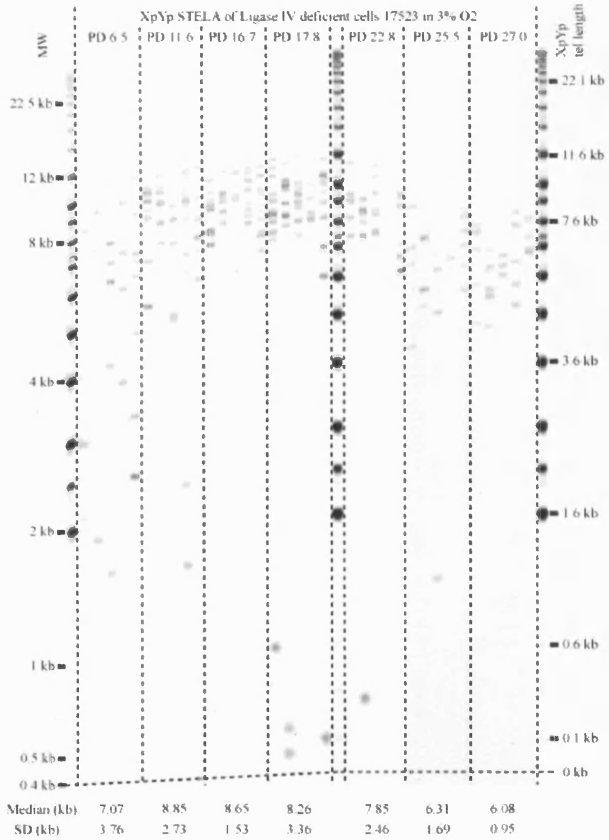

Figure 4.7 a STELA gel displaying the XpYp telomere length profile of DNA Ligase IV syndrome firbroblasts 17523 in 3% oxygen. Starting from the point cells were taken into culture, population doublings (PD) are presented above the gel. Molecular Weight (MW) is indicated on the left and corrected telomere length is indicated on the right. Median telomere length and corresponding standard deviation (SD) are detailed below the gel

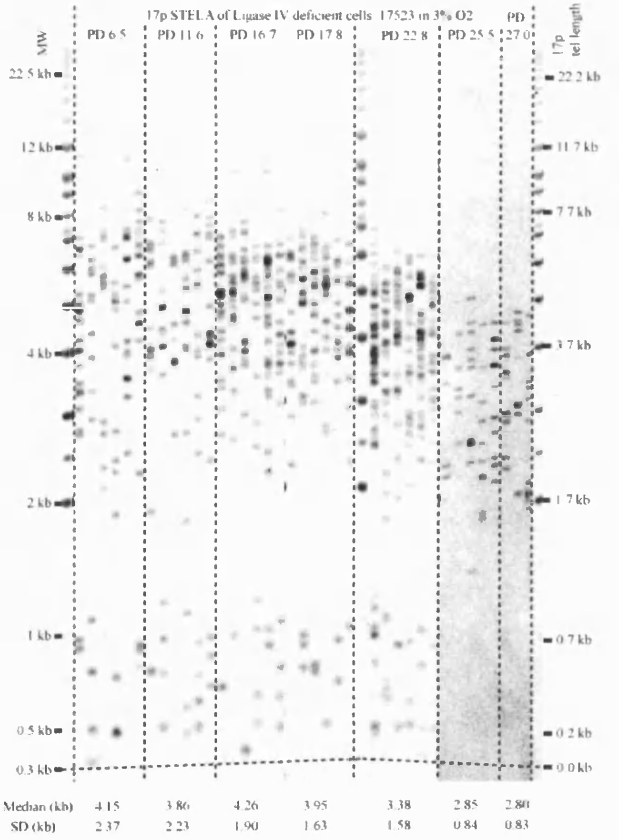

Figure 4.7 b STELA gel diplaying the 17p telomere length profile of DNA Ligase IV syndrome fibroblasts 17523 in 3% oxygen. Starting from the point cells were taken in culture, population doublings (PD) are presented above the gel. Molecular Weight (MW) is indicated on the left and corrected telomere length is indicated on the right. Median telomere length and corresponding standard deviation (SD) in kb are detailed below the gel

a)

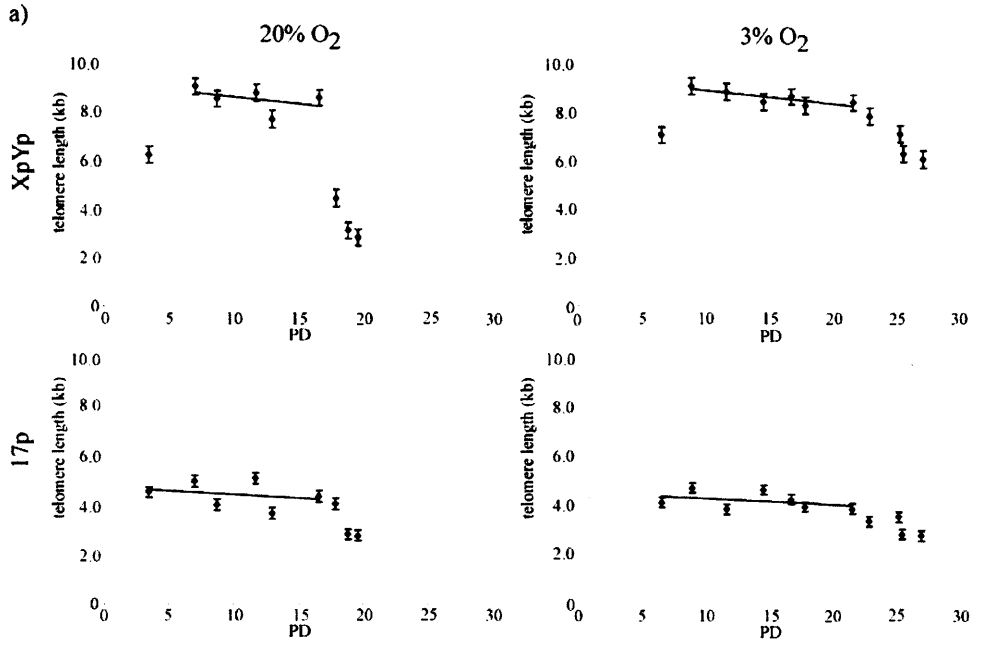

b)

telomere	Erosion rate bp/PD	20% O_2 R2	Number of Data points	Erosion rate bp/PD	3% O_2 R2	Number of Data points
XpYp	56.9	0.185	5	56.4	0.701	6
17p	30.8	0.069	6	26.4	0.153	7
Overall mean	43.9		Overall mean	41.5		
Overall SD	13.1		Overall SD	14.1		

Figure 4.8 Summarising the telomere erosion rate data of DNA Ligase IV syndrome cells 17523 in 20 and 3% oxygen. a) Telomere erosion rate is calculated as the slope of the regression line after plotting the median telomere length against the corresponding PD. Individual telomere are detailed on the right, oxygen concentration is displayed above, error bars are ± standard error, y-axis presents median telomere length, x-axis presents PD. b) Erosion rates, accompanying R2 and the number of data points for each chromosome are displayed. Overall mean and corresponding standard deviation (SD) are also detailed.

culture (Fig. 4.1b). During this phase of growth the loss of telomere length at 20% O_2 for XpYp was 0.46 kb and 0.61 kb for the 17p telomere, over 9.57 PDs. At 3% O_2 the loss for XpYp was 0.66 kb and 0.84 kb at the 17p telomere over 15 PDs. The erosion rates were calculated for the exponential growth phase for XpYp and 17p at each oxygen concentration and are shown in Fig. 4.8. The overall mean rates of erosion of GM17523 were determinded to be 43.85 ± 13.05 bp/PD at 20% O_2 and 41.50 ± 14.09 bp/PD at 3% O_2 (mean ± SD).

4.3.3 Telomere dynamics of DNA Ligase IV syndrome fibroblast expressing HPV E6E7 oncoproteins

In order to examine the role of Ligase IV in telomere fusion, the cells were forced to proliferate beyond the point of senescence. To do this both Ligase IV deficient fibroblasts cultures GM 16088 and GM17523 were transfected with HPV16 E6E7. The HPV16 E6E7 oncoproteins abrogate the function of p53 and Rb and therefore can extend the replicative lifespan of normal cells by typically 26 – 28 PDs (Bond et al., 1999, Capper et al., 2007). Thus, allowing cells to continue to divide and consequently the telomeres to erode within the length range where they become de-protected and can undergo fusion.

Initial experiments in Ligase IV deficient cells showed that transfection of HPV16 E6E7 approximately 3 PDs before the point of senescence was lethal, with no extension of proliferate lifespan. Transfection was therefore repeated at an earlier PD point (PD 9). This was carried out for both DNA Ligase IV syndrome strains at both 20 and 3% oxygen. However it was clear that these cells do not tolerate the presence of HPV16 E6E7, or they were sensitive to transfection, as they displayed low transfection efficiencies compared to similar experiments in normal cells. The cells grew poorly in highly diluted cultures and clones could only be established in 20% O_2 with GM16088 and in 3% O_2 with GM17523, with the other two conditions yielding no viable cell clones. The presence of E6E7 did not yield any obvious extension in the replicative lifespan (Fig. 4.9). Indeed the control clones of GM17523 expressing neomycin exhibit a

longer replicative capacity than the clones expressing E6E7. However the presence of E6E7 resulted in large quantity of non-viable floating cells in the cultures at both 20% and 3% oxygen.

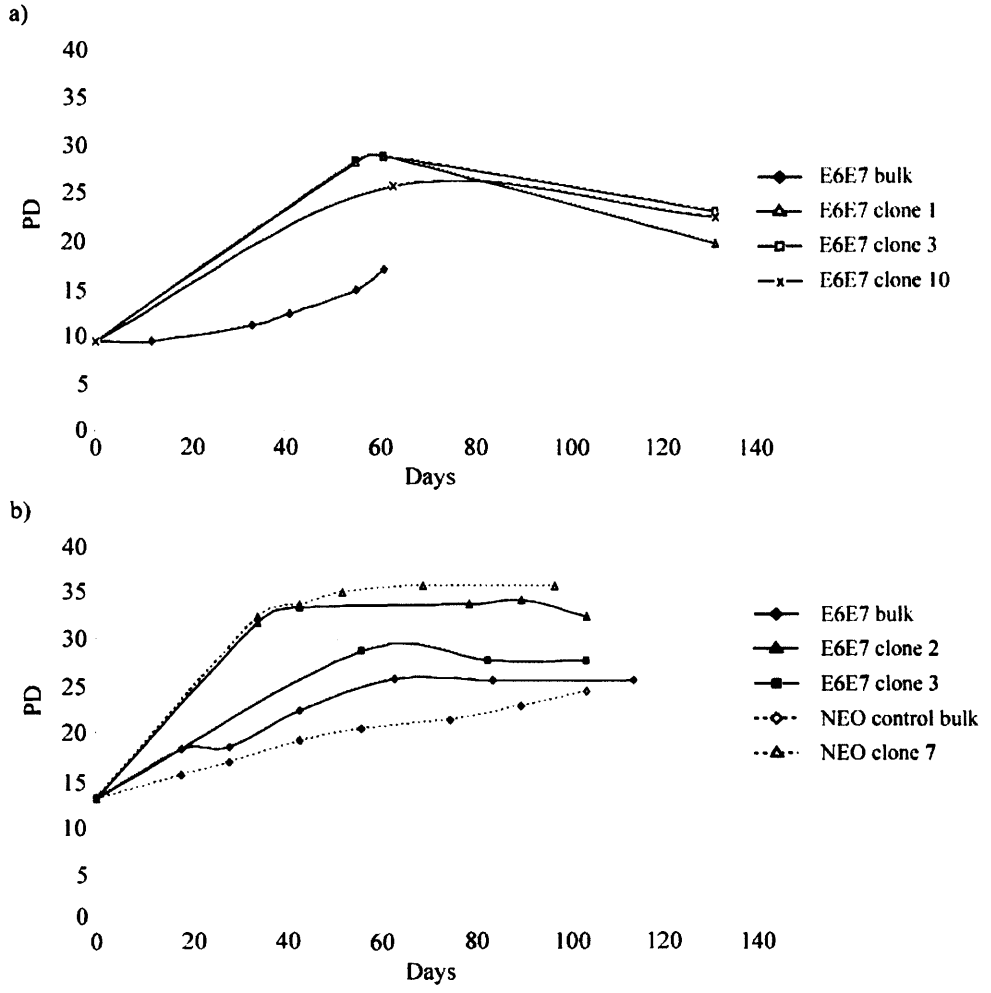

Figure 4.9 Growth curves of parental bulk populations and clonal derivatives of Ligase IV syndrome firoblast strains GM16088 and GM 17523 expressing HPV16 E6E7. Growth curves were plotted as a function of population doublings (PD) versus time in days. a) GM16088 expressing E6E7 in 20% O_2 b) GM17523 expressing E6E7 in 3% O_2

A total of 7 GM16088 clones expressing E6E7 were obtained. However after 130 days post transfection, only an average cell count of 1×10^4 cells for E6E7 clones could be achieved in 20% O_2. None of the clones expressing empty vector accomplished viable cell numbers (Fig. 4.10). At 3% O_2 no clones either E6E7 or neomycin attained usable cell numbers. For GM17523 a total of 10 E6E7 clones were obtained in 3% O_2 with less than 1×10^4 cells per clone after 104 days in culture, no clones were obtained in 20% O_2. 3 clones with the neomycin expressing empty vector (clones 2, 7 and 17) were also obtained (Fig 4.11).

Given the small number of cells obtained from the HPV16 E6E7 and control clones, DNA was extracted using the special Qiagen micro kit designed for the analysis of forensic DNA samples. STELA was undertaken to examine the telomere length profiles of all the clones (Fig 4.10 and 4.11). The GM16088 E6E7 clones at 20% O_2 and the GM17523 E6E7 clones at 3% O_2 display similar modal distribution like the parental populations (Fig. 4.2 and 4.7). In line with previous observations of clonal growth (Baird and Farr, 2006, Baird et al., 2003, Britt-Compton et al., 2006, Capper et al., 2007), the telomere length distribution were much more homogenous than the parental bulk populations despite the long period in culture. However, comparing the telomere length of the isolated clones to the parental cultures undergoing replicative senescence (Fig. 4.2), it was apparent that no obvious difference in telomere length could be observed. This is in contrast to the STELA profiles from similar experiments in the normal human MRC5 fibroblasts where E6E7 expression extends the lifespan for 26 – 28 PDs and consequently telomeres continued to loose another 2 kb resulting in the complete loss of one or more telomeric alleles (Capper et al., 2007) (chapter 3 in this thesis).

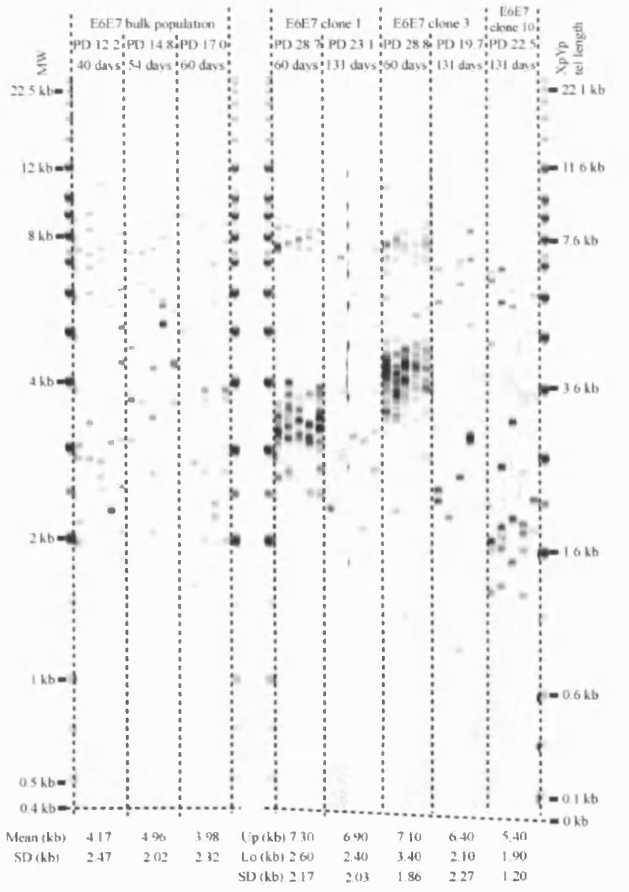

Figure 4.10 a XpYp STELA gel displaying the telomere length profile of DNA Ligase IV deficient fibroblast 16088 expressing HPV16 E6E7 in 20% oxygen. The gel was probed with the telomere adjacent probe. Starting from the point cells were taken into culture, population doublings (PD) are presented in the first line above the gel. In the second line above the gel displays the the days cells were kept in culture after infection. Molecular Weight (MW) is indicated on the left and the corrected telomere length is indicated on the right. Mean or modal telomere length and corresponding standard deviation (SD) in kb are detailed below the gel. (Up) upper modal telomere length, (Lo) lower modal telomere length

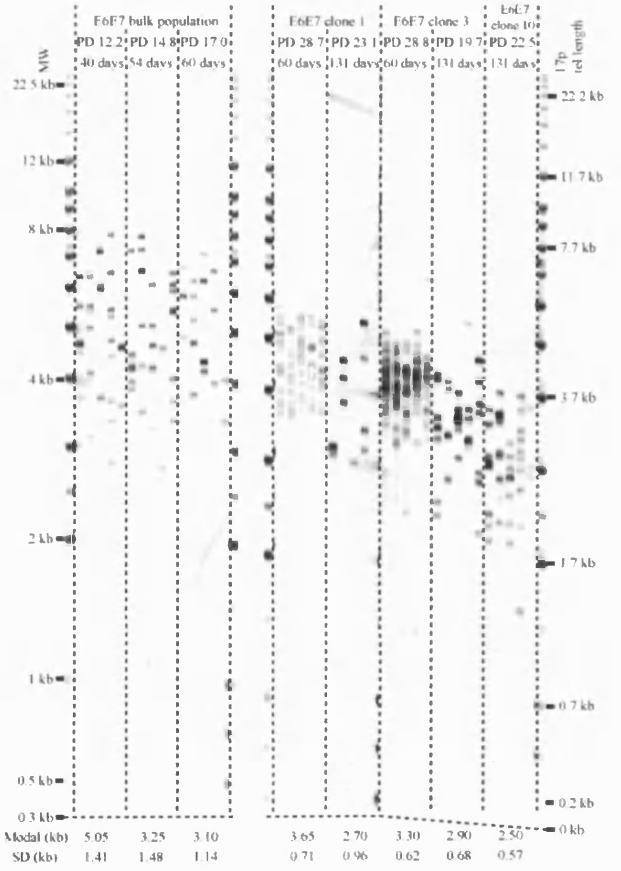

Figure 4.10 b 17p STELA gel displaying the telomere length profile of DNA Ligase IV deficient fibroblast 16088 expressing HPV16 E6E7 in 20% oxygen. The gel was probed with the telomere adjacent probe. Starting from the point cells were taken into culture, population doublings (PD) are presented in the first line above the gel. In the second line above the gel displays the the days cells were kept in culture after infection. Molecular Weight (MW) is indicated on the left and the corrected telomere length is indicated on the right. Modal telomere length and corresponding standard deviation (SD) in kb are detailed below the gel

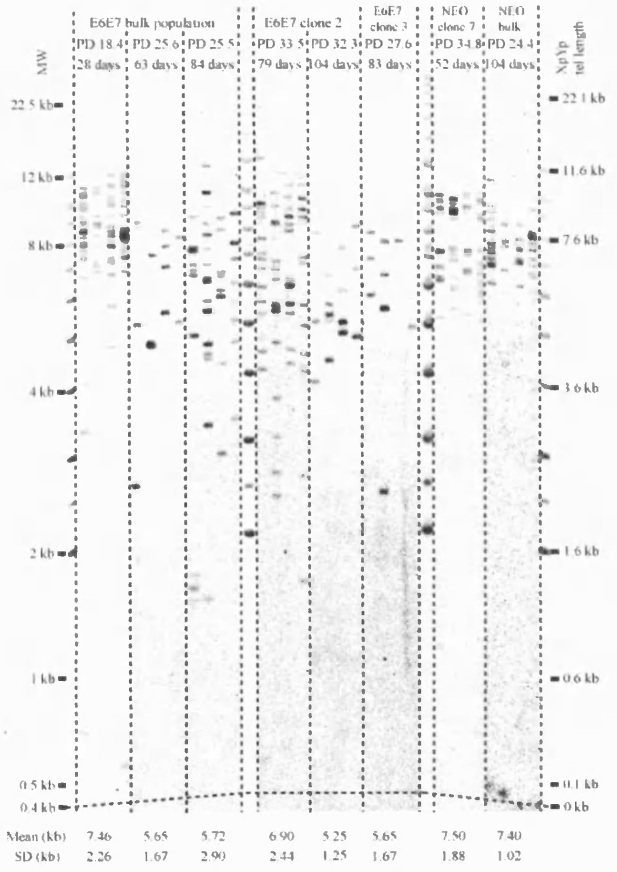

Figure 4.11 a XpYp STELA gel displaying the telomere length profile of DNA Ligase IV syndrome fibroblast 17523 expressing HPV16 E6E7 in 3% oxygen. The Gel was probed with the telomere adjacent probe. Starting from the point cells were taken into culture, population doublings (PD) are presented above the gel. Molecular Weight (MW) is indicated on the left and the corrected telomere length is indicated on the right. Mean telomere length and corresponding standard deviation (SD) in kb are detailed below the gel.

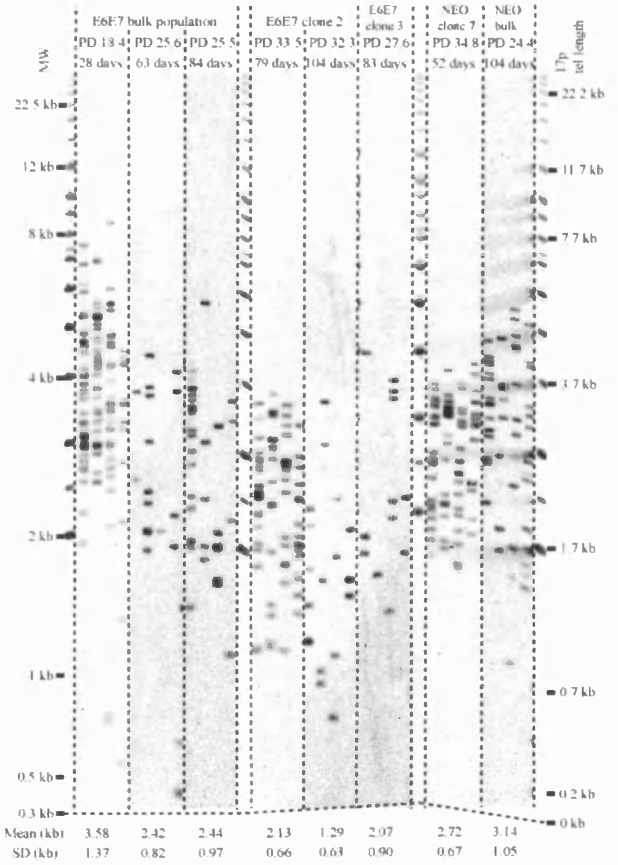

Figure 4.11 b 17p STELA gel displaying the telomere length profile of DNA Ligase IV deficient fibroblast 17523 expressing HPV16 E6E7 in 3% oxygen. The Gel was probed with the telomere adjacent probe. Starting from the point cells were taken into culture, population doublings (PD) are presented above the gel. Molecular Weight (MW) is indicated on the left and the corrected telomere length is indicated on the right. Mean telomere length and corresponding standard deviation (SD) in kb are detailed below the gel.

4.3.4 Fusion Assay of DNA Ligase IV deficient fibroblasts expressing HPV16 E6E7

The expression of HPV16 E6E7 in DNA Ligase IV syndrome cells lines GM16088 and GM17523 failed to push average telomere length distribution of DNA Ligase IV deficient fibroblasts into the length range at which telomeres become unprotected and undergo fusion (Figures 4.10 and 4.11). Nevertheless an accumulation of critically short telomeres could be detected in both fibroblast cultures (Figures 4.2b, 4.3b, 4.6 b, 4.7 and 4.11). Previous work in the group has shown that even sporadic stochastically deleted telomeres can lead to fusion events in normal human cells (Capper et al., 2007). The presence and quantity of telomere-telomere fusion events in DNA Ligase IV syndrome cells was determined by using long-range single molecule PCR amplifications with 3 primers for XpYp, 17p and 21q group telomeres (21q, 1q, 2q, 5q, 6q, 6p, 8p, 10q, 13q, 17q, 19p, 19q, 22q and the 2q13 interstitial telomeric locus) (Letsolo et al., 2009) (Fig. 4.12). However due to the limited number of cells that could be obtained from both the bulk parental populations (max. 5×10^5 cells; min. 2×10^4 cells) or the HPV16 E6E7 expressing fibroblast cultures (average 1×10^4 cells), there was a limited amount of DNA that could be analysed. The fusion assay detects a limited number of possible fusion events in the human genome and thus large number of input cells equivalents are required to detect single fusions (Capper et al., 2007, Letsolo et al., 2009). Nine fusion reactions were undertaken containing 10ng of DNA (20-40 times less that typically is used for this type of analysis). Despite this limitation it was possible to detect fusions in the Ligase IV syndrome fibroblast. Interestingly these were detected in the bulk parental populations, whilst rare, the frequency of fusion in GM16088 involving XpYp and 17p was 1.3×10^{-4}, 30 times higher than the frequency of 4×10^{-6} observed in normal fibroblasts with a similar relatively long telomere distribution (Capper et al., 2007). In the second Ligase IV syndrome fibroblast culture GM17523, only one fusion involving the 17p telomere was observed giving a fusion frequency of 6.7×10^{-5}. Even being very low, the frequency is still 16 times higher than the frequency observed in normal fibroblasts. In addition, it was apparent that more fusions could be detected in the 21q group of telomeres. However the specificity of the probe used to detect the 21q group is not good enough to allow any meaningful estimation of fusion frequency.

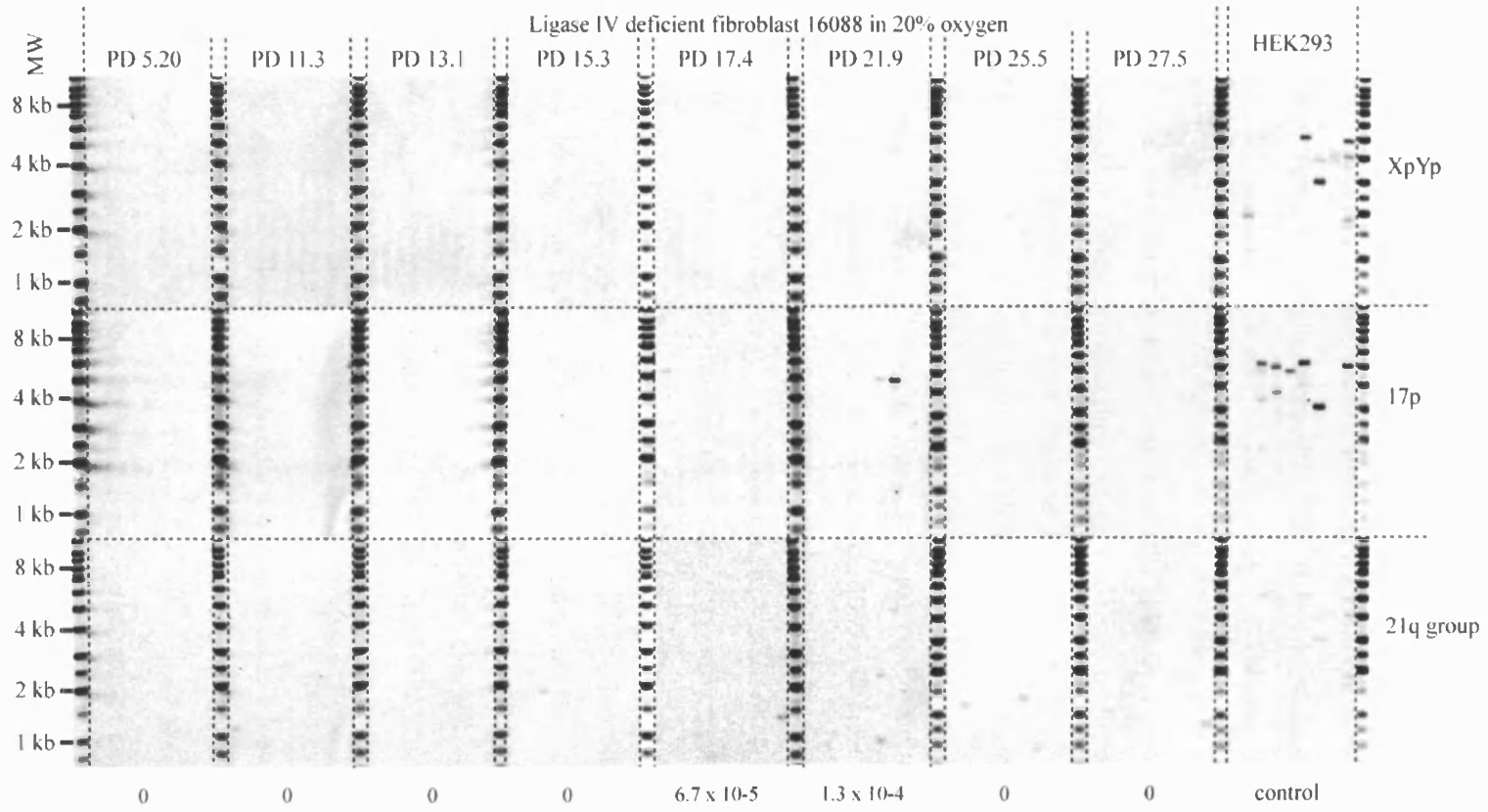

Figure 4.12 Fusion of Ligase IV deficient cells 16088 in 20% oxygen for the XpYp, 17p and 21q group chromosomes. Each reaction contains 10 ng of DNA. Bands are detected by the specific probe detailed on the right. The fusion frequency was calculated for the 17p chromosome and is stated below each sample. Molecular weight markers are indicated on the left.

4.4 Discussion

4.4.1 Replicative lifespan and telomere erosion in DNA Ligase IV deficient cells

The DNA ligase IV syndrome cell lines, GM16088 and GM17523, exhibit a similar replicative capacity of approximately 25 PDs. Both fibroblast strains were derived from relatively young patients (9 and 14 years of age). GM16088 and GM17523 were both obtained from the Coriell Cell Repository and no information on the replicative history of the cells prior to this study was available. However two other studies of these fibroblast cultures indicated that they exhibit a reduced replicative lifespan compared to normal diploid fibroblasts strains (Badie et al., 1997, Cabuy et al., 2005). This is typical of many cell strains derived from individuals with mutated members of DNA damage repair mechanisms like DNA Ligase I (chapter 3), NBS1 (chapter 5) and WRN (Martin et al., 1970, Tollefsbol and Cohen, 1984). Classical NHEJ is disrupted in patient derived DNA Ligase IV syndrome cultures (Badie et al., 1995a, Badie et al., 1995b, Girard et al., 2004, O'Driscoll et al., 2001) however the hypomorphic mutation in Lig4 gene does not impair the DNA damage response in these cells (Badie et al., 1997, O'Driscoll et al., 2001). This raises the possibility that these cells may suffer high levels of genomic stress that signals a cell cycle arrest. This may lead to a telomere independent reduction in the proliferative capacity. Alternatively, the deficit in NHEJ may directly influence telomere dynamics increasing the rate of telomere erosion and thus undergo telomere-driven premature replicative senescence. However in this study the erosion rate in DNA Ligase IV deficient cells was not obviously different from that observed in normal fibroblast cultures, 113 bp/PD in GM16088 and 43 bp/PD in GM17523 compared to 60 to 120 bp per cell division in normal fibroblasts (Baird et al., 2003, Harley et al., 1990). This argues against the hypothesis that the Ligase IV deficiency impacts directly upon telomere dynamics. However these data are in contrast to a previous study (Cabuy et al., 2005) were elevated rates of erosion was observed in GM16088 (>200 bp/PD) and signal free ends were detected. The Cabuy et al study was undertaken using TRF Southern blot analysis, Flow-FISH and Q-FISH and rates of erosion varied between the different techniques used. These techniques are hybridisation based and thus suffer from

a lower telomere length threshold below which telomeres cannot be detected. STELA does not suffer in this regard as it is capable of determining the length of the shortest telomeres. Therefore the distinction between the apparent rates of erosion may be a function of the difference in the technologies used to determine telomere length. The rate of erosion documented with STELA in the Ligase deficient cell strain GM17523 is just 43 bp/PD, we conclude that Ligase IV deficient cells exhibit no change in the rates of erosion of the bulk of the telomere length distribution.

4.4.2 Influence of Oxidative Stress on the Replicative Capacity and Telomere Dynamics of DNA Ligase IV syndrome fibroblasts

One aspect of this study was to test if the replicative lifespan of Ligase IV syndrome fibroblast cultures was sensitive to oxidative stress. The less severely affected fibroblast culture GM 16088 displayed no increase in replicative capacity at low oxygen concentrations. This is mirrored in the similar growth rates and telomere erosion rates at both oxygen concentrations. The more severe phenotype of the second Ligase IV syndrome strain was reflected in more limited replicative capacity of less than 20 PDs. However, the reduction of the oxidative tension increased the replicative lifespan of GM17523 by 20% compared to that obtained when cultured in 20% oxygen. This is consistent with observations in both foetal and adult human lung fibroblasts and Werner cells (Britt-Compton et al., 2009, Forsyth et al., 2003, Kashino et al., 2003) where culturing at low oxygen concentrations extended the lifespan of these cells. Comparing the exponential growth rate and telomere erosion rate at both oxygen concentrations, only the growth rate of GM17523 at 3% oxygen is increased by 27%.

4.4.3 Short telomere distribution in DNA Ligase IV deficient cells GM17523

Another distinct aspect of telomere dynamics in the GM 17523 cell strain, derived from the more severely affected patient, was the apparent presence of a population of very short telomeres at the 17p telomere (Fig 4.7 b). This telomere length distribution was invariant, exhibiting no apparent telomere erosion despite the bulk of the telomere length distribution suffering erosion. The frequency (average 14.4%) of the short telomeres

remained constant during the lifespan of the culture only disappearing in the final 2 PD. These short telomeres may be consistent with the observations of signal free ends (3%) by Cabuy et al in Ligase IV deficient cells. These telomere dynamics using STELA have not been seen in telomerase negative cells. Two possibilities present themselves: Firstly, cells that contain these short telomeres have activated some form of telomere maintenance system; however this does not appear to result in telomere lengthening and the frequency of these telomeres does not increase as be predicted if they were being maintained. Alternatively, the Ligase IV deficiency confers a telomere instability phenotype that results in constant rate of production of short telomeres. Cells that contain these telomeres either exit the cell cycle and do not contribute to the growth of the culture or the short telomeres are repaired through an Ligase IV independent DNA repair pathway resulting in fusions to another chromosome ends. The latter possibility appears more likely given the DNA repair deficiency of these cells.

Telomeres represent difficult loci to replicate and have recently been described as fragile sites (Sfeir et al., 2009). Furthermore G-rich telomeric DNA is considered to form G-quadruplex structures which are difficult to replicate and require specialised helicase activity to resolve. Thus, replication fork stalling and resolution as a double-strand DNA break may result in telomeric mutation. I speculate that Ligase IV deficient cells exhibit an enhanced telomere replication defect. Why this phenomena was only observed at the 17p telomere is also a matter of speculation, however one explanation could be the presence of telomere variant repeats within the proximal regions of the telomere repeat array. These distributions are hypervariable and each telomere of each individual will display a unique telomere variant repeat pattern (TVR) (Baird et al., 1995). Some repeat types exhibit differing levels of stability, for example CTAGGG is particular mutable (Mendez-Bermudez et al., 2009). It is conceivable that the TVR region at the 17p telomere in GM17523 presents a particular problem during replication compared to the XpYp telomere. Consistent with this CTAGGG repeats have been detected within the 17p telomere (Letsolo et al., 2009).

These hypothesises could be tested by attempting to clone out this telomere phenotype, however despite multiple attempts it was not possible to obtain viable clones from these cell strains.

4.4.4 Fusions in DNA Ligase IV deficient fibroblast cultures

The purpose of these experiments was to produce Ligase IV deficient fibroblasts with short dysfunctional telomeres that are capable of fusion. Unfortunately the particular cell strains used here did not have very short telomeres at the particular telomeres analysed. Furthermore it was apparent that the introduction of HPV E6E7 did not confer a lifespan extension. It was thus not possible to obtain sufficiently short telomeres that would undergo fusion. Previous analysis of this type in normal fibroblasts (Capper et al., 2007) as well as in Ligase I deficient cells (chapter 3), have shown short dysfunctional telomere are subjected to fusion. Despite the severe difficulties in obtaining sufficient DNA for analysis, telomere fusion was detected in the Ligase IV deficient cells in the absence of HPV16 E6E7. There was an apparent increase in fusion frequency in both Ligase IV deficient strains with ongoing cell division. Fusion frequencies were greater within the 21q family of telomeres, indicating that other telomeres could be shorter and undergo fusion compared to the here analysed 17p and XpYp telomeres. It would therefore be of interest to examine the telomere dynamics at these ends. The fusion frequency was low (GM16088: 1.3×10^{-4}, GM17523: 6.7×10^{-5}) but still significantly higher than in normal other fibroblast cell lines with similar average telomere length (Capper et al., 2007) where a fusion frequency of 4×10^{-6} was observed. These observations are consistent with the increased presence of anaphase bridges observed previously in 180BR (GM16088) compared to normal fibroblasts (Cabuy et al., 2005). Similar to the here observed fusions, the frequency of anaphase bridges increased with ongoing cell division (Cabuy et al., 2005). The apparent increase in fusion frequencies compared to normal cells, may be consistent with the presence of the short telomeres observed in these Ligase IV deficient cells being subjected to fusion.

The DNA Ligase IV activity in the GM16088 cells is below 10% and in GM17523 below 1% of levels found in normal fibroblast. Both cells strains are radiation sensitive indicating a defect in DSB repair. Despite being compromised for NHEJ, these cells exhibit a 30 times higher fusion frequencies than that observed in normal cells. These observations are consistent with data from Ligase IV mutants in fission yeast (Baumann and Cech, 2000), telomerase negative mice (Maser et al., 2007) and Arabidopsis (Heacock et al., 2007). All these studies show that short dysfunctional telomeres can be subjected to fusion despite the absence of DNA ligase IV and consequently functional C-NHEJ. The observation of fusion in Ligase IV deficient cells is also consistent with the hypothesis that fusion of short dysfunctional telomeres is dependent on alternative NHEJ. This hypothesis is based upon the distinct mutational profile observed following the fusion of short telomeres in human cells, compromising of large sub-telomeric deletions and microhomology at the fusion point (Capper et al., 2007, Letsolo et al., 2009). The profile is in contrast to telomeric fusion following the experimental abrogation of TRF2. These chromosomal fusion events display several kilo bases of telomeric repeats at the fusion point and are dependent on DNA Ligase IV, Ku70/80 and DNA-Pk_{cs} (Smogorzewska et al., 2002, Stansel et al., 2001). Therefore classical NHEJ may not be the predominant mechanism underlying the fusion of short dysfunctional telomeres.

4.5 Conclusion

It appears that premature senescence of DNA Ligase IV syndrome cells is not a result of elevated telomere attrition as telomere erosion rates are in the range observed in normal human fibroblasts. However a distinct and constant distribution of short telomeres could trigger a DNA damage response inducing premature senescence. Telomere fusion events could be detected despite the lack of DNA Ligase IV activity. This is consistent with error-prone alternative end-joining processes operating to facilitate the fusion of short dysfunctional telomeres.

Chapter 5: Nijmegen Breakage Syndrome

5.1 Abstract

NBS1 is a part of the MRN complex and plays a critical role in the repair and processing of DNA double strand breaks. The primary human Nijmegen Breakage Syndrome fibroblast cells analysed in this study contain a hypomorphic 657del5 mutation found in 90% of all NBS patients.

The telomere dynamics in NBS1 deficient cells were investigated using STELA. It appears that in contrast to previous observations NBS1 deficiency does not influence the rate of telomere attrition. Therefore the limited replicative capacity of NBS fibroblast is not a consequence of elevated telomere loss. In addition, the NBS1 deficient primary fibroblasts display a significant paucity of sporadic telomere deletions events, thus indicating a possible role of NBS1 in the process. In conclusion, sporadic telomere deletion events might be the result of the resolution of Holliday junctions at the bottom of t-loops and are accompanied by the formation of t-circles.

Another aspect of this study was to determine if NBS1 participates in the fusion of short dysfuntional telomeres. However the expression of HPV16 E6E7 in NBS1 deficient cells failed to push average telomere length into the length range at which telomeres become unprotected and undergo fusion. The large scale analysis of the parental culture did not yield any fusion events. This was not surprising as average telomere is relatively long and no sporadic telomere deletions could be observed. Thus no conclusion could be reached regarding the role of NBS1 in telomeric fusion events.

5.2 Introduction

5.2.1 NBS1/nibrin

As a component of the MRN protein complex, NBS1 plays a critical role in the repair and processing of DNA double strand breaks (DSB) (Carney et al., 1998, Varon et al., 1998). NBS1 is essential for the nuclear location of Mre11 and RAD50 (Carney et al., 1998). In addition, NBS1 binds to histone γ–H2AX foci and initiates the rapid assembly of MRN at DSBs (Kobayashi et al., 2002). NBS1 is involved in the initiation of the DNA damage response by mediating protein-protein interactions at DSBs (Lloyd et al., 2009, Williams et al., 2009). Furthermore, the MRN complex is associated with telomeres through its interaction with telomere binding protein TRF2 which is a mediator in t-loop formation (Kass-Eisler and Greider, 2000, Zhu et al., 2000).

The NBS1 gene contains 3 distinct domains. The N-terminal region includes a fork head associated domain (FHD) and two breast cancer C-terminal (BRCT) domains. The FHD domain binds to DNA damage proteins like Mdc1 and Ctp1 and most importantly acts as a tether to Mre11. The BRCT domains are involved in the recruitment of repair and checkpoint proteins to DSBs (Lloyd et al., 2009, Williams et al., 2009). The central region comprises several conserved sequences for phosphorylation by ATM and ATM/RAD3 associated (ATR) kinases. The C-terminal region incorporates the Mre11 binding domain (MBD) and ATM recruitment motif (Becker et al., 2006, Williams et al., 2002).

5.2.2 Nijmegen breakage syndrome

Nijmegen breakage syndrome (NBS) is a rare autosomal recessive disorder and belongs in the group of human chromosomal instability syndromes like Bloom's Syndrome and ataxia-telangiectasia (AT) (Weemaes et al., 1981). Characteristic symptoms of NBS are microcephaly, immunodeficiency, distinct facial features, growth retardation, hypersensitivity to ionizing radiation (IR), chromosomal instability and a strong predisposition for lymphomas (Williams et al., 2009, Digweed and Sperling, 2004,

Weemaes et al., 1981). NBS is caused by mutations in NBS1 gene located at chromosome 8q21.3 (Carney et al., 1998, Varon et al., 1998). 90% of all NBS patients are homozygous for a hypomorphic 5 bp deletion event at position 657 in exon 6 of NBS1 (Varon et al., 1998). The 657del5 germline mutation has the highest frequency in the Slavic population in central Europe, presenting a common founder mutation (Varon et al., 2000). The 657del5 missense mutation splits the NBS1 directly in the BRCT linker region into two separate peptides of 26 kDa and 70 kDa. The smaller peptide contains the FHD and one of the BRCT domains and the larger peptide includes the Mre11 binding domain and ATM binding motif. The larger peptide retains the ability to interact with Mre11, suggesting that this interaction is essential for viability (Becker et al., 2006, Williams et al., 2002). Seven other mutations in NBS1 result in the expression of a truncated protein and lead to NBS (Attwooll et al., 2009).

5.2.3 GM07166

GM07166 fibroblasts were derived from a NBS patient carrying the homozygous 657del5 mutation. Like all NBS patient derived cells, GM07166 cells display an abrogated p53 function which results in an abnormal cell cycle arrest in G1-S and a prolonged accumulation in G2 phase following ionizing radiation (Jongmans et al., 1997). Furthermore, GM07166 is impaired in the intra S-phase checkpoint as cells continue to synthesize DNA despite the presence of radiation induced DNA damage (Girard et al., 2002, Shiloh, 1997). GM07166 cells show high sensitivity to ionizing radiation, chromosomal instability, decreased homologous recombination and accelerated telomere shortening (Ranganathan et al., 2001, Tauchi et al., 2002). The DNA-PK activity appears to be normal (Sullivan et al., 1997).

5.2.4 Animal models of NBS

NBS1-null phenotype in mice causes embryonic lethality (Zhu et al., 2001) whereas those expressing the C-terminal region of NBS1 are viable and share many symptoms of NBS (Williams et al., 2002, Kang et al., 2002). The chicken cell line DT40 is disrupted

in NBS1 expression. As a consequence, cell cycle progression is slowed down due to a defect in the intra-S phase checkpoint regulation. DT40 is also hypersensitive to DNA damaging agents and chromosomal instability (Tauchi et al., 2002).

5.2.5 Stochastic Telomere Deletion Events

STELA analysis revealed that most telomeres erode gradually as a consequence of the end replication problem (Olovnikov, 1971). However superimposed on this telomere loss were sporadic large scale telomere deletion events (Baird et al., 2003). Similar telomere deletion events referred to as telomere rapid deletions (TRD) have been observed in yeast and are dependent on RAD52 and MRX complex (Bucholc et al., 2001, Lustig, 2003). However the mechanism creating TRDs in yeast may be distinct from the mechanisms inducing sporadic telomere deletions in humans. The mechanistic basis of these human sporadic telomere deletion events is still unknown. Several mechanisms are to be considered: sister chromatid exchange (SCE) (Bailey et al., 2004, Rudd et al., 2007), replication fork stalling (Crabbe et al., 2004), oxidative damage (Petersen et al., 1998) and T-loop recombination, first characterized in yeast (Lustig, 2003). High levels of sister chromatid exchange (SCE) have been observed at mammalian telomeres. Evidence in mouse cells indicates that SCE is 20 times higher at telomeres than at genomic loci (Bailey et al., 2004). Furthermore, human telomeres are subjected to a SCE rate which is 1600 times higher than the rest of the genome (Rudd et al., 2007). Moreover, SCE might lead to unequal sister chromatid exchange if the newly replicated chromatids are misaligned. The resulting long and short telomere product might give rise to dramatic changes in telomere length. Observations on telomere variant repeats are consistent with unequal SCE generating diversity (Baird et al., 1995, Baird et al., 2000, Britt-Compton and Baird, 2006). However, there is no data so far to suggest that SCE might lead to large scale telomere deletion events. Sporadic telomere deletion events do not accumulate with ongoing cell division, implying they are either repaired by an unknown DNA repair pathway, trigger a DNA damage response followed by the exit of the cell from the cell cycle or undergo fusion. Previous observations in our group have proven that these sporadic telomeric deletions can undergo fusion (Capper et al.,

2007). Assuming that an estimated 2% of the each telomere population undergo sporadic telomere deletions, this may represent a significant contributor to genomic instability and therefore could aid cancer progression in normal fibroblasts.

5.2.6 Aims

The aim of this work was to determine if NBS1 influences telomere dynamics and if NBS1 participates in the fusion of short dysfuntional telomeres. Furthermore, this study tried to determine if NBS1 deficiency abolishes the presence of sporadic telomere rapid deletion events in humans.

5.3 Results

5.3.1 Optimising the replicative lifespan of NBS1 deficient fibroblasts

Previous studies have shown that radical oxygen species (ROS) can give rise to varying levels of DNA damage in primary human fibroblasts inducing premature cell cycle arrest and consequently a significant reduction of the replicative capacity of the primary cells (Chen et al., 1995). Large quantities of non-proliferating cells in a culture can simulate an increase telomere erosion rate in particular near the end of the replicative lifespan of the cells (Forsyth et al., 2003). Moreover, another hypothesis suggests that the TTAGGG repeats of the telomere are sensitive to ROS induced DNA damage resulting in increased, end-replication independent telomere shortening (von Zglinicki, 2002). The NBS1 deficient cells GM07166 are sensitive to DNA damaging agents (Nove et al., 1986). Oxidative stress may further aggravate the severely compromised cell phenotype of NBS1 deficient cells and consequently attenuate the cultures replicative lifespan and influence the telomere dynamics observed in these cells.

In order to monitor the influence of oxidative stress on NBS1 deficient cells GM07166 the parental bulk population was split at PD 7.5 and was either cultured under normal oxygen concentrations of 20% O_2 and physiological oxygen concentration of 3% O_2. The cells were cultured by Mrs Rebecca Capper. The cells were passaged serially and the accumulated PDs were plotted as a function of time (Fig. 5.1).

Culturing NBS1 deficient fibroblasts GM07166 at physiological oxygen levels of 3% did not extend of the replicative capacity of the patient derived cells (Fig 5.1). The cells at 20% and 3% oxygen reached their replicative limit at PD 25 and 26.5 respectively. This represents a truncated replicative lifespan compared to normal fibroblast cultures (Hayflick, 1965) and is consistent with other DNA repair deficient cells strains analysed in this thesis. This data is also in line with previous observations in several model organisms (Kang et al., 2002, Tauchi et al., 2002), where the NBS1 deficient cells presented a significantly slower cell cycle time and cell growth rates compared to normal cells. The cells were kept in culture for 217 days in the different oxygen

concentrations and during that time 16.5 PD in 20% O_2 and 18.0 PD in 3% O_2 were achieved. The overall growth rates during the oxygen experiment were determined to be 0.087 PD/day ± 0.092 PD/day at 20% O_2 and 0.091 PD/day ± 0.062 PD/day at 3% O_2 (mean ± SD). However in both oxygen concentrations the growth rate varied during the course of the experiment slowing and speeding up in irregular intervals resulting in the step-like appearance of the growth curve (Fig. 5.1). It was not obvious if this is a result of the NBS1 deficiency or experimental circumstances.

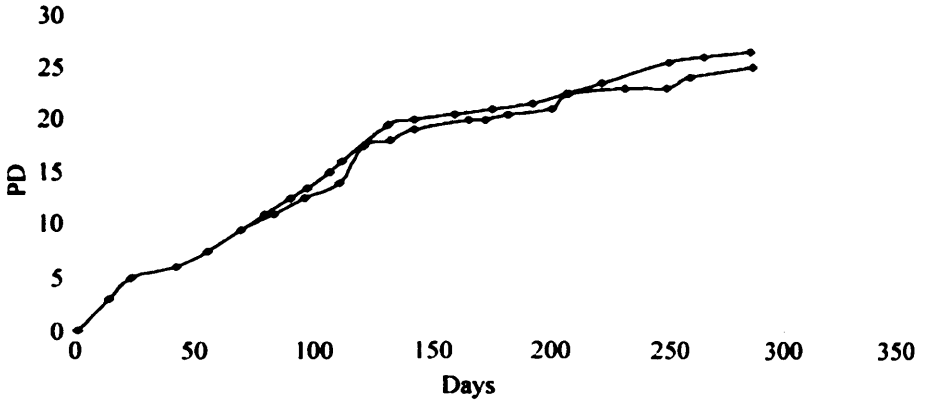

Figure 5.1 Growth curves of NBS1 deficient cells cultured in 3% and 20% oxygen. Plotting growth curves as function of population doublings (PD) verus time in days.Filled markers represent cells cultured at 20% oxygen and open markers represent those cultured in 3% O2.

5.3.2 Telomere dynamics of NBS1 deficient fibroblasts

In order to determine if NBS1 has a role in telomere dynamics, the XpYp and 17p telomere length distributions of GM07166 under 20% and 3% oxygen were investigated using single telomere length analysis (STELA) (Baird et al., 2003). In line with previous studies in the group (Baird and Farr, 2006, Baird et al., 2003, Britt-Compton et al., 2006), only the XpYp and 17p telomere were analysed as both chromosome are representative for average chromosomal telomere length and average telomere erosion rates resulting from the end-replication problem. Multiple cell samples were taken during the course of the experiment and STELA was used to track the telomere

dynamics with ongoing cell division. The STELA southern blots for the experiment are shown in figures 5.2 to 5.3.

In both oxygen concentrations, the telomere length distributions of GM07166 were bimodal at the XpYp telomere (Fig 5.2 a and Fig 5.3 a). At 20 % O_2, an apparent change in the distributions could be observed, the upper modal distribution disappeared as the cell reached the end of their replicative capacity. Albeit less obvious, the 17p telomere in both oxygen concentrations displayed a similar bimodal distribution, with evidence of the loss of the lower distribution after approximately 132 days in culture (Fig. 5.2 b and Fig 5.3 b). During the 6.5 PD between which telomere dynamics were analysed at 20% O_2, the lower XpYp distribution decreased by 0.9 kb whereas the upper distribution decreased by 0.7 kb disappearing after 3.5 PDs making it difficult to determine an accurate erosion rate. For the 17p telomere, the culture at 20% O_2, displayed a loss of 1.7 kb at the upper modal distribution whereas the lower distribution was more difficult to define and disappeared after 3.5 PDs, therefore an accurate telomere erosion rates could not be determined. At 3% O_2, the upper XpYp length distribution lost 2.1 kb and the lower telomere length lost 1.05 kb over 10 PDs. The 17p telomere lost 0.3 kb at the upper distribution during this period and again the lower distribution disappeared after 3.5 PDs, hence an accurate erosion rate could not be determined. The telomere erosion rate data for NBS1 deficient primary fibroblasts is summarised in Fig. 5.4. The telomere erosion rates were calculated separately for each chromosome. The overall erosion rate for the lower modal XpYp distribution and the upper modal 17p distribution was determined to be 229.4 bp/PD ± 73.2 bp/PD in 20% O_2 and 95.6 bp/PD ± 46.7 bp/PD in 3% O_2 (mean ± SE).

Sporadic telomere deletion events have been observed in normal and diseased primary fibroblasts (Baird and Farr, 2006, Baird et al., 2003, Britt-Compton et al., 2006)(chapter 3 and 4 in this thesis), these represent a significant mutational mechanism creating dysfunctional telomere that are capable of fusion (Capper et al., 2007). One of the objectives of this study was to determine if NBS1 deficiency may play a role in the generation of telomeric deletion. This hypothesis was based on the genetic analysis that

identified RAD50 and Mre11 in the process of telomere rapid deletion (TRD) observed in yeast (Bucholc et al., 2001, Lustig, 2003). The telomere length profiles observed in NBS cells (Fig 5.2 and 5.3) appeared to display a paucity of short telomeres compared to that observed in normal fibroblast cultures as well other DNA repair deficient cell strains analysed in this thesis. The XpYp telomere profiles of the different fibroblast cultures are presented as histograms depicting the observed telomere lengths distribution as a proportion (%) of the number of analysed molecules (Fig 5.5).

Stochastically shorter telomeres are defined as those which deviate from the normal (Gauss) distribution of expected telomere length. However bimodal distributions make it difficult to determine these deleted telomeres. Nevertheless an estimated 2% of all observed telomeres in different fibroblast cultures will be significantly shorter than the mean telomere length. In order to determine if NBS1 deficient cells display no sporadic telomere deletion events, all telomere profiles were combined for analysis and a total of 1051 and 1066 molecules were plotted in a histogram for 20% and 3% O_2 respectively (Fig 5.5 bottom panel). There were no telomeres observed that are shorter than 0.9 kb and 1.1 kb in 20% and 3% O_2 respectively. This differs from the expected 2% of telomeres which should be shorter than 500 bp. This difference is statistically highly significant for both oxygen concentrations (both p-value below 0.001, Chi-Square test).

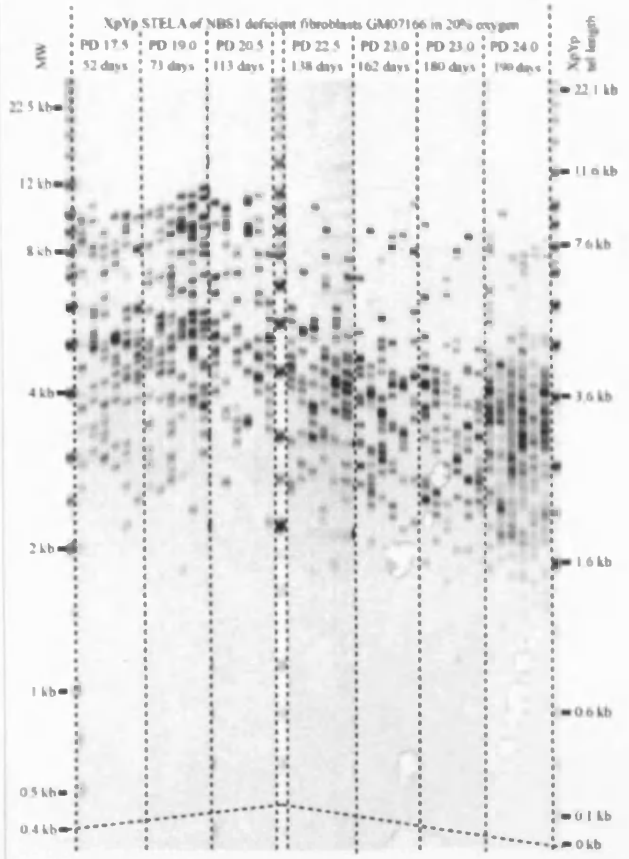

Upper (kb)	7.40	7.20	7.50	6.70	N.A.	N.A.	N.A.
Lower (kb)	3.80	3.80	3.50	3.20	3.10	2.90	2.90
SD (kb)	2.20	2.15	2.09	1.41	1.61	1.37	1.64

Figure 5.2a XpYp STELA gel displaying the telomere length profile of NBS1 deficient fibroblast GM07166 in 20% oxygen. Starting from the point cells were taken into culture, population doublings (PD) are presented in the first line above the gel. The second line above the gel displays the days cells were kept in culture. Molecular Weight (MW) is indicated on the left and the corrected telomere length is indicated on the right. Upper modal length, lower modal telomere length and corresponding standard deviation (SD) in kb are detailed below the gel. N.A. not applicable since modal telomere length disappeared.

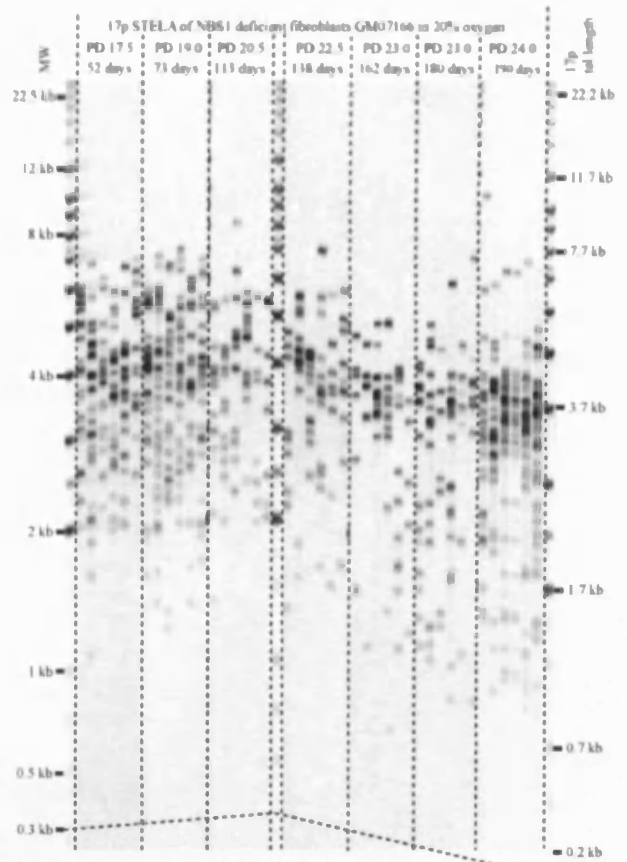

Upper (kb)	4.90	4.40	4.30	3.30	3.30	3.30	3.20
Lower (kb)	3.10	3.10	3.40	N.A.	N.A.	N.A.	N.A.
SD (kb)	1.26	1.35	1.22	1.27	1.10	1.31	1.36

Figure 5.2b 17p STELA gel displaying the telomere length profile of NBS1 deficient fibroblast GM07166 in 20% oxygen. Starting from the point cells were taken into culture, population doublings (PD) are presented in the first line above the gel. The second line above the gel displays the days cells were kept in culture. Molecular Weight (MW) is indicated on the left and the corrected telomere length is indicated on the right. Upper modal length, lower modal telomere length and corresponding standard deviation (SD) in kb are detailed below the gel. N.A. not applicable because modal telomere length disappeared.

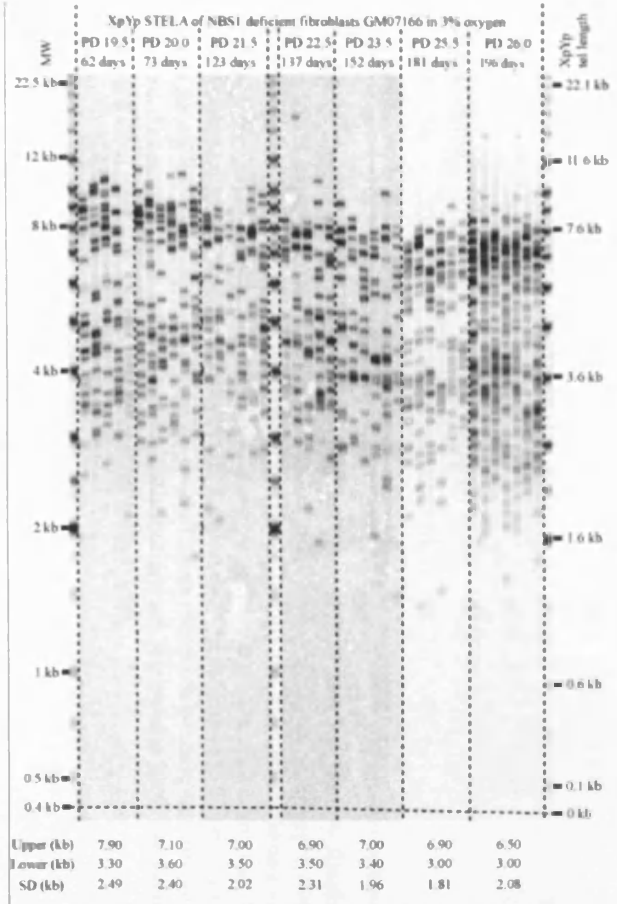

Upper (kb)	7.90	7.10	7.00	6.90	7.00	6.90	6.50
Lower (kb)	3.30	3.60	3.50	3.50	3.40	3.00	3.00
SD (kb)	2.49	2.40	2.02	2.31	1.96	1.81	2.08

Figure 5.3a XpYp STELA gel displaying the telomere length profile of NBS1 deficient fibroblast GM07166 in 3% oxygen. Starting from the point cells were taken into culture, population doublings (PD) are presented in the first line above the gel. The second line above the gel displays the days cells were kept in culture. Molecular Weight (MW) is indicated on the left and the corrected telomere length is indicated on the right. Upper modal length, lower modal telomere length and corresponding standard derivation (SD) in kb are detailed below the gel.

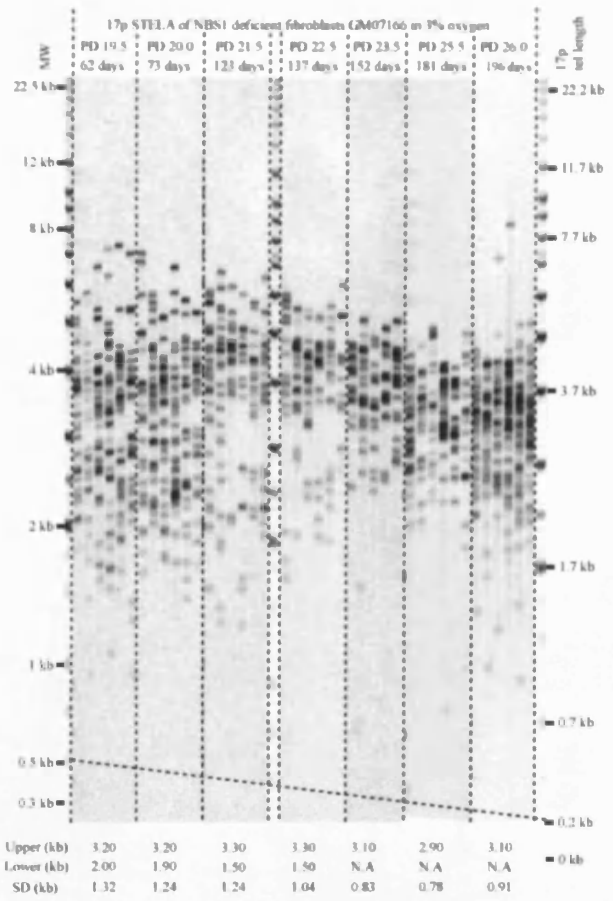

Upper (kb)	3.20	3.20	3.30	3.30	3.10	2.90	3.10
Lower (kb)	2.00	1.90	1.50	1.50	N.A	N.A	N.A
SD (kb)	1.32	1.24	1.24	1.04	0.83	0.78	0.91

Figure 5.3b 17p STELA gel displaying the telomere length profile of NBS1 deficient fibroblast GM07166 in 3% oxygen. Starting from the point cells were taken into culture, population doublings (PD) are presented in the first line above the gel. The second line above the gel displays the days cells were kept in culture. Molecular Weight (MW) is indicated on the left and the corrected telomere length is indicated on the right. Upper modal length, lower modal telomere length and corresponding standard derivation (SD) in kb are detailed below the gel. N.A. not applicable because modal telomere length is lost from the population.

a)

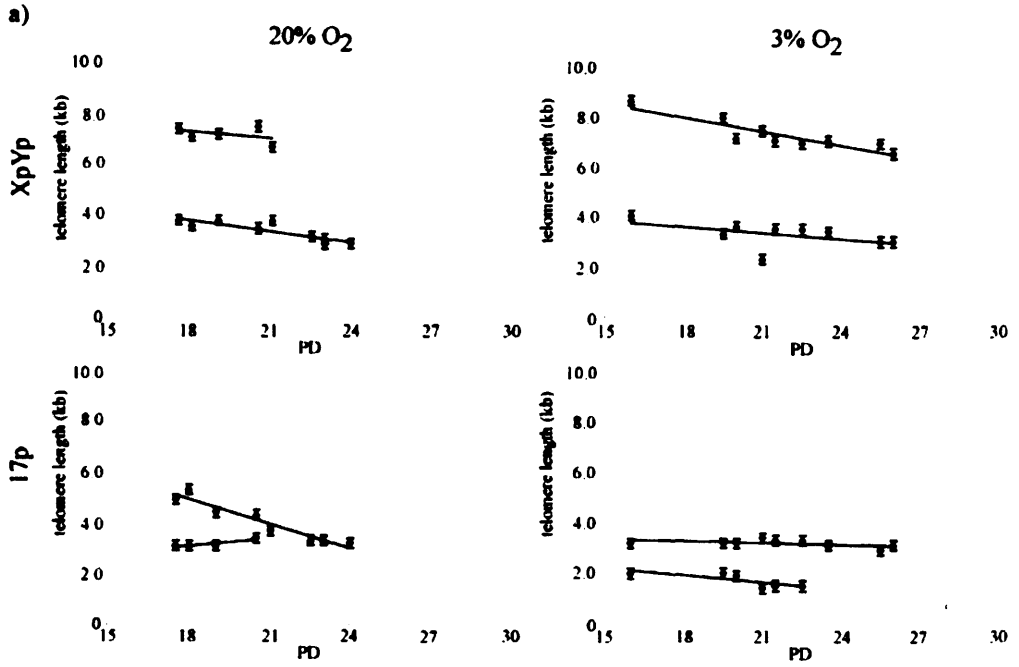

b)

telomere	Erosion rate bp/PD	20% O_2 R2	Number of Data points	Erosion rate bp/PD	3% O_2 R2	Number of Data points
XpYp	78.5	0.148	5	183.2	0.808	9
	139.8	0.753	8	80.1	0.259	9
17p	319	0.921	8	23.6	0.255	9
	100	0.778	4	95.6	0.605	6
Overall mean	229.4		Overall mean	95.6		
Overall SE	73.2		Overall SE	46.7		

Figure 5.4 Summarising the telomere erosion rate data of NBS1 deficient primary fibroblasts GM07166 in 20 and 3% oxygen. a) Telomere erosion rate is calculated as the slope of the regression line after plotting the median telomere length against the corresponding PD. Individual telomere are detailed on the right, oxygen concentration is displayed above, error bars are ± standard error, y-axis presents modal telomere length, x-axis presents PD. b) Erosion rates, accompanying R2 and the number of data points for each chromosome are displayed. Overall mean and corresponding standard error (SE) are also detailed. The erosion rates for the lost modal distibutions are displayed in grey. The estimated values are excluded from the overall mean and overall SE calculations.

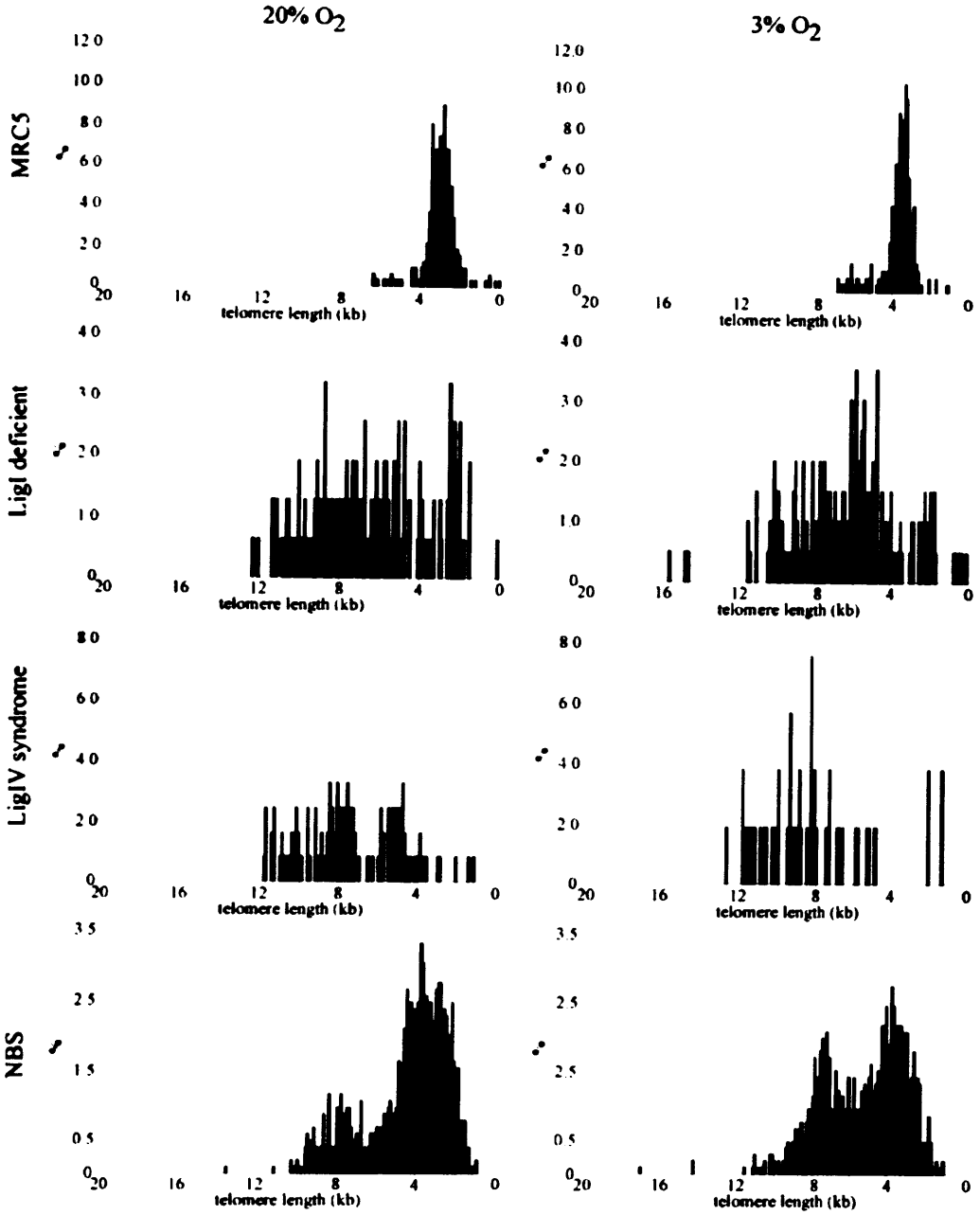

Figure 5.5 Statistically shorter telomeres (Outliers) in normal and diseased primary fibroblast cultures in 20 and 3% oxygen. The histograms display the observed telomere profiles for XpYp as a proportion (%) of the analysed molecules. The dipicted fibroblast cultures are indicated on the left, oxygen concentration is displayed above, y-axis presents the proportion of analysed molecules in %, x-axis presents telomere length in kb. MRC-5: normal lung fibroblasts, LigI deficient: DNA Ligase I deficient fibroblasts GM16096, LigIV syndrome; DNA Ligase IV deficient fibroblasts GM17523, NBS: NBS1 deficient fibroblast GM07166

5.3.3 Telomere dynamics of NBS1 deficient fibroblasts expressing HPV E6E7 oncoproteins

Another objective of this study was to investigate the role of nibrin/NBS1/p95 in telomere fusion events. In order to extend the lifespan of GM07166 and thus allow the telomeres to erode within the length range where to become de-protected and undergo fusion, cells were transfected with HPV16 E6E7 oncoproteins. These oncoproteins abrogate the function of p53 and Rb, allowing the cells to bypass senescence and continue to divide through to crisis.

Initial experiments in NBS1 deficient cells at both oxygen concentrations were carried out and the cells were transfected 3 PDs prior to end of the replicative lifespan of the cells. The transfection proved to be lethal to the cells, no clonal population could be obtained and with no extension of proliferative lifespan was observed in the bulk population. The transfection was therefore repeated at both oxygen concentrations at an earlier PD; PD 3 for 20% O_2 and PD 11 for 3% O_2. Although 24 E6E7 clones and 12 NEO clones were picked at each oxygen concentration, no viable clone could be established. At both oxygen conditions, the transfection efficiencies were low, cells grow poorly in low densities and no apparent lifespan extension could be achieved. After 100 days post transfection most clones contained less then 5×10^4 cells, with an average of 3×10^3 cells. STELA analysis was attempted however DNA content of all samples was not sufficient to obtain usable data (data not shown).

5.3.4 Fusion assay of NBS1 deficient fibroblasts GM07166

The expression of HPV E6E7 in NBS1 deficient cells GM07166 did not extend the proliferative capacity of the fibroblasts and consequently the average telomere length is likely to have remained above the threshold length at which telomeres become de-protected and undergo fusion as observed in un-transfected cells (Capper et al., 2007). Furthermore because these cells failed to proliferate, the obtained DNA samples proved to be insufficient for fusion analysis and thus no data could be compiled. However a total of 25 samples from the parental population was analysed for fusions. Even though a

total of 3.75 x 10^5 molecules were analysed, no fusion events were detected (data not shown).

5.4 Discussion

5.4.1 Cell proliferation and telomere erosion in NBS1 deficient cells

In the study presented here, GM07166 displayed slow cell proliferation achieving less then 20 PDs in 217 days. The slow rates of proliferation could be a consequence of the prolonged cell cycle resulting from the NBS 1 deficiency in these cells (Jongmans et al., 1997, Kang et al., 2002, Tauchi et al., 2002). Notable, a step-like growth curve of the NBS 1 deficient primary fibroblast in 20% O_2 was observed; long stretches of slow growth alternate with short periods of faster cell proliferation (Fig 5.1). One explanation for the shape of the growth curve could be related to the kinetics of single cell growth in slowly growing cultures. In these cultures the main cell population displays little or no cell growth, only a minority of clonal populations are still proliferating. The faster cell growth of these populations could result in a clonal overtake of the parental culture; with stretches of slow growth corresponding to the time the clone needed to over take the culture. These type of cell kinetics are similar to those described in fibroblast cultures derived from Werner's syndrome patients (Baird et al., 2004, Schonberg et al., 1984) and to some extent in normal human fibroblasts (Littlefield and Mailhes, 1975), where clonal succession, attenuation and expansion artificially increased the telomere loss of the bulk population. As described above, the cell growth of the bulk population is driven by a small minority of proliferating cells whereas the majority of the NBS cells exit the cell cycle. In later stages of the culture, these clonal populations overtake the culture. In this situation, the estimated PDs of the culture do not correspond with actual cell divisions (CD) of the individual fibroblasts. Subsequently the telomere erosion which is measured in bp/PD will appear to be increased as the estimated PDs are significantly lower than the actual CDs. This might suggest that the elevated telomere erosion rate of 229.4 bp/PD ± 73.2 bp/PD (mean ± SD) in 20% O_2 is a product of this discrepancy. Moreover the erosion rate of 95.6 bp/PD ± 46.7 bp/PD in 3% O_2 is well within in the range of telomere erosion rates observed in normal fibroblast cultures (Baird et al., 2003,

Harley et al., 1990). Taken together with the step-like growth of NBS fibroblasts (Fig 5.1), this could give an explanation for the accelerated telomere attrition of NBS1 deficient cells at 20% O_2. However it was not immediately obvious why the phenomena can only be seen at 20% O_2. One argument could be that higher oxidative tension results in more cells exiting the cell cycle and therefore amplifying the clonal succession, attenuation and expansion phenotype. Attempts were made to examine this issue further by deriving clonal cultures in which the telomere dynamics and grow rates could be examined in isolation from the bulk populations where the complex replicative histories of the various cell lineages can confound the analysis (Smith et al., 1980). Unfortunately it was not possible to obtain viable clones from the parental culture or indeed the HPVE6E7 transfected culture, this may been due the cells inability to grow at low densities. Taken together, this argues against a previous observation that NBS1 deficiency results in an accelerated telomere erosion rate (Ranganathan et al., 2001).

5.4.2 Replicative Lifespan and the Influence of Oxidative Stress on of NBS1 deficient cells

In a previous study GM07166 reached senescence after ~ 10 PDs in culture (Ranganathan et al., 2001). The GM07166 in this study were obtained from the same source as used in this chapter (Corriel Institute) at passage 8 and were cultured for 50 days in which they achieved approximately 10 PDs. They determined senescence using senescence-associated mammalian β-galactosidase activity (SAβ-gal) assay (0.4) or (40%), however senescent cells have a SAβ-gal activity of > 90% (Bond et al., 1999). This may imply that the replicative capacity of GM07166 was not completely utilised in the study by Ranganathan et al.

The NBS1 deficient cells exhibited a limited proliferative capacity of approximately 26 PDs. This is in line with previous observations in NBS1 deficient primary fibroblast cultures (Girard et al., 2000). Furthermore, severe reduction in the replicative lifespan has been observed in other patient derived fibroblast cultures with mutations in DNA damage repair components; DNA ligase I deficient fibroblasts (chapter 3), DNA Ligase

IV syndrome cells (chapter 4) and Werner Cells (Martin et al., 1970, Tollefsbol and Cohen, 1984). One explanation for this could again be related to the explanation articulated in the earlier chapters on Ligase I deficiency and Ligase IV syndrome. Another aspect of this study was to test if the replicative capacity of NBS1 deficient fibroblast would be extended by lowering the oxidative tension. However the patient derived NBS culture displayed no increase in replicative lifespan at low oxygen concentrations.

5.4.3 Failed Replicative Lifespan Extension of NBS1 deficient cells

Abrogation of p53 and Rb does not extend the replicative capacity of primary NBS1 deficient fibroblast GM07166. A previous study on these fibroblast showed that NBS deficiency leads to reduction and delays in the p53 up-regulation (Jongmans et al., 1997) indicating that the p53 response pathway is defective in these cells. Thus experimentally interfering in this pathway may not have any effect on replicative lifespan.

5.4.4 NBS1 Deficiency and Telomeric Fusion Events

The main aspect of this study was to extend the replicative lifespan of NBS1 deficient fibroblast and consequently to produce cells with short dysfunctional telomeres that are capable to undergo fusion. Unfortunately the introduction of HPV16 E6E7 did not result in the expected lifespan extension. Furthermore, no sporadic telomere deletions events could be detected in the NBS fibroblast cultures which in normal human fibroblasts can undergo fusion (Capper et al., 2007). Another approach to observe the influence of NBS1 on telomeric fusion events would be to abrogate function of the complete MRN complex via a small molecule inhibitor, called mirin (Dupre et al., 2008, Garner et al., 2009). Mirin abolishes the Mre11-associated exonuclease function of the MRN complex and inhibits all homology mediated DNA repair in the treated cells. Similar to the experiment described in chapter 6, a clonal derivative of human fetal lung diploid MRC5 fibroblasts expressing HPV16 E6E7 (clone 1) could be treated with mirin. The inhibitor might create an effect on the mutational fusion profile of MRC5 HPV16 E6E7.

5.4.5 Sporadic Telomere Deletions in NBS

Sporadic telomere deletions are not consistent with gradual telomere loss resulting from the end replication problem (Olovnikov, 1971). Instead it appears these deletion events are generated by a currently unknown mechanism. One possible explanation could be a process previously described in *S. cerevisiae* termed telomere rapid deletion (TRD) (Li and Lustig, 1996). Initial observation in yeast showed that TRD results in the rapid reduction of artificially elongated yeast telomeres to wild-type telomere length. Following the observations that TRD increased in the absence of the hyper recombination gene HPR1 and decreased in the absence of the recombination protein RAD52 (Aguilera and Klein, 1989, Li and Lustig, 1996), it has been proposed that TRD occurs through intra-chromosomal recombination within the telomere array. Moreover, the MRX (homolog of human MRN complex) participates in TRD by initiating the branch invasion of the 3' chromosome termini into the proximal telomere repeat sequence. The strand invasion displaces the telomeric DNA forming a D-loop and therefore creating a structure which resembles a T-loop. The D-loop is nicked resulting in a Holliday junction like structure at the strand invasion point which is resolved into a truncated telomere and a TTAGGG rich circular DNA molecule referred to as telomeric circle (T-circle) (Bucholc et al., 2001, Lustig, 2003). Evidence for TRD has also been observed in mammalian cells with a mutated allele of TRF2, $TRF2^{\Delta B}$ (Wang et al., 2004). The abrogation of functional TRF2 led to the suppression of NHEJ and rapid loss of large segments of telomeric DNA which form circular loops. Further investigation showed that these deletion events were dependent on NBS1 and X-ray repair cross-complementing 3 (XRCC3). The latter, together with its partner RAD51C, is thought to be involved in the resolution of Holliday junctions (Liu et al., 2004c). Following this observation, it has been proposed that t-circles are a result of t-loop deletion via homologous recombination (HR) and might contribute to rapid telomere deletion (Wang et al., 2004). T-circles have also been observed in cell with an alternative lengthening of telomeres (ALT) phenotype (Cesare and Griffith, 2004, Wang et al., 2004). In line with the previous hypothesis of T-circle formation, NBS1 and XRCC3 are required for the ALT phenotype and the formation of T-circles in these cells (Compton et al., 2007, Tomaska et al., 2009, Zhong et al., 2007).

In the data presented here, NBS1 deficient fibroblasts display a paucity of sporadic telomere deletion events. Based on the model described above, this indicates that sporadic telomere deletions might be the result of resolution of Holliday junctions at the base of the t-loop by homologous recombination. One way to test this hypothesis would be to reintroduce functional NBS1 into the NBS fibroblast which might lead to the re-appearance of sporadic telomere deletions.

5.5 Conclusion

In contrast to previous observations, the telomere erosion in NBS deficient fibroblasts is not elevated and consequently not the reason for premature senescence in these cells. Notable, the investigated primary fibroblasts display a significant paucity of sporadic telomere deletions events. This implies that sporadic telomere deletion events might be the result of the resolution of Holliday junctions at the bottom of t-loops and are accompanied by the formation of t-circles. No conclusion could be made regarding the role of NBS1 in telomeric fusion events.

Chapter 6: PARP inhibitors

6.1 Abstract

Poly(ADP-ribose) polymerase1 (PARP1) transfers ADP-ribose subunits from NAD^+ to target proteins forming poly(ADP-ribose) (pADPr or PAR) polymers. Recent studies have described an alternative end-joining pathway in absence of classic members of non homologous end joining. This pathway is dependent on PARP1 and DNA ligase III/XRCC1 complex. The mutational profile of this alternative NHEJ pathway is reminiscent of the mutational profile observed in fusions between short dysfunctional telomeres. Furthermore, clinical trials with PARP1 inhibitors have shown that tumours with pre-existing defects in DSB repair are sensitive to PARP1 inhibition.

The telomere dynamics in MRC5 fibroblast expressing HPV16 E6E7 following PARP1 inhibition were monitored using STELA. In line with previous studies, PARP1 inhibition resulted in a rapid decline of average telomere length. The loss of telomere length may have been induced by PARP1 inhibition or by an earlier onset of crisis which is characterised by increase of telomere attrition. This latter explanation provides the intriguing possibility that PARP inhibition may sensitise cells to telomere dysfunction.

The main aspect of this study was to examine the role which PARP1 plays in fusion events between short dysfunctional human telomeres. However the limited data set from MRC5 E6E7 after PARP inhibition did not allow to draw any conclusions as to how PARP inhibition influences fusions between short dysfunctional telomeres.

6.2 Introduction

6.2.1 Poly(ADP-ribose) polymerase 1 (PARP1)

Poly(ADP-ribosyl)ation through PARP1 transfers ADP-ribose subunits from nicotinamide adenine dinucleotide (NAD^+) to target proteins forming poly(ADP-ribose) (pADPr or PAR) polymers (Kameshita et al., 1984, Rouleau et al., 2010). Poly(ADP-ribosyl)ation is a posttranslational protein modification and is an immediate response to DSBs. PARP1 is the founding member of poly(ADP-ribose) polymerase (PARP) family which all feature the same catalytic domain which implements poly(ADP-ribosyl)ation (Otto et al., 2005). In response to DNA damage, PARP1 is recruited to the site of single stranded and double stranded DNA breaks. It has been shown that poly(ADP-ribosyl)ation is involved in BER (Masson et al., 1998), HR (Hochegger et al., 2006) and NHEJ (Wang et al., 2004). In addition to recognising DNA damage, PARP1 rapidly recruits MRN and ATM to DSBs (Haince et al., 2007, Haince et al., 2008) and is involved in restarting of the replication fork (Bryant et al., 2009, Levy et al., 2009).

6.2.2 PARP inhibitors

Initial experiments with PARP inhibitors such as 3-aminobenzamide (3-AB) and 1,5-Isoquinolinediol (DIQ) indicated that cancer cell lines and human tumours that lack BRCA1 and BRCA2, both members of HR, are highly sensitive to PARP inhibition. The inhibition resulted in chromosomal instability, cell cycle arrest and consequently apoptosis of the treated cells (Bryant et al., 2009, Farmer et al., 2005). This gave the impulse to develop PARP1 inhibitors as an alternative to traditional chemotherapy for the treatment of tumours with pre-existing defects in DSB repair. However as 3-AB and DIQ are neither selective enough nor potent enough to result in a specific and complete inhibition of PARP1 (>90%), a new generation of PARP inhibitors has been developed. These inhibitors are created to actively compete with NAD^+ and thus prevent the poly(ADP-ribosyl)ation through PARP1 and related proteins(Rouleau et al., 2010, Zaremba and Curtin, 2007).

Several preliminary clinical trials have shown that PARP1 inhibition in BRCA-negative breast and ovarian cancer gives promising results (Fong et al., 2009, Rouleau et al., 2010).

6.2.3 PARPs and Telomeres

Several members of the PARP family interact with telomere binding proteins. Human PARP5 (Tankyrase, TNK) interacts with TRF1 (Smith and de Lange, 2000, Smith et al., 1998), PARP 1 and 2 with TRF2 (Dantzer et al., 2004, Gomez et al., 2006). In human, TNKS and TNKS2 both localise to human telomeres and both are involved in telomere length maintenance. They both interact with TRF1 and poly(ADP-ribosyl)ate TRF1 as well (Hsiao and Smith, 2008). Consequently inhibiting the binding of TRF1 to telomeres and therefore leaving the chromosome end accessible for telomerase to allow the gradual elongation of the telomere (Cook et al., 2002, Smith and de Lange, 2000). In mice, the abrogation of PARP1 gave controversial observation either having no impact on telomere erosion rates, telomere capping and the overall viability of the mice or resulting in shortened telomeres compared to wild type mice (d'Adda di Fagagna et al., 1999, Espejel et al., 2004). The individual deletions of TNKS 1 and TNKS 2 in mice produce viable and active animals. Furthermore, both deletions have no effect on telomere maintenance or telomere capping (Chiang et al., 2008, Chiang et al., 2006, Yeh et al., 2006).

6.2.4 Alternative NHEJ (A-NHEJ)

Recent studies described an alternative non-homologous end-joining (NHEJ) pathway which is independent of DNA-PKcs and Ku70/80. Instead the pathway relies on poly(ADP-ribose) polymerase 1 (PARP-1) and XRCC1/DNA Ligase III complex (Audebert et al., 2004, Audebert et al., 2006, Wang et al., 2005). This slower back-up process (A-NHEJ) can be observed in wild-type cells and cells with defects in DNA-PK dependent NHEJ (C-NHEJ). The pathway utilizes microhomologies and is prone to missjoining (Roth and Wilson, 1986, Verkaik et al., 2002). In addition, the joining process is biased to a high G:C content at the joining point (Audebert et al., 2008).

6.2.5 Fusion of short dysfunctional telomeres

Alternative NHEJ is reminiscent of the mutational profile of fusion events between short telomeres previously observed in our group. The profile comprises large deletion events, short patches of microhomology and a bias toward G:C at the fusion point between dysfunctional human telomeres (Capper et al., 2007, Letsolo et al., 2009). Furthermore, recent observations in telomerase negative mice have indicated that critically short telomeres undergo fusion in the absence of Lig4 and DNA-PKcs (Maser et al., 2007). This suggests that A-NHEJ could be the predominant mechanism to fuse short dysfunctional telomeres.

6.2.6 Aims

To test the hypothesis, a clonal derivative of human fetal lung diploid MRC5 fibroblasts expressing HPV16 E6E7 (clone 1) was treated with PARP-1 inhibitor, 1,5-Isoquinolinediol (DIQ). MRC5 E6E7 presents a well defined and reproducible model to investigate fusion events between short and dysfunctional telomeres. The inhibitor may disrupt the A-NHEJ pathway and create an effect on the mutational profile of MRC5 HPV16 E6E7.

6.3 Results

6.3.1 Culture kinetics of MRC5 HPV16 E6E7 incubated with PARP inhibitor

The clonal derivative of human fetal lung diploid fibroblast MRC5 fibroblasts expressing HPV16 E6E7 (clone 1) was previously described (Baird et al., 2003, Capper et al., 2007, Letsolo et al., 2009). Briefly, the lifespan of the clone was extended by forcing the expression of the human papillomavirus (HPV)16 E6E7 oncoproteins, which abrogate the function of RB and p53. The cells bypassed senescence and reached crisis after further 26-28 PDs. The XpYp telomere presents two alleles. The longer allele erodes with an erosion rate of 86 bp/PD which was indistinguishable from the erosion rate of the parental culture before senescence. The short XpYp allele and the 17p telomere continued to erode beyond a threshold length were they were no longer detectable with STELA. No XpYp telomeres derived from the shorter allele were present in crisis cells. The 17p telomere was lost in 85% of analysed cells as cells approached crisis. The disappearance of the short XpYp telomere and the 17p telomere coincided with the increase of fusion events.

MRC5 cells expressing HPV16 E6E7 were cultured at PD 32.9 in the absence and presence of dimethyl-sulfoxide (DMSO), 10 μM DIQ and 100 μM DIQ in 20% oxygen. For the experiment, the inhibitor DIQ was dissolved in DMSO and was added to the cell culture medium at a concentration of 10μM and 100μM. The cells were grown and treated by Mrs Rebecca Capper. Compared to the untreated cells, treatment with 10 μM and 100 μM DIQ reduced the replicative lifespan of MRC5 cells by 1.94% and 3.88% respectively (Fig. 6.1). Interestingly, the addition of 0.1% DMSO to the culture medium increased the lifespan of the cells by 1.94%. Investigating the growth rates during the exponential growth phase, the growth rate of all four cultures slowed from 1 PD per day to less than 1/5 of a PD per day, with an average value of 0.453 PD/day ± 0.284 PD/day for the untreated cells, 0.469 PD/day ± 0.317 PD/day for the DMSO treated cells, 0.425 PD/day ± 0.295 PD/day for the 10 μM DIQ treated cells and 0.399 PD/day ± 0.273 PD/day for the 100 μM DIQ treated cells (mean ± SD). No significant difference in the average growth rate could be found between the four cultures (p-value 0.977, ANOVA:

Single Factor). PARP inhibition at 10 μM and 100 μM DIQ concentration has no apparent effect on cell growth and cell viability.

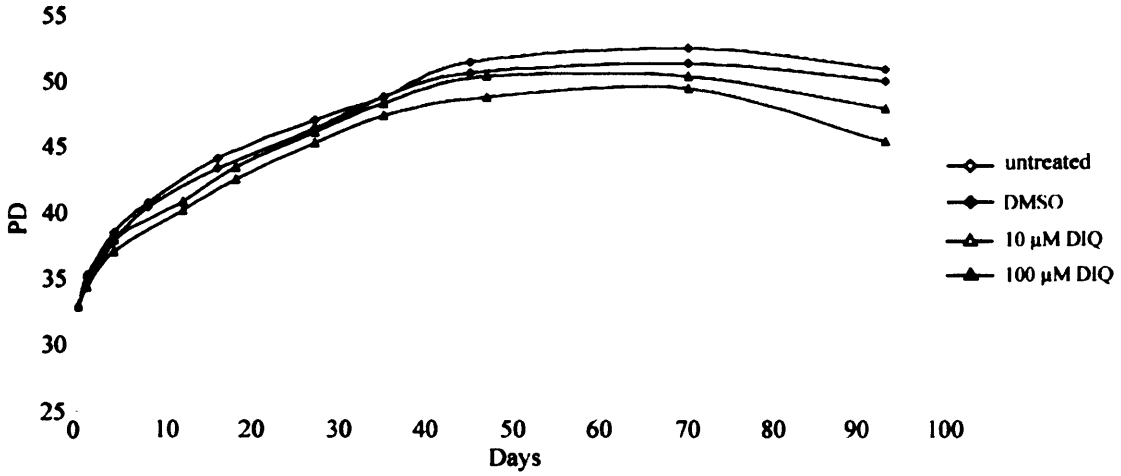

Figure 6.1 Growth curves of MRC5 HPV16 E6E7 cells in the presence and absence of PARP inhibitor DIQ.

6.3.2 Telomere dynamics of MRC5 HPV16 E6E7 after PARP inhibition

In order to monitor the telomere dynamics following the inhibition of PARP, the XpYp and 17p telomere length distributions of the untreated, DMSO treated, 10 μM DIQ and 100 μM DIQ treated cells were determined by using single telomere length analysis (STELA). Only the XpYp and 17p telomere were analysed as both chromosome are representative for average chromosomal telomere length and average telomere erosion rates resulting from the end-replication problem (Baird and Farr, 2006, Baird et al., 2003, Britt-Compton et al., 2006). Multiple cell samples were taken and subjected to STELA in order to track telomere dynamics with ongoing cell division as the cells approached crisis. Only the STELA southern blots for the DMSO and the 100 μM DIQ treated cells are presented here (Fig 6.2 and 6.3).

Both the DMSO and 100μM DIQ cells display the same bimodal distribution at the XpYp telomere. In both cultures, the shorter XpYp allele disappeared after

approximately 52 PDs. The 17p telomere was gradually lost as cells reached the end of their replicative lifespan. Both cultures appear to be similar and no obvious differences to the previous study could be observed (Capper et al., 2007). The minimal telomere length was determined after 70 days before PD values decreased due to the onset of crisis (Fig. 6.1). Comparing both cultures at this time point, both cultures attain a similar telomere length at both analysed chromosome ends. For the XpYp telomere, the control culture reached a minimal telomere length of 3.8 kb whereas the DIQ treated culture obtained a minimal length of 3.4 kb (p-value: 0.354, two tailed t-test). The 17p telomere attained the minimal telomere length of 0.57 kb and 0.58 kb at the control and PARP inhibited culture respectively (p-value: 0.788, two tailed t-test).

During the 70 days of the experiment, the DMSO and 100μM DIQ treated culture, lost 1.6 kb and 2.0 kb at the upper XpYp modal telomere length respectively. The 17p telomere decreased by 890 bp in the DMSO treated culture and by 650 bp in DIQ treated culture in this time period. During the exponential growth phase of the culture (47 days), the erosion rates for the XpYp and 17p telomere were calculated separately and are shown in Fig. 6.4. From the erosion rate diagrams it became apparent that treatment with a PARP inhibitor resulted in a rapid decrease in the XpYp telomere length in the later stages of the culture whereas the XpYp telomere in the control cells eroded more gradually. The same event could be observed at the 17p telomere in the DIQ treated cells. However it was not clear from these observations if the elevated telomere attrition was either a result of the influences of PARP inhibition on telomere dynamics or if PARP inhibition had induced an earlier onset of crisis which is characterised by an increase in the rate of telomere erosion (Britt-Compton et al., 2006, Capper et al., 2007).

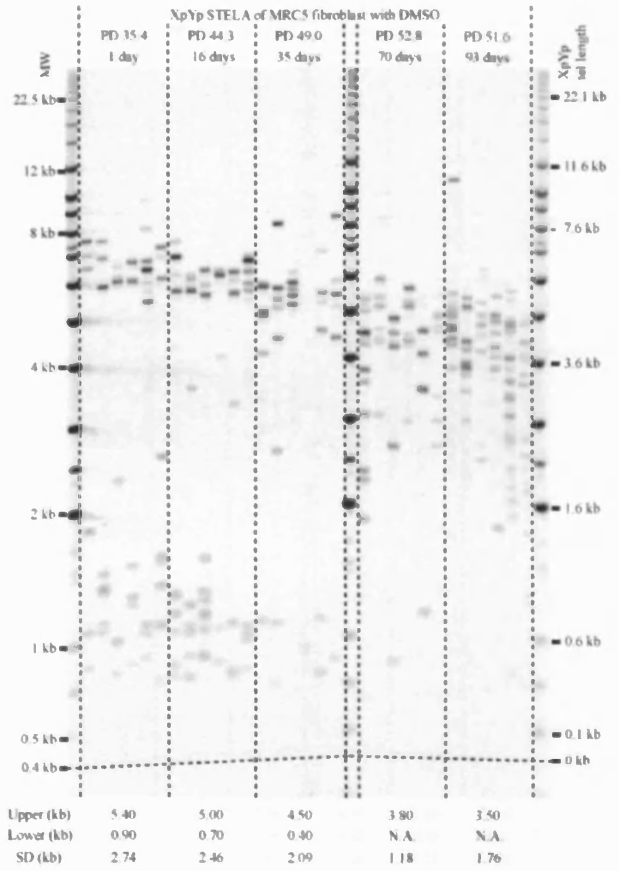

Figure 6.2 a XpYp Stela displaying the telomere length profile of MRC5 fibroblasts expressing E6E7 The PDs starting from the point cells were taken into culture are presented in the first line above the gel The days of treatment are displayed below the PDs. Molecular weight (MW) is indicated on the left and c orrected telomere length is indicated on the right. Modal telomere length and corresponding standard deviation (SD) are detailed below the gel.

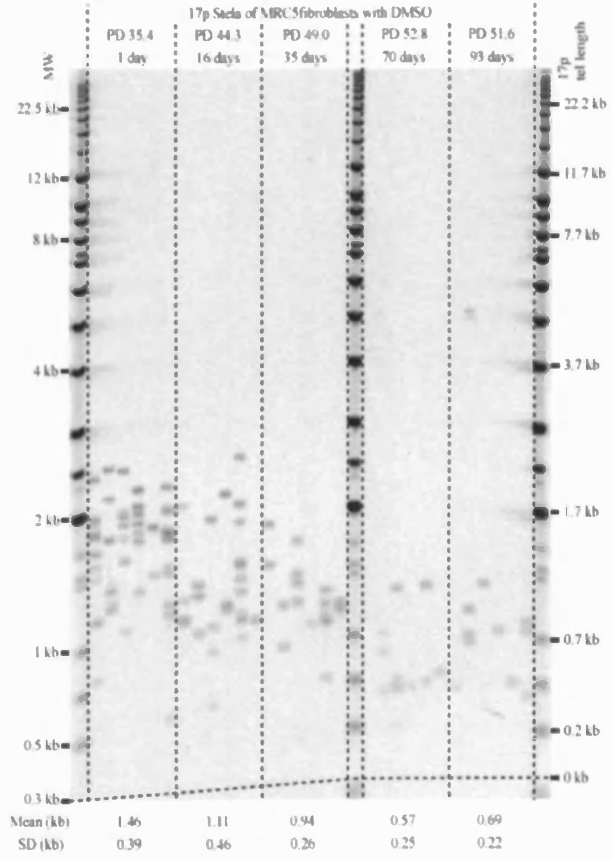

Figure 6.2 b 17p Stela displaying the telomere length profile of MRC5 fibroblasts expressing E6E7 with DMSO. The PD starting from the point cells were taken into culture are presented in the first line above the gel. The days of treatment are displayed in the second line above the gel. Molecular Weight (MW) is indicated on the left and corrected telomere length is indicated on the right. Mean telomere lengths and corresponding standard deviation (SD) are detailed below the gel.

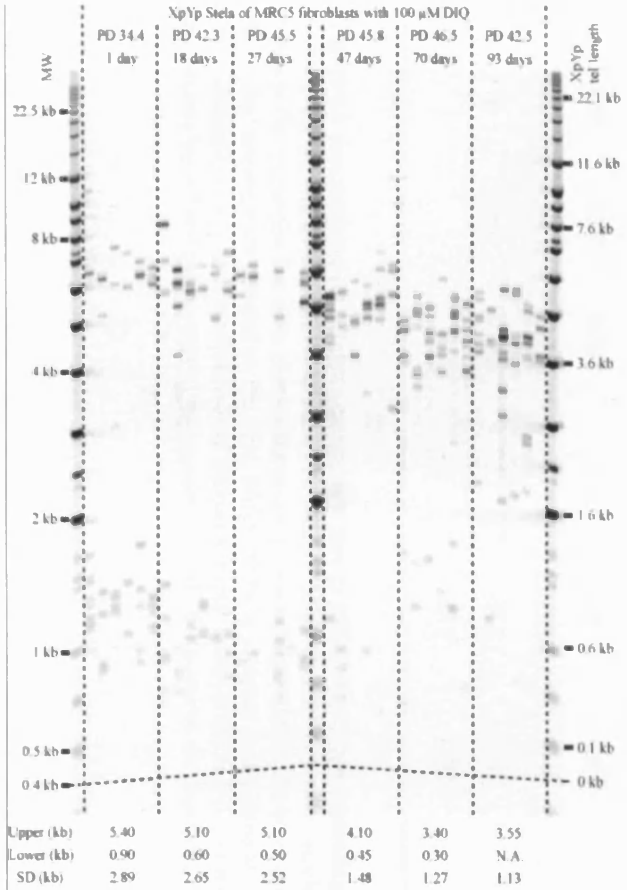

Figure 6.3 a. XpYp Stela displaying the telomere length profile of MRC5 fibroblasts expression E6E7 with 100nM DIQ. The PD starting from the point cells were taken into culture are presented in the first line above the gel. The days of treatment with DIQ are displayed in second line above the gel. Molecular Weight (MW) is indicated on the left and corrected telomere length is indicated on the right. Modal telomere length and corresponding standard deviation (SD) are detailed below the gel.

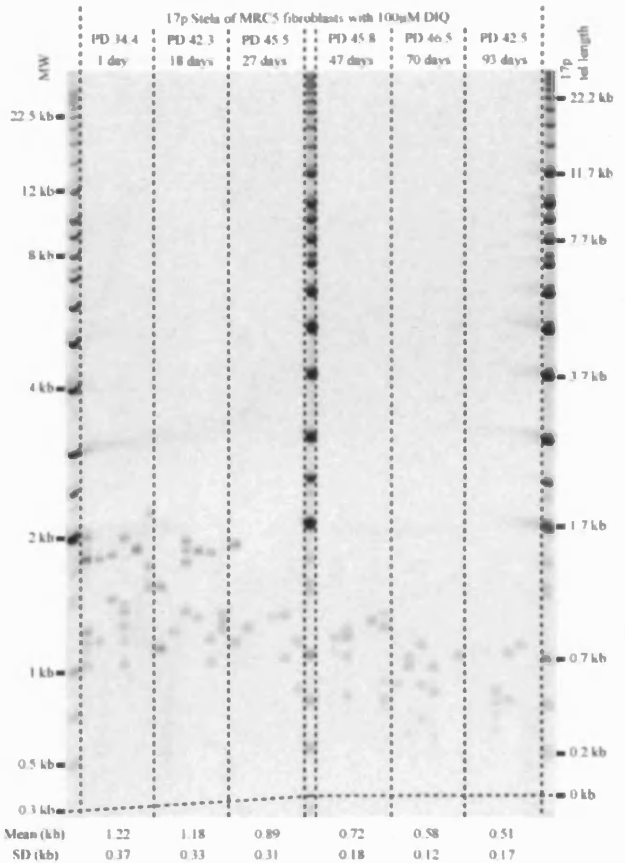

Figure 6.3 b. 17p Stela displaying the telomere length profile of MRC5 fibroblast expressing E6E7 with 100nM DIQ. The PD starting from the point were cells were taken back into culture are presented in the fist line above the gel. The days of treatment are displayed in the second line above the gel. Molecular Weight (MW) is indicated on the left and corrected telomere length is indicated on the right. Mean telomere length and corresponding standard deviation (SD) are detailed below the gel.

a)

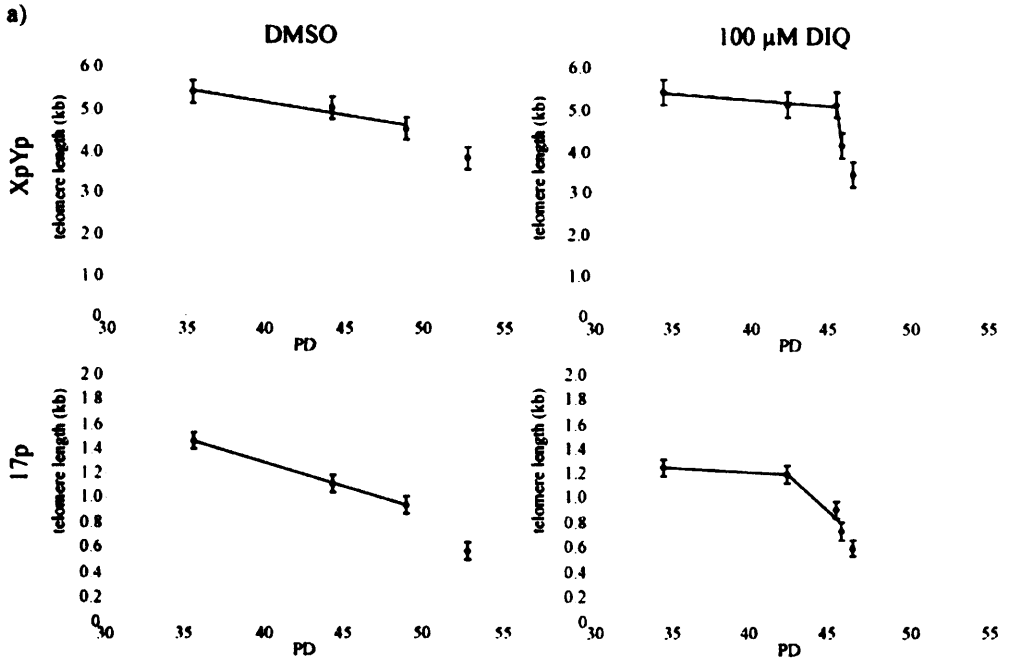

b)

telomere	Erosion rate bp/PD	DMSO R2	Number of Data points	Erosion rate bp/PD	100 µM DIQ R2	Number of Data points
XpYP	63.5	0.944	3	29.3	0.925	3
				2788.7	1	2
17p	38.4	0.995	3	6.3	1	2
				117	0.924	3

Figure 6.4 Summarising the telomere erosion rate data of MRC5 fibroblasts expressing HPV16 E6E7 in the presence and absence of PARP inhibitor, DIQ. a) Telomere erosion rate is calculated as the slope of the regression line after plotting the mean telomere length against the corresponding PD. Individual telomere are detailed on the right, PARP inhibitor presence is displayed above, error bars are ± standard error, y-axis presents means telomere length, x-axis presents PD. b) Erosion rates, accompanying R2 and the number of data points for each chromosome are displayed.

6.3.3 Fusion assay of MRC5 HPV16 E6E7 after PARP inhibition

Previous studies with MRC5 expressing HPV16 E6E7 have shown that the non-detectable telomeres become de-protected and can undergo fusion (Capper et al., 2007, Letsolo et al., 2009). The presence and quantity of telomere-telomere fusion events was determined using long-range single–molecules PCR amplifications with 3 primers for 17p, XpYp and 21q group telomeres (21q, 1q, 2q, 5q, 6q, 6p, 8p, 10q, 13q, 17q, 19p, 19q, 22q and the 2q13 interstitial telomeric locus) (Letsolo et al., 2009) (Fig. 6.5).

Fusion events between all chromosome ends could be detected. The fusion frequency was calculated for the 17p telomere in order to avoid the clonal fusion event between XpYp and 21q group in later PDs in DIQ treated cells. In a previous study the fusion frequency for MRC5 E6E7 fibroblasts was estimated for the XpYp telomere which is not suitable for comparing fusion frequencies in this thesis (Letsolo et al., 2009). However comparing the fusion frequency for the XpYp telomere in the control cells at PD 52.5 (4×10^{-4}) from this thesis to the frequency of the previous study (3.9×10^{-4} at PD 52.8) no obvious difference was apparent. As expected, the fusion frequency increased near crisis in both the control and treated cells. This is consistent with previous studies (Capper et al., 2007, Letsolo et al., 2009). Notably, after 70 days of treatment, fusion frequency is approximately 2 times higher in the PARP inhibited fibroblasts than in the control cells. The decrease in fusion frequency at the end of the DIQ treated culture (93 days) maybe attributed to the smaller amount of viable cells and reduction of diversity in fusion events. In addition, it was evident that the DIQ treated culture was overtaken by a clonal fusion between the XpYp telomere and a member of the 21q group. These fusion events from in an earlier PD, are maintained throughout the cell cycle and can overtake a clonal culture (Artandi and DePinho, 2000a, Capper et al., 2007).

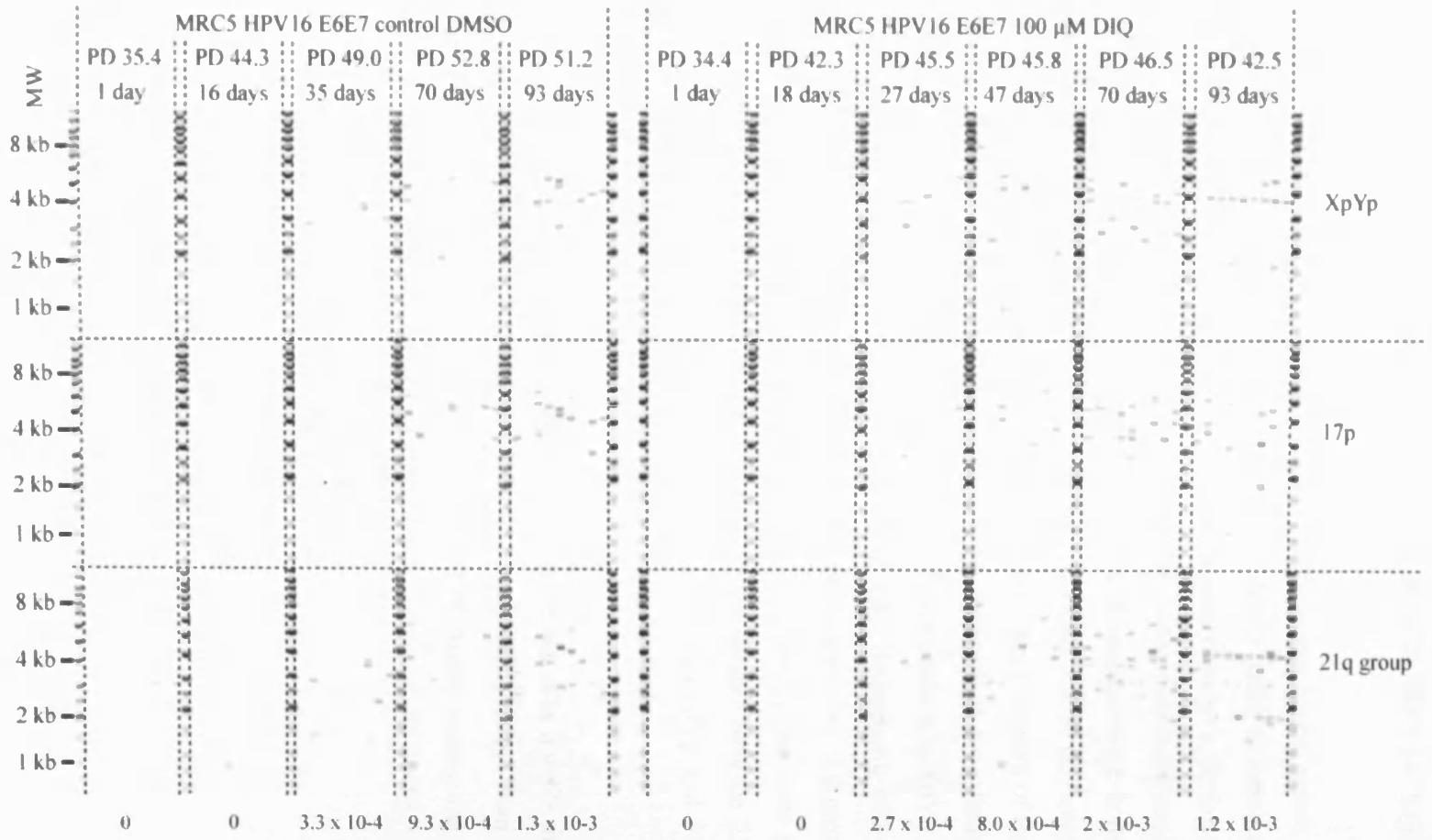

Figure 6.5 Fusion assay of MRC5 HPV16 E6E7 cells for the XpYp, 17p and 21q group chromosomes. Each reaction contains 10 ng of DNA. Bands are detected by the specific probe detailed on the right. The fusion frequency was calculated for the 17p chromosome and is stated below each sample. Molecular weight markers are indicated on the left.

6.3.4 Internal Structure of Fusions in MRC5 HPV16 E6E7 after PARP inhibition

In order to examine the internal structure of telomere fusion events following PARP inhibition for 95 days, 30 fusion events in MRC5 cells expressing E6E7 were re-amplified and sequenced (Fig. 6.6). Unfortunately only 3 fusion points could be determined by direct sequencing. The nature of fusion events between members of the 21q group made it difficult to obtain the fusion points, however in three fusion events the double sequence of the fusion could be separated due to the location of the fusion points (Fig 6.6). In addition six more fusions involving members of the 21q group were initiated though the fusion point could not be determined to a limit in the available DNA. All attempts to determine the sequence of prominent 21q-XpYp fusion event after 93 days of PARP inhibition were in vain (Fig 6.5). Sequencing with an XpYp primer revealed a clear sequence of the XpYp telomere whereas the 21q group primer gives a double sequence which could not be allocated to a specific telomere (data not shown). The same phenomena could be observed in fusion events between 21q group and the 17p telomere. Reamplification for fusions between the XpYp and 17p telomere were attempted however no true fusion event could be identified.

Whilst this does not represent a significant sample set, it is notable that the mean sub-telomeric deletion size is 2706 bp. This is considerably larger than the deletion size observed in a large analysis of MRC5 E6E7 fibroblasts undergoing crisis in culture, where a mean of 1496 bp has been documented (Letsolo et al., 2009).

6.3.5 Efficiency of PARP1 inhibition

Attempts have been made to confirm the efficiency of PARP1 inhibition by western-blot analysis. Following a standard protocol, soluble protein was isolated and quantified, but both PARP inhibition samples presented negative protein quantities. It was not clear if this was either the result of PARP1 inhibition or just a technical problem. Furthermore, it was decided to measure PARP activity by using an antibody against poly(ADP-ribose) (PAR) polymers. Several antibody dilutions (ranging form 1:1000 (recommended) to 1:100) were used, but not even a clear signal for the positive control samples could be achieved. Due to the time limit it was not possible to repeat the experiment (data not shown).

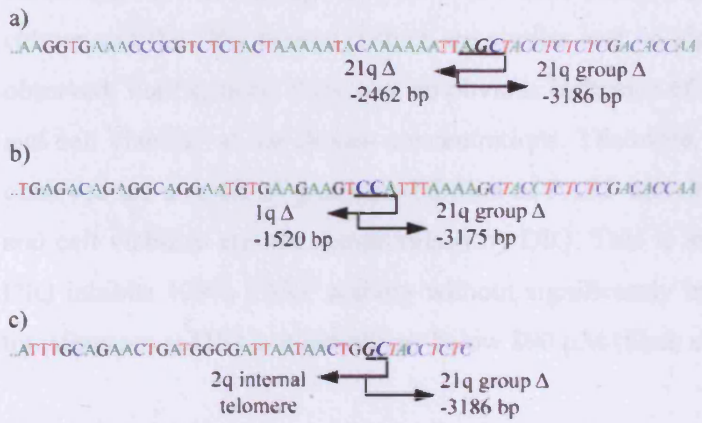

Figure 6.6 DNA sequences data of fusion events in MRC5 lung fibroblasts expressing E6E7 after PARP inhibition. Three fusion events between two members of the 21q group are presented. a) 21q:21q group fusion; b) 1q:21q group fusion; c) 2q (internal telomere):21q group fusion. Telomere-adjacent DNA is shown in multicolor, Fusion points, deletions size in bp, microhomoloy (bold and underlined) are displayed below the fusion event. The reamplification primer is indicated in italics.

6.4 Discussion

6.4.1 Effect of PARP inhibition on telomere length and lifespan of MRC5 E6E7 fibroblasts

In contrast to the DMSO treated MRC5 cells, PARP1 inhibition resulted in a rapid decline in average telomere length at the XpYp and 17p telomere in the later stages of culture. The reason behind these phenomena was not immediately apparent. One explanation could be that the rapid decrease of telomere length is the result of population doublings (PDs) not matching cells divisions (CDs) as it has been seen in cultures approaching crisis. In cultures at the end of their replicative capacity, long periods of constant cell number though with still significant cell division present an elevated telomere erosion rate (Capper et al., 2007). This raises the intriguing possibility that PARP inhibition could sensitise cells to telomere dysfunction driving them to crisis. However, what counts against this is the observation that growth rates of the control culture and the DIQ treated culture are similar and no significant slow down could be observed. Furthermore, there was no obvious influence of PARP inhibitors on cell cycle and cell viability at the chosen concentrations. Therefore, it can be assumed all effects observed are a result of gradual inhibition of PARP activity since cell cycle progression and cell viability are not compromised by DIQ. This is in agreement with the fact that DIQ inhibits 100% PARP activity without significantly inhibiting mono-(ADP-ribosyl) transfereases at DIQ concentrations below 890 μM (Shah et al., 1996).

Rapid decrease in telomere length has been observed before in human and hamster cells (Beneke et al., 2008). However, observations in mice are more ambiguous. Whereas one group showed rapidly shortening telomeres (d'Adda di Fagagna et al., 1999, Tong et al., 2001), others observed no impact after PARP inhibition (Espejel et al., 2004, Samper et al., 2001). Benke et al carried out a similar experiment in human and hamster cells observing similar rapid telomere erosion as seen in the MRC5 expressing E6E7. Furthermore, following the release from the PARP1 inhibitor, average telomere length reversed back to control levels in telomerase expressing cells. They speculated that PARP1 inhibition interferes with TRF2 activity. However it is not clear if PARP1

interacts with TRF2 in a permanent or more transient way. Both models propose that PARP1 is required for TRF2 modification, t-loop opening and replication fork passage (Beneke et al., 2008).

DIQ treated cells attain the same minimal telomere length as control culture. It is not possible to determine if the telomere lenght at XpYp and 17p levels out as it has been observed in previous observations (Beneke et al., 2008) or continuous to decrease further. Following previous observations the short unprotected telomeres undergo fusion.

6.4.2 Effect of PARP inhibition on fusion frequency of MRC5 E6E7 fibroblasts

The fusion frequency in the DMSO control cells was in the same range than observed in previous studies (Letsolo et al., 2009), whereas the fusion frequency of the DIQ treated MRC5 E6E7 fibroblasts is elevated (2x) compared to the control cells. Similar to the fusion events in DNA Ligase I deficient fibroblasts (chapter 3), the increase in fusion frequency could be an indicator that the fusion process is more efficient and therefore the unprotected chromosome termini undergo less processing prior to the final ligation step of end joining. However the few fusion events sequenced involved the chromosomes of the 21q group and indicated that most of the re-amplifiable fusion events are right at the limit of the fusion assay which detects deletion up to 3.5 kb (Letsolo et al., 2009). Interestingly, the mean deletion size was considerably larger in the three fusion events sequenced from the cells treated with the PARP inhibitor. Clearly more data are required to validate this result. However, if the assumption can be supported these data indicate that PARP inhibition may modulate the mechanism underlying telomere fusion, possibly by reducing the efficiency of ligation and thus facilitating continued 5′ – 3′ nucleolytic resection.

Fusions sequencing in MRC5 fibroblasts expressing E6E7 proved to be not as straight forward as expected. Recent observation of fusion events in ataxia telangiectasia-like

disorder (ATLD) fibroblasts, resulting from a deficiency in Mre11 have shown that telomere fusion in these cells display a more erratic mutational profile (Maira Tankimanova, personal communications). The fusion events in ATLD cells contain a higher frequency of insertions events. Closer inspection of which indicated that they are derived from duplicated sequences adjacent to the fusion point. From these data it was concluded that Mre11 is required to stabilise the end-joining complex to facilitate ligation. Furthermore, and consistent with its role in this process, fusion in ATLD cells exhibit more extensive sub-telomeric deletions. A similar pattern might be observed in MRC5 expressing E6E7 following the PARP1 inhibition. PARP1 is essential for the rapid recruitment of the MRN complex to end of DNA lesions (Haince et al., 2007). The structure of the MRN complex provides a stable DNA-chromatin bridging scaffold between two DNA ends in homologous recombination and NHEJ (Hopfner et al., 2002, Williams et al., 2008). This may account for the possible increase in sub-telomeric deletion size in presence of PARP inhibition. However it is clear that more sequencing analysis of fusion events is required before any firm conclusion can be drawn.

6.5 Conclusion

The limited data set from MRC5 E6E7 after PARP inhibition does not allow making any assumption how PARP inhibition influences fusions between short dysfunctional telomeres.

Chapter 7: General Discussion and Further Investigations

7.1 Reduced Replicative Lifespan in DNA Repair Deficiency Syndromes is not a Result of Elevated Telomere Erosion

All DNA repair deficient and patient derived human fibroblast strains observed in this thesis exhibit a similar limited replicative capacity of less than 30 PDs. This is in contrast to normal fibroblasts where 40 to 70 PDs at the point of replicative senescence are expected (Hayflick, 1965). The reduced replicative lifespan is in line with previous observations of these strains (DNA Ligase I deficiency: (Cabuy et al., 2005, Soza et al., 2009); DNA Ligase IV syndrome: (Badie et al., 1997, Cabuy et al., 2005); NBS: (Girard et al., 2000, Ranganathan et al., 2001) and also other DNA repair deficient fibroblasts cultures such as Werner Syndrome (Martin et al., 1970, Tollefsbol and Cohen, 1984). Furthermore, previous studies have implied that elevated telomere erosion might be the cause of the attenuated lifespan in these DNA repair deficient fibroblasts (Cabuy et al., 2005, Ranganathan et al., 2001). However, these studies were undertaken using TRF Southern Blots, Flow-Fish and Q-Fish. All these techniques are hybridisation based and suffer from a lower telomere length threshold below which telomeres cannot be detected. STELA does not suffer from this limitation as it is able to detect the length of the shortest telomere. In addition, the investigated DNA repair deficiency syndrome strains display a type of cell kinetics similar to those described in Werner's syndrome patients (Baird et al., 2004, Schonberg et al., 1984) and to some extent in normal human fibroblasts (Littlefield and Mailhes, 1975), where clonal succession, attenuation and expansion artificially elevate the average telomere erosion rate of the bulk population. In this case, the estimated population doublings (PDs) of the bulk population do not correspond with the actual cell divisions (CDs) of the single fibroblasts. In order to further address this issue, normally clonal derivatives of the parental bulk population are isolated which allow the observation of growth rates and telomere dynamics of an individual cell lineage (Smith et al., 1980). However, it was not possible to obtain viable clones from either the parental bulk population or the HPV16 E6E7 transfected cultures

of three of the DNA repair deficiency syndromes. Only the DNA Ligase I syndrome culture expressing HPV 16 E6E7 yielded viable clones. However due to the limited amount of samples and the cells reaching crisis, it was not possible to determine the average telomere erosion rate of these fibroblast cultures.

Telomere erosion is not the sole cause of replicative senescence. Also oxidative stress, DNA damaging agents and oncogene over expression can induce premature replicative senescence and thereby decrease the replicative lifespan of human fibroblast significantly (Dumont et al., 2000, Robles and Adami, 1998, Serrano et al., 1997). In order to determine the influence of oxidative stress on DNA repair deficient primary fibroblasts, all four fibroblast strains were cultured at 20% and 3% oxygen. Reducing oxidative stress increased the replicative capacity of the Ligase I deficient fibroblasts strain GM16096 and DNA Ligase IV syndrome strain GM 17523 (1% of remaining Ligase IV activity) by an average 22% compared to those cultured at 20% oxygen. However there was no significant increase in the growth rate in the exponential growth phase of these two DNA repair deficient strain. In contrast to these two, the second DNA Ligase IV Syndrome strain GM 16088 which retained less than 10% Ligase IV activity and the NBS1 deficient strain, both displayed no increase in replicative capacity at low oxygen concentrations.

The average telomere erosion rate documented with STELA in all four DNA repair deficiency fibroblast strains at 3% O_2 is within in the range of telomere erosion observed in normal human fibroblasts (40 to 120 bp per cell division) (DNA Ligase I deficiency: 99.6 ± 47.5 bp/PD; DNA Ligase IV syndrome GM16088: 112.4 ± 41.5 bp/PD; DNA Ligase IV syndrome GM17523: 41.5 ± 14.1 bp/PD; NBS: 95.6 ± 46.7 bp/PD) (Baird et al., 2003, Harley et al., 1990). At 20% oxygen, only the erosion rates of DNA Ligase I and NBS1 deficient fibroblast strains are elevated by an average 110% (DNA Ligase I deficiency: 180.1 ± 27.5 bp/PD; DNA Ligase IV syndrome GM16088: 115.4 ± 43.9 bp/PD; DNA Ligase IV syndrome GM17523: 43.9 ± 13.1 bp/PD; NBS: 229.4 ± 73.2 bp/PD). Notably, the erosion rates for the two DNA Ligase IV syndrome strains are similar at both oxygen concentrations.

The elevated telomere erosion rate and the even more truncated replicative capacity of DNA Ligase I deficient fibroblast at 20% oxygen indicates that the cells are sensitive to oxidative stress. This might be because oxidative tension can generate reactive oxygen species which in turn can cause cytotoxic lesions. These DNA lesions are repaired by base excision repair (BER) in normal human fibroblast (Laval et al., 1998). DNA Ligase I deficient fibroblasts are defective for long-patch BER and subsequently favour short-patch BER (Levin et al., 2000). It might be reasonable to assume that the defect in long-patch BER might promote a higher sensitivity to oxidative stress. This sensitivity might lead to more cells exiting the cell cycle and therefore no longer contributing to the overall growth of the culture. In consequence, the estimated PDs of the population would not correspond with the actual cell divisions and thereby increase the telomere erosion rate artificially.

In contrast to the DNA Ligase I deficient fibroblasts, NBS1 deficient fibroblast present elevated telomere erosion rate at 20% oxygen. However, this does not result in a further reduction in replicative lifespan of these cells. As described above, NBS cells at 20% oxygen displayed a type of cell kinetics in which clonal succession, attenuation and expansion artificially increase observed telomere erosion rates due to the estimated PDs not matching to the actual CDs.

Taking all of this together, this data supports the assumption that DNA repair deficiency does not result in accelerated telomere erosion and therefore the reduced replicative lifespan of these fibroblast cultures appears to be telomere independent.

The next step to further address this issue would be the forced ectopic expression of telomerase in these DNA repair deficient fibroblast cultures. In the case that the reduced replicative capacity of these patient derived strains is telomere dependent, the introduction of hTERT into these strains should result in telomere elongation, facilitate vigorous cell growth and consequently the cells should overcome replicative senescence extending the lifespan of the cells indefinitely (Bodnar et al., 1998, McSharry et al.,

2001). However preliminary experiments (data not shown) have shown that this may not be the case. Following the transfection with hTERT, the growth rate stayed similar to the control cultures. Furthermore, no clonal population could be obtained and no replicative capacity extension was observed in the bulk population. Due to the time limit, no STELA analysis of these samples has been carried out. In line with the previous speculation, this might also indicate that the limited replicative capacity of DNA repair deficient fibroblast strains is telomere independent.

7.2 The Mechanistic Basis of Telomere Fusions in DNA Repair Deficient Human Fibroblasts Cultures

The expression of HPV E6E7 extended the lifespan of DNA Ligase I deficient fibroblasts GM16096 resulting in short dysfunctional telomeres capable to undergo fusion. The observed fusion frequency was 10 fold higher than detected in normal MRC5 fibroblasts expressing HPV16 E6E7 (Capper et al., 2007, Letsolo et al., 2009) analysed using the same fusion technology. This might be attributed to a more efficient fusion process which is devoid of extensive end-processing which creates large sub-telomeric deletion events. Furthermore, in conjunction with low levels of DNA Ligase I activity, DNA Ligase I deficient cells display up-regulated levels of DNA Ligase III and are sensitive to PARP1 inhibition (Liang et al., 2008, Lonn et al., 1989, Moser et al., 2007). As the survival of GM16096 depends on DNA Ligase III and PARP1, this might suggest that the observed fusion events in GM16096 are dependent on these two proteins.

In contrast to DNA Ligase I deficient cells, the introduction of HPV E6E7 did not confer a lifespan extension in the two Ligase IV syndrome and NBS1 deficient fibroblast cultures. Therefore it was not possible to obtain sufficiently short telomeres that would undergo fusion. However, analysis of the two parental DNA Ligase IV deficient fibroblast strains revealed an apparent increase in fusion frequency in both cultures with ongoing cell division. The elevated fusion frequency, compared to normal cells with a similar average telomere length, coincides with the presence of a population of short

telomeres observed in both DNA Ligase IV syndrome strains. Several studies have shown (Baumann and Cech, 2000, Heacock et al., 2007, Maser et al., 2007) that short dysfunctional telomeres are subjected to fusion in the absence of functional NHEJ. Furthermore a previous study has shown that DSBs in human DNA Ligase IV deficient cells are joined by a microhomology driven, error-prone mechanism (Smith et al., 2003).

Similar to the fusion frequency in DNA Ligase I deficient fibroblast, the fusion frequency in MRC5 fibroblasts expressing E6E7 is elevated compared to the controls. Again this might indicate that the fusion process is more efficient and therefore the chromosome ends undergoes less processing prior the joining process. However, in contrast to previous observation, initial analysis revealed that all sub-telomeric deletion events of the analysed fusions are right at the limit of the fusion assay. Furthermore, the preliminary sequence analysis uncovered a large number of more complex fusion events. This resembles observations in ATLD cells, indicating that PARP1 inhibition might interfere with the recruitment of the MRN complex to DSBs.

Following these observations it might be safe to speculate that the fusion of short dysfunctional telomere is largely independent of DNA Ligase I and DNA Ligase IV. Furthermore, this leads to the final assumption that DNA Ligase III might be the predominant ligase involved in the fusion of short dysfunctional telomeres. From the here presented data, it was not possible to draw a conclusion about the involvement of NBS1 and PARP in the fusion of short telomeres.

The data presented here does not allow a definite statement about the mechanistic basis of fusions in short dysfunctional telomeres. Further sequence analysis and statistical analysis are necessary. For the fusion events detected in DNA Ligase I deficient fibroblasts, it could be interesting to determine if a paucity of large scale deletion events can be detected on the other chromosome ends from the 21q group (21q, 10q, 13q etc) similar to the 17p telomere. As it is not possible to carry out STELA on these telomeres to investigate the actual telomere length, it might be possible to determine if either all the observable fusion points are clustered in a specific range on the individual

chromosomes or are spread through out the whole sub-telomeric region. Furthermore, it might be of interest to determine if the deletion size pattern of the individual chromosomes is different to previous observations in our group (Letsolo et al., 2009).

In order to determine the predominant DNA repair pathway involved in the fusion of short dysfunctional telomeres it might be necessary to inhibit more than one DNA repair pathway. However, it is not expected that cells will survive this procedure. Instead it might be interesting to observe the formation of fusions in a more isolated environment in regards to the preferred DNA repair pathway in the cells. A previous study has shown that high grade bladder tumours which are associated with a high levels of genomic instability (Bentley et al., 2004) favour a highly mutagenic, microhomology mediated alternative end joining pathway. This pathway is independent of Ku 70/80, DNA-Pk_{cs} and XRCC4, all prominent components of C-NHEJ (Bentley et al., 2004). As this alternative NHEJ pathway dominates the end joining of mismatched DSBs in these bladder tumours, it might be reasonable to assume that short dysfunctional telomeres in these tumours are joined favouring the same error-prone pathway. If this is the case the resulting fusion profile should be similar or even more distinct than the fusion profile previously observed in human MRC5 fibroblast expressing HPV E6E7 (Capper et al., 2007, Letsolo et al., 2009).

Another possibility would be to approach the problem from another direction. As we have a good understanding how telomeres presents themselves in terms of TTAGGG repeat content, length of the TVR region and sub-telomeric region, it should be possible to create an artificial telomere template in a similar way like DSB templates are used to investigate end joining pathways (Bentley et al., 2004, Feldmann et al., 2000, Smith et al., 2001).

7.3 Sporadic Telomere Deletion Events in NBS1 Deficient Fibroblasts

The patient derived NBS1 deficient fibroblasts present a paucity of sporadic telomere deletion events. These deletion events do not conform to gradual telomere loss resulting

from the end replication problem (Olovnikov, 1971). In line with observations in *S. cerevisiae* (Bucholc et al., 2001, Lustig, 2003), it has been speculated that loss of large segments of telomeric DNA (rapid telomere deletions) in mammalians are the result of the resolution of Holliday junctions at the base of the t-loop by homologous recombination. These events are dependent on NBS1 and XRCC3 (Liu et al., 2004c, Wang et al., 2004). The observations presented here are in line with this hypothesis. One way to further investigate the involvement of NBS1 in sporadic telomere deletions events would be to re-introduce functional NBS1 into NBS fibroblasts which might lead to the re-appearance of the deletion of large segments of telomeric DNA.

7.4 Short Telomere Distribution in DNA Ligase IV Syndrome cells

STELA analysis of DNA Ligase IV deficient fibroblasts GM 17523, which retained less than 1% of DNA Ligase IV activity, revealed the presence of a distinct short telomere distribution on the 17p telomere. The distribution remained constant throughout the first 23 PDs and represented an average 14.4% of the total numbers of telomeres. A similar short distribution was observed at the 17p telomere of the second DNA Ligase IV syndrome strain GM16088. However, the result was ambiguous as the telomere adjacent probe for the 17p telomere yielded a number of recurring bands which could not be excluded to be a contamination. The consistent distribution in the more severely affected fibroblast culture appeared to be resistant against telomere erosion despite the average telomere length distribution declining with ongoing cell division. This lead to the speculation that DNA Ligase IV deficiency might facilitate a telomere replication defect which results in either premature exit from the cell cycle of the individual cell or an increased amount of telomeric fusion events through an DNA Ligase IV independent DNA repair pathway.

Interestingly, culturing the more severely effected DNA Ligase IV syndrome strain GM17523 at lower oxygen concentration increased the replicative capacity of the cells by 20%. However, no notable difference could be observed between telomere erosion rates of the cultures at the different oxygen concentrations. Furthermore, STELA

analysis revealed the distinct distribution of short telomeres being more prominent in the culture at 3% O_2. It has been speculated in this thesis that DNA Ligase IV deficiency confers an unknown telomere instability phenotype which results in a constant rate of production of short telomeres.

This phenotype may be related to the presence of specific TVR distributions that present a problem for telomeric replication. It may therefore be informative to examine the TVR distribution of the 17p telomere in these cell strains by TVR-PCR. It may also be informative to isolate and sequence the short 17p telomeric mutants observed in Ligase IV deficient cells. Little is known about the TVR composition of the 17p telomere, the only data coming from sequence analysis of fusion events that include the 17p TVR region. Some alleles contain CTAGGG repeats that have previously been documented to exhibit enhanced instability compared to the other TVR types (Mendez-Bermudez et al., 2009). CTAGGG repeats favour G-quadruplex formation (Lim et al., 2009), it is thus possible that the presence of CTAGGG repeats at the 17p telomere exacerbate replication fork stalling that may, in the absence of Ligase IV, preferentially lead to 17p specific mutation.

7.5 Increased Frequency of Single Nucleotide Mutations in DNA Ligase I Deficient Cells

While analysing the sequence of the observed fusion events in DNA Ligase I deficient human fibroblast expressing HPV E6E7, an increased frequency of single nucleotide mutations has been observed in the sub-telomeric sequence of the 17p telomere and the members of the 21q group (data not shown). Previous studies have shown that DNA Ligase I syndrome fibroblast have a defect in Okazaki fragment joining and single strand nick sealing during DNA damage repair (Prasad et al., 1996, Prigent et al., 1994). In contrast to unaffected fibroblasts, the ligation reaction in 46BR is stalled as a consequence of the accumulation of two normally transient intermediate products, Ligase I-AMP and nicked DNA-AMP (Henderson et al., 1985, Lonn et al., 1989, Prigent et al., 1994). The retarded ligation reaction could be the cause of the elevated single

nucleotide mutations frequency and subsequently may explain the significantly increased level of genomic instability in DNA Ligase I deficiency mouse models (Harrison et al., 2002).

7.6 Effect of PARP Inhibition on Telomere Length and Lifespan

The inhibition of PARP1 in MRC5 fibroblast expressing HPV E6E7 resulted in the rapid loss in average telomere length at the investigated XpYp and 17p telomere in the later stages of the culture. It was initially speculated that PARP1 inhibition could sensitise cells to telomere dysfunction and therefore drive cells to crisis. However this speculation was rejected as this and previous observations did not observe any changes in cell proliferation and cell viability during PARP1 inhibition (Beneke et al., 2008). Benke at al suggested that PARP1 inhibition interferes with TRF2 activity. However it is not clear yet, how PARP1 interacts with TRF2. One proposed model suggests PARP1 acts as a permanent "key" for the replication fork complex, modifying TRF2 and thereby opening the t-loop to facilitate the passage of the replication fork. The second model implies that PARP1 is transiently recruited to stalled or collapsed replication forks, where it modifies TRF2 and subsequently reactivates the progression of the replication fork. In both cases the replication fork stalling in the telomeric regions as a consequence of PARP1 inhibition might be the cause of the rapid decline in average telomere length. It is apparent that speculation about the effect of PARP1 inhibition are obsolete in this thesis as long as the actual PARP1 inhibition is not verified by western blotting.

References

AGUILERA, A. & KLEIN, H. L. (1989) Genetic and molecular analysis of recombination events in Saccharomyces cerevisiae occurring in the presence of the hyper-recombination mutation hpr1. *Genetics,* 122, 503-17.

AHEL, D., HOREJSI, Z., WIECHENS, N., POLO, S. E., GARCIA-WILSON, E., AHEL, I., FLYNN, H., SKEHEL, M., WEST, S. C., JACKSON, S. P., OWEN-HUGHES, T. & BOULTON, S. J. (2009) Poly(ADP-ribose)-dependent regulation of DNA repair by the chromatin remodeling enzyme ALC1. *Science,* 325, 1240-3.

AHNESORG, P., SMITH, P. & JACKSON, S. P. (2006) XLF interacts with the XRCC4-DNA ligase IV complex to promote DNA nonhomologous end-joining. *Cell,* 124, 301-13.

ALDER, J. K., CHEN, J. J., LANCASTER, L., DANOFF, S., SU, S. C., COGAN, J. D., VULTO, I., XIE, M., QI, X., TUDER, R. M., PHILLIPS, J. A., 3RD, LANSDORP, P. M., LOYD, J. E. & ARMANIOS, M. Y. (2008) Short telomeres are a risk factor for idiopathic pulmonary fibrosis. *Proc Natl Acad Sci U S A,* 105, 13051-6.

ALLSOPP, R. C., CHANG, E., KASHEFI-AAZAM, M., ROGAEV, E. I., PIATYSZEK, M. A., SHAY, J. W. & HARLEY, C. B. (1995) Telomere shortening is associated with cell division in vitro and in vivo. *Exp Cell Res,* 220, 194-200.

ALLSOPP, R. C., VAZIRI, H., PATTERSON, C., GOLDSTEIN, S., YOUNGLAI, E. V., FUTCHER, A. B., GREIDER, C. W. & HARLEY, C. B. (1992) Telomere length predicts replicative capacity of human fibroblasts. *Proc Natl Acad Sci U S A,* 89, 10114-8.

ALTMEYER, M., MESSNER, S., HASSA, P. O., FEY, M. & HOTTIGER, M. O. (2009) Molecular mechanism of poly(ADP-ribosyl)ation by PARP1 and identification of lysine residues as ADP-ribose acceptor sites. *Nucleic Acids Res,* 37, 3723-38.

ANDRES, S. N., MODESTI, M., TSAI, C. J., CHU, G. & JUNOP, M. S. (2007) Crystal structure of human XLF: a twist in nonhomologous DNA end-joining. *Mol Cell,* 28, 1093-101.

ARLETT, C. F. & PRIESTLEY, A. (1984) Deficient recovery from potentially lethal damage in some gamma-irradiated human fibroblast cell strains. *Br J Cancer Suppl,* 6, 227-32.

ARMANIOS, M. Y., CHEN, J. J., COGAN, J. D., ALDER, J. K., INGERSOLL, R. G., MARKIN, C., LAWSON, W. E., XIE, M., VULTO, I., PHILLIPS, J. A., 3RD, LANSDORP, P. M., GREIDER, C. W. & LOYD, J. E. (2007) Telomerase mutations in families with idiopathic pulmonary fibrosis. *N Engl J Med,* 356, 1317-26.

AROSIO, D., CUI, S., ORTEGA, C., CHOVANEC, M., DI MARCO, S., BALDINI, G., FALASCHI, A. & VINDIGNI, A. (2002) Studies on the mode of Ku interaction with DNA. *J Biol Chem,* 277, 9741-8.

ARTANDI, S. E., CHANG, S., LEE, S. L., ALSON, S., GOTTLIEB, G. J., CHIN, L. & DEPINHO, R. A. (2000) Telomere dysfunction promotes non-reciprocal translocations and epithelial cancers in mice. *Nature,* 406, 641-5.

ARTANDI, S. E. & DEPINHO, R. A. (2000a) A critical role for telomeres in suppressing and facilitating carcinogenesis. *Curr Opin Genet Dev,* 10, 39-46.

ARTANDI, S. E. & DEPINHO, R. A. (2000b) Mice without telomerase: what can they teach us about human cancer? *Nat Med,* 6, 852-5.

ATTWOOLL, C. L., AKPINAR, M. & PETRINI, J. H. (2009) The mre11 complex and the response to dysfunctional telomeres. *Mol Cell Biol,* 29, 5540-51.

AUDEBERT, M., SALLES, B. & CALSOU, P. (2004) Involvement of poly(ADP-ribose) polymerase-1 and XRCC1/DNA ligase III in an alternative route for DNA double-strand breaks rejoining. *J Biol Chem,* 279, 55117-26.

AUDEBERT, M., SALLES, B. & CALSOU, P. (2008) Effect of double-strand break DNA sequence on the PARP-1 NHEJ pathway. *Biochem Biophys Res Commun,* 369, 982-8.

AUDEBERT, M., SALLES, B., WEINFELD, M. & CALSOU, P. (2006) Involvement of polynucleotide kinase in a poly(ADP-ribose) polymerase-1-dependent DNA double-strand breaks rejoining pathway. *J Mol Biol,* 356, 257-65.

AZZALIN, C. M., REICHENBACH, P., KHORIAULI, L., GIULOTTO, E. & LINGNER, J. (2007) Telomeric repeat containing RNA and RNA surveillance factors at mammalian chromosome ends. *Science,* 318, 798-801.

BADIE, C., GOODHARDT, M., WAUGH, A., DOYEN, N., FORAY, N., CALSOU, P., SINGLETON, B., GELL, D., SALLES, B., JEGGO, P., ARLETT, C. F. & MALAISE, E. P. (1997) A DNA double-strand break defective fibroblast cell line (180BR) derived from a radiosensitive patient represents a new mutant phenotype. *Cancer Res,* 57, 4600-7.

BADIE, C., ILIAKIS, G., FORAY, N., ALSBEIH, G., CEDERVALL, B., CHAVAUDRA, N., PANTELIAS, G., ARLETT, C. & MALAISE, E. P. (1995a) Induction and rejoining of DNA double-strand breaks and interphase chromosome breaks after exposure to X rays in one normal and two hypersensitive human fibroblast cell lines. *Radiat Res,* 144, 26-35.

BADIE, C., ILIAKIS, G., FORAY, N., ALSBEIH, G., PANTELLIAS, G. E., OKAYASU, R., CHEONG, N., RUSSELL, N. S., BEGG, A. C., ARLETT, C. F. & ET AL. (1995b) Defective repair of DNA double-strand breaks and chromosome damage in fibroblasts from a radiosensitive leukemia patient. *Cancer Res,* 55, 1232-4.

BAE, N. S. & BAUMANN, P. (2007) A RAP1/TRF2 complex inhibits nonhomologous end-joining at human telomeric DNA ends. *Mol Cell,* 26, 323-34.

BAILEY, S. M., BRENNEMAN, M. A. & GOODWIN, E. H. (2004) Frequent recombination in telomeric DNA may extend the proliferative life of telomerase-negative cells. *Nucleic Acids Res,* 32, 3743-51.

BAIRD, D. M., COLEMAN, J., ROSSER, Z. H. & ROYLE, N. J. (2000) High levels of sequence polymorphism and linkage disequilibrium at the telomere of 12q: implications for telomere biology and human evolution. *Am J Hum Genet,* 66, 235-50.

BAIRD, D. M., DAVIS, T., ROWSON, J., JONES, C. J. & KIPLING, D. (2004) Normal telomere erosion rates at the single cell level in Werner syndrome fibroblast cells. *Hum Mol Genet,* 13, 1515-24.

BAIRD, D. M. & FARR, C. J. (2006) The organization and function of chromosomes. *EMBO Rep,* 7, 372-6.

BAIRD, D. M., JEFFREYS, A. J. & ROYLE, N. J. (1995) Mechanisms underlying telomere repeat turnover, revealed by hypervariable variant repeat distribution patterns in the human Xp/Yp telomere. *Embo J,* 14, 5433-43.

BAIRD, D. M., ROWSON, J., WYNFORD-THOMAS, D. & KIPLING, D. (2003) Extensive allelic variation and ultrashort telomeres in senescent human cells. *Nat Genet,* 33, 203-7.

BALIN, A. K., FISHER, A. J. & CARTER, D. M. (1984) Oxygen modulates growth of human cells at physiologic partial pressures. *J Exp Med,* 160, 152-66.

BANIK, S. S. & COUNTER, C. M. (2004) Characterization of interactions between PinX1 and human telomerase subunits hTERT and hTR. *J Biol Chem,* 279, 51745-8.

BARNES, D. E., JOHNSTON, L. H., KODAMA, K., TOMKINSON, A. E., LASKO, D. D. & LINDAHL, T. (1990) Human DNA ligase I cDNA: cloning and functional expression in Saccharomyces cerevisiae. *Proc Natl Acad Sci U S A,* 87, 6679-83.

BARNES, D. E., STAMP, G., ROSEWELL, I., DENZEL, A. & LINDAHL, T. (1998) Targeted disruption of the gene encoding DNA ligase IV leads to lethality in embryonic mice. *Curr Biol,* 8, 1395-8.

BARNES, D. E., TOMKINSON, A. E., LEHMANN, A. R., WEBSTER, A. D. & LINDAHL, T. (1992) Mutations in the DNA ligase I gene of an individual with immunodeficiencies and cellular hypersensitivity to DNA-damaging agents. *Cell,* 69, 495-503.

BASS, H. W., MARSHALL, W. F., SEDAT, J. W., AGARD, D. A. & CANDE, W. Z. (1997) Telomeres cluster de novo before the initiation of synapsis: a three-dimensional spatial analysis of telomere positions before and during meiotic prophase. *J Cell Biol,* 137, 5-18.

BAUMANN, P. & CECH, T. R. (2000) Protection of telomeres by the Ku protein in fission yeast. *Mol Biol Cell,* 11, 3265-75.

BAUMANN, P. & CECH, T. R. (2001) Pot1, the putative telomere end-binding protein in fission yeast and humans. *Science,* 292, 1171-5.

BEACHY, P. A., KARHADKAR, S. S. & BERMAN, D. M. (2004) Tissue repair and stem cell renewal in carcinogenesis. *Nature,* 432, 324-31.

BECKER, E., MEYER, V., MADAOUI, H. & GUEROIS, R. (2006) Detection of a tandem BRCT in Nbs1 and Xrs2 with functional implications in the DNA damage response. *Bioinformatics,* 22, 1289-92.

BENEKE, S., COHAUSZ, O., MALANGA, M., BOUKAMP, P., ALTHAUS, F. & BURKLE, A. (2008) Rapid regulation of telomere length is mediated by poly(ADP-ribose) polymerase-1. *Nucleic Acids Res,* 36, 6309-17.

BENTLEY, D., SELFRIDGE, J., MILLAR, J. K., SAMUEL, K., HOLE, N., ANSELL, J. D. & MELTON, D. W. (1996) DNA ligase I is required for fetal liver erythropoiesis but is not essential for mammalian cell viability. *Nat Genet,* 13, 489-91.

BENTLEY, D. J., HARRISON, C., KETCHEN, A. M., REDHEAD, N. J., SAMUEL, K., WATERFALL, M., ANSELL, J. D. & MELTON, D. W. (2002) DNA ligase I null mouse cells show normal DNA repair activity but altered DNA replication and reduced genome stability. *J Cell Sci,* 115, 1551-61.

BENTLEY, J., DIGGLE, C. P., HARNDEN, P., KNOWLES, M. A. & KILTIE, A. E. (2004) DNA double strand break repair in human bladder cancer is error prone and involves microhomology-associated end-joining. *Nucleic Acids Res,* 32, 5249-59.

BIANCHI, A., SMITH, S., CHONG, L., ELIAS, P. & DE LANGE, T. (1997) TRF1 is a dimer and bends telomeric DNA. *Embo J,* 16, 1785-94.

BIANCHI, A., STANSEL, R. M., FAIRALL, L., GRIFFITH, J. D., RHODES, D. & DE LANGE, T. (1999) TRF1 binds a bipartite telomeric site with extreme spatial flexibility. *Embo J,* 18, 5735-44.

BLACKBURN, E. H. & GALL, J. G. (1978) A tandemly repeated sequence at the termini of the extrachromosomal ribosomal RNA genes in Tetrahymena. *J Mol Biol,* 120, 33-53.

BLASCO, M. A. (2007) The epigenetic regulation of mammalian telomeres. *Nat Rev Genet,* 8, 299-309.

BLASCO, M. A. & HAHN, W. C. (2003) Evolving views of telomerase and cancer. *Trends Cell Biol,* 13, 289-94.

BLOCK, W. D., YU, Y., MERKLE, D., GIFFORD, J. L., DING, Q., MEEK, K. & LEES-MILLER, S. P. (2004) Autophosphorylation-dependent remodeling of the DNA-dependent protein kinase catalytic subunit regulates ligation of DNA ends. *Nucleic Acids Res,* 32, 4351-7.

BLOOM, D. (1954) Congenital telangiectatic erythema resembling lupus erythematosus in dwarfs; probably a syndrome entity. *AMA Am J Dis Child,* 88, 754-8.

BODNAR, A. G., OUELLETTE, M., FROLKIS, M., HOLT, S. E., CHIU, C. P., MORIN, G. B., HARLEY, C. B., SHAY, J. W., LICHTSTEINER, S. & WRIGHT, W. E. (1998) Extension of life-span by introduction of telomerase into normal human cells. *Science,* 279, 349-52.

BOGENHAGEN, D. F., PINZ, K. G. & PEREZ-JANNOTTI, R. M. (2001) Enzymology of mitochondrial base excision repair. *Prog Nucleic Acid Res Mol Biol,* 68, 257-71.

BOND, J. A., HAUGHTON, M. F., ROWSON, J. M., SMITH, P. J., GIRE, V., WYNFORD-THOMAS, D. & WYLLIE, F. S. (1999) Control of replicative life span in human cells: barriers to clonal expansion intermediate between M1 senescence and M2 crisis. *Mol Cell Biol,* 19, 3103-14.

BOULTON, S. J. & JACKSON, S. P. (1996) Saccharomyces cerevisiae Ku70 potentiates illegitimate DNA double-strand break repair and serves as a barrier to error-prone DNA repair pathways. *Embo J,* 15, 5093-103.

BRADSHAW, P. S., STAVROPOULOS, D. J. & MEYN, M. S. (2005) Human telomeric protein TRF2 associates with genomic double-strand breaks as an early response to DNA damage. *Nat Genet,* 37, 193-7.

BRAIG, M. & SCHMITT, C. A. (2006) Oncogene-induced senescence: putting the brakes on tumor development. *Cancer Res,* 66, 2881-4.

BRITT-COMPTON, B. & BAIRD, D. M. (2006) Intra-allelic mutation at human telomeres. *Biochem Soc Trans,* 34, 581-2.

BRITT-COMPTON, B., CAPPER, R., ROWSON, J. & BAIRD, D. M. (2009) Short telomeres are preferentially elongated by telomerase in human cells. *FEBS Lett,* 583, 3076-80.

BRITT-COMPTON, B., ROWSON, J., LOCKE, M., MACKENZIE, I., KIPLING, D. & BAIRD, D. M. (2006) Structural stability and chromosome-specific telomere length is governed by cis-acting determinants in humans. *Hum Mol Genet,* 15, 725-33.

BROCCOLI, D., SMOGORZEWSKA, A., CHONG, L. & DE LANGE, T. (1997) Human telomeres contain two distinct Myb-related proteins, TRF1 and TRF2. *Nat Genet,* 17, 231-5.

BROCCOLI, D., YOUNG, J. W. & DE LANGE, T. (1995) Telomerase activity in normal and malignant hematopoietic cells. *Proc Natl Acad Sci U S A,* 92, 9082-6.

BROWN, W. R., MACKINNON, P. J., VILLASANTE, A., SPURR, N., BUCKLE, V. J. & DOBSON, M. J. (1990) Structure and polymorphism of human telomere-associated DNA. *Cell,* 63, 119-32.

BRYAN, T. M., ENGLEZOU, A., DALLA-POZZA, L., DUNHAM, M. A. & REDDEL, R. R. (1997) Evidence for an alternative mechanism for maintaining telomere length in human tumors and tumor-derived cell lines. *Nat Med,* 3, 1271-4.

BRYANS, M., VALENZANO, M. C. & STAMATO, T. D. (1999) Absence of DNA ligase IV protein in XR-1 cells: evidence for stabilization by XRCC4. *Mutat Res,* 433, 53-8.

BRYANT, H. E., PETERMANN, E., SCHULTZ, N., JEMTH, A. S., LOSEVA, O., ISSAEVA, N., JOHANSSON, F., FERNANDEZ, S., MCGLYNN, P. &

HELLEDAY, T. (2009) PARP is activated at stalled forks to mediate Mre11-dependent replication restart and recombination. *Embo J,* 28, 2601-15.

BUCHOLC, M., PARK, Y. & LUSTIG, A. J. (2001) Intrachromatid excision of telomeric DNA as a mechanism for telomere size control in Saccharomyces cerevisiae. *Mol Cell Biol,* 21, 6559-73.

BUCK, D., MALIVERT, L., DE CHASSEVAL, R., BARRAUD, A., FONDANECHE, M. C., SANAL, O., PLEBANI, A., STEPHAN, J. L., HUFNAGEL, M., LE DEIST, F., FISCHER, A., DURANDY, A., DE VILLARTAY, J. P. & REVY, P. (2006) Cernunnos, a novel nonhomologous end-joining factor, is mutated in human immunodeficiency with microcephaly. *Cell,* 124, 287-99.

CABUY, E., NEWTON, C., JOKSIC, G., WOODBINE, L., KOLLER, B., JEGGO, P. A. & SLIJEPCEVIC, P. (2005) Accelerated telomere shortening and telomere abnormalities in radiosensitive cell lines. *Radiat Res,* 164, 53-62.

CAHILL, D. P., KINZLER, K. W., VOGELSTEIN, B. & LENGAUER, C. (1999) Genetic instability and darwinian selection in tumours. *Trends Cell Biol,* 9, M57-60.

CAMPISI, J. & D'ADDA DI FAGAGNA, F. (2007) Cellular senescence: when bad things happen to good cells. *Nat Rev Mol Cell Biol,* 8, 729-40.

CAPPER, R., BRITT-COMPTON, B., TANKIMANOVA, M., ROWSON, J., LETSOLO, B., MAN, S., HAUGHTON, M. & BAIRD, D. M. (2007) The nature of telomere fusion and a definition of the critical telomere length in human cells. *Genes Dev,* 21, 2495-508.

CARNEY, J. P., MASER, R. S., OLIVARES, H., DAVIS, E. M., LE BEAU, M., YATES, J. R., 3RD, HAYS, L., MORGAN, W. F. & PETRINI, J. H. (1998) The hMre11/hRad50 protein complex and Nijmegen breakage syndrome: linkage of double-strand break repair to the cellular DNA damage response. *Cell,* 93, 477-86.

CELLI, G. B. & DE LANGE, T. (2005) DNA processing is not required for ATM-mediated telomere damage response after TRF2 deletion. *Nat Cell Biol,* 7, 712-8.

CEROSALETTI, K. M., LANGE, E., STRINGHAM, H. M., WEEMAES, C. M., SMEETS, D., SOLDER, B., BELOHRADSKY, B. H., TAYLOR, A. M., KARNES, P., ELLIOTT, A., KOMATSU, K., GATTI, R. A., BOEHNKE, M. & CONCANNON, P. (1998) Fine localization of the Nijmegen breakage syndrome gene to 8q21: evidence for a common founder haplotype. *Am J Hum Genet,* 63, 125-34.

CERVANTES, R. B. & LUNDBLAD, V. (2002) Mechanisms of chromosome-end protection. *Curr Opin Cell Biol,* 14, 351-6.

CESARE, A. J. & GRIFFITH, J. D. (2004) Telomeric DNA in ALT cells is characterized by free telomeric circles and heterogeneous t-loops. *Mol Cell Biol,* 24, 9948-57.

CESARE, A. J., QUINNEY, N., WILLCOX, S., SUBRAMANIAN, D. & GRIFFITH, J. D. (2003) Telomere looping in P. sativum (common garden pea). *Plant J,* 36, 271-9.

CESARE, A. J. & REDDEL, R. R. (2010) Alternative lengthening of telomeres: models, mechanisms and implications. *Nat Rev Genet,* 11, 319-30.

CHAI, W., SHAY, J. W. & WRIGHT, W. E. (2005) Human telomeres maintain their overhang length at senescence. *Mol Cell Biol,* 25, 2158-68.

CHANG, C. C., WU, J. Y., CHIEN, C. W., WU, W. S., LIU, H., KANG, C. C., YU, L. J. & CHANG, T. C. (2003) A fluorescent carbazole derivative: high sensitivity for quadruplex DNA. *Anal Chem,* 75, 6177-83.

CHANG, P., COUGHLIN, M. & MITCHISON, T. J. (2005) Tankyrase-1 polymerization of poly(ADP-ribose) is required for spindle structure and function. *Nat Cell Biol,* 7, 1133-9.

CHEN, C. Y., HUANG, Y. L. & LIN, T. H. (1998) Association between oxidative stress and cytokine production in nickel-treated rats. *Arch Biochem Biophys,* 356, 127-32.

CHEN, L., TRUJILLO, K., SUNG, P. & TOMKINSON, A. E. (2000) Interactions of the DNA ligase IV-XRCC4 complex with DNA ends and the DNA-dependent protein kinase. *J Biol Chem,* 275, 26196-205.

CHEN, L. Y., LIU, D. & SONGYANG, Z. (2007) Telomere maintenance through spatial control of telomeric proteins. *Mol Cell Biol,* 27, 5898-909.

CHEN, Q., FISCHER, A., REAGAN, J. D., YAN, L. J. & AMES, B. N. (1995) Oxidative DNA damage and senescence of human diploid fibroblast cells. *Proc Natl Acad Sci U S A,* 92, 4337-41.

CHEN, Q. M., PROWSE, K. R., TU, V. C., PURDOM, S. & LINSKENS, M. H. (2001) Uncoupling the senescent phenotype from telomere shortening in hydrogen peroxide-treated fibroblasts. *Exp Cell Res,* 265, 294-303.

CHEN, Y., YANG, Y., VAN OVERBEEK, M., DONIGIAN, J. R., BACIU, P., DE LANGE, T. & LEI, M. (2008) A shared docking motif in TRF1 and TRF2 used for differential recruitment of telomeric proteins. *Science,* 319, 1092-6.

CHENG, M. L., HO, H. Y., WU, Y. H. & CHIU, D. T. (2004) Glucose-6-phosphate dehydrogenase-deficient cells show an increased propensity for oxidant-induced senescence. *Free Radic Biol Med,* 36, 580-91.

CHIANG, Y. J., HSIAO, S. J., YVER, D., CUSHMAN, S. W., TESSAROLLO, L., SMITH, S. & HODES, R. J. (2008) Tankyrase 1 and tankyrase 2 are essential but redundant for mouse embryonic development. *PLoS One,* 3, e2639.

CHIANG, Y. J., NGUYEN, M. L., GURUNATHAN, S., KAMINKER, P., TESSAROLLO, L., CAMPISI, J. & HODES, R. J. (2006) Generation and characterization of telomere length maintenance in tankyrase 2-deficient mice. *Mol Cell Biol,* 26, 2037-43.

CHIN, L. S., MURRAY, S. F., DOHERTY, P. F. & SINGH, S. K. (1999) K252a induces cell cycle arrest and apoptosis by inhibiting Cdc2 and Cdc25c. *Cancer Invest,* 17, 391-5.

CHIURILLO, M. A., CANO, I., DA SILVEIRA, J. F. & RAMIREZ, J. L. (1999) Organization of telomeric and sub-telomeric regions of chromosomes from the protozoan parasite Trypanosoma cruzi. *Mol Biochem Parasitol,* 100, 173-83.

COHEN, H. Y., LAVU, S., BITTERMAN, K. J., HEKKING, B., IMAHIYEROBO, T. A., MILLER, C., FRYE, R., PLOEGH, H., KESSLER, B. M. & SINCLAIR, D. A. (2004) Acetylation of the C terminus of Ku70 by CBP and PCAF controls Bax-mediated apoptosis. *Mol Cell,* 13, 627-38.

COHEN, S. B., GRAHAM, M. E., LOVRECZ, G. O., BACHE, N., ROBINSON, P. J. & REDDEL, R. R. (2007) Protein composition of catalytically active human telomerase from immortal cells. *Science,* 315, 1850-3.

COHN, M. & BLACKBURN, E. H. (1995) Telomerase in yeast. *Science,* 269, 396-400.

COLGIN, L. M., BARAN, K., BAUMANN, P., CECH, T. R. & REDDEL, R. R. (2003) Human POT1 facilitates telomere elongation by telomerase. *Curr Biol,* 13, 942-6.

COMPTON, S. A., CHOI, J. H., CESARE, A. J., OZGUR, S. & GRIFFITH, J. D. (2007) Xrcc3 and Nbs1 are required for the production of extrachromosomal telomeric circles in human alternative lengthening of telomere cells. *Cancer Res,* 67, 1513-9.

COOK, B. D., DYNEK, J. N., CHANG, W., SHOSTAK, G. & SMITH, S. (2002) Role for the related poly(ADP-Ribose) polymerases tankyrase 1 and 2 at human telomeres. *Mol Cell Biol,* 22, 332-42.

COSTANTINI, S., WOODBINE, L., ANDREOLI, L., JEGGO, P. A. & VINDIGNI, A. (2007) Interaction of the Ku heterodimer with the DNA ligase IV/Xrcc4 complex and its regulation by DNA-PK. *DNA Repair (Amst),* 6, 712-22.

COTNER-GOHARA, E., KIM, I. K., TOMKINSON, A. E. & ELLENBERGER, T. (2008) Two DNA-binding and nick recognition modules in human DNA ligase III. *J Biol Chem,* 283, 10764-72.

CRABBE, L., VERDUN, R. E., HAGGBLOM, C. I. & KARLSEDER, J. (2004) Defective telomere lagging strand synthesis in cells lacking WRN helicase activity. *Science,* 306, 1951-3.

CREISSEN, D. & SHALL, S. (1982) Regulation of DNA ligase activity by poly(ADP-ribose). *Nature,* 296, 271-2.

CRITCHLOW, S. E., BOWATER, R. P. & JACKSON, S. P. (1997) Mammalian DNA double-strand break repair protein XRCC4 interacts with DNA ligase IV. *Curr Biol,* 7, 588-98.

CUMMING, G., FIDLER, F. & VAUX, D. L. (2007) Error bars in experimental biology. *J Cell Biol,* 177, 7-11.

D'ADDA DI FAGAGNA, F., HANDE, M. P., TONG, W. M., LANSDORP, P. M., WANG, Z. Q. & JACKSON, S. P. (1999) Functions of poly(ADP-ribose) polymerase in controlling telomere length and chromosomal stability. *Nat Genet,* 23, 76-80.

D'ADDA DI FAGAGNA, F., HANDE, M. P., TONG, W. M., ROTH, D., LANSDORP, P. M., WANG, Z. Q. & JACKSON, S. P. (2001) Effects of DNA nonhomologous end-joining factors on telomere length and chromosomal stability in mammalian cells. *Curr Biol,* 11, 1192-6.

D'ADDA DI FAGAGNA, F., REAPER, P. M., CLAY-FARRACE, L., FIEGLER, H., CARR, P., VON ZGLINICKI, T., SARETZKI, G., CARTER, N. P. & JACKSON, S. P. (2003) A DNA damage checkpoint response in telomere-initiated senescence. *Nature,* 426, 194-8.

D'AMOURS, D. & JACKSON, S. P. (2002) The Mre11 complex: at the crossroads of dna repair and checkpoint signalling. *Nat Rev Mol Cell Biol,* 3, 317-27.

DAHM, K. (2007) Functions and regulation of human artemis in double strand break repair. *J Cell Biochem,* 100, 1346-51.

DANTZER, F., GIRAUD-PANIS, M. J., JACO, I., AME, J. C., SCHULTZ, I., BLASCO, M., KOERING, C. E., GILSON, E., MENISSIER-DE MURCIA, J., DE MURCIA, G. & SCHREIBER, V. (2004) Functional interaction

between poly(ADP-Ribose) polymerase 2 (PARP-2) and TRF2: PARP activity negatively regulates TRF2. *Mol Cell Biol,* 24, 1595-607.

DAVID, S. S., O'SHEA, V. L. & KUNDU, S. (2007) Base-excision repair of oxidative DNA damage. *Nature,* 447, 941-50.

DAVIS, T., BAIRD, D. M., HAUGHTON, M. F., JONES, C. J. & KIPLING, D. (2005) Prevention of accelerated cell aging in Werner syndrome using a p38 mitogen-activated protein kinase inhibitor. *J Gerontol A Biol Sci Med Sci,* 60, 1386-93.

DAVIS, T. & KIPLING, D. (2009) Assessing the role of stress signalling via p38 MAP kinase in the premature senescence of ataxia telangiectasia and Werner syndrome fibroblasts. *Biogerontology,* 10, 253-66.

DE BRUIN, D., ZAMAN, Z., LIBERATORE, R. A. & PTASHNE, M. (2001) Telomere looping permits gene activation by a downstream UAS in yeast. *Nature,* 409, 109-13.

DE JAGER, M., VAN NOORT, J., VAN GENT, D. C., DEKKER, C., KANAAR, R. & WYMAN, C. (2001) Human Rad50/Mre11 is a flexible complex that can tether DNA ends. *Mol Cell,* 8, 1129-35.

DE LANGE, T. (2004) T-loops and the origin of telomeres. *Nat Rev Mol Cell Biol,* 5, 323-9.

DE LANGE, T. (2005) Shelterin: the protein complex that shapes and safeguards human telomeres. *Genes Dev,* 19, 2100-10.

DE LANGE, T., SHIUE, L., MYERS, R. M., COX, D. R., NAYLOR, S. L., KILLERY, A. M. & VARMUS, H. E. (1990) Structure and variability of human chromosome ends. *Mol Cell Biol,* 10, 518-27.

DEBACKER, K. & KOOY, R. F. (2007) Fragile sites and human disease. *Hum Mol Genet,* 16 Spec No. 2, R150-8.

DEBACKER, K., WINNEPENNINCKX, B., LONGMAN, C., COLGAN, J., TOLMIE, J., MURRAY, R., VAN LUIJK, R., SCHEERS, S., FITZPATRICK, D. & KOOY, F. (2007) The molecular basis of the folate-sensitive fragile site FRA11A at 11q13. *Cytogenet Genome Res,* 119, 9-14.

DEFAZIO, L. G., STANSEL, R. M., GRIFFITH, J. D. & CHU, G. (2002) Synapsis of DNA ends by DNA-dependent protein kinase. *Embo J,* 21, 3192-200.

DEJARDIN, J. & KINGSTON, R. E. (2009) Purification of proteins associated with specific genomic Loci. *Cell,* 136, 175-86.

DENCHI, E. L. (2009) Give me a break: how telomeres suppress the DNA damage response. *DNA Repair (Amst),* **8,** 1118-26.

DENCHI, E. L. & DE LANGE, T. (2007) Protection of telomeres through independent control of ATM and ATR by TRF2 and POT1. *Nature,* 448, 1068-71.

DENG, Y., GUO, X., FERGUSON, D. O. & CHANG, S. (2009) Multiple roles for MRE11 at uncapped telomeres. *Nature,* 460, 914-8.

DERNBURG, A. F., SEDAT, J. W., CANDE, W. Z. & BASS, H. W. (1995) Cytology of telomeres. In *Telomeres* (ed. E. H. Blackburn and C. W. Greider) *New York: Laboratories Press,* pp. 295-338.

DESAI-MEHTA, A., CEROSALETTI, K. M. & CONCANNON, P. (2001) Distinct functional domains of nibrin mediate Mre11 binding, focus formation, and nuclear localization. *Mol Cell Biol,* 21, 2184-91.

DI LEONARDO, A., LINKE, S. P., CLARKIN, K. & WAHL, G. M. (1994) DNA damage triggers a prolonged p53-dependent G1 arrest and long-term induction of Cip1 in normal human fibroblasts. *Genes Dev,* 8, 2540-51.

DI MICCO, R., FUMAGALLI, M., CICALESE, A., PICCININ, S., GASPARINI, P., LUISE, C., SCHURRA, C., GARRE, M., NUCIFORO, P. G., BENSIMON, A., MAESTRO, R., PELICCI, P. G. & D'ADDA DI FAGAGNA, F. (2006) Oncogene-induced senescence is a DNA damage response triggered by DNA hyper-replication. *Nature,* 444, 638-42.

DIGWEED, M. & SPERLING, K. (2004) Nijmegen breakage syndrome: clinical manifestation of defective response to DNA double-strand breaks. *DNA Repair (Amst),* 3, 1207-17.

DIMITROVA, N. & DE LANGE, T. (2009) Cell cycle-dependent role of MRN at dysfunctional telomeres: ATM signaling-dependent induction of nonhomologous end joining (NHEJ) in G1 and resection-mediated inhibition of NHEJ in G2. *Mol Cell Biol,* 29, 5552-63.

DIMRI, G. P., ITAHANA, K., ACOSTA, M. & CAMPISI, J. (2000) Regulation of a senescence checkpoint response by the E2F1 transcription factor and p14(ARF) tumor suppressor. *Mol Cell Biol,* 20, 273-85.

DIONNE, I. & WELLINGER, R. J. (1996) Cell cycle-regulated generation of single-stranded G-rich DNA in the absence of telomerase. *Proc Natl Acad Sci U S A,* 93, 13902-7.

DIONNE, I. & WELLINGER, R. J. (1998) Processing of telomeric DNA ends requires the passage of a replication fork. *Nucleic Acids Res,* 26, 5365-71.

DUMONT, P., BALBEUR, L., REMACLE, J. & TOUSSAINT, O. (2000) Appearance of biomarkers of in vitro ageing after successive stimulation of WI-38 fibroblasts with IL-1alpha and TNF-alpha: senescence associated beta-galactosidase activity and morphotype transition. *J Anat,* 197 Pt 4, 529-37.

DUNHAM, M. A., NEUMANN, A. A., FASCHING, C. L. & REDDEL, R. R. (2000) Telomere maintenance by recombination in human cells. *Nat Genet,* 26, 447-50.

DUPRE, A., BOYER-CHATENET, L., SATTLER, R. M., MODI, A. P., LEE, J. H., NICOLETTE, M. L., KOPELOVICH, L., JASIN, M., BAER, R., PAULL, T. T. & GAUTIER, J. (2008) A forward chemical genetic screen reveals an inhibitor of the Mre11-Rad50-Nbs1 complex. *Nat Chem Biol,* 4, 119-25.

DURKIN, S. G., RAGLAND, R. L., ARLT, M. F., MULLE, J. G., WARREN, S. T. & GLOVER, T. W. (2008) Replication stress induces tumor-like microdeletions in FHIT/FRA3B. *Proc Natl Acad Sci U S A,* 105, 246-51.

DYNAN, W. S. & YOO, S. (1998) Interaction of Ku protein and DNA-dependent protein kinase catalytic subunit with nucleic acids. *Nucleic Acids Res,* 26, 1551-9.

ELLIS, N. A., GRODEN, J., YE, T. Z., STRAUGHEN, J., LENNON, D. J., CIOCCI, S., PROYTCHEVA, M. & GERMAN, J. (1995) The Bloom's syndrome gene product is homologous to RecQ helicases. *Cell,* 83, 655-66.

ESPEJEL, S., KLATT, P., MENISSIER-DE MURCIA, J., MARTIN-CABALLERO, J., FLORES, J. M., TACCIOLI, G., DE MURCIA, G. & BLASCO, M. A. (2004) Impact of telomerase ablation on organismal viability, aging, and tumorigenesis in mice lacking the DNA repair proteins PARP-1, Ku86, or DNA-PKcs. *J Cell Biol,* 167, 627-38.

FAIRALL, L., CHAPMAN, L., MOSS, H., DE LANGE, T. & RHODES, D. (2001) Structure of the TRFH dimerization domain of the human telomeric proteins TRF1 and TRF2. *Mol Cell,* 8, 351-61.

FAJKUS, J., KRALOVICS, R., KOVARIK, A. & FAJKUSOVA, L. (1995) The telomeric sequence is directly attached to the HRS60 subtelomeric tandem repeat in tobacco chromosomes. *FEBS Lett,* 364, 33-5.

FAJKUS, J., SYKOROVA, E. & LEITCH, A. R. (2005) Telomeres in evolution and evolution of telomeres. *Chromosome Res,* 13, 469-79.

FALCK, J., COATES, J. & JACKSON, S. P. (2005) Conserved modes of recruitment of ATM, ATR and DNA-PKcs to sites of DNA damage. *Nature,* 434, 605-11.

FARAGHER, R. G., KILL, I. R., HUNTER, J. A., POPE, F. M., TANNOCK, C. & SHALL, S. (1993) The gene responsible for Werner syndrome may be a cell division "counting" gene. *Proc Natl Acad Sci U S A,* 90, 12030-4.

FARMER, H., MCCABE, N., LORD, C. J., TUTT, A. N., JOHNSON, D. A., RICHARDSON, T. B., SANTAROSA, M., DILLON, K. J., HICKSON, I., KNIGHTS, C., MARTIN, N. M., JACKSON, S. P., SMITH, G. C. & ASHWORTH, A. (2005) Targeting the DNA repair defect in BRCA mutant cells as a therapeutic strategy. *Nature,* 434, 917-21.

FELDMANN, E., SCHMIEMANN, V., GOEDECKE, W., REICHENBERGER, S. & PFEIFFER, P. (2000) DNA double-strand break repair in cell-free extracts from Ku80-deficient cells: implications for Ku serving as an alignment factor in non-homologous DNA end joining. *Nucleic Acids Res,* 28, 2585-96.

FONG, P. C., BOSS, D. S., YAP, T. A., TUTT, A., WU, P., MERGUI-ROELVINK, M., MORTIMER, P., SWAISLAND, H., LAU, A., O'CONNOR, M. J., ASHWORTH, A., CARMICHAEL, J., KAYE, S. B., SCHELLENS, J. H. & DE BONO, J. S. (2009) Inhibition of poly(ADP-ribose) polymerase in tumors from BRCA mutation carriers. *N Engl J Med,* 361, 123-34.

FORSYTH, N. R., EVANS, A. P., SHAY, J. W. & WRIGHT, W. E. (2003) Developmental differences in the immortalization of lung fibroblasts by telomerase. *Aging Cell,* 2, 235-43.

FORTINI, P., PARLANTI, E., SIDORKINA, O. M., LAVAL, J. & DOGLIOTTI, E. (1999) The type of DNA glycosylase determines the base excision repair pathway in mammalian cells. *J Biol Chem,* 274, 15230-6.

FROSINA, G., FORTINI, P., ROSSI, O., CARROZZINO, F., RASPAGLIO, G., COX, L. S., LANE, D. P., ABBONDANDOLO, A. & DOGLIOTTI, E. (1996) Two pathways for base excision repair in mammalian cells. *J Biol Chem,* 271, 9573-8.

FU, D. & COLLINS, K. (2007) Purification of human telomerase complexes identifies factors involved in telomerase biogenesis and telomere length regulation. *Mol Cell,* 28, 773-85.

FUKUCHI, K., MARTIN, G. M. & MONNAT, R. J., JR. (1989) Mutator phenotype of Werner syndrome is characterized by extensive deletions. *Proc Natl Acad Sci U S A,* 86, 5893-7.

GAO, Y., SUN, Y., FRANK, K. M., DIKKES, P., FUJIWARA, Y., SEIDL, K. J., SEKIGUCHI, J. M., RATHBUN, G. A., SWAT, W., WANG, J., BRONSON, R. T., MALYNN, B. A., BRYANS, M., ZHU, C., CHAUDHURI, J., DAVIDSON, L., FERRINI, R., STAMATO, T., ORKIN, S. H., GREENBERG, M. E. & ALT, F. W. (1998) A critical role for DNA end-joining proteins in both lymphogenesis and neurogenesis. *Cell,* 95, 891-902.

GARNER, K. M., PLETNEV, A. A. & EASTMAN, A. (2009) Corrected structure of mirin, a small-molecule inhibitor of the Mre11-Rad50-Nbs1 complex. *Nat Chem Biol,* 5, 129-30; author reply 130.

GERMAN, J., ARCHIBALD, R. & BLOOM, D. (1965) Chromosomal Breakage in a Rare and Probably Genetically Determined Syndrome of Man. *Science,* 148, 506-7.

GERMAN, J., SCHONBERG, S., LOUIE, E. & CHAGANTI, R. S. (1977) Bloom's syndrome. IV. Sister-chromatid exchanges in lymphocytes. *Am J Hum Genet,* 29, 248-55.

GIRARD, P. M., FORAY, N., STUMM, M., WAUGH, A., RIBALLO, E., MASER, R. S., PHILLIPS, W. P., PETRINI, J., ARLETT, C. F. & JEGGO, P. A. (2000) Radiosensitivity in Nijmegen Breakage Syndrome cells is attributable to a repair defect and not cell cycle checkpoint defects. *Cancer Res,* 60, 4881-8.

GIRARD, P. M., KYSELA, B., HARER, C. J., DOHERTY, A. J. & JEGGO, P. A. (2004) Analysis of DNA ligase IV mutations found in LIG4 syndrome patients: the impact of two linked polymorphisms. *Hum Mol Genet,* 13, 2369-76.

GIRARD, P. M., RIBALLO, E., BEGG, A. C., WAUGH, A. & JEGGO, P. A. (2002) Nbs1 promotes ATM dependent phosphorylation events including those required for G1/S arrest. *Oncogene,* 21, 4191-9.

GIRE, V., ROUX, P., WYNFORD-THOMAS, D., BRONDELLO, J. M. & DULIC, V. (2004) DNA damage checkpoint kinase Chk2 triggers replicative senescence. *Embo J,* 23, 2554-63.

GOMEZ, D., AOUALI, N., RENAUD, A., DOUARRE, C., SHIN-YA, K., TAZI, J., MARTINEZ, S., TRENTESAUX, C., MORJANI, H. & RIOU, J. F. (2003) Resistance to senescence induction and telomere shortening by a G-quadruplex ligand inhibitor of telomerase. *Cancer Res,* 63, 6149-53.

GOMEZ, D., O'DONOHUE, M. F., WENNER, T., DOUARRE, C., MACADRE, J., KOEBEL, P., GIRAUD-PANIS, M. J., KAPLAN, H., KOLKES, A., SHIN-YA, K. & RIOU, J. F. (2006) The G-quadruplex ligand telomestatin inhibits POT1 binding to telomeric sequences in vitro and induces GFP-POT1 dissociation from telomeres in human cells. *Cancer Res,* 66, 6908-12.

GRADWOHL, G., MENISSIER DE MURCIA, J. M., MOLINETE, M., SIMONIN, F., KOKEN, M., HOEIJMAKERS, J. H. & DE MURCIA, G. (1990) The second zinc-finger domain of poly(ADP-ribose) polymerase determines specificity for single-stranded breaks in DNA. *Proc Natl Acad Sci U S A,* 87, 2990-4.

GRANOTIER, C., PENNARUN, G., RIOU, L., HOFFSCHIR, F., GAUTHIER, L. R., DE CIAN, A., GOMEZ, D., MANDINE, E., RIOU, J. F., MERGNY, J. L., MAILLIET, P., DUTRILLAUX, B. & BOUSSIN, F. D. (2005) Preferential binding of a G-quadruplex ligand to human chromosome ends. *Nucleic Acids Res,* 33, 4182-90.

GREIDER, C. W. & BLACKBURN, E. H. (1985) Identification of a specific telomere terminal transferase activity in Tetrahymena extracts. *Cell,* 43, 405-13.

GREIDER, C. W. & BLACKBURN, E. H. (1996) Telomeres, telomerase and cancer. *Sci Am,* 274, 92-7.

GRIFFITH, J., BIANCHI, A. & DE LANGE, T. (1998) TRF1 promotes parallel pairing of telomeric tracts in vitro. *J Mol Biol,* 278, 79-88.

GRIFFITH, J. D., COMEAU, L., ROSENFIELD, S., STANSEL, R. M., BIANCHI, A., MOSS, H. & DE LANGE, T. (1999) Mammalian telomeres end in a large duplex loop. *Cell,* 97, 503-14.

GU, J., LU, H., TIPPIN, B., SHIMAZAKI, N., GOODMAN, M. F. & LIEBER, M. R. (2007) XRCC4:DNA ligase IV can ligate incompatible DNA ends and can ligate across gaps. *Embo J,* 26, 1010-23.

GUPTA, V. & EBERLE, R. (1984) Modulation of tumour cell colony growth in soft agar by oxygen and its mechanism. *Br J Cancer,* 49, 587-93.

HAINCE, J. F., KOZLOV, S., DAWSON, V. L., DAWSON, T. M., HENDZEL, M. J., LAVIN, M. F. & POIRIER, G. G. (2007) Ataxia telangiectasia mutated (ATM) signaling network is modulated by a novel poly(ADP-ribose)-dependent pathway in the early response to DNA-damaging agents. *J Biol Chem,* 282, 16441-53.

HAINCE, J. F., MCDONALD, D., RODRIGUE, A., DERY, U., MASSON, J. Y., HENDZEL, M. J. & POIRIER, G. G. (2008) PARP1-dependent kinetics of recruitment of MRE11 and NBS1 proteins to multiple DNA damage sites. *J Biol Chem,* 283, 1197-208.

HALBERT, C. L., DEMERS, G. W. & GALLOWAY, D. A. (1991) The E7 gene of human papillomavirus type 16 is sufficient for immortalization of human epithelial cells. *J Virol,* 65, 473-8.

HALLIWELL, B. (1996) Antioxidants in human health and disease. *Annu Rev Nutr,* 16, 33-50.

HAMMARSTEN, O. & CHU, G. (1998) DNA-dependent protein kinase: DNA binding and activation in the absence of Ku. *Proc Natl Acad Sci U S A,* 95, 525-30.

HANAOKA, S., NAGADOI, A., YOSHIMURA, S., AIMOTO, S., LI, B., DE LANGE, T. & NISHIMURA, Y. (2001) NMR structure of the hRap1 Myb motif reveals a canonical three-helix bundle lacking the positive surface charge typical of Myb DNA-binding domains. *J Mol Biol,* 312, 167-75.

HARA, E., TSURUI, H., SHINOZAKI, A., NAKADA, S. & ODA, K. (1991) Cooperative effect of antisense-Rb and antisense-p53 oligomers on the extension of life span in human diploid fibroblasts, TIG-1. *Biochem Biophys Res Commun,* 179, 528-34.

HARLEY, C. B., FUTCHER, A. B. & GREIDER, C. W. (1990) Telomeres shorten during ageing of human fibroblasts. *Nature,* 345, 458-60.

HARPER, L., GOLUBOVSKAYA, I. & CANDE, W. Z. (2004) A bouquet of chromosomes. *J Cell Sci,* 117, 4025-32.

HARRISON, C., KETCHEN, A. M., REDHEAD, N. J., O'SULLIVAN, M. J. & MELTON, D. W. (2002) Replication failure, genome instability, and increased cancer susceptibility in mice with a point mutation in the DNA ligase I gene. *Cancer Res,* 62, 4065-74.

HARTLERODE, A. J. & SCULLY, R. (2009) Mechanisms of double-strand break repair in somatic mammalian cells. *Biochem J,* 423, 157-68.

HASSA, P. O. & HOTTIGER, M. O. (2008) The diverse biological roles of mammalian PARPS, a small but powerful family of poly-ADP-ribose polymerases. *Front Biosci,* 13, 3046-82.

HAYFLICK, L. (1965) The Limited in Vitro Lifetime of Human Diploid Cell Strains. *Exp Cell Res,* 37, 614-36.

HE, H., MULTANI, A. S., COSME-BLANCO, W., TAHARA, H., MA, J., PATHAK, S., DENG, Y. & CHANG, S. (2006) POT1b protects telomeres from end-to-end chromosomal fusions and aberrant homologous recombination. *Embo J,* 25, 5180-90.

HEACOCK, M. L., IDOL, R. A., FRIESNER, J. D., BRITT, A. B. & SHIPPEN, D. E. (2007) Telomere dynamics and fusion of critically shortened telomeres in plants lacking DNA ligase IV. *Nucleic Acids Res,* 35, 6490-500.

HEMANN, M. T., RUDOLPH, K. L., STRONG, M. A., DEPINHO, R. A., CHIN, L. & GREIDER, C. W. (2001a) Telomere dysfunction triggers developmentally regulated germ cell apoptosis. *Mol Biol Cell,* 12, 2023-30.

HEMANN, M. T., STRONG, M. A., HAO, L. Y. & GREIDER, C. W. (2001b) The shortest telomere, not average telomere length, is critical for cell viability and chromosome stability. *Cell,* 107, 67-77.

HENDERSON, L. M., ARLETT, C. F., HARCOURT, S. A., LEHMANN, A. R. & BROUGHTON, B. C. (1985) Cells from an immunodeficient patient (46BR) with a defect in DNA ligation are hypomutable but hypersensitive to the induction of sister chromatid exchanges. *Proc Natl Acad Sci U S A,* 82, 2044-8.

HENDERSON, S., ALLSOPP, R., SPECTOR, D., WANG, S. S. & HARLEY, C. (1996) In situ analysis of changes in telomere size during replicative aging and cell transformation. *J Cell Biol,* 134, 1-12.

HERBIG, U., JOBLING, W. A., CHEN, B. P., CHEN, D. J. & SEDIVY, J. M. (2004) Telomere shortening triggers senescence of human cells through a pathway involving ATM, p53, and p21(CIP1), but not p16(INK4a). *Mol Cell,* 14, 501-13.

HIEL, J. A., WEEMAES, C. M., VAN ENGELEN, B. G., SMEETS, D., LIGTENBERG, M., VAN DER BURGT, I., VAN DEN HEUVEL, L. P., CEROSALETTI, K. M., GABREELS, F. J. & CONCANNON, P. (2001) Nijmegen breakage syndrome in a Dutch patient not resulting from a defect in NBS1. *J Med Genet,* 38, E19.

HIRAOKA, Y., HENDERSON, E. & BLACKBURN, E. H. (1998) Not so peculiar: fission yeast telomere repeats. *Trends Biochem Sci,* 23, 126.

HIYAMA, E. & HIYAMA, K. (2002) Clinical utility of telomerase in cancer. *Oncogene,* 21, 643-9.

HIYAMA, E., YAMAOKA, H., MATSUNAGA, T., HAYASHI, Y., ANDO, H., SUITA, S., HORIE, H., KANEKO, M., SASAKI, F., HASHIZUME, K., NAKAGAWARA, A., OHNUMA, N. & YOKOYAMA, T. (2004) High expression of telomerase is an independent prognostic indicator of poor outcome in hepatoblastoma. *Br J Cancer,* 91, 972-9.

HOCHEGGER, H., DEJSUPHONG, D., FUKUSHIMA, T., MORRISON, C., SONODA, E., SCHREIBER, V., ZHAO, G. Y., SABERI, A., MASUTANI, M., ADACHI, N., KOYAMA, H., DE MURCIA, G. & TAKEDA, S. (2006) Parp-1 protects homologous recombination from interference by Ku and Ligase IV in vertebrate cells. *Embo J,* 25, 1305-14.

HOEIJMAKERS, J. H. (2001) Genome maintenance mechanisms for preventing cancer. *Nature,* 411, 366-74.

HOEKSTRA, M. F. (1997) Responses to DNA damage and regulation of cell cycle checkpoints by the ATM protein kinase family. *Curr Opin Genet Dev,* 7, 170-5.

HOLT, S. E. & SHAY, J. W. (1999) Role of telomerase in cellular proliferation and cancer. *J Cell Physiol,* 180, 10-8.

HOPFNER, K. P., KARCHER, A., CRAIG, L., WOO, T. T., CARNEY, J. P. & TAINER, J. A. (2001) Structural biochemistry and interaction architecture of the DNA double-strand break repair Mre11 nuclease and Rad50-ATPase. *Cell,* 105, 473-85.

HOPFNER, K. P., KARCHER, A., SHIN, D., FAIRLEY, C., TAINER, J. A. & CARNEY, J. P. (2000) Mre11 and Rad50 from Pyrococcus furiosus: cloning and biochemical characterization reveal an evolutionarily conserved multiprotein machine. *J Bacteriol,* 182, 6036-41.

HOPFNER, K. P., PUTNAM, C. D. & TAINER, J. A. (2002) DNA double-strand break repair from head to tail. *Curr Opin Struct Biol,* 12, 115-22.

HOUGHTALING, B. R., CUTTONARO, L., CHANG, W. & SMITH, S. (2004) A dynamic molecular link between the telomere length regulator TRF1 and the chromosome end protector TRF2. *Curr Biol,* 14, 1621-31.

HSIAO, S. J. & SMITH, S. (2008) Tankyrase function at telomeres, spindle poles, and beyond. *Biochimie,* 90, 83-92.

HSIAO, S. J. & SMITH, S. (2009) Sister telomeres rendered dysfunctional by persistent cohesion are fused by NHEJ. *J Cell Biol,* 184, 515-26.

HSIEH, C. L., ARLETT, C. F. & LIEBER, M. R. (1993) V(D)J recombination in ataxia telangiectasia, Bloom's syndrome, and a DNA ligase I-associated immunodeficiency disorder. *J Biol Chem,* 268, 20105-9.

HSU, H. L., GILLEY, D., BLACKBURN, E. H. & CHEN, D. J. (1999) Ku is associated with the telomere in mammals. *Proc Natl Acad Sci U S A,* 96, 12454-8.

HSU, H. L., GILLEY, D., GALANDE, S. A., HANDE, M. P., ALLEN, B., KIM, S. H., LI, G. C., CAMPISI, J., KOHWI-SHIGEMATSU, T. & CHEN, D. J. (2000) Ku acts in a unique way at the mammalian telomere to prevent end joining. *Genes Dev,* 14, 2807-12.

IWANO, T., TACHIBANA, M., RETH, M. & SHINKAI, Y. (2004) Importance of TRF1 for functional telomere structure. *J Biol Chem,* 279, 1442-8.

JACKSON, P., GRIMM, M. O., KINGSLEY, E. A., BROSIUS, U., ANTALIS, T., YARDLEY, G. & RUSSELL, P. J. (2002) Relationship between expression of KAI1 metastasis suppressor gene, mRNA levels and p53 in human bladder and prostate cancer cell lines. *Urol Oncol,* 7, 99-104.

JACKSON, S. P. & BARTEK, J. (2009) The DNA-damage response in human biology and disease. *Nature,* 461, 1071-8.

JIRICNY, J. (2006) The multifaceted mismatch-repair system. *Nat Rev Mol Cell Biol,* 7, 335-46.

JOHNSON, B. F., CALLEJA, G. B., BOISCLAIR, I. & YOO, B. Y. (1979) Cell division in yeasts. III. The biased, asymmetric location of the septum in the fission yeast cell, Schizosaccharomyces pombe. *Exp Cell Res,* 123, 253-9.

JONGMANS, W., VUILLAUME, M., CHRZANOWSKA, K., SMEETS, D., SPERLING, K. & HALL, J. (1997) Nijmegen breakage syndrome cells fail to induce the p53-mediated DNA damage response following exposure to ionizing radiation. *Mol Cell Biol,* 17, 5016-22.

JOYCE, R. M. & VINCENT, P. C. (1983) Advantage of reduced oxygen tension in growth of human melanomas in semi-solid cultures: quantitative analysis. *Br J Cancer,* 48, 385-93.

KAMESHITA, I., MATSUDA, Z., TANIGUCHI, T. & SHIZUTA, Y. (1984) Poly (ADP-Ribose) synthetase. Separation and identification of three proteolytic fragments as the substrate-binding domain, the DNA-binding domain, and the automodification domain. *J Biol Chem,* 259, 4770-6.

KANG, J., BRONSON, R. T. & XU, Y. (2002) Targeted disruption of NBS1 reveals its roles in mouse development and DNA repair. *Embo J,* 21, 1447-55.

KARLSEDER, J., BROCCOLI, D., DAI, Y., HARDY, S. & DE LANGE, T. (1999) p53- and ATM-dependent apoptosis induced by telomeres lacking TRF2. *Science,* 283, 1321-5.

KARLSEDER, J., HOKE, K., MIRZOEVA, O. K., BAKKENIST, C., KASTAN, M. B., PETRINI, J. H. & DE LANGE, T. (2004) The telomeric protein TRF2 binds the ATM kinase and can inhibit the ATM-dependent DNA damage response. *PLoS Biol,* 2, E240.

KARLSEDER, J., KACHATRIAN, L., TAKAI, H., MERCER, K., HINGORANI, S., JACKS, T. & DE LANGE, T. (2003) Targeted deletion reveals an essential function for the telomere length regulator Trf1. *Mol Cell Biol,* 23, 6533-41.

KAROW, J. K., CHAKRAVERTY, R. K. & HICKSON, I. D. (1997) The Bloom's syndrome gene product is a 3'-5' DNA helicase. *J Biol Chem,* 272, 30611-4.

KAROW, J. K., CONSTANTINOU, A., LI, J. L., WEST, S. C. & HICKSON, I. D. (2000) The Bloom's syndrome gene product promotes branch migration of holliday junctions. *Proc Natl Acad Sci U S A,* 97, 6504-8.

KASHINO, G., KODAMA, S., NAKAYAMA, Y., SUZUKI, K., FUKASE, K., GOTO, M. & WATANABE, M. (2003) Relief of oxidative stress by ascorbic acid delays cellular senescence of normal human and Werner syndrome fibroblast cells. *Free Radic Biol Med,* 35, 438-43.

KASS-EISLER, A. & GREIDER, C. W. (2000) Recombination in telomere-length maintenance. *Trends Biochem Sci,* 25, 200-4.

KASTAN, M. B. & LIM, D. S. (2000) The many substrates and functions of ATM. *Nat Rev Mol Cell Biol,* 1, 179-86.

KEITH, W. N. (2003) In situ analysis of telomerase RNA gene expression as a marker for tumor progression. *Methods Mol Med,* 75, 163-76.

KEITH, W. N., BILSLAND, A., HARDIE, M. & EVANS, T. R. (2004) Drug insight: Cancer cell immortality-telomerase as a target for novel cancer gene therapies. *Nat Clin Pract Oncol,* 1, 88-96.

KIM, N. W., PIATYSZEK, M. A., PROWSE, K. R., HARLEY, C. B., WEST, M. D., HO, P. L., COVIELLO, G. M., WRIGHT, W. E., WEINRICH, S. L. & SHAY, J. W. (1994) Specific association of human telomerase activity with immortal cells and cancer. *Science,* 266, 2011-5.

KIM, R. A., CARON, P. R. & WANG, J. C. (1995) Effects of yeast DNA topoisomerase III on telomere structure. *Proc Natl Acad Sci U S A,* 92, 2667-71.

KIM, S. H., BEAUSEJOUR, C., DAVALOS, A. R., KAMINKER, P., HEO, S. J. & CAMPISI, J. (2004) TIN2 mediates functions of TRF2 at human telomeres. *J Biol Chem,* 279, 43799-804.

KIM, S. H., KAMINKER, P. & CAMPISI, J. (1999) TIN2, a new regulator of telomere length in human cells. *Nat Genet,* 23, 405-12.

KIPLING, D. & COOKE, H. J. (1990) Hypervariable ultra-long telomeres in mice. *Nature,* 347, 400-2.

KIYONO, T., FOSTER, S. A., KOOP, J. I., MCDOUGALL, J. K., GALLOWAY, D. A. & KLINGELHUTZ, A. J. (1998) Both Rb/p16INK4a inactivation and

telomerase activity are required to immortalize human epithelial cells. *Nature,* 396, 84-8.

KOBAYASHI, J., TAUCHI, H., SAKAMOTO, S., NAKAMURA, A., MORISHIMA, K., MATSUURA, S., KOBAYASHI, T., TAMAI, K., TANIMOTO, K. & KOMATSU, K. (2002) NBS1 localizes to gamma-H2AX foci through interaction with the FHA/BRCT domain. *Curr Biol,* 12, 1846-51.

KOLQUIST, K. A., ELLISEN, L. W., COUNTER, C. M., MEYERSON, M., TAN, L. K., WEINBERG, R. A., HABER, D. A. & GERALD, W. L. (1998) Expression of TERT in early premalignant lesions and a subset of cells in normal tissues. *Nat Genet,* 19, 182-6.

KRAUS, W. L. (2009) New functions for an ancient domain. *Nat Struct Mol Biol,* 16, 904-7.

KULCZYK, A. W., YANG, J. C. & NEUHAUS, D. (2004) Solution structure and DNA binding of the zinc-finger domain from DNA ligase IIIalpha. *J Mol Biol,* 341, 723-38.

KYSELA, B., CHOVANEC, M. & JEGGO, P. A. (2005) Phosphorylation of linker histones by DNA-dependent protein kinase is required for DNA ligase IV-dependent ligation in the presence of histone H1. *Proc Natl Acad Sci U S A,* 102, 1877-82.

KYSELA, B., DOHERTY, A. J., CHOVANEC, M., STIFF, T., AMEER-BEG, S. M., VOJNOVIC, B., GIRARD, P. M. & JEGGO, P. A. (2003) Ku stimulation of DNA ligase IV-dependent ligation requires inward movement along the DNA molecule. *J Biol Chem,* 278, 22466-74.

LAFFERTY-WHYTE, K., CAIRNEY, C. J., WILL, M. B., SERAKINCI, N., DAIDONE, M. G., ZAFFARONI, N., BILSLAND, A. & KEITH, W. N. (2009) A gene expression signature classifying telomerase and ALT immortalization reveals an hTERT regulatory network and suggests a mesenchymal stem cell origin for ALT. *Oncogene,* 28, 3765-74.

LAKSHMIPATHY, U. & CAMPBELL, C. (2001) Antisense-mediated decrease in DNA ligase III expression results in reduced mitochondrial DNA integrity. *Nucleic Acids Res,* 29, 668-76.

LANGELIER, M. F., SERVENT, K. M., ROGERS, E. E. & PASCAL, J. M. (2008) A third zinc-binding domain of human poly(ADP-ribose) polymerase-1 coordinates DNA-dependent enzyme activation. *J Biol Chem,* 283, 4105-14.

LAVAL, J., JURADO, J., SAPARBAEV, M. & SIDORKINA, O. (1998) Antimutagenic role of base-excision repair enzymes upon free radical-induced DNA damage. *Mutat Res,* 402, 93-102.

LAVIN, M. F. & SHILOH, Y. (1997) The genetic defect in ataxia-telangiectasia. *Annu Rev Immunol,* 15, 177-202.

LEHMANN, A. R., WILLIS, A. E., BROUGHTON, B. C., JAMES, M. R., STEINGRIMSDOTTIR, H., HARCOURT, S. A., ARLETT, C. F. & LINDAHL, T. (1988) Relation between the human fibroblast strain 46BR and cell lines representative of Bloom's syndrome. *Cancer Res,* 48, 6343-7.

LETSOLO, B. T., ROWSON, J. & BAIRD, D. M. (2009) Fusion of short telomeres in human cells is characterized by extensive deletion and microhomology, and can result in complex rearrangements. *Nucleic Acids Res,* 38, 1841-52.

LEVIN, D. S., BAI, W., YAO, N., O'DONNELL, M. & TOMKINSON, A. E. (1997) An interaction between DNA ligase I and proliferating cell nuclear antigen: implications for Okazaki fragment synthesis and joining. *Proc Natl Acad Sci U S A,* 94, 12863-8.

LEVIN, D. S., MCKENNA, A. E., MOTYCKA, T. A., MATSUMOTO, Y. & TOMKINSON, A. E. (2000) Interaction between PCNA and DNA ligase I is critical for joining of Okazaki fragments and long-patch base-excision repair. *Curr Biol,* 10, 919-22.

LEVY, N., OEHLMANN, M., DELALANDE, F., NASHEUER, H. P., VAN DORSSELAER, A., SCHREIBER, V., DE MURCIA, G., MENISSIER-DE MURCIA, J., MAIORANO, D. & BRESSON, A. (2009) XRCC1 interacts with the p58 subunit of DNA Pol alpha-primase and may coordinate DNA repair and replication during S phase. *Nucleic Acids Res,* 37, 3177-88.

LI, B. & COMAI, L. (2002) Displacement of DNA-PKcs from DNA ends by the Werner syndrome protein. *Nucleic Acids Res,* 30, 3653-61.

LI, B. & DE LANGE, T. (2003) Rap1 affects the length and heterogeneity of human telomeres. *Mol Biol Cell,* 14, 5060-8.

LI, B. & LUSTIG, A. J. (1996) A novel mechanism for telomere size control in Saccharomyces cerevisiae. *Genes Dev,* 10, 1310-26.

LI, B., OESTREICH, S. & DE LANGE, T. (2000) Identification of human Rap1: implications for telomere evolution. *Cell,* 101, 471-83.

LI, C., GOODCHILD, J. & BARIL, E. F. (1994) DNA ligase I is associated with the 21 S complex of enzymes for DNA synthesis in HeLa cells. *Nucleic Acids Res,* 22, 632-8.

LIANG, L., DENG, L., NGUYEN, S. C., ZHAO, X., MAULION, C. D., SHAO, C. & TISCHFIELD, J. A. (2008) Human DNA ligases I and III, but not ligase IV, are required for microhomology-mediated end joining of DNA double-strand breaks. *Nucleic Acids Res,* 36, 3297-310.

LIEBER, M. R. (2008) The mechanism of human nonhomologous DNA end joining. *J Biol Chem,* 283, 1-5.

LIEBER, M. R. (2010) The mechanism of double-strand DNA break repair by the nonhomologous DNA end-joining pathway. *Annu Rev Biochem,* 79, 181-211.

LIEBER, M. R., MA, Y., PANNICKE, U. & SCHWARZ, K. (2003) Mechanism and regulation of human non-homologous DNA end-joining. *Nat Rev Mol Cell Biol,* 4, 712-20.

LILLARD-WETHERELL, K., MACHWE, A., LANGLAND, G. T., COMBS, K. A., BEHBEHANI, G. K., SCHONBERG, S. A., GERMAN, J., TURCHI, J. J., ORREN, D. K. & GRODEN, J. (2004) Association and regulation of the BLM helicase by the telomere proteins TRF1 and TRF2. *Hum Mol Genet,* 13, 1919-32.

LIM, K. W., ALBERTI, P., GUEDIN, A., LACROIX, L., RIOU, J. F., ROYLE, N. J., MERGNY, J. L. & PHAN, A. T. (2009) Sequence variant (CTAGGG)n in the human telomere favors a G-quadruplex structure containing a G.C.G.C tetrad. *Nucleic Acids Res,* 37, 6239-48.

LIN, A. W., BARRADAS, M., STONE, J. C., VAN AELST, L., SERRANO, M. & LOWE, S. W. (1998) Premature senescence involving p53 and p16 is activated in response to constitutive MEK/MAPK mitogenic signaling. *Genes Dev,* 12, 3008-19.

LINGNER, J., CECH, T. R., HUGHES, T. R. & LUNDBLAD, V. (1997) Three Ever Shorter Telomere (EST) genes are dispensable for in vitro yeast telomerase activity. *Proc Natl Acad Sci U S A,* 94, 11190-5.

LITTLEFIELD, L. G. & MAILHES, J. B. (1975) Observations of de novo clones of cytogentically aberrant cells in primary fibroblast cell strains from phenotypically normal women. *Am J Hum Genet,* 27, 190-7.

LIU, D., O'CONNOR, M. S., QIN, J. & SONGYANG, Z. (2004a) Telosome, a mammalian telomere-associated complex formed by multiple telomeric proteins. *J Biol Chem,* 279, 51338-42.

LIU, D., SAFARI, A., O'CONNOR, M. S., CHAN, D. W., LAEGELER, A., QIN, J. & SONGYANG, Z. (2004b) PTOP interacts with POT1 and regulates its localization to telomeres. *Nat Cell Biol,* 6, 673-80.

LIU, Y., MASSON, J. Y., SHAH, R., O'REGAN, P. & WEST, S. C. (2004c) RAD51C is required for Holliday junction processing in mammalian cells. *Science,* 303, 243-6.

LLOYD, J., CHAPMAN, J. R., CLAPPERTON, J. A., HAIRE, L. F., HARTSUIKER, E., LI, J., CARR, A. M., JACKSON, S. P. & SMERDON, S. J. (2009) A supramodular FHA/BRCT-repeat architecture mediates Nbs1 adaptor function in response to DNA damage. *Cell,* 139, 100-11.

LOAYZA, D. & DE LANGE, T. (2003) POT1 as a terminal transducer of TRF1 telomere length control. *Nature,* 423, 1013-8.

LOAYZA, D., PARSONS, H., DONIGIAN, J., HOKE, K. & DE LANGE, T. (2004) DNA binding features of human POT1: a nonamer 5'-TAGGGTTAG-3' minimal binding site, sequence specificity, and internal binding to multimeric sites. *J Biol Chem,* 279, 13241-8.

LOEB, L. A. & MONNAT, R. J., JR. (2008) DNA polymerases and human disease. *Nat Rev Genet,* 9, 594-604.

LOMBARD, D. B. & GUARENTE, L. (2000) Nijmegen breakage syndrome disease protein and MRE11 at PML nuclear bodies and meiotic telomeres. *Cancer Res,* 60, 2331-4.

LONN, U., LONN, S., NYLEN, U. & WINBLAD, G. (1989) Altered formation of DNA replication intermediates in human 46 BR fibroblast cells hypersensitive to 3-aminobenzamide. *Carcinogenesis,* 10, 981-5.

LOURIA-HAYON, I., GROSSMAN, T., SIONOV, R. V., ALSHEICH, O., PANDOLFI, P. P. & HAUPT, Y. (2003) The promyelocytic leukemia protein protects p53 from Mdm2-mediated inhibition and degradation. *J Biol Chem,* 278, 33134-41.

LUDERUS, M. E., VAN STEENSEL, B., CHONG, L., SIBON, O. C., CREMERS, F. F. & DE LANGE, T. (1996) Structure, subnuclear distribution, and nuclear matrix association of the mammalian telomeric complex. *J Cell Biol,* 135, 867-81.

LUKAS, J. & BARTEK, J. (2004) Cell division: the heart of the cycle. *Nature,* 432, 564-7.

LUKE, B. & LINGNER, J. (2009) TERRA: telomeric repeat-containing RNA. *Embo J,* 28, 2503-10.

LUKE, B., PANZA, A., REDON, S., IGLESIAS, N., LI, Z. & LINGNER, J. (2008) The Rat1p 5' to 3' exonuclease degrades telomeric repeat-containing RNA

and promotes telomere elongation in Saccharomyces cerevisiae. *Mol Cell,* 32, 465-77.

LUSTIG, A. J. (2003) Clues to catastrophic telomere loss in mammals from yeast telomere rapid deletion. *Nat Rev Genet,* 4, 916-23.

LYONS, R. J., DEANE, R., LYNCH, D. K., YE, Z. S., SANDERSON, G. M., EYRE, H. J., SUTHERLAND, G. R. & DALY, R. J. (2001) Identification of a novel human tankyrase through its interaction with the adaptor protein Grb14. *J Biol Chem,* 276, 17172-80.

MA, J. L., KIM, E. M., HABER, J. E. & LEE, S. E. (2003) Yeast Mre11 and Rad1 proteins define a Ku-independent mechanism to repair double-strand breaks lacking overlapping end sequences. *Mol Cell Biol,* 23, 8820-8.

MA, Y., LU, H., TIPPIN, B., GOODMAN, M. F., SHIMAZAKI, N., KOIWAI, O., HSIEH, C. L., SCHWARZ, K. & LIEBER, M. R. (2004) A biochemically defined system for mammalian nonhomologous DNA end joining. *Mol Cell,* 16, 701-13.

MA, Y., PANNICKE, U., SCHWARZ, K. & LIEBER, M. R. (2002) Hairpin opening and overhang processing by an Artemis/DNA-dependent protein kinase complex in nonhomologous end joining and V(D)J recombination. *Cell,* 108, 781-94.

MA, Y., SCHWARZ, K. & LIEBER, M. R. (2005) The Artemis:DNA-PKcs endonuclease cleaves DNA loops, flaps, and gaps. *DNA Repair (Amst),* 4, 845-51.

MACKEY, Z. B., NIEDERGANG, C., MURCIA, J. M., LEPPARD, J., AU, K., CHEN, J., DE MURCIA, G. & TOMKINSON, A. E. (1999) DNA ligase III is recruited to DNA strand breaks by a zinc finger motif homologous to that of poly(ADP-ribose) polymerase. Identification of two functionally distinct DNA binding regions within DNA ligase III. *J Biol Chem,* 274, 21679-87.

MAKAROV, V. L., HIROSE, Y. & LANGMORE, J. P. (1997) Long G tails at both ends of human chromosomes suggest a C strand degradation mechanism for telomere shortening. *Cell,* 88, 657-66.

MANI, R. S., FANTA, M., KARIMI-BUSHERI, F., SILVER, E., VIRGEN, C. A., CALDECOTT, K. W., CASS, C. E. & WEINFELD, M. (2007) XRCC1 stimulates polynucleotide kinase by enhancing its damage discrimination and displacement from DNA repair intermediates. *J Biol Chem,* 282, 28004-13.

MANI, R. S., KARIMI-BUSHERI, F., FANTA, M., CALDECOTT, K. W., CASS, C. E. & WEINFELD, M. (2004) Biophysical characterization of human

XRCC1 and its binding to damaged and undamaged DNA. *Biochemistry,* 43, 16505-14.

MARINTCHEV, A., MULLEN, M. A., MACIEJEWSKI, M. W., PAN, B., GRYK, M. R. & MULLEN, G. P. (1999) Solution structure of the single-strand break repair protein XRCC1 N-terminal domain. *Nat Struct Biol,* 6, 884-93.

MARRONE, A. & MASON, P. J. (2003) Dyskeratosis congenita. *Cell Mol Life Sci,* 60, 507-17.

MARTENS, U. M., CHAVEZ, E. A., POON, S. S., SCHMOOR, C. & LANSDORP, P. M. (2000) Accumulation of short telomeres in human fibroblasts prior to replicative senescence. *Exp Cell Res,* 256, 291-9.

MARTIN, G. M. (1982) Syndromes of accelerated aging. *Natl Cancer Inst Monogr,* 60, 241-7.

MARTIN, G. M., SPRAGUE, C. A. & EPSTEIN, C. J. (1970) Replicative life-span of cultivated human cells. Effects of donor's age, tissue, and genotype. *Lab Invest,* 23, 86-92.

MARTIN, I. V. & MACNEILL, S. A. (2002) ATP-dependent DNA ligases. *Genome Biol,* 3, REVIEWS3005.

MASER, R. S., WONG, K. K., SAHIN, E., XIA, H., NAYLOR, M., HEDBERG, H. M., ARTANDI, S. E. & DEPINHO, R. A. (2007) DNA-dependent protein kinase catalytic subunit is not required for dysfunctional telomere fusion and checkpoint response in the telomerase-deficient mouse. *Mol Cell Biol,* 27, 2253-65.

MASON, J. M. & BIESSMANN, H. (1995) The unusual telomeres of Drosophila. *Trends Genet,* 11, 58-62.

MASON, P. J. (2003) Stem cells, telomerase and dyskeratosis congenita. *Bioessays,* 25, 126-33.

MASSON, M., NIEDERGANG, C., SCHREIBER, V., MULLER, S., MENISSIER-DE MURCIA, J. & DE MURCIA, G. (1998) XRCC1 is specifically associated with poly(ADP-ribose) polymerase and negatively regulates its activity following DNA damage. *Mol Cell Biol,* 18, 3563-71.

MASUTOMI, K. & HAHN, W. C. (2003) Telomerase and tumorigenesis. *Cancer Lett,* 194, 163-72.

MCCLINTOCK, B. (1939) The Behavior in Successive Nuclear Divisions of a Chromosome Broken at Meiosis. *Proc Natl Acad Sci U S A,* 25, 405-16.

MCCLINTOCK, B. (1941) The Stability of Broken Ends of Chromosomes in Zea Mays. *Genetics,* 26, 234-82.

MCELLIGOTT, R. & WELLINGER, R. J. (1997) The terminal DNA structure of mammalian chromosomes. *Embo J,* 16, 3705-14.

MCKEE, B. D. (2004) Homologous pairing and chromosome dynamics in meiosis and mitosis. *Biochim Biophys Acta,* 1677, 165-80.

MCSHARRY, B. P., JONES, C. J., SKINNER, J. W., KIPLING, D. & WILKINSON, G. W. (2001) Human telomerase reverse transcriptase-immortalized MRC-5 and HCA2 human fibroblasts are fully permissive for human cytomegalovirus. *J Gen Virol,* 82, 855-63.

MENDEZ-BERMUDEZ, A., HILLS, M., PICKETT, H. A., PHAN, A. T., MERGNY, J. L., RIOU, J. F. & ROYLE, N. J. (2009) Human telomeres that contain (CTAGGG)n repeats show replication dependent instability in somatic cells and the male germline. *Nucleic Acids Res,* 37, 6225-38.

METCALFE, J. A., PARKHILL, J., CAMPBELL, L., STACEY, M., BIGGS, P., BYRD, P. J. & TAYLOR, A. M. (1996) Accelerated telomere shortening in ataxia telangiectasia. *Nat Genet,* 13, 350-3.

MEYN, M. S. (1999) Ataxia-telangiectasia, cancer and the pathobiology of the ATM gene. *Clin Genet,* 55, 289-304.

MEYNE, J., RATLIFF, R. L. & MOYZIS, R. K. (1989) Conservation of the human telomere sequence (TTAGGG)n among vertebrates. *Proc Natl Acad Sci U S A,* 86, 7049-53.

MICHALOGLOU, C., VREDEVELD, L. C., SOENGAS, M. S., DENOYELLE, C., KUILMAN, T., VAN DER HORST, C. M., MAJOOR, D. M., SHAY, J. W., MOOI, W. J. & PEEPER, D. S. (2005) BRAFE600-associated senescence-like cell cycle arrest of human naevi. *Nature,* 436, 720-4.

MICHISHITA, E., MCCORD, R. A., BERBER, E., KIOI, M., PADILLA-NASH, H., DAMIAN, M., CHEUNG, P., KUSUMOTO, R., KAWAHARA, T. L., BARRETT, J. C., CHANG, H. Y., BOHR, V. A., RIED, T., GOZANI, O. & CHUA, K. F. (2008) SIRT6 is a histone H3 lysine 9 deacetylase that modulates telomeric chromatin. *Nature,* 452, 492-6.

MILMAN, N., HIGUCHI, E. & SMITH, G. R. (2009) Meiotic DNA double-strand break repair requires two nucleases, MRN and Ctp1, to produce a single size class of Rec12 (Spo11)-oligonucleotide complexes. *Mol Cell Biol,* 29, 5998-6005.

MIMORI, T., AKIZUKI, M., YAMAGATA, H., INADA, S., YOSHIDA, S. & HOMMA, M. (1981) Characterization of a high molecular weight acidic nuclear protein recognized by autoantibodies in sera from patients with polymyositis-scleroderma overlap. *J Clin Invest,* 68, 611-20.

MITCHELL, J. R., WOOD, E. & COLLINS, K. (1999) A telomerase component is defective in the human disease dyskeratosis congenita. *Nature,* 402, 551-5.

MORIN, G. B. (1989) The human telomere terminal transferase enzyme is a ribonucleoprotein that synthesizes TTAGGG repeats. *Cell,* 59, 521-9.

MORTUSEWICZ, O. & LEONHARDT, H. (2007) XRCC1 and PCNA are loading platforms with distinct kinetic properties and different capacities to respond to multiple DNA lesions. *BMC Mol Biol,* 8, 81.

MOSER, J., KOOL, H., GIAKZIDIS, I., CALDECOTT, K., MULLENDERS, L. H. & FOUSTERI, M. I. (2007) Sealing of chromosomal DNA nicks during nucleotide excision repair requires XRCC1 and DNA ligase III alpha in a cell-cycle-specific manner. *Mol Cell,* 27, 311-23.

MOSHOUS, D., CALLEBAUT, I., DE CHASSEVAL, R., CORNEO, B., CAVAZZANA-CALVO, M., LE DEIST, F., TEZCAN, I., SANAL, O., BERTRAND, Y., PHILIPPE, N., FISCHER, A. & DE VILLARTAY, J. P. (2001) Artemis, a novel DNA double-strand break repair/V(D)J recombination protein, is mutated in human severe combined immune deficiency. *Cell,* 105, 177-86.

MUELLER, J. H. (1938) A Synthetic Medium for the Cultivation of C. diphtheriae. *J Bacteriol,* 36, 499-515.

MUNOZ-JORDAN, J. L., CROSS, G. A., DE LANGE, T. & GRIFFITH, J. D. (2001) t-loops at trypanosome telomeres. *Embo J,* 20, 579-88.

MUNTONI, A. & REDDEL, R. R. (2005) The first molecular details of ALT in human tumor cells. *Hum Mol Genet,* 14 Spec No. 2, R191-6.

NASMYTH, K. (1978) Eukaryotic gene cloning and expression in yeast. *Nature,* 274, 741-3.

NICK MCELHINNY, S. A., SNOWDEN, C. M., MCCARVILLE, J. & RAMSDEN, D. A. (2000) Ku recruits the XRCC4-ligase IV complex to DNA ends. *Mol Cell Biol,* 20, 2996-3003.

NIJNIK, A., DAWSON, S., CROCKFORD, T. L., WOODBINE, L., VISETNOI, S., BENNETT, S., JONES, M., TURNER, G. D., JEGGO, P. A., GOODNOW, C. C. & CORNALL, R. J. (2009) Impaired lymphocyte development and

antibody class switching and increased malignancy in a murine model of DNA ligase IV syndrome. *J Clin Invest,* 119, 1696-705.

NOVE, J., LITTLE, J. B., MAYER, P. J., TROILO, P. & NICHOLS, W. W. (1986) Hypersensitivity of cells from a new chromosomal-breakage syndrome to DNA-damaging agents. *Mutat Res,* 163, 255-62.

O'CONNOR, M. S., SAFARI, A., LIU, D., QIN, J. & SONGYANG, Z. (2004) The human Rap1 protein complex and modulation of telomere length. *J Biol Chem,* 279, 28585-91.

O'DRISCOLL, M., CEROSALETTI, K. M., GIRARD, P. M., DAI, Y., STUMM, M., KYSELA, B., HIRSCH, B., GENNERY, A., PALMER, S. E., SEIDEL, J., GATTI, R. A., VARON, R., OETTINGER, M. A., NEITZEL, H., JEGGO, P. A. & CONCANNON, P. (2001) DNA ligase IV mutations identified in patients exhibiting developmental delay and immunodeficiency. *Mol Cell,* 8, 1175-85.

O'DRISCOLL, M., GENNERY, A. R., SEIDEL, J., CONCANNON, P. & JEGGO, P. A. (2004) An overview of three new disorders associated with genetic instability: LIG4 syndrome, RS-SCID and ATR-Seckel syndrome. *DNA Repair (Amst),* 3, 1227-35.

OGAWA, H., JOHZUKA, K., NAKAGAWA, T., LEEM, S. H. & HAGIHARA, A. H. (1995) Functions of the yeast meiotic recombination genes, MRE11 and MRE2. *Adv Biophys,* 31, 67-76.

OKA, Y., SHIOTA, S., NAKAI, S., NISHIDA, Y. & OKUBO, S. (1980) Inverted terminal repeat sequence in the macronuclear DNA of Stylonychia pustulata. *Gene,* 10, 301-6.

OLOVNIKOV, A. M. (1971) [Principle of marginotomy in template synthesis of polynucleotides]. *Dokl Akad Nauk SSSR,* 201, 1496-9.

OPRESKO, P. L., MASON, P. A., PODELL, E. R., LEI, M., HICKSON, I. D., CECH, T. R. & BOHR, V. A. (2005) POT1 stimulates RecQ helicases WRN and BLM to unwind telomeric DNA substrates. *J Biol Chem,* 280, 32069-80.

OPRESKO, P. L., VON KOBBE, C., LAINE, J. P., HARRIGAN, J., HICKSON, I. D. & BOHR, V. A. (2002) Telomere-binding protein TRF2 binds to and stimulates the Werner and Bloom syndrome helicases. *J Biol Chem,* 277, 41110-9.

OTTAVIANI, A., GILSON, E. & MAGDINIER, F. (2008) Telomeric position effect: from the yeast paradigm to human pathologies? *Biochimie,* 90, 93-107.

OTTO, H., RECHE, P. A., BAZAN, F., DITTMAR, K., HAAG, F. & KOCH-NOLTE, F. (2005) In silico characterization of the family of PARP-like poly(ADP-ribosyl)transferases (pARTs). *BMC Genomics,* 6, 139.

PALM, W. & DE LANGE, T. (2008) How shelterin protects mammalian telomeres. *Annu Rev Genet,* 42, 301-34.

PALM, W., HOCKEMEYER, D., KIBE, T. & DE LANGE, T. (2009) Functional dissection of human and mouse POT1 proteins. *Mol Cell Biol,* 29, 471-82.

PARDUE, M. L. & DEBARYSHE, P. G. (2003) Retrotransposons provide an evolutionarily robust non-telomerase mechanism to maintain telomeres. *Annu Rev Genet,* 37, 485-511.

PARKINSON, G. N., LEE, M. P. & NEIDLE, S. (2002) Crystal structure of parallel quadruplexes from human telomeric DNA. *Nature,* 417, 876-80.

PARRINELLO, S., SAMPER, E., KRTOLICA, A., GOLDSTEIN, J., MELOV, S. & CAMPISI, J. (2003) Oxygen sensitivity severely limits the replicative lifespan of murine fibroblasts. *Nat Cell Biol,* 5, 741-7.

PASCAL, J. M., O'BRIEN, P. J., TOMKINSON, A. E. & ELLENBERGER, T. (2004) Human DNA ligase I completely encircles and partially unwinds nicked DNA. *Nature,* 432, 473-8.

PAULL, T. T. & GELLERT, M. (1999) Nbs1 potentiates ATP-driven DNA unwinding and endonuclease cleavage by the Mre11/Rad50 complex. *Genes Dev,* 13, 1276-88.

PETERSEN, S., SARETZKI, G. & VON ZGLINICKI, T. (1998) Preferential accumulation of single-stranded regions in telomeres of human fibroblasts. *Exp Cell Res,* 239, 152-60.

PETRACEK, M. E., LEFEBVRE, P. A., SILFLOW, C. D. & BERMAN, J. (1990) Chlamydomonas telomere sequences are A+T-rich but contain three consecutive G-C base pairs. *Proc Natl Acad Sci U S A,* 87, 8222-6.

PETRINI, J. H., DONOVAN, J. W., DIMARE, C. & WEAVER, D. T. (1994) Normal V(D)J coding junction formation in DNA ligase I deficiency syndromes. *J Immunol,* 152, 176-83.

PETRINI, J. H. & STRACKER, T. H. (2003) The cellular response to DNA double-strand breaks: defining the sensors and mediators. *Trends Cell Biol,* 13, 458-62.

PICH, U., FUCHS, J. & SCHUBERT, I. (1996) How do Alliaceae stabilize their chromosome ends in the absence of TTTAGGG sequences? *Chromosome Res,* 4, 207-13.

PLOWMAN, P. N., BRIDGES, B. A., ARLETT, C. F., HINNEY, A. & KINGSTON, J. E. (1990) An instance of clinical radiation morbidity and cellular radiosensitivity, not associated with ataxia-telangiectasia. *Br J Radiol,* 63, 624-8.

PLUTA, A. F., KAINE, B. P. & SPEAR, B. B. (1982) The terminal organization of macronuclear DNA in Oxytricha fallax. *Nucleic Acids Res,* 10, 8145-54.

PRASAD, R., SINGHAL, R. K., SRIVASTAVA, D. K., MOLINA, J. T., TOMKINSON, A. E. & WILSON, S. H. (1996) Specific interaction of DNA polymerase beta and DNA ligase I in a multiprotein base excision repair complex from bovine testis. *J Biol Chem,* 271, 16000-7.

PRIGENT, C., SATOH, M. S., DALY, G., BARNES, D. E. & LINDAHL, T. (1994) Aberrant DNA repair and DNA replication due to an inherited enzymatic defect in human DNA ligase I. *Mol Cell Biol,* 14, 310-7.

PRITCHETT, C. J., SENIOR, P. V., SUNTER, J. P., WATSON, A. J., WILSON, R. G. & APPLETON, D. R. (1985) Cell proliferation in human colorectal mucosa in organ culture: the early adaptive changes. *J Anat,* 141, 171-9.

PROWSE, K. R., AVILION, A. A. & GREIDER, C. W. (1993) Identification of a nonprocessive telomerase activity from mouse cells. *Proc Natl Acad Sci U S A,* 90, 1493-7.

PUEBLA-OSORIO, N., LACEY, D. B., ALT, F. W. & ZHU, C. (2006) Early embryonic lethality due to targeted inactivation of DNA ligase III. *Mol Cell Biol,* 26, 3935-41.

RAMSDEN, D. A. & GELLERT, M. (1998) Ku protein stimulates DNA end joining by mammalian DNA ligases: a direct role for Ku in repair of DNA double-strand breaks. *Embo J,* 17, 609-14.

RANGANATHAN, V., HEINE, W. F., CICCONE, D. N., RUDOLPH, K. L., WU, X., CHANG, S., HAI, H., AHEARN, I. M., LIVINGSTON, D. M., RESNICK, I., ROSEN, F., SEEMANOVA, E., JAROLIM, P., DEPINHO, R. A. & WEAVER, D. T. (2001) Rescue of a telomere length defect of Nijmegen breakage syndrome cells requires NBS and telomerase catalytic subunit. *Curr Biol,* 11, 962-6.

RASS, U., COMPTON, S. A., MATOS, J., SINGLETON, M. R., IP, S. C., BLANCO, M. G., GRIFFITH, J. D. & WEST, S. C. (2010) Mechanism of

Holliday junction resolution by the human GEN1 protein. *Genes Dev,* 24, 1559-69.

REYA, T., MORRISON, S. J., CLARKE, M. F. & WEISSMAN, I. L. (2001) Stem cells, cancer, and cancer stem cells. *Nature,* 414, 105-11.

RIBALLO, E., CRITCHLOW, S. E., TEO, S. H., DOHERTY, A. J., PRIESTLEY, A., BROUGHTON, B., KYSELA, B., BEAMISH, H., PLOWMAN, N., ARLETT, C. F., LEHMANN, A. R., JACKSON, S. P. & JEGGO, P. A. (1999) Identification of a defect in DNA ligase IV in a radiosensitive leukaemia patient. *Curr Biol,* 9, 699-702.

RIBALLO, E., DOHERTY, A. J., DAI, Y., STIFF, T., OETTINGER, M. A., JEGGO, P. A. & KYSELA, B. (2001) Cellular and biochemical impact of a mutation in DNA ligase IV conferring clinical radiosensitivity. *J Biol Chem,* 276, 31124-32.

RIHA, K., MCKNIGHT, T. D., FAJKUS, J., VYSKOT, B. & SHIPPEN, D. E. (2000) Analysis of the G-overhang structures on plant telomeres: evidence for two distinct telomere architectures. *Plant J,* 23, 633-41.

RIHA, K. & SHIPPEN, D. E. (2003) Telomere structure, function and maintenance in Arabidopsis. *Chromosome Res,* 11, 263-75.

RIOU, J. F., GOMEZ, D., LEMARTELEUR, T. & TRENTESAUX, C. (2003) [G-quadruplex DNA: myth or reality?]. *Bull Cancer,* 90, 305-13.

ROBERSON, R. S., KUSSICK, S. J., VALLIERES, E., CHEN, S. Y. & WU, D. Y. (2005) Escape from therapy-induced accelerated cellular senescence in p53-null lung cancer cells and in human lung cancers. *Cancer Res,* 65, 2795-803.

ROBLES, S. J. & ADAMI, G. R. (1998) Agents that cause DNA double strand breaks lead to p16INK4a enrichment and the premature senescence of normal fibroblasts. *Oncogene,* 16, 1113-23.

ROONEY, S., SEKIGUCHI, J., ZHU, C., CHENG, H. L., MANIS, J., WHITLOW, S., DEVIDO, J., FOY, D., CHAUDHURI, J., LOMBARD, D. & ALT, F. W. (2002) Leaky Scid phenotype associated with defective V(D)J coding end processing in Artemis-deficient mice. *Mol Cell,* 10, 1379-90.

ROTH, D. B. & WILSON, J. H. (1986) Nonhomologous recombination in mammalian cells: role for short sequence homologies in the joining reaction. *Mol Cell Biol,* 6, 4295-304.

ROULEAU, M., PATEL, A., HENDZEL, M. J., KAUFMANN, S. H. & POIRIER, G. G. (2010) PARP inhibition: PARP1 and beyond. *Nat Rev Cancer,* 10, 293-301.

RUCCI, F., NOTARANGELO, L. D., FAZELI, A., PATRIZI, L., HICKERNELL, T., PAGANINI, T., COAKLEY, K. M., DETRE, C., KESZEI, M., WALTER, J. E., FELDMAN, L., CHENG, H. L., POLIANI, P. L., WANG, J. H., BALTER, B. B., RECHER, M., ANDERSSON, E. M., ZHA, S., GILIANI, S., TERHORST, C., ALT, F. W. & YAN, C. T. (2010) Homozygous DNA ligase IV R278H mutation in mice leads to leaky SCID and represents a model for human LIG4 syndrome. *Proc Natl Acad Sci U S A,* 107, 3024-9.

RUDD, M. K., FRIEDMAN, C., PARGHI, S. S., LINARDOPOULOU, E. V., HSU, L. & TRASK, B. J. (2007) Elevated rates of sister chromatid exchange at chromosome ends. *PLoS Genet,* 3, e32.

SALK, D. (1982) Werner's syndrome: a review of recent research with an analysis of connective tissue metabolism, growth control of cultured cells, and chromosomal aberrations. *Hum Genet,* 62, 1-5.

SAMPER, E., GOYTISOLO, F. A., MENISSIER-DE MURCIA, J., GONZALEZ-SUAREZ, E., CIGUDOSA, J. C., DE MURCIA, G. & BLASCO, M. A. (2001) Normal telomere length and chromosomal end capping in poly(ADP-ribose) polymerase-deficient mice and primary cells despite increased chromosomal instability. *J Cell Biol,* 154, 49-60.

SAN FILIPPO, J., SUNG, P. & KLEIN, H. (2008) Mechanism of eukaryotic homologous recombination. *Annu Rev Biochem,* 77, 229-57.

SARTHY, J., BAE, N. S., SCRAFFORD, J. & BAUMANN, P. (2009) Human RAP1 inhibits non-homologous end joining at telomeres. *Embo J,* 28, 3390-9.

SATOH, M. S. & LINDAHL, T. (1992) Role of poly(ADP-ribose) formation in DNA repair. *Nature,* 356, 356-8.

SAVAGE, S. A., GIRI, N., BAERLOCHER, G. M., ORR, N., LANSDORP, P. M. & ALTER, B. P. (2008) TINF2, a component of the shelterin telomere protection complex, is mutated in dyskeratosis congenita. *Am J Hum Genet,* 82, 501-9.

SAVITSKY, K., SFEZ, S., TAGLE, D. A., ZIV, Y., SARTIEL, A., COLLINS, F. S., SHILOH, Y. & ROTMAN, G. (1995) The complete sequence of the coding region of the ATM gene reveals similarity to cell cycle regulators in different species. *Hum Mol Genet,* 4, 2025-32.

SAWADA, M., SUN, W., HAYES, P., LESKOV, K., BOOTHMAN, D. A. & MATSUYAMA, S. (2003) Ku70 suppresses the apoptotic translocation of Bax to mitochondria. *Nat Cell Biol,* 5, 320-9.

SCHERTHAN, H. (2001) A bouquet makes ends meet. *Nat Rev Mol Cell Biol,* 2, 621-7.

SCHERTHAN, H., WEICH, S., SCHWEGLER, H., HEYTING, C., HARLE, M. & CREMER, T. (1996) Centromere and telomere movements during early meiotic prophase of mouse and man are associated with the onset of chromosome pairing. *J Cell Biol,* 134, 1109-25.

SCHMITT, C. A., FRIDMAN, J. S., YANG, M., LEE, S., BARANOV, E., HOFFMAN, R. M. & LOWE, S. W. (2002) A senescence program controlled by p53 and p16INK4a contributes to the outcome of cancer therapy. *Cell,* 109, 335-46.

SCHOEFTNER, S. & BLASCO, M. A. (2008) Developmentally regulated transcription of mammalian telomeres by DNA-dependent RNA polymerase II. *Nat Cell Biol,* 10, 228-36.

SCHONBERG, S., NIERMEIJER, M. F., BOOTSMA, D., HENDERSON, E. & GERMAN, J. (1984) Werner's syndrome: proliferation in vitro of clones of cells bearing chromosome translocations. *Am J Hum Genet,* 36, 387-97.

SCHULZ, V. P., ZAKIAN, V. A., OGBURN, C. E., MCKAY, J., JARZEBOWICZ, A. A., EDLAND, S. D. & MARTIN, G. M. (1996) Accelerated loss of telomeric repeats may not explain accelerated replicative decline of Werner syndrome cells. *Hum Genet,* 97, 750-4.

SELMAN, M. & PARDO, A. (2002) Idiopathic pulmonary fibrosis: an epithelial/fibroblastic cross-talk disorder. *Respir Res,* 3, 3.

SERRANO, M., LIN, A. W., MCCURRACH, M. E., BEACH, D. & LOWE, S. W. (1997) Oncogenic ras provokes premature cell senescence associated with accumulation of p53 and p16INK4a. *Cell,* 88, 593-602.

SFEIR, A., KOSIYATRAKUL, S. T., HOCKEMEYER, D., MACRAE, S. L., KARLSEDER, J., SCHILDKRAUT, C. L. & DE LANGE, T. (2009) Mammalian telomeres resemble fragile sites and require TRF1 for efficient replication. *Cell,* 138, 90-103.

SHAH, G. M., POIRIER, D., DESNOYERS, S., SAINT-MARTIN, S., HOFLACK, J. C., RONG, P., APSIMON, M., KIRKLAND, J. B. & POIRIER, G. G. (1996) Complete inhibition of poly(ADP-ribose) polymerase activity prevents the recovery of C3H10T1/2 cells from oxidative stress. *Biochim Biophys Acta,* 1312, 1-7.

SHAMPAY, J., SZOSTAK, J. W. & BLACKBURN, E. H. (1984) DNA sequences of telomeres maintained in yeast. *Nature,* 310, 154-7.

SHAY, J. W. & BACCHETTI, S. (1997) A survey of telomerase activity in human cancer. *Eur J Cancer,* 33, 787-91.

SHAY, J. W., WRIGHT, W. E., BRASISKYTE, D. & VAN DER HAEGEN, B. A. (1993) E6 of human papillomavirus type 16 can overcome the M1 stage of immortalization in human mammary epithelial cells but not in human fibroblasts. *Oncogene,* 8, 1407-13.

SHILOH, Y. (1997) Ataxia-telangiectasia and the Nijmegen breakage syndrome: related disorders but genes apart. *Annu Rev Genet,* 31, 635-62.

SHILOH, Y. (2006) The ATM-mediated DNA-damage response: taking shape. *Trends Biochem Sci,* 31, 402-10.

SHIPPEN-LENTZ, D. & BLACKBURN, E. H. (1989) Telomere terminal transferase activity from Euplotes crassus adds large numbers of TTTTGGGG repeats onto telomeric primers. *Mol Cell Biol,* 9, 2761-4.

SIBANDA, B. L., CRITCHLOW, S. E., BEGUN, J., PEI, X. Y., JACKSON, S. P., BLUNDELL, T. L. & PELLEGRINI, L. (2001) Crystal structure of an Xrcc4-DNA ligase IV complex. *Nat Struct Biol,* 8, 1015-9.

SMITH, J., BALDEYRON, C., DE OLIVEIRA, I., SALA-TREPAT, M. & PAPADOPOULO, D. (2001) The influence of DNA double-strand break structure on end-joining in human cells. *Nucleic Acids Res,* 29, 4783-92.

SMITH, J., RIBALLO, E., KYSELA, B., BALDEYRON, C., MANOLIS, K., MASSON, C., LIEBER, M. R., PAPADOPOULO, D. & JEGGO, P. (2003) Impact of DNA ligase IV on the fidelity of end joining in human cells. *Nucleic Acids Res,* 31, 2157-67.

SMITH, J. R., PEREIRA-SMITH, O. M., BRAUNSCHWEIGER, K. I., ROBERTS, T. W. & WHITNEY, R. G. (1980) A general method for determining the replicative age of normal animal cell cultures. *Mech Ageing Dev,* 12, 355-65.

SMITH, S. & DE LANGE, T. (2000) Tankyrase promotes telomere elongation in human cells. *Curr Biol,* 10, 1299-302.

SMITH, S., GIRIAT, I., SCHMITT, A. & DE LANGE, T. (1998) Tankyrase, a poly(ADP-ribose) polymerase at human telomeres. *Science,* 282, 1484-7.

SMOGORZEWSKA, A., KARLSEDER, J., HOLTGREVE-GREZ, H., JAUCH, A. & DE LANGE, T. (2002) DNA ligase IV-dependent NHEJ of deprotected mammalian telomeres in G1 and G2. *Curr Biol,* 12, 1635-44.

SMOGORZEWSKA, A., VAN STEENSEL, B., BIANCHI, A., OELMANN, S., SCHAEFER, M. R., SCHNAPP, G. & DE LANGE, T. (2000) Control of human telomere length by TRF1 and TRF2. *Mol Cell Biol,* 20, 1659-68.

SOZA, S., LEVA, V., VAGO, R., FERRARI, G., MAZZINI, G., BIAMONTI, G. & MONTECUCCO, A. (2009) DNA ligase I deficiency leads to replication-dependent DNA damage and impacts cell morphology without blocking cell cycle progression. *Mol Cell Biol,* 29, 2032-41.

STANSEL, R. M., DE LANGE, T. & GRIFFITH, J. D. (2001) T-loop assembly in vitro involves binding of TRF2 near the 3' telomeric overhang. *Embo J,* 20, 5532-40.

SULLIVAN, K. E., VEKSLER, E., LEDERMAN, H. & LEES-MILLER, S. P. (1997) Cell cycle checkpoints and DNA repair in Nijmegen breakage syndrome. *Clin Immunol Immunopathol,* 82, 43-8.

SWIGGERS, S. J., NIBBELING, H. A., ZEILEMAKER, A., KUIJPERS, M. A., MATTERN, K. A. & ZIJLMANS, J. M. (2004) Telomerase activity level, but not hTERT mRNA and hTR level, regulates telomere length in telomerase-reconstituted primary fibroblasts. *Exp Cell Res,* 297, 434-43.

TAKAI, H., SMOGORZEWSKA, A. & DE LANGE, T. (2003) DNA damage foci at dysfunctional telomeres. *Curr Biol,* 13, 1549-56.

TAO, Z., GAO, P., HOFFMAN, D. W. & LIU, H. W. (2008) Domain C of human poly(ADP-ribose) polymerase-1 is important for enzyme activity and contains a novel zinc-ribbon motif. *Biochemistry,* 47, 5804-13.

TAO, Z., GAO, P. & LIU, H. W. (2009) Identification of the ADP-ribosylation sites in the PARP-1 automodification domain: analysis and implications. *J Am Chem Soc,* 131, 14258-60.

TARSOUNAS, M., MUNOZ, P., CLAAS, A., SMIRALDO, P. G., PITTMAN, D. L., BLASCO, M. A. & WEST, S. C. (2004) Telomere maintenance requires the RAD51D recombination/repair protein. *Cell,* 117, 337-47.

TAUCHI, H., MATSUURA, S., KOBAYASHI, J., SAKAMOTO, S. & KOMATSU, K. (2002) Nijmegen breakage syndrome gene, NBS1, and molecular links to factors for genome stability. *Oncogene,* 21, 8967-80.

TAYLOR, R. M., WICKSTEAD, B., CRONIN, S. & CALDECOTT, K. W. (1998) Role of a BRCT domain in the interaction of DNA ligase III-alpha with the DNA repair protein XRCC1. *Curr Biol,* 8, 877-80.

TCHIRKOV, A. & LANSDORP, P. M. (2003) Role of oxidative stress in telomere shortening in cultured fibroblasts from normal individuals and patients with ataxia-telangiectasia. *Hum Mol Genet,* 12, 227-32.

TEO, I. A., BROUGHTON, B. C., DAY, R. S., JAMES, M. R., KARRAN, P., MAYNE, L. V. & LEHMANN, A. R. (1983) A biochemical defect in the repair of alkylated DNA in cells from an immunodeficient patient (46BR). *Carcinogenesis,* 4, 559-64.

THOMPSON, L. H., BROOKMAN, K. W., DILLEHAY, L. E., MOONEY, C. L. & CARRANO, A. V. (1982) Hypersensitivity to mutation and sister-chromatid-exchange induction in CHO cell mutants defective in incising DNA containing UV lesions. *Somatic Cell Genet,* 8, 759-73.

TIMINSZKY, G., TILL, S., HASSA, P. O., HOTHORN, M., KUSTATSCHER, G., NIJMEIJER, B., COLOMBELLI, J., ALTMEYER, M., STELZER, E. H., SCHEFFZEK, K., HOTTIGER, M. O. & LADURNER, A. G. (2009) A macrodomain-containing histone rearranges chromatin upon sensing PARP1 activation. *Nat Struct Mol Biol,* 16, 923-9.

TOLLEFSBOL, T. O. & COHEN, H. J. (1984) The effect of age on the accumulation of labile triosephosphate isomerase and thymidine incorporation in pokeweed mitogen stimulated human lymphocytes. *J Gerontol,* 39, 398-405.

TOMASKA, L., NOSEK, J., KRAMARA, J. & GRIFFITH, J. D. (2009) Telomeric circles: universal players in telomere maintenance? *Nat Struct Mol Biol,* 16, 1010-5.

TOMASKA, L., WILLCOX, S., SLEZAKOVA, J., NOSEK, J. & GRIFFITH, J. D. (2004) Taz1 binding to a fission yeast model telomere: formation of telomeric loops and higher order structures. *J Biol Chem,* 279, 50764-72.

TONG, W. M., HANDE, M. P., LANSDORP, P. M. & WANG, Z. Q. (2001) DNA strand break-sensing molecule poly(ADP-Ribose) polymerase cooperates with p53 in telomere function, chromosome stability, and tumor suppression. *Mol Cell Biol,* 21, 4046-54.

TRUJILLO, K. M., YUAN, S. S., LEE, E. Y. & SUNG, P. (1998) Nuclease activities in a complex of human recombination and DNA repair factors Rad50, Mre11, and p95. *J Biol Chem,* 273, 21447-50.

TSAI, C. J., KIM, S. A. & CHU, G. (2007) Cernunnos/XLF promotes the ligation of mismatched and noncohesive DNA ends. *Proc Natl Acad Sci U S A,* 104, 7851-6.

VAN STEENSEL, B. & DE LANGE, T. (1997) Control of telomere length by the human telomeric protein TRF1. *Nature,* 385, 740-3.

VAN STEENSEL, B., SMOGORZEWSKA, A. & DE LANGE, T. (1998) TRF2 protects human telomeres from end-to-end fusions. *Cell,* 92, 401-13.

VARON, R., SEEMANOVA, E., CHRZANOWSKA, K., HNATEYKO, O., PIEKUTOWSKA-ABRAMCZUK, D., KRAJEWSKA-WALASEK, M., SYKUT-CEGIELSKA, J., SPERLING, K. & REIS, A. (2000) Clinical ascertainment of Nijmegen breakage syndrome (NBS) and prevalence of the major mutation, 657del5, in three Slav populations. *Eur J Hum Genet,* 8, 900-2.

VARON, R., VISSINGA, C., PLATZER, M., CEROSALETTI, K. M., CHRZANOWSKA, K. H., SAAR, K., BECKMANN, G., SEEMANOVA, E., COOPER, P. R., NOWAK, N. J., STUMM, M., WEEMAES, C. M., GATTI, R. A., WILSON, R. K., DIGWEED, M., ROSENTHAL, A., SPERLING, K., CONCANNON, P. & REIS, A. (1998) Nibrin, a novel DNA double-strand break repair protein, is mutated in Nijmegen breakage syndrome. *Cell,* 93, 467-76.

VENTEICHER, A. S., ABREU, E. B., MENG, Z., MCCANN, K. E., TERNS, R. M., VEENSTRA, T. D., TERNS, M. P. & ARTANDI, S. E. (2009) A human telomerase holoenzyme protein required for Cajal body localization and telomere synthesis. *Science,* 323, 644-8.

VENTEICHER, A. S., MENG, Z., MASON, P. J., VEENSTRA, T. D. & ARTANDI, S. E. (2008) Identification of ATPases pontin and reptin as telomerase components essential for holoenzyme assembly. *Cell,* 132, 945-57.

VERDUN, R. E., CRABBE, L., HAGGBLOM, C. & KARLSEDER, J. (2005) Functional human telomeres are recognized as DNA damage in G2 of the cell cycle. *Mol Cell,* 20, 551-61.

VERKAIK, N. S., ESVELDT-VAN LANGE, R. E., VAN HEEMST, D., BRUGGENWIRTH, H. T., HOEIJMAKERS, J. H., ZDZIENICKA, M. Z. & VAN GENT, D. C. (2002) Different types of V(D)J recombination and end-joining defects in DNA double-strand break repair mutant mammalian cells. *Eur J Immunol,* 32, 701-9.

VEUGER, S. J., CURTIN, N. J., SMITH, G. C. & DURKACZ, B. W. (2004) Effects of novel inhibitors of poly(ADP-ribose) polymerase-1 and the DNA-dependent protein kinase on enzyme activities and DNA repair. *Oncogene,* 23, 7322-9.

VON ZGLINICKI, T. (2002) Oxidative stress shortens telomeres. *Trends Biochem Sci,* 27, 339-44.

VULLIAMY, T., MARRONE, A., GOLDMAN, F., DEARLOVE, A., BESSLER, M., MASON, P. J. & DOKAL, I. (2001) The RNA component of telomerase is mutated in autosomal dominant dyskeratosis congenita. *Nature,* 413, 432-5.

VULLIAMY, T. J., WALNE, A., BASKARADAS, A., MASON, P. J., MARRONE, A. & DOKAL, I. (2005) Mutations in the reverse transcriptase component of telomerase (TERT) in patients with bone marrow failure. *Blood Cells Mol Dis,* 34, 257-63.

WAGA, S., BAUER, G. & STILLMAN, B. (1994) Reconstitution of complete SV40 DNA replication with purified replication factors. *J Biol Chem,* 269, 10923-34.

WAGA, S. & STILLMAN, B. (1994) Anatomy of a DNA replication fork revealed by reconstitution of SV40 DNA replication in vitro. *Nature,* 369, 207-12.

WAGA, S. & STILLMAN, B. (1998) The DNA replication fork in eukaryotic cells. *Annu Rev Biochem,* 67, 721-51.

WALKER, J. R., CORPINA, R. A. & GOLDBERG, J. (2001) Structure of the Ku heterodimer bound to DNA and its implications for double-strand break repair. *Nature,* 412, 607-14.

WANG, H., ROSIDI, B., PERRAULT, R., WANG, M., ZHANG, L., WINDHOFER, F. & ILIAKIS, G. (2005) DNA ligase III as a candidate component of backup pathways of nonhomologous end joining. *Cancer Res,* 65, 4020-30.

WANG, M., WU, W., ROSIDI, B., ZHANG, L., WANG, H. & ILIAKIS, G. (2006) PARP-1 and Ku compete for repair of DNA double strand breaks by distinct NHEJ pathways. *Nucleic Acids Res,* 34, 6170-82.

WANG, R. C., SMOGORZEWSKA, A. & DE LANGE, T. (2004) Homologous recombination generates T-loop-sized deletions at human telomeres. *Cell,* 119, 355-68.

WANG, S. S. & ZAKIAN, V. A. (1990) Sequencing of Saccharomyces telomeres cloned using T4 DNA polymerase reveals two domains. *Mol Cell Biol,* 10, 4415-9.

WANG, Y. & PATEL, D. J. (1993) Solution structure of a parallel-stranded G-quadruplex DNA. *J Mol Biol,* 234, 1171-83.

WATSON, J. M. & RIHA, K. (2010) Comparative biology of telomeres: Where plants stand. *FEBS Lett,* 584, 3752-3759.

WEBSTER, A. D., BARNES, D. E., ARLETT, C. F., LEHMANN, A. R. & LINDAHL, T. (1992) Growth retardation and immunodeficiency in a patient with mutations in the DNA ligase I gene. *Lancet,* 339, 1508-9.

WEEMAES, C. M., HUSTINX, T. W., SCHERES, J. M., VAN MUNSTER, P. J., BAKKEREN, J. A. & TAALMAN, R. D. (1981) A new chromosomal instability disorder: the Nijmegen breakage syndrome. *Acta Paediatr Scand,* 70, 557-64.

WELLINGER, R. J., WOLF, A. J. & ZAKIAN, V. A. (1993) Saccharomyces telomeres acquire single-strand TG1-3 tails late in S phase. *Cell,* 72, 51-60.

WETERINGS, E. & CHEN, D. J. (2008) The endless tale of non-homologous end-joining. *Cell Res,* 18, 114-24.

WILLIAMS, B. R., MIRZOEVA, O. K., MORGAN, W. F., LIN, J., DUNNICK, W. & PETRINI, J. H. (2002) A murine model of Nijmegen breakage syndrome. *Curr Biol,* 12, 648-53.

WILLIAMS, R. S., DODSON, G. E., LIMBO, O., YAMADA, Y., WILLIAMS, J. S., GUENTHER, G., CLASSEN, S., GLOVER, J. N., IWASAKI, H., RUSSELL, P. & TAINER, J. A. (2009) Nbs1 flexibly tethers Ctp1 and Mre11-Rad50 to coordinate DNA double-strand break processing and repair. *Cell,* 139, 87-99.

WILLIAMS, R. S., MONCALIAN, G., WILLIAMS, J. S., YAMADA, Y., LIMBO, O., SHIN, D. S., GROOCOCK, L. M., CAHILL, D., HITOMI, C., GUENTHER, G., MOIANI, D., CARNEY, J. P., RUSSELL, P. & TAINER, J. A. (2008) Mre11 dimers coordinate DNA end bridging and nuclease processing in double-strand-break repair. *Cell,* 135, 97-109.

WILLIAMS, R. S., WILLIAMS, J. S. & TAINER, J. A. (2007) Mre11-Rad50-Nbs1 is a keystone complex connecting DNA repair machinery, double-strand break signaling, and the chromatin template. *Biochem Cell Biol,* 85, 509-20.

WRIGHT, W. E. & SHAY, J. W. (2001) Cellular senescence as a tumor-protection mechanism: the essential role of counting. *Curr Opin Genet Dev,* 11, 98-103.

WU, G. J., SINCLAIR, C. S., PAAPE, J., INGLE, J. N., ROCHE, P. C., JAMES, C. D. & COUCH, F. J. (2000) 17q23 amplifications in breast cancer involve the PAT1, RAD51C, PS6K, and SIGma1B genes. *Cancer Res,* 60, 5371-5.

WU, L., DAVIES, S. L., LEVITT, N. C. & HICKSON, I. D. (2001) Potential role for the BLM helicase in recombinational repair via a conserved interaction with RAD51. *J Biol Chem,* 276, 19375-81.

WYATT, H. D., WEST, S. C. & BEATTIE, T. L. (2010) InTERTpreting telomerase structure and function. *Nucleic Acids Res,* 38, 5609-22.

WYLLIE, F. S., LEMOINE, N. R., BARTON, C. M., DAWSON, T., BOND, J. & WYNFORD-THOMAS, D. (1993) Direct growth stimulation of normal human epithelial cells by mutant p53. *Mol Carcinog,* 7, 83-8.

XIN, H., LIU, D., WAN, M., SAFARI, A., KIM, H., SUN, W., O'CONNOR, M. S. & SONGYANG, Z. (2007) TPP1 is a homologue of ciliate TEBP-beta and interacts with POT1 to recruit telomerase. *Nature,* 445, 559-62.

YE, J. Z., DONIGIAN, J. R., VAN OVERBEEK, M., LOAYZA, D., LUO, Y., KRUTCHINSKY, A. N., CHAIT, B. T. & DE LANGE, T. (2004a) TIN2 binds TRF1 and TRF2 simultaneously and stabilizes the TRF2 complex on telomeres. *J Biol Chem,* 279, 47264-71.

YE, J. Z., HOCKEMEYER, D., KRUTCHINSKY, A. N., LOAYZA, D., HOOPER, S. M., CHAIT, B. T. & DE LANGE, T. (2004b) POT1-interacting protein PIP1: a telomere length regulator that recruits POT1 to the TIN2/TRF1 complex. *Genes Dev,* 18, 1649-54.

YEAGER, T. R., NEUMANN, A. A., ENGLEZOU, A., HUSCHTSCHA, L. I., NOBLE, J. R. & REDDEL, R. R. (1999) Telomerase-negative immortalized human cells contain a novel type of promyelocytic leukemia (PML) body. *Cancer Res,* 59, 4175-9.

YEH, T. Y., SBODIO, J. I. & CHI, N. W. (2006) Mitotic phosphorylation of tankyrase, a PARP that promotes spindle assembly, by GSK3. *Biochem Biophys Res Commun,* 350, 574-9.

YEHEZKEL, S., SEGEV, Y., VIEGAS-PEQUIGNOT, E., SKORECKI, K. & SELIG, S. (2008) Hypomethylation of subtelomeric regions in ICF syndrome is associated with abnormally short telomeres and enhanced transcription from telomeric regions. *Hum Mol Genet,* 17, 2776-89.

YOU, Z. & BAILIS, J. M. (2010) DNA damage and decisions: CtIP coordinates DNA repair and cell cycle checkpoints. *Trends Cell Biol,* 20, 402-9.

YU, C. E., OSHIMA, J., FU, Y. H., WIJSMAN, E. M., HISAMA, F., ALISCH, R., MATTHEWS, S., NAKURA, J., MIKI, T., OUAIS, S., MARTIN, G. M., MULLIGAN, J. & SCHELLENBERG, G. D. (1996) Positional cloning of the Werner's syndrome gene. *Science,* 272, 258-62.

ZAHLER, A. M. & PRESCOTT, D. M. (1988) Telomere terminal transferase activity in the hypotrichous ciliate Oxytricha nova and a model for replication of the ends of linear DNA molecules. *Nucleic Acids Res,* 16, 6953-72.

ZAREMBA, T. & CURTIN, N. J. (2007) PARP inhibitor development for systemic cancer targeting. *Anticancer Agents Med Chem,* 7, 515-23.

ZHONG, Z., SHIUE, L., KAPLAN, S. & DE LANGE, T. (1992) A mammalian factor that binds telomeric TTAGGG repeats in vitro. *Mol Cell Biol,* 12, 4834-43.

ZHONG, Z. H., JIANG, W. Q., CESARE, A. J., NEUMANN, A. A., WADHWA, R. & REDDEL, R. R. (2007) Disruption of telomere maintenance by depletion of the MRE11/RAD50/NBS1 complex in cells that use alternative lengthening of telomeres. *J Biol Chem,* 282, 29314-22.

ZHOU, X. Z. & LU, K. P. (2001) The Pin2/TRF1-interacting protein PinX1 is a potent telomerase inhibitor. *Cell,* 107, 347-59.

ZHU, J., PETERSEN, S., TESSAROLLO, L. & NUSSENZWEIG, A. (2001) Targeted disruption of the Nijmegen breakage syndrome gene NBS1 leads to early embryonic lethality in mice. *Curr Biol,* 11, 105-9.

ZHU, J., WOODS, D., MCMAHON, M. & BISHOP, J. M. (1998) Senescence of human fibroblasts induced by oncogenic Raf. *Genes Dev,* 12, 2997-3007.

ZHU, X. D., KUSTER, B., MANN, M., PETRINI, J. H. & DE LANGE, T. (2000) Cell-cycle-regulated association of RAD50/MRE11/NBS1 with TRF2 and human telomeres. *Nat Genet,* 25, 347-52.

ZHU, X. D., NIEDERNHOFER, L., KUSTER, B., MANN, M., HOEIJMAKERS, J. H. & DE LANGE, T. (2003) ERCC1/XPF removes the 3' overhang from uncapped telomeres and represses formation of telomeric DNA-containing double minute chromosomes. *Mol Cell,* 12, 1489-98.

ZHUANG, J., JIANG, G., WILLERS, H. & XIA, F. (2009) Exonuclease function of human Mre11 promotes deletional nonhomologous end joining. *J Biol Chem,* 284, 30565-73.